ITERATIVE TECHNIQUES FOR CONTROLLER TUNING

Teză destinată obţinerii
titlului ştiinţific de doctor inginer
la
Universitatea "Politehnica" din Timişoara
în domeniul Ingineria Sistemelor
de către

ing. Mircea-Bogdan Rădac

Conducător ştiinţific:	Prof.Dr.Eng. Radu-Emil Precup
Referenţi ştiinţifici:	Prof.Dr.Eng. Octavian Proştean
	Prof.Dr.Eng. Sergiu Caraman
	Prof.Dr.Eng. Corneliu Lazăr
	Prof.Dr.Eng. Stefan Preitl

Data susţinerii tezei:30.09.2011

Seriile Teze de doctorat ale UPT sunt:

1. Automatică
2. Chimie
3. Energetică
4. Ingineria Chimică
5. Inginerie Civilă
6. Inginerie Electrică
7. Inginerie Electronică şi Telecomunicaţii
8. Inginerie Industrială
9. Inginerie Mecanică
10. Ştiinţa Calculatoarelor
11. Ştiinţa şi Ingineria Materialelor
12. Ingineria sistemelor
13. Inginerie energetică
14. Calculatoare şi tehnologia informaţiei

Universitatea „Politehnica” din Timişoara a iniţiat seriile de mai sus în scopul diseminării expertizei, cunoştinţelor şi rezultatelor cercetărilor întreprinse în cadrul şcolii doctorale a universităţii. Seriile conţin, potrivit H.B.Ex.S Nr. 14 / 14.07.2006, tezele de doctorat susţinute în universitate începând cu 1 octombrie 2006.

România, 300159 Timişoara, Bd. Republicii 9,
tel. 0256 403823, fax. 0256 403221
e-mail: editura@edipol.upt.ro

Preface

This thesis presents the research results of the author between 2008 and 2011, in the framework of the PhD studies in Systems Engineering at the "Politehnica" University of Timişoara, Romania, within the Department of Automation and Applied Informatics.

First of all I would like to thank my supervisor, Prof. Dr. Eng. Radu-Emil Precup, for the support and guidance throughout the development process of this thesis which started early with the elaboration of my Diploma thesis. His energy and ability to push things forward despite the obstacles has been a great inspiration for me.

I would also like to thank Prof. Dr. Eng. Stefan Preitl and M. Sc. Dipl. Eng. Claudia-Adina Dragoş for the fruitful and close co-operation throughout this time. Nevertheless many thanks go to my collaborators from the University of Ottawa, Canada, and from the Óbuda University, Budapest, Hungary. They were near me, we experienced an excellent co-operation in several projects, they were my co-authors in journal and conference papers, and they offered me the best advices when I needed them.

I also express my gratitude to the members of the PhD evaluation and defense committee, Prof. Dr. Eng. Octavian Proştean, the Dean of the Faculty of Automation and Computers, "Politehnica" University of Timişoara, Romania, and the president of the committee, Prof. Dr. Eng. Sergiu Caraman from the "Dunărea de Jos" University of Galaţi, Romania, Prof. Dr. Eng. Corneliu Lazăr from the "Gheorghe Asachi" Technical University of Iaşi, Romania, and Prof. Dr. Eng. Stefan Preitl from the "Politehnica" University of Timişoara, Romania, for accepting to be a part of this committee and for their time spent in the evaluation of my PhD thesis. Their comments and insightful discussions before publication helped me shape the final form of this thesis.

Timişoara, September 2011 Mircea-Bogdan Rădac

Rădac, Mircea-Bogdan

Iterative Techniques for Controller Tuning

Teze de doctorat ale UPT, Seria 12, Nr. 1, Editura Politehnica, 2011, 176 pagini, 69 figuri, 2 tabele.

Cuvinte cheie:

Tehnici iterative de acordare, Iterative Feedback Tuning, Virtual Reference Feedback Tuning, Iterative Regression Tuning, Simultaneous Perturbation Stochastic Approximation, reglare fuzzy, optimizare, LQR, LQG.

Rezumat:
În cadrul tezei sunt propuse diverse tehnici iterative dedicate acordării sistematice a parametrilor regulatoarelor automate în vederea îmbunătăţirii performanţelor sistemelor de reglare automată. Rezultatele de cercetare prezentate se referă la două direcţii distincte: îmbunătăţirea aspectelor particulare aferente fiecărei tehnici în parte şi folosirea acestor tehnici în combinaţie cu diferite structuri convenţionale de reglare automată exemplificate prin structurile cu reacţie după stare şi cele cu regulatoare fuzzy. Ambele direcţii sunt validate pe o gamă largă de aplicaţii de laborator urmărind investigarea diferitelor clase de procese cărora li se pot aplica tehnicile dezvoltate. Sunt efectuate studii comparative privind performanţele şi sunt analizate costurile de implementare ale tehncilor iterative.

CONTENTS

List of Acronyms

1-DOF, 2-DOF	One Degree Of Freedon, Two Degrees Of Freedom
BFGS	Broyden - Fletcher - Goldfarb - Shanno
CbT	Correlation-based Tuning
CSs	Control Systems
D-ARE	Discrete time Algebraic Riccati Equation
DbC	Data-based Control
DC	Direct current
DFT	Discrete Fourier Transform
ETFE	Empirical Transfer Function Estimate
FCSs	Fuzzy Control Systems
FDA	Finite Difference Approximations
FDSA	Finite Difference Stochastic Approximations
FdT	Frequency-domain Tuning
FFT	Fast Fourier Transform
FPGA	Field-Programmable Gate Array
FRFs	Frequency Response Functions
IFT	Iterative Feedback Tuning
ILC	Iterative Learning Control
IRT	Iterative Regression Tuning
LMA	Levenberg-Marquardt Algorithm
LMIs	Linear Matrix Inequalities
LQG	Linear Quadratic Gaussian
LQR	Linear Quadratic Regulator
LTI	Linear Time-Invariant
MFC	Model Free Control

MIMO	Multiple-Input Multiple-Ouput
MQ	Model Quality
MRAC	Model Reference Adaptive Control
NL	Nonlinear
OF	Objective Function
PI, PID	Proportional-Integral, Proportional-Integral-Derivative
PRBS	Pseudo Random Binary Sequence
PWM	Pulse-Width Modulation
RM	Reference Model
SA	Stochastic Approximation
SISO	Single Input-Single Output
SNR	Signal-to-Noise Ratio
SPA	SPectral correlation-based Analysis
SPSA	Simulatenous Perturbation Stochastic Approximation
STR	Self Tuning Regulators
t.f.s	transfer functions
TISO-FC	Two Inputs-Single Output Fuzzy Controller
TS-PI-FCs	Takagi-Sugeno PI Fuzzy Controllers
USB	Universal Serial Bus
VRFT	Virtual Reference Feedback Tuning

1. Introduction

1.1. Motivation behind the research

Model reference control is a paradigm that has evolved in time to capture all the developments in control systems (CSs) design from the beginnings till nowadays. It has always been representative for the approach on the design phase where the control system engineer receives specifications over the CS that has to be designed. In many situations, these specifications come as constraints on the time response of the output of the controlled process, such as rising time, overshoot, settling time, steady-state error. This has always been the most direct way of asserting the behavior and the quality of the controlled systems. Other specifications can be in the frequency domain such as bandwidth, phase and gain margins, etc.

A common way around with model reference control is formulated as follows: given some performance specifications that can be often described by the behavior of a (typically second order system) reference model response to a input excitation signal, design a CS that makes the output(s) of interest of the process behave like the reference model in terms of time response when driven by the same exactly input excitation signal. In most of the cases, the difference between the output of the CS's output and the reference model output defines a measure of the quality of the match between the two. The cost function (CF) or the objective function (OF) expressed that way depends on the parameters of the controller. The model reference problem requires finding the suitable set of design parameters that minimize the OF, which brings close the responses that form the aforementioned error. Thus, the model reference control problem becomes and optimization problem that can be solved analytically or by some optimization technique.

This is also a superficial view of the design problem as it hides important aspects. All the approaches to the problem eventually lead to the basic conclusion that in automatic control the design boils down to compromise. The central players in this game of compromise are of course the process and the controller for it is the relationship between them that determine the two other extremely important aspects of the CS: the disturbance rejection and the parameter sensitivity (which in turn determines the robust stability and the robust performance).

With these two objects in hand it has to be stressed the fact that the controller is subject to designer's choice both as structure complexity and parameters values whereas the process can only be known partially. We use models for the processes which are inherently simplifications of the reality. Therefore, with models available, the design task can be carried out and tested but with no guarantee that the implementation of the proposed solution would give satisfactory results under real conditions.

As for obtaining the models, the user always has at hand tools such as first-principle modeling or system identification for obtaining mathematical models. So, one aspect that has always been fixed with respect to the design of CS's is the

model-based approach. Whether we operate on nominal models, simplified models, the knowledge of the process model has been essential to the design and analysis of the CS's. Knowing the model allows for a better insight into the limitations of the design process and allows testing before implementation through simulation.

On the shaky grounds of model uncertainty and parameters variations, tools had to be developed such that the specifications would be met under a broad range of conditions. That is the reason for development of fields such as adaptive control and robust control.

Adaptive control has emerged as a solution to cope with parameter variations by means of automatically redesigning the controller. In general, the difficulty which arises with this approach is mainly the analysis that has to be carried out in a time-varying nonlinear context and possibly the cost of implementation. Some variations of the adaptive control include Gain-scheduling, Model Reference Adaptive Control (MRAC) (both direct and indirect) and Self Tuning Regulators (STR). Even by using approaches like the "MIT rule" or the Lyapunov redesign, we still make use of process model and just the thought of bringing together the issues of stability analysis, convergence and robustness, all of them in the time-varying nonlinear framework, could make the best of control engineers tremble.

In the recent years, some techniques have emerged and earned the classification name as "data-based techniques" that claim to help in the design and tuning of control structures making no use of the process model, so being "model−free". Such popular techniques investigated in this thesis are *Iterative Feedback Tuning* (IFT), *Virtual Reference Feedback Tuning* (VRFT), *Correlation-based Tuning* (CbT), *Iterative Regression Tuning* (IRT). At first sight, they throw a bold challenge, an idea we could call as "Controlling the unknown". The logic behind these techniques is apparently simple: since the classical two step design procedure (modeling and control, respectively) can miss the specifications because of the mismatch between the model and the real process, one should skip the modeling step and try to make a design (or tuning) without using a model. The idea has been advocated by studies showing that the modeling (identification) should not be seen as a purpose in itself, but rather a mean to help the unique purpose of control design [56]. Only the relevant aspects for control should be captured within the model in the model-based design paradigm.

As it will be seen in the following, the label "model−free" is only valid in certain situations, under certain assumptions which can not be made unless some insight is available about the process in cause. And, as always, we will eventually reach the same position of compromise, but this time, with a new problem in hands: how much information about the process is sufficient to reach the specifications in design? How can the empirical observations be used to infer limitations in the design beforehand? If a model will prove to be necessary, how detailed should it be for the design purpose (this is the same as saying: how much are we willing to cut costs in identification and relax the quality constraints on the model)?

From the point of view of the tradeoff between model quality (MQ), design complexity (DC) and performance requirements (PR), the data-based control (DbC) techniques are focused on achieving performances with no process model at hand (or a very crude approximation) and meeting the specifications with simple, easy to maintain and interpret controllers such as the one that predominate in the industry (e.g., PI, PID). This idea is highlighted in terms of the diagram presented in Fig. 1.1.

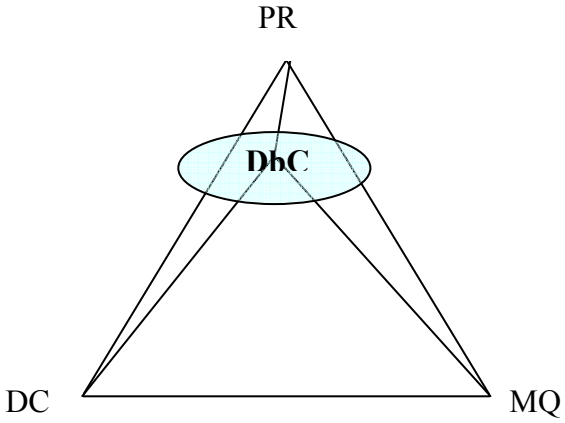

Fig. 1.1. Data-based control as a tradeoff between model quality, design complexity and performance requirements.

1.2. Thesis overview

Iterative Feedback Tuning (**IFT**) is a data-based technique that tunes the controller parameters iteratively along the gradient direction of a given objective function and it is applicable when an initial stabilizing controller is given in advance.

Variations between IFT algorithms are introduced by the choice of the objective function and of the adopted structure of the controller as well. IFT algorithms are formulated in the discrete time domain.

The designer selects the controller's structure and complexity, which means that the controller is available in analytical form. The parameterization should be such that the transfer function of the controller is differentiable with respect to its parameters gathered in the parameter vector $\underline{\rho}$.

IFT usually deals with LQG-like objective functions expressed as

$$J(\underline{\rho}) = \frac{1}{2N} E\{ \sum_{k=1}^{N} \left\{ \left[L_y(q^{-1}) \delta y(k, \underline{\rho}) \right]^2 + \lambda \left[L_u(q^{-1}) u(k, \underline{\rho}) \right]^2 \right\} \}, \qquad (1.2.1)$$

where $L_y(q^{-1})$ and $L_u(q^{-1})$ are frequency dependent weightings that penalize the output difference δy and the control input u according to the designer's needs. The expectation $E\{.\}$ is taken with respect to the stochastic disturbances that enter the process and thus affect the closed-loop. The objective of iterative feedback tuning is to determine the optimal set of parameters $\underline{\rho}^*$ which minimizes the objective function

$$\underline{\rho}^* = \underset{\underline{\rho}}{\textbf{arg min}}\, J(\underline{\rho}). \qquad (1.2.2)$$

The major stumbling block for the solution to this optimal control problem is the computation of the gradient of the objective function with respect to the controller parameters. An estimate of the gradient of the objective function with respect to the controller parameters can be obtained by conducting special "gradient" experiments on the closed-loop system at each iteration of the IFT. The

solution is approached iteratively using different gradient-based search algorithms such as

$$\underline{\rho}^{i+1} = \underline{\rho}^{i} - \gamma_i (\underline{R}^{i})^{-1} est\left[\frac{\partial J}{\partial \underline{\rho}}(\underline{\rho}^{i})\right]. \tag{1.2.3}$$

It should be pointed out right from the beginning that the technique is not only a sensitivity-based tuning but it also holds a stochastic convergence results which is of crucial importance in experiment-based tuning where all measurements are affected by random effects.

The thesis has a strong focus on IFT, offering an exhaustive analysis of the technique, which serves both as a starting point in the analysis and as a comparison basis for the subsequent analyzed techniques.

Virtual Reference Feedback Tuning (**VFRT**), viewed in the model-reference control framework, is a technique that achieves the minimization of an objective function which penalizes the difference between the behavior of the designed closed-loop system and the behavior of the desired reference model [53], [54], [55]. This idea can be expressed as

$$J_{MR}(\underline{\rho}) = \left\| \left(\frac{P(z)C(z,\underline{\rho})}{1+P(z)C(z,\underline{\rho})} - M(z) \right) W(z) \right\|_2^2, \tag{1.2.4}$$

where $M(z)$ is the reference model expressed as a discrete time transfer function, $P(z)$ and $C(z)$ stand for the process discrete-time transfer function and for the controller discrete-time transfer function respectively. $W(z)$ is a weighting filter and can be understood in frequency domain while being used as a degree of freedom in the design. The criterion makes use of the two-norm of a transfer function in discrete form. Another expression in the frequency domain can be employed due to the Parseval's theorem as:

$$J_{MR}(\underline{\rho}) = \frac{1}{2\pi} \int_{-\pi}^{\pi} \left| \frac{P(e^{j\omega})C(e^{j\omega},\underline{\rho})}{1+P(e^{j\omega})C(e^{j\omega},\underline{\rho})} - M(e^{j\omega}) \right|^2 \left| W(e^{j\omega}) \right|^2 d\omega. \tag{1.2.5}$$

To solve the VRFT problem means to try and find the controller which minimizes the objective function. The solution reduces to an identification problem as explained. The following discussion assumes single input single output linear time-invariant process. The time argument is omitted for simplicity. Also, the deterministic case is considered leaving the situation when the noise affects the signals for another discussion. An excitation for the open loop process is considered as u for which the output y is recorded. The same output is considered to have been obtained by filtering a reference signal through the reference model M. Although M is causal and the inverse of it is not, the filtering can be done to obtain this virtual reference signal called r since y is available. A virtual feedback control structure is built with the controlled error $e = r - y$ feeding a controller with pre-specified structure called $C(z)$. Passing e through $C(z)$ should give us the initial signal used for excitation which is u. The parameters of the proposed structure of the controller which achieve the best fit between the filtered virtual error e and input signal u are the solution to an identification-like problem defined as an optimization problem which can be solved via least-squares if the parameterization of the controller is linear. Several manipulations lead to the fact that the solution to this problem can also be the solution to the model reference following problem.

Correlation-based Tuning (**CbT**) is another approach to controller tuning that has been developed in the past decade. Its aim is to design the controller for the closed-loop feedback control structure in a manner which makes the closed-loop response to a reference input signal resemble the response of a reference model. Thus the same paradigm – that is specific to the objective of the MRAC and to the IFT and VRFT techniques – is preserved. The development of the technique does not make use of the process model and thus CbT can be considered as a member of the "model-free data-based" techniques group.

An initial stabilizing controller is assumed to exist for the closed-loop and the behavior of the closed-loop is assumed to be different from the one of the reference model. This can also be called the output error since it is the sample-wise difference between the closed-loop output and the reference model output, both of them being excited by the same reference input. The model reference tracking error depends on one hand on the noise that affects the real closed-loop. On the other hand, it also depends on the reference input signal because of the difference between the actual closed-loop and the desired closed-loop (which is the reference model). The relation between the reference input and the output error can be easily surprised in the correlation function of the two signals when the quasi-stationary framework [116] is assumed which is a pretty realistic assumption. If the closed-loop system model and the reference model were the same, the output error would not be correlated anymore with the reference input. Therefore, the idea emerges that in order to make the two outputs resemble, a decorrelation procedure is performed. A measure for the correlation function of the two signals is chosen to be

$$J(\underline{\rho}) = \sum_{\tau=-N}^{N} [R_{r,\varepsilon_{oe}}(\tau,\underline{\rho})]^2 \ , \tag{1.2.6}$$

where $R_{r,\varepsilon_{oe}}(\tau,\underline{\rho})$ is the correlation function between the reference input signal $r(k)$ and the output error $\varepsilon_{oe}(k,\underline{\rho})$. The dependence on the parameter vector $\underline{\rho}$ is emphasized which is the set of parameters that characterizes the linear controller. The correlation function for each τ is calculated over a finite time horizon which is the length of the experiment and the objective function J is calculated over $2N+1$ samples.

A particular situation is considered when it can be possible to fiind a controller which perfectly decorrelates the output error and the reference input. This implies the fact that with an aprioric choice of the controller structure, we need to know at least the process model structure (not necessarily the model parameters) in order to check if the closed-loop equivalent behavior is a perfect match for the reference model structure. This is rarely the case although, because we usually choose reference models that are of second order with performance indices specifications such as damping factor and rise time. With the prespecified parameterization of the controller it may not be possible to achieve the desired behavior of a second order model. In an equivalent formulation, given a process model, the matching controller that results as an analytical solution may be improper. Thus, if we want to eliminate as much as possible the knowledge on the process and go for an aprioric selection on the controller structure and parameterization, what actually remains is a measure of the degree of correlation that can be reduced to the extent which gives a minimal decorrelation of the reference input and the output error. This is the most general case and although zero decorrelation is not possible, the problem then becomes amenable to numerical optimization. Different algorithms can be used such as steepest- descent or Gauss-

Newton. The gradients that need to be computed can be obtained as in the IFT technique by performing special „gradient" experiments on the closed-loop. From case to case, one can select a stochastic approximation algorithm or a pure deterministic one. This idea is backed-up by the fact that the estimate of the correlation function obtained over a finite horizon is itself a random variable but depending on the length of the time horizon it gets more or less deterministic.

The same issues related to any iterative tuning procedure are also specific to CbT, namely the convergence analysis of the algorithm and the preservation of the stability of the closed-loop along the iterations which has to be checked.

Frequency-domain Tuning (**FdT**) has a similar formulation to that of IFT with general linear quadratic objective function which penalizes the output tracking error of a reference model and the control signal [29], [30], [110], [111], [113]. FdT gives a different solution to the gradient-based stochastic approximation algorithm, which resides in the computation of the estimate of the gradient of the objective function. The objective function is expressed in the frequency domain via Parseval's theorem and by using spectral analysis techniques that allow the calculation of different auto and cross-correlation sequences of the signals in the closed-loop system. Spectral estimates are obtained for the transfer functions involved in the algorithm. The derivatives of the objective function with respect to the controller parameters are thus obtained in the frequency domain. This approach is appealing since it makes use of the spectral analysis techniques and circumvents the problem of using estimated parametric models by instead using non-parametric models in the form of the frequency response functions.

The stability is ensured between iterations by calculating the Vinnicombe distance and the generalized stability margin. These quantities that are calculated here make use of the same nonparametric models that were obtained via spectral analysis. A general issue which is not taken into account for the described technique is the concern for quality estimates of the nonparametric models.

Iterative Regression Tuning (**IRT**) is another recent data-based algorithm for tuning controllers, and it is based on a computational approach [11], [12]. Similar in formulation to the IFT or VRFT approach, the idea behind this technique is to minimize a objective function which is dependent on the controller's parameters in a typical negative feedback control structure. The solution to the optimization problem however resembles with the one used in IFT. This technique uses a similar gradient descent approach to search for the set of parameters which minimize the objective function. It also assumes to be model-free in the sense that it makes no use of a process model in the tuning procedure. All the fallacies of this approach are the same as in the case of IFT since the convergence of the algorithm and the stability of the loop have to be tested. Moreover, the algorithm could stop in a local minimum instead of finding the global one.

The typical objective concerning IRT is to find the optimal parameter vector $\underline{\rho}^*$ to minimize the objective function

$$J(\underline{q}(\underline{\rho})) = \underline{w}^T \underline{q} = \sum_{i=1}^{M} w_i q_i \ , \tag{1.2.7}$$

where $\underline{w} = [w_1 \ \ldots \ w_m]^T$ is the weighting vector, $w_i \geq 0$, $i = 1...m$, are the weights, $q_i \geq 0, i = 1...m$, are the empirical CS performance indices,

$\underline{q} = [q_1 \ \ldots \ q_m]^T$, and $\underline{\rho} = [\rho_1 \ \ldots \ \rho_n]^T$ is the parameter vector containing the tuning parameters of the controller.

What is very interesting about the idea behind IRT is the aggregation in the objective function of performance indices of different nature which is quite awkward at first sight. The performance measures need only be smooth functions of the design parameters.

The problem is solved as in IFT via a gradient-based search of the minimum of the objective function and it is done by finding linear local models which express the dependency of the indices q_i on the design parameters $\underline{\rho}$. In the original approach these local models were obtain by intensively simulating on the model and this fact makes the original approach not amenable to implementation on real processes in order to extract information. However, the local linear models can also be derived by finite difference approximations by doing experiments on the real closed-loop. Accepting the fact that the estimates are affected by noise, a Robbins-Monro stochastic approximation algorithm can be employed which is the gradient-based approach but with a stochastic converge results in addition.

Simultaneous Perturbation Stochastic Approximation (**SPSA**) is based on the fact that unlike with the deterministic steepest descent, the gradient-based stochastic approximation algorithms (including IFT and SPSA) use estimated gradients of the OF

$$\underline{\rho}^{i+1} = \underline{\rho}^i - a^i est[\frac{\partial J}{\partial \underline{\rho}}(\underline{\rho}^i)] . \tag{1.2.8}$$

In IFT it is possible to calculate the gradients by using data from the real time experiments. However, when such schemes cannot be employed, according to Kiefer-Wolfovitz's Stochastic Approximation (SA) algorithm the gradients have to be estimated on the basis of the noisy measurements of the OF in terms of the calculation of finite difference approximations around the current point. Under specific conditions regarding the existence of a minimum of the OF, the differentiability with respect to the parameters, and a suitable selection of $\{a^i\}_{i\in N}$, Robbins-Monro's SA algorithm and Kiefer-Wolfowitz's SA algorithm state that the sequence of parameter vectors $\{\underline{\rho}^i\}_{i\in N}$ converges to the parameter vector $\underline{\rho}^*$ that minimizes the OF J.

The idea behind finite difference approximations is to evaluate the argument of the OF around the current iteration argument and to use next the noisy measurements to calculate the estimates of the gradient. One-sided approximations or two-sided approximations can be used with this regard. For two-sided approximations, a general estimated gradient is

$$est[\frac{\partial J}{\partial \underline{\rho}}(\underline{\rho}^i)] = \begin{bmatrix} \frac{\tilde{J}(\underline{\rho}^i + c^i \underline{\xi}_1) - \tilde{J}(\underline{\rho}^i - c^i \underline{\xi}_1)}{2c^i} \\ \ldots \\ \frac{\tilde{J}(\underline{\rho}^i + c^i \underline{\xi}_p) - \tilde{J}(\underline{\rho}^i - c^i \underline{\xi}_p)}{2c^i} \end{bmatrix}, \tag{1.2.9}$$

where $\underline{\xi}_i = \begin{bmatrix} 0 & \ldots & \overset{i-th\ position}{\overset{\downarrow}{1}} & \ldots & 0 \end{bmatrix}^T$ is a p-dimensional vector, with p – the dimension of the parameter vector, and c^i is the difference magnitude coefficient. The variables $\tilde{J}$ in (1.2.9) represent noisy measurements of the OF The sequences $\{a^i\}_{i\in N}$ and $\{c^i\}_{i\in N}$ are degrees of freedom in the FDSA algorithm. The FDSA-based estimate is biased due to the random perturbations in the parameter vector and the convergence to $\underline{\rho}^*$ is ensured for a proper choice of the sequences $\{a^i\}_{i\in N}$ and $\{c^i\}_{i\in N}$, namely:

$$a^i > 0,\ c^i > 0,\ a^i \to 0,\ c^i \to 0,$$
$$\sum_{i=0}^{\infty} a^i = \infty,\ \sum_{i=0}^{\infty} (a^i / c^i)^2 < \infty. \tag{1.2.10}$$

Another problem of this approach is the fact that $2p$ measurements of the OF are needed at each iteration, and this affects the experiment's costs. The costs increase with the number of parameters. That is the reason why SPSA reduces the costs burden by means of only two evaluations of the OF per iteration. With this regard the arguments are first randomly disturbed, and next the approximations of the gradient are calculated as follows using finite differences:

$$est[\frac{\partial J}{\partial \underline{\rho}}(\underline{\rho}^i)] = \begin{bmatrix} \frac{\tilde{J}(\underline{\rho}^i + c^i \underline{\Delta}_i) - \tilde{J}(\underline{\rho}^i - c^i \underline{\Delta}_i)}{2c^i \Delta_{i1}} \\ \ldots \\ \frac{\tilde{J}(\underline{\rho}^i + c^i \underline{\Delta}_i) - \tilde{J}(\underline{\rho}^i - c^i \underline{\Delta}_i)}{2c^i \Delta_{ip}} \end{bmatrix}, \tag{1.2.11}$$

where $\underline{\Delta}_i = [\Delta_{i1}\ \ldots\ \Delta_{ip}]^T$.

The aforementioned characteristics of the SPSA algorithm make it suitable for experiments on the real process and obviously for tuning schemes based on numerical search like in IFT.

Other two related techniques are presented as follows because of their innovative nature and because of the similarities to the previously mentioned concepts:

Iterative Learning Control (**ILC**) [202] is similar to the aforementioned techniques in the sense that it works batch-wise, between experiments, but its' purpose is not to modify some control parameters. Rather than that, it learns from previous experiments, incorporating knowledge on the previously obtained performance in order to modify the control such that the process output tracks a desired trajectory. In the simplest form, it is used to control open loop processes. However the loop can be conceptually regarded as "closed" in the iteration domain rather than in the time horizon that is specific to each experiment with the process.

ILC is designed to work in environments where the control task is repeated exactly, with a critical emphasis on the trajectory initial conditions that have to be the same every time. This approach can be viewed as a constraint but it can actually

be useful in domains such as robotics. The technique needs the capability of memorizing the past control activity in order to being able to transfer it to the next iteration. It may frequently use a process model in order to develop the learning laws and ensure the convergence to the desired performance. Thus it can not be labeled as "model-free". The algorithm is combined with feedback control structures in order to endow the ILC structures with further capabilities specific to the classical control.

Model Free Control (**MFC**) is a model-free adaptive-based approach to the process control. It does not work batch-wise as in the rest of the iterative algorithms but instead it advocates the fact that it makes no use of the process model and can solve the model reference tracking problem. MFC works in an adaptive fashion, employing a phenomenological local model that is valid for a very short period of time (typically during one sample time). For a single-input single-output process, this can be of the form

$$y^{(n)} = F + \alpha u \,, \tag{1.2.12}$$

where n is usually 1 or 2 and it represents the derivative of n-th order with respect to time, α is a constant and F is to be computed periodically from the previous relation and u, y have the usual meaning of input and output respectively. The difficulty of the problem however is the calculation of the derivative of the output with respect to time. Numerical differentiation of a function with respect to time argument is a good approximation when the sample time is small and if the function of time is smooth. When this is not the case and even more, when the noise affects the measurement, the estimate of the derivative can be extremely erroneous. Different solutions were proposed in order to circumvent this problem as, for example, the solution given in [203].

Next a PI (or PID-type) control is implemented in the form

$$u = -\frac{F}{\alpha} + \frac{y^{*(n)}}{\alpha} + K_P e + K_I \int e \,, \tag{1.2.13}$$

where y^* is the reference trajectory, $e=y-y^*$ is the output tracking error. This control gives for the closed-loop system a manifold in which the error e goes to zero if appropriate choices are made for the parameters in the control law.

MFC shows a great potential especially when dealing with nonlinear systems. However, there is no systematic technique to choose the local model parameters, and when it comes to ensuring the stability of the control system the difficulties that are specific to adaptive systems arise.

This thesis is structured in six chapters (with Introduction and Conclusions) and two appendices. Some details on these chapters and appendices are given as follows.

Chapter 2 is a comprehensive study of Iterative Feedback Tuning. A general presentation of the tuning scheme is attempted for one- and two-degree-of-freedom controllers (1-DOF and 2-DOF). For the 2-DOF control structure, two subsequent situations are detailed for both simultaneous and separate parameter tuning. General aspects concerning the reference model selection, the search direction of the searching algorithm and issues related to the convergence of the algorithm to the solution, are presented. Subchapters 9 and 10 are dedicated to the translation of IFT to multiple-input multiple-output (MIMO) systems. Ideas on how to reduce the number of experiments at each iteration are suggested, and they are important due to the rapidly increasing number of parameters in MIMO controllers.

An original tuning scheme using IFT is next presented on a setup using state feedback control. The scheme shows to be effective for pole-placement-based solutions that need retuning either because of process aging or due to the large differences between the model and the real process. A solution to the search algorithm convergence is proposed in terms of Popov's hyperstability analysis theory. The results are validated on laboratory equipment represented by a modular servo system. These results are the subject of the 11th subchapter.

Using the same structure with state-feedback control, the approach is translated to optimal control systems. The Linear Quadratic Regulator (LQR) and the Linear Quadratic Gaussian (LQG) control problems can be casted into optimization problems that are amenable for tuning via IFT. The optimality of the model-based paradigm in the design of optimal control systems is discussed in the light of the discrepancies between the process model and reality. In order to benefit from the guaranteed robustness properties of the LQR-based designed CSs, tuning via IFT is attempted. The case studies show some important facts: The optimal solution can be reached when we start from near a vicinity of the solution even if the process model is poor. Also, the optimal solution can be reached from an initial pole-placement solution which by its nature does not guarantee good robustness properties for the state-feedback structure. Thirdly, the inherent noise that affects the experimental-based tuning is shown to weaken the robustness of the CS but not to a substantial degree. The novel tuning scheme is also validated on laboratory equipment with a servo system. All the aforementioned subjects form the 12th subchapter.

Subchapter 13 deals with the stability issue between the iterations of the IFT. The solution makes use of a coprime factor uncertainty representation for the controller subject to tuning, and the small gain theorem for linear time-invariant (LTI) discrete-time systems is applied with this regard. Bounds on the gain of the systems involved in the stability analysis are found from nonparametric models in frequency domain, which are typically easier to obtain than the parametric models. The frequency response functions can be obtained either via empirical transfer function estimate (ETFE) or by spectral correlation-based analysis (SPA). The results are supported by a simulation case study. The ideas can be considered to enlarge the overview of the iterative schemes and can render the approach into a suitable tool for maintaining the stability throughout the iterations. Several other techniques fall within the incidence of this approach, such as IRT, SPSA or CbT.

Chapter 3 is dedicated to the VRFT used as a tool in CSs design. VRFT and IFT can be viewed as counterparts of a complete tool aimed at CS design and fine tuning. For a proper formulation of the design objective (i.e., the objective function formulation), VRFT and IFT have an identical purpose. Benefiting from the flexibility of IFT which consists in the possibility of modifying the objective function along the iterations, different aims can be targeted such as control effort penalty or translation to control error penalty, and finally all the signals being weighted in time (or frequency domain) by using flexible filters.

The formulation of VRFT makes it suitable for the design of low complexity controllers such as the ones that predominate in industry. They have a major advantage which is also the key point of the VRFT algorithm: the linear parameterization of the controller. Using a linear parameterization, the combination with IFT can be shown to be very effective in terms of obtaining estimates of the Hessian of the objective function, which is the major contribution of the chapter. This in turn can speed up the convergence of the algorithm since the use of the estimate of the Hessian is recommended when close to the solution. The idea is

backed-up by simulations and real-time experiments on both angular velocity and angular position control for a laboratory servo system.

Chapter 4 introduces two additional techniques that can be used in the CS tuning. Since their development, IRT and SPSA were seen as more "computational approach" tools rather than suitable for experiment-based tuning. The major contribution of this chapter is that it indicates different possibilities of adapting these schemes to efficient practical real-time application. The substantial advantages of the iterative schemes presented in this thesis are pinpointed again in this context since they represent more than sensitivity-based tuning schemes. They also hold a stochastic convergence results which is a crucial development that is necessary whenever we talk about real-time processes inherently affected by measurement noise. Concluding, these techniques are situated on the increasingly blurred border between the metaheuristic approach in optimization and the data-based approach.

IRT is translated to a real-process implementation for a servo system position control and is shown to be efficient.

In the same setting as for the IFT and the LQG-based tuning for the process plus Kalman filter, the SPSA is also employed with results comparable in terms of efficiency with IFT. The tuning setup is novel since it is designed entirely in the state-space formulation for the ensemble formed by the process dynamics and the Kalman filter dynamics. The results allow for a thorough comparison between the two techniques.

Chapter 5 is devoted to studying the possible improvements that can arise from the mixing of fuzzy control with IFT. The main contribution of this chapter is a three-step stable design technique for fuzzy control systems (FCSs) with Takagi-Sugeno PI fuzzy controllers (TS-PI-FCs). This new technique is based on the combination of IFT and fuzzy control, and it aims discrete-time input affine Single Input-Single Output (SISO) processes. Starting with a poor process model and using a linear controller, the CS performance can be improved in two additional steps. The first step concerns the IFT, and the second step is related to the use of fuzzy control.

Chapter 6 reiterates the contributions of this thesis both generally and punctually. It also suggests future research directions and how the results of this thesis were disseminated.

Appendix A serves the subchapter 2.12, and it concerns the illustration of the objectives that pursued in a LQR based problem where all state variables are available to measurements, and they are therefore subject to measurement noise. The three objectives are the minimization of the state energy, the minimization of the control effort and the minimization of the energy transfer from the process noise to the state variables.

Appendix B presents the proof of Theorem 5.1 in Chapter 5 dedicated to the globally asymptotically stability of the equilibrium point at the origin of the fuzzy control system.

The new contributions of the current thesis are developed on two directions, 1) and 2), pointed out as follows.

1) Combination of the different techniques with other control structures:

- IFT in tandem with state-feedback control design via pole-placement is analyzed in Chapter 2. The main new contribution is a direct state-space formulation of IFT gradient experiments. The results were published in:

  ***Rădac, M.-B.**, Precup, R.-E., Preitl, St., Petriu, E. M., Dragoş, C.-A., Paul, A. S. and Kilyeni, St. (2009): Signal Processing Aspects in State Feedback Control Based on Iterative Feedback Tuning. Proceedings of 2nd International Conference on Human System Interaction HSI'09, Catania, Italy, pp. 40-45, indexed in* **ISI Proceedings**.

  ***Rădac, M.-B.**, Precup, R.-E., Petriu, E. M., Preitl, St. and Dragoş, C.-A. (2009): Iterative Feedback Tuning Approach to a Class of State Feedback-Controlled Servo Systems. Proceedings of 6th International Conference on Informatics in Control, Automation and Robotics ICINCO 2009, Milan, Italy, vol. 1 Intelligent Control Systems and Optimization, pp. 41-48, indexed in* **ISI Proceedings**.

  ***Rădac, M.-B.**, Precup, R.-E., Petriu, E. M., Preitl, St. and Dragoş, C.-A. (2011): Convergent Iterative Feedback Tuning of State Feedback-Controlled Servo Systems. In: Informatics in Control Automation and Robotics, Eds. Andrade Cetto, J., Filipe, J. and Ferrier, J.-L. (Springer-Verlag), pp. 99-111, indexed in* **SCOPUS**.

- IFT and state-feedback optimal control has been tackled in Chapter 2. The new contribution is a thorough study regarding the tuning for LQR/LQG problems in case of poor model available. The results are not yet published, but they belong to a journal paper which is in the review process.

- IFT in combination with fuzzy control systems are the subject of Chapter 5. The results were published in:

  *Precup, R.-E., **Rădac, M.-B.**, Preitl, St., Tomescu, M.-L., Petriu, E. M. and Paul, A. S. (2009): IFT-based PI-fuzzy Controllers: Signal Processing and Implementation. Proceedings of 6th International Conference on Informatics in Control, Automation and Robotics ICINCO 2009, Milan, Italy, vol. 1 Intelligent Control Systems and Optimization, pp. 207-212, indexed in* **ISI Proceedings**.

  *Precup, R.-E., **Rădac, M.-B.**, Preitl, St., Petriu, E. M. and Dragoş, C.-A. (2009): Iterative Feedback Tuning in Linear and Fuzzy Control Systems. In: Towards Intelligent Engineering and Information Technology, Eds. Rudas, I. J., Fodor, J. and Kacprzyk, J. (Springer-Verlag), pp. 179-192, indexed in* **SCOPUS**.

- The combination of IFT and VRFT is carried out in Chapter 3. The results were published in:

  ***Rădac, M.-B.**, Grad, R.-B., Precup, R.-E., Preitl, St., Dragoş, C.-A., Petriu, E. M. and Kilyeni, A. (2011): Mixed Virtual Reference Feedback Tuning - Iterative Feedback Tuning Approach to the Position Control of a Laboratory Servo System. Proceedings of International Conference on Computer as a Tool EUROCON 2011, Lisbon, Portugal, paper index 453, 4 pp., indexed in* **INSPEC**.

  ***Rădac, M.-B.**, Grad. R.-B., Precup, R.-E., Petriu, E. M., Preitl, St. and Dragoş, C.-A. (2011): Mixed Virtual Reference Feedback Tuning – Iterative Feedback Tuning: Method and Laboratory Assessment. Proceedings of 20th*

IEEE International Symposium on Industrial Electronics ISIE 2011, Gdansk, Poland, pp. 649-654, indexed in **INSPEC**.

2) Improvements of the different techniques in both theoretical and practical implementation aspects together with validation on laboratory equipment:

- IFT's convergence is studied in the Chapter 2 and the results were published in

  ***Rădac, M.-B.**, Precup, R.-E., Petriu, E. M., Preitl, St. and Dragoş, C.-A. (2011): Convergent Iterative Feedback Tuning of State Feedback-Controlled Servo Systems. In: Informatics in Control Automation and Robotics, Eds. Andrade Cetto, J., Filipe, J. and Ferrier, J.-L. (Springer-Verlag), pp. 99-111, indexed in* **SCOPUS**.

- Stability of IFT throughout the iterations is also discussed in Chapter 2 and the results were published in:

  ***Rădac, M.-B.**, Precup, R.-E., Petriu, E. M., Preitl, St. and David, R.-C. (2011): Stable Iterative Feedback Tuning Method for Servo Systems. Proceedings of 20th IEEE International Symposium on Industrial Electronics ISIE 2011, Gdansk, Poland, pp. 1943-1948, indexed in* **INSPEC**.

- Experimental validations of IFT, VRFT, IRT, ILC on laboratory equipment are highlithted in:

  ***Rădac, M.-B.**, Precup, R.-E., Preitl, St., Tar, J. K., Fodor, J. and Petriu, E. M. (2008): Gain-Scheduling and Iterative Feedback Tuning of PI Controllers for Longitudinal Slip Control. Proceedings of 6th IEEE International Conference on Computational Cybernetics ICCC 2008, Stara Lesna, Slovakia, pp. 183-188, indexed in* **SCOPUS, INSPEC**.

  *Precup, R.-E., Moşincat, I., **Rădac, M.-B.**, Preitl, St., Kilyeni, St., Petriu, E. M. and Dragoş, C.-A. (2010): Experiments in Iterative Feedback Tuning for Level Control of Three-Tank System. Proceedings of 15th IEEE Mediterranean Electromechanical Conference MELECON 2010, Valletta, Malta, pp. 564-569, indexed in* **ISI Proceedings**.

  *Precup, R.-E., Borchescu, C., **Rădac, M.-B.**, Preitl, St., Dragoş, C.-A., Petriu, E. M. and Tar, J. K. (2010): Implementation and Signal Processing Aspects of Iterative Regression Tuning. Proceedings of 2010 IEEE International Symposium on Industrial Electronics ISIE 2010, Bari, Italy, pp. 1657-1662, indexed in* **SCOPUS, INSPEC**.

A list of the papers that provide new contributions of the current thesis is presented as follows:

1. ***Rădac, M.-B.**, Precup, R.-E., Preitl, St., Tar, J. K., Fodor, J. and Petriu, E. M. (2008): Gain-Scheduling and Iterative Feedback Tuning of PI Controllers for Longitudinal Slip Control. Proceedings of 6th IEEE International Conference on Computational Cybernetics ICCC 2008, Stara Lesna, Slovakia, pp. 183-188, indexed in* **SCOPUS, INSPEC**.

2. ***Rădac, M.-B.**, Precup, R.-E., Preitl, St., Petriu, E. M., Dragoş, C.-A., Paul, A. S. and Kilyeni, St. (2009): Signal Processing Aspects in State Feedback Control Based on Iterative Feedback Tuning. Proceedings of 2nd International Conference on Human System Interaction HSI'09, Catania, Italy, pp. 40-45, indexed in* **ISI Proceedings**.

3. *Precup, R.-E., **Rădac, M.-B.**, Preitl, St., Tomescu, M.-L., Petriu, E. M. and Paul, A. S. (2009): IFT-based PI-fuzzy Controllers: Signal Processing and Implementation. Proceedings of 6th International Conference on Informatics in Control, Automation and Robotics ICINCO 2009, Milan, Italy, vol. 1 Intelligent Control Systems and Optimization, pp. 207-212, indexed in* **ISI Proceedings**.

4. ***Rădac, M.-B.**, Precup, R.-E., Petriu, E. M., Preitl, St. and Dragoş, C.-A. (2009): Iterative Feedback Tuning Approach to a Class of State Feedback-Controlled Servo Systems. Proceedings of 6th International Conference on Informatics in Control, Automation and Robotics ICINCO 2009, Milan, Italy, vol. 1 Intelligent Control Systems and Optimization, pp. 41-48, indexed in* **ISI Proceedings**.

5. ***Rădac, M.-B.**, Precup, R.-E., Preitl, St., Tar, J. K. and Burnham, K. J. (2009): Tire Slip Fuzzy Control of a Laboratory Anti-lock Braking System. Proceedings of the European Control Conference 2009 ECC'09, Budapest, Hungary, pp. 940-945.*

6. *Precup, R.-E., Gavriluţă, C., **Rădac, M.-B.**, Preitl, St., Dragoş, C.-A., Tar, J. K. and Petriu, E. M. (2009): Iterative Learning Control Experimental Results for Inverted Pendulum Crane Mode Control. Proceedings of 7th International Symposium on Intelligent Systems and Informatics SISY 2009, Subotica, Serbia, pp. 323-328, indexed in* **ISI Proceedings**.

7. ***Rădac, M.-B.**, Precup, R.-E., Preitl, St. and Dragoş, C.-A. (2009): Iterative Feedback Tuning in MIMO Systems. Signal Processing and Application. Proceedings of 5th International Symposium on Applied Computational Intelligence and Informatics SACI 2009, Timişoara, Romania, pp. 77-82, indexed in* **ISI Proceedings**.

8. *Precup, R.-E., Moşincat, I., **Rădac, M.-B.**, Preitl, St., Kilyeni, St., Petriu, E. M. and Dragoş, C.-A. (2010): Experiments in Iterative Feedback Tuning for Level Control of Three-Tank System. Proceedings of 15th IEEE Mediterranean Electromechanical Conference MELECON 2010, Valletta, Malta, pp. 564-569, indexed in* **ISI Proceedings**.

9. *Precup, R.-E., Borchescu, C., **Rădac, M.-B.**, Preitl, St., Dragoş, C.-A., Petriu, E. M. and Tar, J. K. (2010): Implementation and Signal Processing Aspects of Iterative Regression Tuning. Proceedings of 2010 IEEE International Symposium on Industrial Electronics ISIE 2010, Bari, Italy, pp. 1657-1662, indexed in* **SCOPUS, INSPEC**.

10. *Precup, R.-E., **Rădac, M.-B.**, Preitl, St., Petriu, E. M. and Dragoş, C.-A. (2009): Iterative Feedback Tuning in Linear and Fuzzy Control Systems. In: Towards Intelligent Engineering and Information Technology, Eds. Rudas, I. J., Fodor, J. and Kacprzyk, J. (Springer-Verlag), pp. 179-192, indexed in* **SCOPUS**.

11. *Precup, R.-E., Preitl, St., **Rădac, M.-B.**, Petriu, E. M., Dragoş, C.-A. and Tar, J. K. (online first, Date of Publication: 03 August 2010): Experiment-based teaching in advanced control engineering. IEEE Transactions on Education, vol. PP, no. 99, pp. 1-11, DOI: 10.1109/TE.2010.2058575, **ISI** Science Citation Index impact factor (in 2009) = 1.157.*

12. ***Rădac, M.-B.**, Precup, R.-E., Petriu, E. M., Preitl, St. and Dragoş, C.-A. (2011): Convergent Iterative Feedback Tuning of State Feedback-Controlled Servo Systems. In: Informatics in Control Automation and Robotics, Eds. Andrade Cetto, J., Filipe, J. and Ferrier, J.-L. (Springer-Verlag), pp. 99-111, indexed in* **SCOPUS**.

13. ***Rădac, M.-B.**, Grad, R.-B., Precup, R.-E., Preitl, St., Dragoş, C.-A., Petriu, E. M. and Kilyeni, A. (2011): Mixed Virtual Reference Feedback Tuning - Iterative*

Feedback Tuning Approach to the Position Control of a Laboratory Servo System. Proceedings of International Conference on Computer as a Tool EUROCON 2011, Lisbon, Portugal, paper index 453, 4 pp., indexed in **INSPEC**.

14. ***Rădac, M.-B.****, Grad. R.-B., Precup, R.-E., Petriu, E. M., Preitl, St. and Dragoş, C.-A. (2011): Mixed Virtual Reference Feedback Tuning – Iterative Feedback Tuning: Method and Laboratory Assessment. Proceedings of 20th IEEE International Symposium on Industrial Electronics ISIE 2011, Gdansk, Poland, pp. 649-654, indexed in* **INSPEC**.

15. ***Rădac, M.-B.****, Precup, R.-E., Petriu, E. M., Preitl, St. and David, R.-C. (2011): Stable Iterative Feedback Tuning Method for Servo Systems. Proceedings of 20th IEEE International Symposium on Industrial Electronics ISIE 2011, Gdansk, Poland, pp. 1943-1948, indexed in* **INSPEC**.

Concluding, the new contributions of this thesis belong to the results published in 15 papers. The author of this thesis is the first author of 10 of these papers. All papers are classified as follows as function of their indexing and visibility:

- one paper published in an ISI journal with impact factor (IEEE Transactions on Education),
- six papers published in the volumes of academic conferences indexed in ISI Proceedings,
- five papers published in the volumes of academic conferences indexed in the international databases SCOPUS and/or INSPEC,
- two book chapters published in Springer-Verlag and indexed in SCOPUS as well.

All papers are visible, and this is proved by the organizing societies, IEEE (for ten papers), IFAC (for two papers) and EUCA (for one paper, published at European Control Conference ECC'09), and by Springer-Verlag (for the two book chapters). It is also highlighted that 14 out of the 15 papers are published abroad.

2. Iterative Feedback Tuning (IFT)

2.1. Introduction to Iterative Feedback Tuning

Iterative Feedback Tuning (IFT) is a data-based technique that tunes the controller parameters iteratively along the gradient direction of a given objective function and it is applicable when an initial stabilizing controller is given in advance [1]. Variations between IFT algorithms are introduced by the choice of the objective function, as well as by the adopted structure of the controller.

The control design via IFT is carried out in the discrete time domain. The designer selects the controller's structure and complexity, which means that the controller is available in analytical form. The parameterization should be such that the transfer function of the controller is differentiable with respect to its parameters.

In this theoretical part, first the case of one-degree-of-freedom, and then the case of two-degree-of-freedom controllers will be discussed.

The next set of controller parameters are obtained by using a Gauss-Newton scheme:

$$\underline{\rho}^{i+1} = \underline{\rho}^{i} - \gamma_i (\underline{R}^{i})^{-1} est\left[\frac{\partial J}{\partial \underline{\rho}}(\underline{\rho}^{i})\right], \tag{2.1.1}$$

where $i \in N$ is the iteration number, γ_i is a positive real number which determines the step size of the current iteration, and $\underline{R}^i$ is a positive definite matrix typically chosen equal to an estimate of the Hessian of J.

A separate subchapter is dedicated to the presentation of some options on how to choose the matrix $\underline{R}$. Subchapter *2.6. Search direction* presents aspects concerning three techniques to obtain the matrix $\underline{R}$.

2.2. Criterion minimization

A separate paragraph has been dedicated to the issue of minimization of the objective function, because $J(\underline{\rho})$ can be chosen of different structure.

For example in [1], for the two-mass-spring system with friction, two objective functions were chosen, a different one for each controller. In [4], for the comparison a of PID controller parameters obtained with IFT and with classical tuning rules, a particular form of the objective function from [16] was used, viz. the control weight was considered to be null.

For the case studies presented in this work the following quadratic criterion was implemented. The form of the objective function is the one suggested in [14] and [16]

$$J(\underline{\rho}) = \frac{1}{2N} E\{ \sum_{k=1}^{N} \left\{ \left[L_y(q^{-1})\delta y(k,\underline{\rho}) \right]^2 + \lambda \left[L_u(q^{-1})u(k,\underline{\rho}) \right]^2 \right\} \}, \qquad (2.2.1)$$

where $L_y(q^{-1})$ and $L_u(q^{-1})$ are frequency dependent weightings that penalize the output difference δy and the control input u according to the designer's needs. The expectation $E\{.\}$ is taken with respect to the stochastic disturbances that enter the process and thus affect the closed-loop. The objective of IFT is to determine the optimal set of parameters $\underline{\rho}^*$ which minimizes the objective function [3]

$$\underline{\rho}^* = \arg\min_{\underline{\rho}} J(\underline{\rho}). \qquad (2.2.2)$$

The major stumbling block for the solution of this optimal control problem is the computation of the gradient of the objective function with respect to the controller parameters [16]. The gradient of the objective function is

$$\frac{\partial J}{\partial \underline{\rho}}(\underline{\rho}) = \frac{1}{N} \sum_{k=1}^{N} \left[L_y(q^{-1})\delta y \frac{\partial \delta y}{\partial \underline{\rho}}(k;\underline{\rho}) + \lambda L_y(q^{-1})u \frac{\partial u}{\partial \underline{\rho}}(k;\underline{\rho}) \right]. \qquad (2.2.3)$$

The necessary condition for optimality is

$$\frac{\partial J}{\partial \underline{\rho}}(\underline{\rho})\Big|_{\underline{\rho}=\underline{\rho}^*} = \underline{0}. \qquad (2.2.4)$$

To solve equation (2.2.4) for $\underline{\rho}^*$, one has to know how the signals δy and u are related to $\underline{\rho}$ and one has to be able to compute the gradients of these signals in respect with $\underline{\rho}$. The process is supposed to contain unknown dynamics, therefore the required analytical form relations cannot be established.

The main contribution of IFT is that it offers a technique to calculate the gradient $\frac{\partial J}{\partial \underline{\rho}}(\underline{\rho})$ directly from the closed-loop system. According to (2.2.3) the required data are the signals δy and u and the gradients of these signals, $\frac{\partial \delta y}{\partial \underline{\rho}}(\underline{\rho})$ and $\frac{\partial u}{\partial \underline{\rho}}(\underline{\rho})$. δy and u can be obtained by direct measurements, while the gradients are obtained from the closed – loop system.

After computing the unbiased estimates of the gradients $\frac{\partial \delta y}{\partial \underline{\rho}}(\underline{\rho})$ and $\frac{\partial u}{\partial \underline{\rho}}(\underline{\rho})$, one can calculate the estimate of the gradient of the OF $est\left[\frac{\partial J}{\partial \underline{\rho}}(\underline{\rho}) \right]$

$$est\left[\frac{\partial J}{\partial \underline{\rho}}(\underline{\rho}) \right] = \frac{1}{N} \sum_{k=1}^{N} \left[L_y(q^{-1})\delta y(k) \cdot est\left[\frac{\partial \delta y}{\partial \rho}(k;\underline{\rho}) \right] + \lambda L_y(q^{-1})u(k) \cdot est\left[\frac{\partial u}{\partial \rho}(k;\underline{\rho}) \right] \right]. \qquad (2.2.5)$$

The methodology to obtain the gradient of the objective function is the same no matter which other quadratic criterion is used. Therefore the particular cases of the objective function presented above will not be detailed anymore.

The methodology to obtain the gradients of the signals y and u or δy and u will be presented in the following next sections for different controller structures.

2.3. Design criterion for one-degree-of-freedom controllers

Considering the structure with a one-degree-of-freedom controller given in Fig. 2.3.1, the signals in the closed-loop system are all dependent on the actual controller tuning, which is explicitly indicated by using the $\underline{\rho}$ argument.

IFT is a technique based on several experiments; therefore we consider each experiment of finite length. Then the reference input is $\{r(k)\}_{k=1,\dots,N}$; the argument k abbreviates the sampling period T_s.

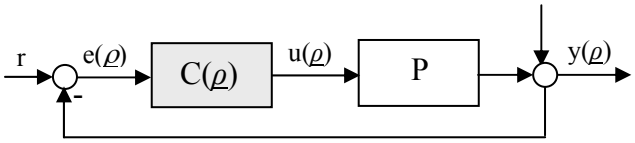

Fig. 2.3.1. Block diagram of the closed loop system with one-degree-of-freedom controller.

$P(q^{-1})$ is a SISO process and $C(q^{-1},\underline{\rho})$ is a feedback controller suitably parameterized by some parameter vector $\underline{\rho}=[\rho_0\ \rho_1\ \dots\ \rho_n\ ]^T$.

Let $S(q^{-1},\underline{\rho})$ denote the achieved sensitivity function and $T(q^{-1},\underline{\rho})$ the complementary sensitivity function, respectively:

$$S(q^{-1},\underline{\rho}) = \frac{1}{1+P(q^{-1})C(q^{-1},\underline{\rho})}, \qquad (2.3.1.a)$$

$$T(q^{-1},\underline{\rho}) = 1 - S(q^{-1},\underline{\rho}) = \frac{P(q^{-1})C(q^{-1},\underline{\rho})}{1+P(q^{-1})C(q^{-1},\underline{\rho})}. \qquad (2.3.1.b)$$

Let $y_d(k)$ be the desired output response to the reference $r(k)$ generated by a reference model selected by the designer. The system with the tuned controller is desired to give a response very close to the response of the reference model (Fig. 2.3.2).

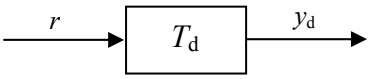

Fig. 2.3.2. Block diagram of the reference model.

The difference between the achieved and the desired response is an output error:

$$\delta y(k,\underline{\rho}) = y(k,\underline{\rho}) - y_d(k). \qquad (2.3.2)$$

By virtue of Fig. 2.3.1 one can establish the following relations:

$$y(k,\underline{\rho}) = T(k,\underline{\rho})r(k) + S(k,\underline{\rho})v(k), \qquad (2.3.3.a)$$

$$u(k,\underline{\rho}) = C(k,\underline{\rho})S(k,\underline{\rho})(r(k) - v(k)). \qquad (2.3.3.b)$$

The analytical expressions of the gradients of δy and u are obtained using relations (2.3.1.a,b), (2.3.2) and (2.3.3.a,b):

$$\frac{\partial \delta y}{\partial \underline{\rho}}(k,\underline{\rho}) \underset{(2.8)}{=} \frac{\partial y}{\partial \underline{\rho}}(k,\underline{\rho}) \Leftarrow \frac{\partial y_d}{\partial \underline{\rho}}(k,\underline{\rho}) = \underline{0}$$

$$\frac{\partial y}{\partial \underline{\rho}}(k,\underline{\rho}) \underset{(2.9a)}{=} \frac{\partial T}{\partial \underline{\rho}}(q^{-1},\underline{\rho})\cdot r(k) + \frac{\partial S}{\partial \underline{\rho}}(q^{-1},\underline{\rho})\cdot v(k),$$

$$\frac{\partial y}{\partial \underline{\rho}}(k,\underline{\rho}) = \frac{\partial C}{\partial \underline{\rho}}(q^{-1},\underline{\rho})\frac{T(q^{-1},\underline{\rho})}{C(q^{-1},\underline{\rho})}(r(k)-y(k)), \qquad (2.3.4.a)$$

$$\frac{\partial u}{\partial \underline{\rho}}(k,\underline{\rho}) \underset{(2.9b)}{=} \left(\frac{\partial C}{\partial \underline{\rho}}(q^{-1},\underline{\rho})\cdot S(q^{-1},\underline{\rho}) + C(q^{-1},\underline{\rho})\frac{\partial S}{\partial \rho}(q^{-1},\underline{\rho})\right)\cdot(r(k)-v(k)),$$

$$\frac{\partial u}{\partial \rho}(k,\rho) = \frac{\partial C}{\partial \rho}(q^{-1},\rho)\cdot S(q^{-1},\rho)\cdot(r(k)-y(k)). \qquad (2.3.4.b)$$

The gradient of the controller, $\frac{\partial C}{\partial \underline{\rho}}(q^{-1},\underline{\rho})$, can be determined in analytical form using the known expression for the discrete controller, $\partial C(q^{-1},\underline{\rho}).\frac{\partial C}{\partial \underline{\rho}}(q^{-1},\underline{\rho})$ is a vector with one column, with as many rows as the number of the controller's parameters:

$$\frac{\partial C}{\partial \underline{\rho}}(q^{-1},\underline{\rho}) = \left[\frac{\partial C}{\partial \rho_0}(q^{-1},\underline{\rho}); \frac{\partial C}{\partial \rho_1}(q^{-1},\underline{\rho}); \ldots; \frac{\partial C}{\partial \rho_n}(q^{-1},\underline{\rho})\right]. \qquad (2.3.5)$$

By assumption, all derivatives in (2.3.5) exist.

Without knowing the model of the process, it is obvious that we cannot calculate the gradients of δy and u, based on the analytical relations (2.3.4.a,b). The formulation of IFT in the case of one-degree-of-freedom controllers needs two experiments in order to compute the next set of controller parameters. The experiments are described in Table 2.3.1.

Table 2.3.1. *Experimental procedure*

Experiment	**(1) "normal"**	**(2) "gradient"**
Reference Input	$r_1(k)=r(k)$	$r_1(k)=r(k)-y_1(k,\rho)$
Measurements	$u_1=C(q^{-1},\underline{\rho})S(q^{-1},\underline{\rho})(r_1(k)-v_1(k))$ $y_1=T(q^{-1},\underline{\rho})r_1(k)+S(q^{-1},\underline{\rho})v_1(k)$	$u_2=C(q^{-1},\underline{\rho})S(q^{-1},\underline{\rho})(r_2(k)-v_1(k))$ $y_2=T(q^{-1},\underline{\rho})r_2(k)+S(q^{-1},\underline{\rho})v_2(k)$

The first experiment is also known as the *normal experiment*. In this first experiment the desired reference signal r is applied. During the first experiment the control signal u_1 the system output y_1 and the control error e are measured.

The second experiment is called the *gradient experiment.* The reference signal to the second experiment is the control error of the first experiment ($e=r-y_1$). During this experiment, the output signal y_2 and the control signal u_2 are measured.

The obtained measurements form the two experiments can be used to estimate the derivatives $\frac{\partial \delta y}{\partial \underline{\rho}}(k,\underline{\rho}) and \frac{\partial u}{\partial \underline{\rho}}(k,\underline{\rho})$:

$$est\left[\frac{\partial y}{\partial \underline{\rho}}(k,\underline{\rho})\right] \underset{(2.3.4a)}{=} \frac{1}{C(q^{-1},\underline{\rho})}\frac{\partial C}{\partial \underline{\rho}}(q^{-1},\underline{\rho})\cdot y_2(k,\underline{\rho}), \qquad (2.3.6.a)$$

$$est\left[\frac{\partial u}{\partial \underline{\rho}}(k,\underline{\rho})\right] \underset{(2.3.4b)}{=} \frac{1}{C(q^{-1},\underline{\rho})}\frac{\partial C}{\partial \rho}(q^{-1},\underline{\rho})\cdot u_2(k,\underline{\rho}). \qquad (2.3.6.b)$$

The disturbances in experiment one and two, v_1 and v_2, respectively, are assumed to be of zero mean and mutually uncorrelated. Under this assumption, the given gradient estimate is unbiased.

2.4. Design criterion for two-degree-of-freedom controllers

Many structures of two-degree-of-freedom controllers are reported in the literature. For example, four structures of two degrees of freedom are presented in [6], with emphasis on the best implementation for dead-time compensation, and a different structure is presented in [4] to aim the achievement of a fast response to set-point changes.

There are several possibilities to apply IFT to different controller structures. In this study, two structures were considered. The first structure of two-degree-of-freedom controller is the one presented in [4] and the second structure is the one suggested in [1]. In the following two subparagraphs the methodology of applying algorithm to these structures is presented in terms of two approaches. The two approaches differ considerably because the controller parameters are tuned differently. The first approach tunes the parameters of the feedback and the feedforward controller simultaneously and the second approach tunes them separately; first the feedback controller parameters and then the feedforward controller parameters.

2.4.1. Simultaneous parameter tuning

The structure for simultaneous parameter tuning, illustrated in Fig. 2.4.1.1, is the one proposed in the first relevant work related to IFT [14], then further developed by the same authors in 1998 [16] and later found in [27].

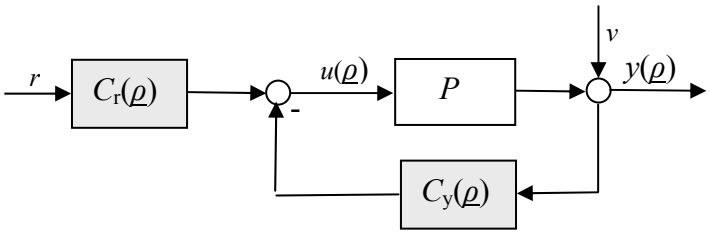

Fig. 2.4.1.1. Block diagram of a two-degree of freedom controller.

In regard with Fig. 2.4.1.1 one can write the following process model:

$$y(k) = Pu(k)+v(k), \quad (2.4.1.1)$$

where $v(k)$ is a stochastic disturbance. This system will be controlled by a two-degree-of-freedom controller, therefore the control signal has the expression

$$u(k) = C_r(\underline{\rho})r(k)- C_y(\underline{\rho})v(k). \quad (2.4.1.2)$$

The controller is operating on the process is $C(\underline{\rho}) = \{C_r(\underline{\rho}), C_y(\underline{\rho})\}$. $C_r(\underline{\rho})$ and $C_y(\underline{\rho})$ are linear time-invariant transfer functions parameterized by a vector parameter $\underline{\rho} \in R^{n_p}$. In [16] it is stated that it is possible for the two controllers to have common parameters.

The desired model is described by Fig. 2.3.2 as in the case of one-degree-of-freedom controllers. The criterion minimization needs to compute the output error

$$\delta y = y(\underline{\rho}) - y_d , \quad (2.4.1.3)$$

$$\delta y = \left(\frac{C_r(\underline{\rho})P}{1+C_y(\underline{\rho})P} - T_d \right) r + \frac{1}{1+C_y(\underline{\rho})P} v . \quad (2.4.1.4)$$

This error consists of a contribution due to incorrect tracking of the reference input r and an error due to the disturbance.

From Fig. 2.4.1.1 one can write the sensitivity function and the complementary sensitivity function.

$$T(\underline{\rho}) = \frac{C_r(\underline{\rho})P}{1+C_y(\underline{\rho})P} , \quad (2.4.1.5.a)$$

$$S(\underline{\rho}) = \frac{1}{1+C_y(\underline{\rho})P} . \quad (2.4.1.5.b)$$

What is interesting to find out for this case is again the estimate of the gradient of the output signal and the estimate of the gradient of the control signal. First it is necessary to note that $\frac{\partial \delta y}{\partial \underline{\rho}}(\underline{\rho}) = \frac{\partial y}{\partial \underline{\rho}}(\underline{\rho})$:

$$\frac{\partial y}{\partial \underline{\rho}}(\underline{\rho}) = \frac{P}{1+C_y(\underline{\rho})P}\frac{\partial C_r}{\partial \underline{\rho}}(\underline{\rho})r - \frac{C_r(\underline{\rho})P^2}{1+C_y(\underline{\rho})P}\frac{\partial C_r}{\partial \underline{\rho}}(\underline{\rho})r - \frac{P}{(1+C_y(\underline{\rho})P)^2}\frac{\partial C_y}{\partial \underline{\rho}}(\underline{\rho})v$$

$$\frac{\partial y}{\partial \underline{\rho}}(\underline{\rho}) = \frac{1}{C_r(\underline{\rho})}\frac{\partial C_r}{\partial \underline{\rho}}(\underline{\rho})T(\underline{\rho})r - \frac{1}{C_r(\underline{\rho})}\frac{\partial C_y}{\partial \underline{\rho}}(\underline{\rho})\left[T^2(\underline{\rho})r + T(\underline{\rho})S(\underline{\rho})v\right].$$

Considering that $\left[T^2(\underline{\rho})r + T(\underline{\rho})S(\underline{\rho})v\right] = T(\underline{\rho})y$, the new result is

$$\frac{\partial y}{\partial \underline{\rho}}(\underline{\rho}) = \frac{1}{C_r(\underline{\rho})}\frac{\partial C_r}{\partial \underline{\rho}}(\underline{\rho})T(\underline{\rho})r - \frac{1}{C_r(\underline{\rho})}\frac{\partial C_y}{\partial \underline{\rho}}(\underline{\rho})T(\underline{\rho})y . \quad (2.4.1.6)$$

The second term can be obtained by using the output signal from one experiment as a reference signal to another experiment. This means that for each of the iterations three experiments are needed.

The gradient of the output can be estimated in the following way:

$$est\frac{\partial y}{\partial \underline{\rho}}(\underline{\rho}) = \frac{1}{C_r(\underline{\rho})}\frac{\partial C_r}{\partial \underline{\rho}}(\underline{\rho})y_3 - \frac{1}{C_r(\underline{\rho})}\frac{\partial C_y}{\partial \underline{\rho}}(\underline{\rho})y_2 . \quad (2.4.1.7)$$

The next step is to obtain an estimate of the gradient of the control signal. The control signal can be written as:

$$u = \frac{C_r(\underline{\rho})}{1+C_y(\underline{\rho})P} r - \frac{C_y(\underline{\rho})}{1+C_y(\underline{\rho})P} v = S(\underline{\rho})\left[C_r(\underline{\rho})r - C_y(\underline{\rho})v\right]. \quad (2.4.1.8)$$

Based on the expression of the sensitivity function in (2.4.1.5.b) one can compute the gradient of $S(\underline{\rho})$:

$$\frac{\partial S}{\partial \underline{\rho}}(\underline{\rho}) = -\frac{1}{C_r(\underline{\rho})} T(\underline{\rho}) S(\underline{\rho}) \frac{\partial C_y}{\partial \underline{\rho}}(\underline{\rho}). \quad (2.4.1.9)$$

It follows that the expression of the gradient of the control signal is

$$\frac{\partial u}{\partial \underline{\rho}}(\underline{\rho}) = S(\underline{\rho})\left(\frac{\partial C_r}{\partial \underline{\rho}}(\underline{\rho})r - \frac{\partial C_y}{\partial \underline{\rho}}(\underline{\rho})\left[T(\underline{\rho})r + S(\underline{\rho})v\right]\right).$$

Observing that $\left[T(\underline{\rho})r + S(\underline{\rho})v\right] = y$, the following result is obtained:

$$\frac{\partial u}{\partial \underline{\rho}}(\underline{\rho}) = S(\underline{\rho})\left(\frac{\partial C_r}{\partial \underline{\rho}}(\underline{\rho})r - \frac{\partial C_y}{\partial \underline{\rho}}(\underline{\rho})y\right). \quad (2.4.1.10)$$

The estimate of the gradient of the control signal has the following expression [16]:

$$\frac{\partial u}{\partial \underline{\rho}}(\underline{\rho}) = \frac{1}{C_r(\underline{\rho})}\left(\frac{\partial C_r}{\partial \underline{\rho}}(\underline{\rho})y_3 - \frac{\partial C_y}{\partial \underline{\rho}}(\underline{\rho})y_2\right). \quad (2.4.1.11)$$

The experimental procedure is detailed in Table 2.4.1.1. Experiments 1 and 3 are the same while experiment 2 has the reference input the output signal from the first experiment.

Table 2.4.1.1 *Experimental procedure*

Experiment	**(1)(3) "normal"**	**(2) "gradient"**
Reference Input	$r_1(k)=r(k)$	$r_2(k)= y_1(k,\underline{\rho})$
Measurements	$u_1=C(q^{-1},\underline{\rho})S(q^{-1},\underline{\rho})(r_1(k)-v_1(k))$ $y_1=T(q^{-1},\underline{\rho})r_1(k)+S(q^{-1},\underline{\rho})v_1(k)$	$u_2=C(q^{-1},\underline{\rho})S(q^{-1},\underline{\rho})(r_2(k)-v_1(k))$ $y_2=T(q^{-1},\underline{\rho})r_2(k)+S(q^{-1},\underline{\rho})v_2(k)$

2.4.2. Separate parameter tuning

For the presentation of the separate parameter tuning by IFT, we choose a structure as the one presented in Fig. 2.4.2.1. This structure consists of two-degree-of-freedom controller (a feedforward controller and a feedback controller), the reference model implemented as a prefilter and the process.

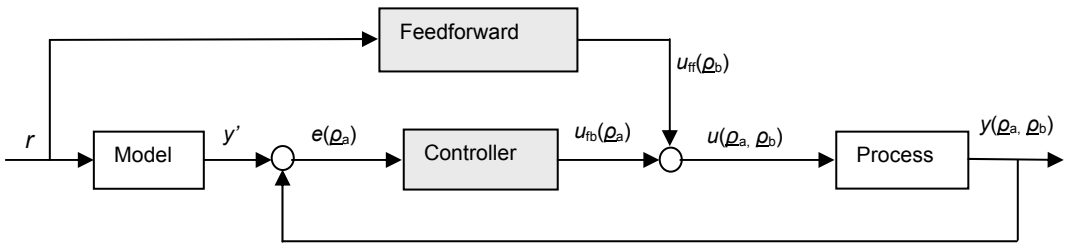

Fig. 2.4.2.1. Block diagram of a system with two-degree-of-freedom controller.

By combining a simple controller with a reference model, one can obtain a better model following. To improve even more the control signal following, one can use a feedforward filter as the one in Fig. 2.4.2.1.

The reference model is typically chosen as a dynamic system of first or second order. It is necessary that the feedback loop be very fast relative to the response of the chosen model.

The feedforward filter has to be chosen in such a manner that the so-called *conditional feedback property* holds. This property states that the closed loop transfer function equals the transfer function of the desired model, no matter of the feedback controller. This is satisfied whenever the feedforward controller equals the product between the transfer functions of the desired model and of the inverse of the process model.

The signal u_{ff} will produce the desired output if the models are correct.

When the output signal deviates from the desired behavior, the control error e will be a non zero number.

It is also possible to combine this structure with an additional feedforward from the measured disturbances. In this case, feedforward is used both to improve set-point response and to reduce the effect of the measurable disturbances.

This structure is used when the system has load disturbances or process uncertainties. In such cases, the feedback controller is designed so that system takes care of these problems while the feedforward controller and the reference model are designed to obtain the desired set-point response.

An IFT controller for a two-mass-spring system with friction, was realised in [1], with a structure like the one presented in Fig. 2.4.2.1. The novelty brought by this work is the idea of separate controller tuning.

Supposing that a stabilizing controller structure is given in advance ($C(\underline{\rho}_a^{(0)})$, $F(\underline{\rho}_b^{(0)})$), in conformity with this approach, one has to tune first the feedback controller $C(\underline{\rho}_a)$ – in order to achieve low sensitivity, and then the feedforward controller $F(\underline{\rho}_b)$ – in order to achieve desired tracking property.

Four experiments are needed to apply IFT to this controller structure. The experiments will be described in the following headers called *Experiment 1* to *4*.

Through experiments 1 and 2, the feedback controller is being tuned and through experiments 3 and 4 the feedforward controller is being tuned.

The parameters are updated by (2.1.1).

The objective functions or the minimization direction can be chosen in different ways. For example in [1], two objective functions were chosen – a different one for each controller tuning, and the minimization direction was chosen to be made by Broyden – Fletcher – Goldfarb – Shanno method.

For the further description of the algorithm through experiments, the approach to calculate the gradients of the control signal and respectively, of the output signal will be shown. These values are needed in order to compute the gradient of the objective function J and R matrix, in order to calculate the next set off controller parameters, whichever optimization method is to be chosen.

Experiment 1

The first experiment consists of the setup depicted in Fig. 2.4.2.2.

Set $u_{ff}(k) = 0$ and $y_d(k) = 0$, and inject a signal $d(k)$, which is white noise of zero mean.

Let $u_1(\rho_a) = 0$ and $y_1(\rho_a) = 0$ be the corresponding I/O signals of the process.

From Fig. 2.4.2.2, one can write the relations for $u_1(\rho_a)$ and $y_1(\rho_a)$.

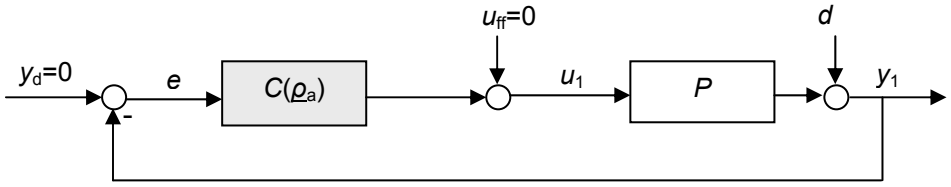

Fig. 2.4.2.2. Block diagram of the system used in Experiment 1.

$$y_1(\underline{\rho}_a) = \frac{1}{1 + P \cdot C(\underline{\rho}_a)} \cdot d\,, \tag{2.4.2.1.a}$$

$$u_1(\underline{\rho}_a) = -C(\underline{\rho}_a) \cdot y(\underline{\rho}_a)\,. \tag{2.4.2.1.b}$$

Experiment 2

The second experiment is different from the first by the fact that, now the test signal is set to zero and to the feed forward, the output signal form the first experiment is being injected. Hence, set $d(k) = 0$, $y_d(k) = 0$ and $u_{ff}(k) = y_1(k, \underline{\rho}_a)$. The corresponding setup for the second experiment is illustrated in Fig. 2.4.2.3.

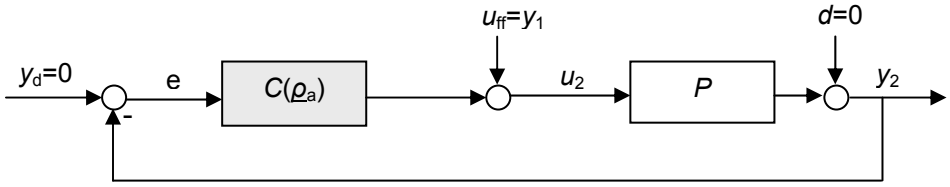

Fig. 2.4.2.3. Block diagram of the system used in Experiment 2.

$$y_2(\underline{\rho}_a) = \frac{P}{1 + P \cdot C(\underline{\rho}_a)} \cdot y_1(\underline{\rho}_a)\,, \tag{2.4.2.2.a}$$

$$u_2(\underline{\rho}_a) = \frac{1}{1 + P \cdot C(\underline{\rho}_a)} \cdot y_1(\underline{\rho}_a)\,. \tag{2.4.2.2.b}$$

The derivatives of $u(\underline{\rho}_a)$ and $y(\underline{\rho}_a)$

$$\frac{\partial y}{\partial \underline{\rho}_a}(k, \underline{\rho}_a) \underset{(2.25.a)}{=} -\frac{\partial C}{\partial \underline{\rho}_a}(q^{-1}, \underline{\rho}_a) \frac{P}{(1 + PC(q^{-1}, \underline{\rho}_a))^2} d(k)\,,$$

$$\frac{\partial y}{\partial \underline{\rho}_a}(k, \underline{\rho}_a) = -\frac{\partial C}{\partial \underline{\rho}_a}(q^{-1}, \underline{\rho}_a) \frac{P}{1 + PC(q^{-1}, \underline{\rho}_a)} \frac{1}{1 + PC(q^{-1}, \underline{\rho}_a)} d(k)\,,$$

$$\frac{\partial y}{\partial \underline{\rho}_a}(k, \underline{\rho}_a) \underset{(2.24.a)}{=} -\frac{\partial C}{\partial \underline{\rho}_a}(q^{-1}, \underline{\rho}_a) \frac{P}{1 + PC(q^{-1}, \underline{\rho}_a)} y_1(k)\,. \tag{2.4.2.3}$$

The gradient of the output signal can be estimated by the following relation:

$$\frac{\partial y}{\partial \underline{\rho}_a}(k,\underline{\rho}_a)\underset{(2..25.a)}{=}-\frac{\partial C}{\partial \underline{\rho}_a}(q^{-1},\underline{\rho}_a)y_2(k), \tag{2.4.2.4}$$

$$\frac{\partial u}{\partial \underline{\rho}_a}(k,\underline{\rho}_a)\underset{(2.24.b)}{=}-\frac{\partial C}{\partial \underline{\rho}_a}(k,\underline{\rho}_a)\cdot y(k,\underline{\rho}_a)-C(k,\rho_a)\frac{\partial y}{\partial \underline{\rho}_a}(k,\rho_a),$$

$$\frac{\partial u}{\partial \underline{\rho}_a}(k,\underline{\rho}_a)\underset{(2.26)}{=}-\frac{\partial C}{\partial \underline{\rho}_a}(k,\underline{\rho}_a)\cdot y(k,\underline{\rho}_a)$$

$$-C(k,\underline{\rho}_a)-\frac{\partial C}{\partial \underline{\rho}_a}(q^{-1},\underline{\rho}_a)\frac{P}{1+PC(q^{-1},\underline{\rho}_a)}y_1(k),$$

$$\frac{\partial u}{\partial \underline{\rho}_a}(k,\underline{\rho}_a)=-\frac{\partial C}{\partial \underline{\rho}_a}(q^{-1},\underline{\rho}_a)\frac{1}{1+PC(q^{-1},\underline{\rho}_a)}y_1(k).$$

The gradient of the control signal can be estimated by the following relation:

$$\frac{\partial u}{\partial \underline{\rho}_a}(k,\underline{\rho}_a)\underset{(2.25.b)}{=}-\frac{\partial C}{\partial \underline{\rho}_a}(q^{-1},\underline{\rho}_a)u_2(k). \tag{2.4.2.5}$$

Having these estimates, one can compute the gradient of the objective function and the matrix $\underline{R}$, of the chosen type and then determine the next set of controller parameters.

After the algorithm starts to converge, with the optimized parameters set for the feedback controller, one has to proceed to experiment 3 and 4, trying to tune the feedforward filter.

Experiment 3

From this point on, we start with a tuned feedback controller K and a non-tuned but stable initial feedforward controller $F(\rho_b)$. The set up for the third experiment is described in Fig. 2.4.2.4.

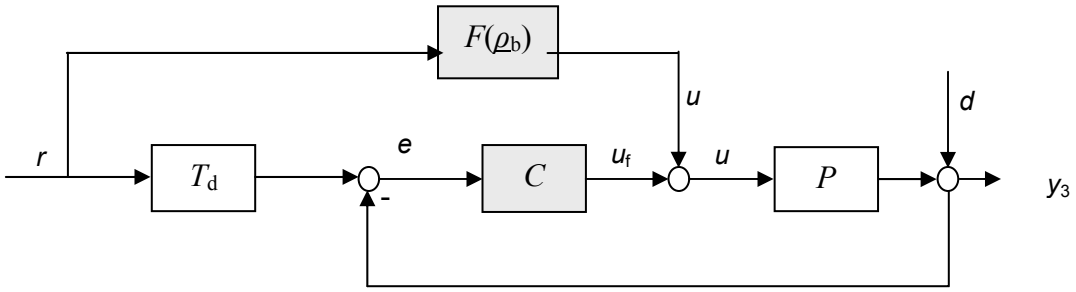

Fig. 2.4.2.4. Block diagram of the system used in Experiment 3.

Based on Fig. 2.4.2.4, one can write the input-output relations for the process:

$$u_3(\underline{\rho}_b)=\left(\frac{1}{1+P(q^{-1})C(q^{-1})}F(q^{-1},\underline{\rho}_b)+\frac{C(q^{-1})}{1+P(q^{-1})C(q^{-1})}T_d(q^{-1})\right)r, \tag{2.4.2.6.b}$$

$$y_3(\underline{\rho}_b)=P(q^{-1})\cdot u_3(\underline{\rho}_b). \tag{2.4.2.6.b}$$

Experiment 4

Experiment 4 is the second experiment needed to help obtain the next set of the parameters of the feedforward controller. The set up for this last experiment is the one depicted in Fig. 2.4.2.5.

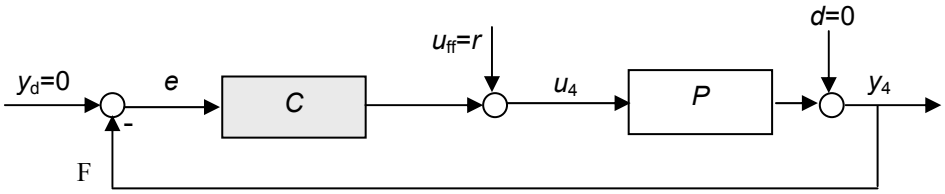

Fig. 2.4.2.5**.** Block Diagram of the system used in Experiment 4.

From Fig. 2.4.2.5, one can write the following relations:

$$u_4(\underline{\rho}_b) = \frac{1}{1+P(q^{-1})C(q^{-1})}r\,, \qquad (2.4.2.7.a)$$

$$y_4(\underline{\rho}_b) = \frac{P(q^{-1})}{1+P(q^{-1})C(q^{-1})}r\,. \qquad (2.4.2.7.b)$$

From the the input-output relations of the process in the Experiment 4, one can see that they both are independent of the feedforward controller parameters. Given this fact, it is enough to perform Experiment 4 only once.

The derivatives of $u(\underline{\rho}_b)$ and $y(\underline{\rho}_b)$

$$\frac{\partial u}{\partial \underline{\rho}}(k,\underline{\rho}_b) = \frac{\partial F}{\partial \underline{\rho}}(q^{-1},\underline{\rho}_b)\frac{1}{1+P(q^{-1})C(q^{-1})}r(k)\,. \qquad (2.4.2.8)$$

The gradient of the control signal can be estimated by the following relation:

$$\frac{\partial u}{\partial \underline{\rho}}(k,\underline{\rho}_b) = \frac{\partial F}{\partial \underline{\rho}}(q^{-1},\underline{\rho}_b)u_4(k)\,, \qquad (2.4.2.9)$$

$$\frac{\partial y}{\partial \underline{\rho}}(k,\underline{\rho}_b) = P(q^{-1})\frac{\partial u}{\partial \underline{\rho}}(k,\underline{\rho}_b)\,,$$

$$\frac{\partial y}{\partial \underline{\rho}}(k,\underline{\rho}_b) = \frac{\partial F}{\partial \underline{\rho}}(q^{-1},\underline{\rho}_b)\frac{P(q^{-1})}{1+P(q^{-1})C(q^{-1})}r(k)\,.$$

The gradient of the output signal can be estimated by the following relation:

$$\frac{\partial y}{\partial \underline{\rho}}(k,\underline{\rho}_b) = \frac{\partial F}{\partial \underline{\rho}}(q^{-1},\underline{\rho}_b)y_4(k)\,. \qquad (2.4.2.10)$$

2.5. Choosing the reference model

The discussion concerns the case when in the objective function formulation, the reference model output tracking is targeted which corresponds to the filtered tracking error penalty in the objective function. The reference model should be

chosen so that the closed-loop response would not be very different. The reference response can be chosen either to increase or to decrease the closed-loop bandwidth. In the case when there is a relative big difference between the closed-loop response and the reference model response, intermediate reference models should be used in order to ensure the convergence step by step. This approach is also known as the *windsurfing*-approach. The reference model is usually taken to be a discrete-time normalized second order transfer function, for which the step response incorporates performance measures such as overshoot, settling time and rise time. However, this is not a constraint and other reference models can be chosen. A typical continuous-time transfer function representation for the reference model is

$$M(s) = \frac{{\omega_0}^2}{s^2 + 2 \cdot \zeta \cdot \omega_0 \cdot s + {\omega_0}^2}, \tag{2.5.1}$$

where ζ is the damping factor and ω_0 is the natural frequency. Different diagrams can then be used such as the ones in [209] in order to illustrate how the choice of the performance indices can be made depending on the damping factor and the natural frequency. Two examples of such diagrams are given in Figs. 2.5.1 and 2.5.2.

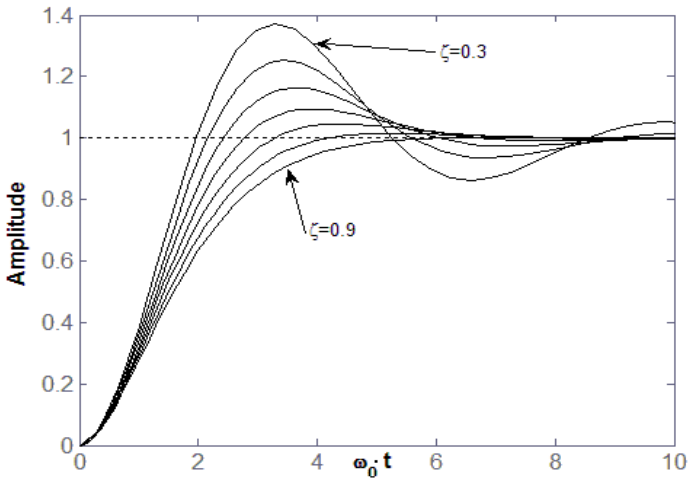

Fig. 2.5.1. Normalized time response of a second-order system for unit step input.

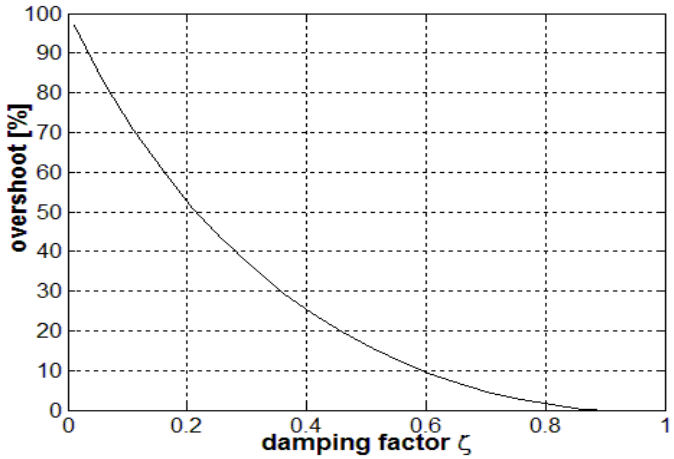

Fig. 2.5.2. Overshoot in percent as a function of the damping factor ζ.

2.6. Search direction

In order to compute the next set of parameters with relation (2.1), the matrix R has to be calculated.

In literature, the matrix $\underline{R}$ is usually taken as an approximate of the Hessian of the objective function J. There are though other possibilities of adopting $\underline{R}$.

For example, if the identity matrix is chosen for $\underline{R}$, the resulting gradient direction is for sure negative. In spite of this, the authors of different works, who applied IFT, have adopted the following form of $\underline{R}$:

$$\underline{R}^i = \frac{1}{N}\sum_{k=1}^{N}\left(est\left[\frac{\partial y}{\partial \underline{\rho}}(k,\underline{\rho}^i)\right]est\left[\frac{\partial y}{\partial \underline{\rho}}(k,\underline{\rho}^i)\right]^T + \lambda \cdot est\left[\frac{\partial u}{\partial \underline{\rho}}(k,\underline{\rho}^i)\right]est\left[\frac{\partial u}{\partial \underline{\rho}}(k,\underline{\rho}^i)\right]^T\right). \tag{2.6.1}$$

The subscript i denotes the iteration number.

Due to disturbances form the *gradient experiment* this will give a biased approximation of the Gauss-Newton direction.

Another interesting choice is to use a quasi-Newton method. One that has been used in literature, in [1], is Broyden – Fletcher – Goldfarb – Shanno (BFGS).

One of the merits of the quasi-Newton methods is that it a good approximation of the Hessian matrix is obtained based on the gradient of the objective function and the design of the controller parameters.

The update law to estimate the Hessian of the matrix based on BFGS is the following:

$$\underline{R}^{i+1} = \underline{R}^i + \frac{\underline{z}^i(\underline{z}^i)^T}{(\underline{z}^i)^T\underline{s}^i} - \frac{\underline{R}^i\underline{s}^i(\underline{s}^i)^T\underline{R}^i}{(\underline{s}^i)^T\underline{R}^i\underline{s}^i}, \tag{2.6.2}$$

where $\underline{R}^i = \underline{R}(\underline{\rho}^i)$, $\underline{s}^i = \underline{\rho}^{i+1} - \underline{\rho}^i$ and $\underline{z}^i = \frac{\partial J}{\partial \underline{\rho}}(\underline{\rho}^{i+1}) - \frac{\partial J}{\partial \underline{\rho}}(\underline{\rho}^i)$

The initial value of the matrix can be any positive definite matrix.

The following facts are known about the BFGS method [1]:

- if $\underline{R}^i$ is symmetric then $\underline{R}^{i+1}$ is symmetric,
- if $\underline{R}^i$ is positive definite and $(\underline{z}^i)^T\underline{s}^i>0$, then $\underline{R}^{i+1}$. If $(\underline{z}^i)^T\underline{s}^i>0$ is not satisfied then we set $\underline{R}^i= \underline{R}^{i+1}$.

Some of the advantages of the BFGS method are:

- global convergence property,
- super linear convergence,
- could be more numerically stable than the Gauss-Newton.

After knowing how to obtain all the necessary data for the algorithm, one can proceed to applying it. The steps of the IFT algorithm are presented in the next section.

2.7. Summary of the Iterative Feedback Tuning algorithm

This section is dedicated to the presentation of the general IFT algorithm. The methodology to obtain all the necessary data for the algorithm has been described in Sections 2.2 to 2.6.

The algorithm will be further presented under the structure of eight steps:

Step1: With the stabilizing controller operating on the process, generate the necessary control signals (e.g. $u_1(k,\underline{\rho}^i)$, $u_2(k,\underline{\rho}^i)$, in the case of one-degree-of-freedom controllers) output signals (e.g. $y_1(k,\underline{\rho}^i)$, $y_2(k,\underline{\rho}^i)$, in the case of one-degree-of-freedom controllers) through the corresponding number of experiments.

Step2: Generate the output signal of the desired model, y_d. Compute the output error as the difference between the output of the first experiment and the output of the reference model $\delta y = y_1 - y_d$.

Step 3: Compute the gradient of the output signal $\frac{\partial y}{\partial \underline{\rho}}(\underline{\rho}^i)$.

Step 4: The control signal is a perfect realization of the control signal of the first experiment.
$u = u_1$.

Step 5: Compute the gradient of the control signal $\frac{\partial u}{\partial \underline{\rho}}(\underline{\rho}^i)$.

Step 6: Compute the objective function $J(\underline{\rho})$ and the estimate of the gradient of the objective function $\frac{\partial J}{\partial \underline{\rho}}(\underline{\rho}^i)$.

Step 7: Compute the matrix $\underline{R}$.

Step 8: Compute the next set of parameters by $\underline{\rho}^{i+1} = \underline{\rho}^i - \gamma_i(\underline{R}^i)^{-1} est\left[\frac{\partial J}{\partial \underline{\rho}}(\underline{\rho}^i)\right]$.

2.8. Convergence analysis of the algorithm and the stability issue throughout the iterations

The convergence properties are given in the next theorem, which is reproduced from [16]:

Theorem 2.8.1: Consider the algorithm presented in section 2.7 with $\underline{R}^i \geq \delta I, \forall i$ for some $\delta > 0$. Assume that the procedure is complemented with the all-pass filtering procedure described above included if necessary so that we have an unconstrained minimization problem, i.e., $\underline{\rho} \in R^d$ (R is the set of reals and it is different from $\underline{R}^i$) for some integer d. Assume that $\{\gamma_i\}$ satisfy the usual conditions for convergence.

$$\sum_{i=1}^{\infty} \gamma_i = \infty \qquad \sum_{i=1}^{\infty} \gamma_i^2 = \infty . \tag{2.8.1}$$

Let the reference signal $\{r\}$ and the disturbances in each experiment $\{v_i^j\}$ be realizations of bounded stationary stochastic processes where these processes are mutually independent. Then, provided that the signals $\{y_i^j\}$; $j = 1, 2, 3$; $i = 1, 2, \ldots$ stay bounded, $\underline{\rho}^i \to \{\underline{\rho} : J'(\underline{\rho}) = 0\}$ with probability 1.

The parameters of the controller are updated in several iterations, until the estimate of the gradient of the objective function approaches zero to a sufficient extent.

A criterion of stopping the algorithm is given in [1] in a statement similar to the following: for a given scalar $\varepsilon > 0$ in advance, if $J(\underline{\rho}^i) - J(\underline{\rho}^{i+1}) < \varepsilon$, then one stops the algorithm and regards the parameters ρ^i as the sub-optimal parameters $\underline{\rho}^*$.

The most important requirement for convergence is that the closed loop signals should stay bounded throughout iterations; the controllers have to remain stabilizing for the process. Unfortunately there is no guarantee that the update law always provides a stable controller. As a measure of precaution one can examine the Bode plot of the controller after each parameter update. If this plot differs significantly from the previous one, then the step size of the iteration should be decreased.

Another more recent approach for ensuring the convergence of the parameters to the optimal solution is suggested in [48] where a Lyapunov function is used which is a function of the set of parameters that are subject to tuning. The update law is then seen as a discrete-time dynamic system for which the stability is assessed. For example, the Lyapunov function can be chosen of the form $V(\underline{\rho}^i) = (\underline{\rho}^i - \underline{\rho}^*)^T (\underline{\rho}^i - \underline{\rho}^*)$, where $\underline{\rho}^*$ is the set of optimal parameters. A ball of radius α centered in $\underline{\rho}^*$ is defined as $B_\alpha(\underline{\rho}) = \{\underline{\rho} \mid (\underline{\rho} - \underline{\rho}^*)^T (\underline{\rho} - \underline{\rho}^*) < \alpha\}$. Then, by using the Lyapunov stability theory, it is shown that there exists a sequence $\{\gamma_i\}$ such that the ball is a domain of attraction for all $\underline{\rho}^i \in B_\alpha(\underline{\rho})$. This translates into $\underline{\rho}^i \to \{\underline{\rho} : J'(\underline{\rho}) = \underline{0}\}$. However, two issues are mentioned in relation to this

approach: one is the fact that $\underline{\rho}^*$ has to be an isolated global minimum for the objective function *J*, and the other fact is that the Lyapunov function is defined with respect to $\underline{\rho}^*$ which is unknown if the process is unknown. So these two facts have to be asserted by using crude model estimates for the process which in turn violates the model-free assumption.

A solution to the algorithm convergence will be provided as a contribution of the current thesis, using Popov's hyperstability theory which in turn allows for a choice of the step scaling sequence $\{\gamma_i\}$ without the need for knowing $\underline{\rho}^*$.

The stability of the closed-loop during the iterations of the IFT is another important aspect that has to be taken into account. The closed-loop should be kept stable in order to respect the assumptions of the theorem related to the convergence of the set of parameters to the optimal solution. It is of course of interest to assert the stability before a new set of parameters of the controller is actually used in the experiments. This would require of course a process model in order to estimate bounds on the stability margins. Sufficient conditions for stability in iterative tuning were developed in [29] in which the Vinnicombe distance (nu-gap) between the actual and the next controller must be kept smaller than the generalized stability margin. In order to evaluate the generalized stability margin, an identification step has to be performed for the complementary sensitivity function by using standard open-loop identification techniques. Moreover, the generalized stability margin and the Vinnicombe metric need to calculate infinity norms for matrices, which implies calculating the largest singular value of a matrix over a finite grid of frequencies. These operations together with the matrix inversion are computationally expensive and thus more difficult to implement on signal processing hardware. However, this entire computational burden is connected to the parametric models that are used. As another contribution of the thesis, a new technique is proposed in order to assert the closed-loop stability, which makes use of non-parametric models such as frequency response functions (FRFs). FRFs are typically easier to obtain than the parametric models.

2.9. Iterative-Feedback Tuning in Multi Input-Multi Output (MIMO) systems

The *Iterative Feedback Tuning* problem extended to *Multiple Input Multiple Output* (MIMO) systems is treated in papers such as [18], [19], [20], [40], [204]. An LTI MIMO system is described as

$$\begin{bmatrix} \underline{y}(k) \\ \underline{y}_m(k) \end{bmatrix} = \underline{G}(q^{-1}) \begin{bmatrix} \underline{r}(k) \\ \underline{d}(k) \\ \underline{u}(k) \end{bmatrix}, \tag{2.9.1}$$

where $\underline{y} \in R^{n_y}$ is the output vector, $\underline{y}_m \in R^{n_{ym}}$ is the measured output vector, $\underline{r} \in R^{n_r}$ is the reference input vector, $\underline{d} \in R^{n_d}$ is the disturbance input vector, and it is zero-mean stationary and with variance σ^2, $\underline{u} \in R^{n_u}$ is the control signal vector.

One can consider that $n_r = n_{ym}$ as is references are prescribed for each measured output. Also it can be considered, without loosing generality that $\underline{y} = \underline{y}_m$. $\underline{G}(q^{-1})$ is a pulse transfer operator matrix that describes the generalized process (2.9.1) as in the robust control context. Let there be a control pulse transfer operator matrix $\underline{C}(q^{-1}, \underline{\rho})$ of dimension $n_u \times n_{ym}$ that is used in a scheme according to Fig. 2.9.1.

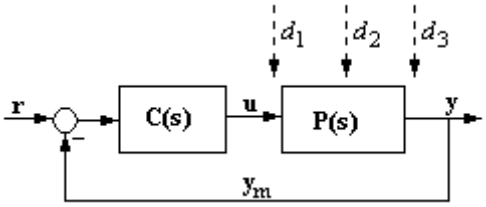

Fig. 2.9.1. The MIMO control system.

The parameter vector of the controller is $\underline{\rho} \in R^{n_\rho}$. The disturbance input d mainly acts upon the output vector $\underline{y}$, and it is suggested by d_3 in Fig. 2.9.1.

Over the IFT problem, one can define the design of the controller $\underline{C}(\underline{\rho})$ based on the minimization of an objective function defined over the time horizon of interest. Let the objective function be

$$J(\underline{\rho}) = \frac{1}{2N} E\left\{ \sum_{k=1}^{N} [\tilde{\underline{y}}(k, \underline{\rho})]^T \tilde{\underline{y}}(k, \underline{\rho}) \right\}, \tag{2.9.2}$$

where $\tilde{\underline{y}}(k, \underline{\rho}) = \underline{y}(k, \underline{\rho}) - \underline{y}_d(k)$ is the reference model tracking error. The objective function can be defined in many ways. It can penalize for example the control effort. The particular form (2.9.2) only penalizes the reference trajectory tracking error. In (2.9.2) $E\{.\}$ is the expectation defined w.r.t to the disturbance $\underline{d}$, N is the finite time horizon. The goal of the optimization problem is to find an optimal controller of parameter vector $\underline{\rho}^*$ which minimizes J. To obtain $\underline{\rho}^*$ one must find $\underline{\rho}$ as a solution to the equation

$$\underline{0} = \frac{dJ}{d\underline{\rho}}(\underline{\rho}) = \frac{1}{N} E\left\{ \sum_{k=1}^{N} \left[\frac{\partial \tilde{\underline{y}}}{\partial \underline{\rho}}(\underline{\rho}) \right]^T \tilde{\underline{y}}(\underline{\rho}) \right\}. \tag{2.9.3}$$

The criterion minimizations is carried out by using an algorithm based on the update law

$$\underline{\rho}^{j+1} = \underline{\rho}^j - \gamma_j (\underline{R}^j)^{-1} est\{ \frac{dJ}{d\underline{\rho}}(\underline{\rho}^j) \}. \tag{2.9.4}$$

In (2.9.4), $\underline{R}^j$ is a positive definite matrix, and it is typically a Gauss-Newton approximation of the Hessian of J. γ_j is the step size scaling coefficient of the search direction and j is the iteration number.

From (2.9.3) one can see that the variable $est\{\frac{dJ}{d\underline{\rho}}\}$ that is used in (2.9.4) should be computed. One can obtain only an unbiased estimate of this variable by obtaining unbiased estimates of the products $\left[\frac{\partial \underline{y}}{\partial \underline{\rho}}(\underline{\rho})\right]^T \underline{y}_t(\underline{\rho})$, as seen from (2.9.3). It was shown by Robbins and Monro in 1951 [13] that the stochastic optimization carried out by (2.9.4) holds in the conditions mentioned above.

The main concern now is to compute the gradients of the output y w.r.t. ρ. The problem was solved by the means of IFT applied to MIMO. The quantities that depend on the controller parameter vector $\underline{\rho}$ are $\underline{y}(\underline{\rho}), \underline{y}_m(\underline{\rho}), \underline{u}(\underline{\rho})$. All the considered signals are time dependent. The time index k is omitted in the following.

Computing the gradient of (2.9.1) w.r.t. one of the parameters of the vector let it be ρ_i, one can obtain:

$$\begin{bmatrix} \underline{y}'(\underline{\rho}) \\ \underline{y}'_m \end{bmatrix} = \underline{G}(q^{-1}) \begin{bmatrix} 0 \\ 0 \\ \underline{u}'(\underline{\rho}) \end{bmatrix}. \tag{2.9.5}$$

Here, we denote $\frac{\partial \bullet}{\partial \rho_i} = \bullet'$. The control signal can also be expressed as follows:

$$\underline{u}(\underline{\rho}) = \underline{C}(q^{-1}, \underline{\rho})(\underline{r} - \underline{y}(\underline{\rho})). \tag{2.9.7}$$

From (2.9.7) the gradient of $\underline{u}(\underline{\rho})$ w.r.t. ρ_i can be computed:

$$\underline{u}' = (\underline{C}(q^{-1}, \underline{\rho})\underline{r} - \underline{C}(q^{-1}, \underline{\rho})\underline{y})' = \underline{C}'(q^{-1}, \underline{\rho})\underline{r} - \underline{C}'(q^{-1}, \underline{\rho})\underline{y} - \underline{C}(q^{-1}, \underline{\rho})\underline{y}' =$$
$$= \underline{C}'(q^{-1}, \underline{\rho})(\underline{r} - \underline{y}) - \underline{C}(q^{-1}, \underline{\rho})\underline{y}'. \tag{2.9.8}$$

The last relation brings the idea of the gradient experiment, in which, using the same closed-loop scheme from Fig. 2.9., where $\underline{C}(q^{-1}, \underline{\rho}), \underline{u}', \underline{y}'$ are involved and adding one additional quantity to the control value, the gradient of $\underline{y}$ w.r.t. ρ_i can be computed. The quantity that is added is $\underline{C}'(q^{-1}, \underline{\rho})(\underline{r} - \underline{y}) = \underline{C}'(q^{-1}, \underline{\rho})\underline{e}^{(1)}$ and is the error from one initial experiment that is filtered through $\underline{C}'(q^{-1}, \underline{\rho})$. Therefore the setup presented in Fig. 2.9.2 can be used, in which $\underline{r}$ is set to $\underline{0}$.

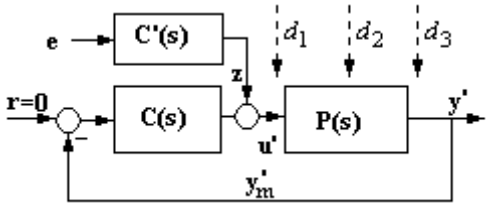

Fig.2.9.2. The setup for the gradient experiment.

In this gradient experiment, the output is a perturbed version of $\underline{y}'$ since disturbance acts on the output. In this form, in every gradient experiment, the partial derivate of each component of $\underline{y}$ is computed w.r.t. one particular ρ_i. It is then needed a total number of $1+n_\rho$ experiments to compute estimates to all gradients involved in (2.9.3).

2.10. How to reduce the number of experiments for MIMO IFT

An approach to reduce the number off experiments for MIMO IFT is suggested in [19]. The setup from Fig.2.9.2 is considered, i.e., the context of the gradient experiment is considered. Let the pulse transfer operator matrix from z to y' be $\underline{P}=\{P_{ij}\}, i=1..n_y, j=1..n_u$, with i, j meaning general matrix indexes. We assume to be known but this will prove to be unnecessary. Then the transfer function matrix from $\underline{e}$ to $\underline{y}'$ will be

$$\begin{bmatrix} y_1 \\ \vdots \\ y_k \\ \vdots \\ y_{n_y} \end{bmatrix} = \begin{bmatrix} P_{11} & \dots & P_{1n_u} \\ \vdots & & \\ & P_{ij} & \\ \vdots & & \\ P_{n_y 1} & \dots & P_{n_y n_u} \end{bmatrix} \begin{bmatrix} C'_{11} & \dots & C'_{1n_{ym}} \\ \vdots & & \\ & C'_{jl} & \\ \vdots & & \\ C'_{n_u 1} & & C'_{n_u n_{ym}} \end{bmatrix} \begin{bmatrix} e_1 \\ \vdots \\ e_l \\ \vdots \\ e_{n_{ym}} \end{bmatrix} + \underline{S}(q^{-1}, \underline{\rho})\underline{d}\,, \qquad (2.10.1)$$

with $k=1..n_y, l=1..n_{ym}$. Here, C'_{jl} denotes the gradient of each transfer function from the matrix $\underline{C}$ w.r.t. ρ_i. The sensitivity function $\underline{S}(\underline{\rho})$ represents the transfer functions from the disturbance to the output. Since $\underline{z}=\underline{C}'\underline{e}$, we can consider further that $\underline{y}=\underline{P}\underline{z}$. Let $\underline{z}$ be chosen of the form

$$\underline{z}=z_{jl}\overset{\Delta}{=}\left(\underbrace{0,\dots,0}_{j-zeros},e_l,0,\dots,0\right)^T. \qquad (2.10.2)$$

Then, from (2.10.1) results that

$$\underline{y}_{jl}=\begin{bmatrix} y_1{}^{jl} \\ \vdots \\ y_{n_y}{}^{jl} \end{bmatrix}=\begin{bmatrix} P_{1j}e_l \\ \vdots \\ P_{n_y j}e_l \end{bmatrix}+\underline{S}(q^{-1},\underline{\rho})\underline{d}^{jl}. \qquad (2.10.3)$$

By conducting an additional number of $n_u \times n_{ym}$ experiments, one can obtain all the products $P_{kj}e_l$ that appear in (2.10.1). Then it is possible to obtain the output vector $\underline{y}$ from (2.10.1) because the operators C'_{jl} commute since they represent transfer functions. The output vector that is obtained is a perturbed version of the gradient vector of $\underline{y}$ w.r.t. ρ_i.

This approach should be very useful when the number of controller's parameters largely exceeds the number $n_u \times n_{ym}$. This case is very often when the number of the inputs is large and the number of total parameters of the controller increases.

Another approach to reduce the number of experiments is presented in [20]. With this regard, Fig. 2.9.1 is referred. In the MIMO case, the sensitivity function and the complementary sensitivity function are defined by

$$\underline{S}(q^{-1},\underline{\rho}) = [\underline{I} + \underline{P}(q^{-1})\underline{C}(q^{-1},\underline{\rho})]^{-1}, \tag{2.10.4}$$

and

$$\underline{T}(q^{-1},\underline{\rho}) = \underline{S}(q^{-1},\underline{\rho})\underline{P}(q^{-1})\underline{C}(q^{-1},\underline{\rho}). \tag{2.10.5}$$

The sensitivity function is considered as the transfer function from disturbance to output when only the d_3 component of the disturbance input vector is considered. The dependency of the output on the inputs from the closed-loop system is

$$\underline{y}(\underline{\rho}) = \underline{T}(q^{-1},\underline{\rho})\underline{r} + \underline{S}(q^{-1},\underline{\rho})\underline{d}. \tag{2.10.6}$$

From (2.9.7) and (2.9.8) it can be shown, considering $\underline{y} = \underline{y}_m$ and eliminating $\underline{u}'$ between equations, that

$$\left.\begin{aligned} &\underline{y}'(\underline{\rho}) = \underline{P}(q^{-1})\underline{u}'(\underline{\rho}) \\ &\underline{u}'(\underline{\rho}) = \underline{C}'(q^{-1},\underline{\rho})\underline{e}(\underline{\rho}) - \underline{C}(q^{-1},\underline{\rho})\underline{y}'(q^{-1},\underline{\rho}) \end{aligned}\right\} \tag{2.10.7}$$

$$\Rightarrow \underline{y}'(\underline{\rho}) = \underline{S}(q^{-1},\underline{\rho})\underline{P}(q^{-1})\underline{C}'(q^{-1},\underline{\rho})\underline{e}(\underline{\rho}).$$

Further, equation (2.10.7) can be written as

$$\underline{y}'(\underline{\rho}) = \underbrace{\underline{S}(q^{-1},\underline{\rho})\underline{P}(q^{-1})\underline{C}(q^{-1},\underline{\rho})}_{\underline{T}(q^{-1},\underline{\rho})}\underbrace{\underline{C}^{-1}(q^{-1},\underline{\rho})\underline{C}'(q^{-1},\underline{\rho})}_{\underline{A}_i(q^{-1},\underline{\rho})}\underline{e}(\underline{\rho}) =$$

$$= \underline{T}(q^{-1},\underline{\rho})\underline{A}_i(q^{-1},\underline{\rho})\underline{e}(\underline{\rho}), \tag{2.10.8}$$

$$\underline{A}_i(q^{-1},\underline{\rho}) = \underline{C}^{-1}(q^{-1},\underline{\rho})\frac{\partial \underline{C}(q^{-1},\underline{\rho})}{\partial \rho_i}.$$

In the last equation, one can see that the initial error signal $\underline{e}(\underline{\rho})$ is filtered through the matrix $\underline{A}_i(q^{-1},\underline{\rho})$ and then filtered through $\underline{T}(q^{-1},\underline{\rho})$ for a number of times equal to the number of parameters in the parameter vector. This is the general case of MIMO as presented above.

But if $\underline{T}(q^{-1},\underline{\rho})$ is known to be close to the identity in the pass band, then in the equation (2.10.8) a commutation is possible, even with commutation errors. This is achieved according to

$$\underline{y}'(\underline{\rho}) = \underline{A}_i(q^{-1},\underline{\rho})\underline{T}(q^{-1},\underline{\rho})\underline{e}(\underline{\rho}), \tag{2.10.9}$$

and it reduces the number of experiments to two, as in the SISO case.

2.11. Convergent Iterative Feedback Tuning of state feedback-controlled servo systems

The second-order servo systems with integral component play an important role as controlled processes in a large category of industrial applications including mechatronics, electrical drives, sub-systems in power process control systems, positioning systems in manipulators, mobile robots, machine tools, flight guidance and control [62]-[69]. Those controlled processes are viewed as special cases of benchmark systems [70]-[72]. A convenient way to develop control solutions dedicated to these controlled processes makes use of linearized models at certain operating points. Therefore the parameter variation associated with the linearization is challenging when very good control system performance indices are required. The design and implementation involve more challenges when low-cost automation solutions are needed.

The control solutions based on state feedback control systems are can cope with the accepted class of processes. The optimal state feedback control systems can fulfill the main control aims i.e. high performance indices in reference input tracking and regulation with respect to several types of load disturbance inputs. With this regard the improvement of the control system performance indices (e.g. settling time and overshoot) is enabled by the minimization of appropriately defined objective functions. The Iterative Feedback Tuning (IFT) [14], [16] is an alternative to the experiment-based minimization of the objective functions. The IFT algorithms employ the input-output data measured from the closed-loop system during its operation to calculate the estimates of the gradients and eventually Hessians of the objective functions. Several experiments are conducted per iteration and the updated controller parameters are calculated on the basis of the input-output data and the estimates.

The extension of IFT according to [38] offers additional steps to improve the convergence properties of IFT while rejecting the disturbances. Several extensions of IFT to Multi Input-Multi Output (MIMO) systems are discussed in [18]-[20], [58]. Linear applications to digitally simulated benchmarks are illustrated in [18], [19]. The need for faster gradient approximations and local convergence in IFT for multivariable processes are thoroughly discussed in [20]. Recently reported industrial applications of IFT include the control of chemical processes [58], servo drives [39] and of anti-lock braking systems [206].

Many experiments are needed for more state feedback control systems and MIMO systems. The need to reduce the number of experiments per iteration has been highlighted in [18]-[20], [38], [204], [206].

The IFT-based state feedback control meant for second-order servo systems with integral component has been suggested in [45]. Building upon [45], twofold new contributions are presented. First, original convergent IFT algorithms are suggested. They are based on the formulation of the parameter update law in the IFT algorithms as a nonlinear dynamical feedback MIMO system in the parameter space and iteration domain. Popov's hyperstability analysis results [73], [74] are applied in this context to derive a new stability theorem which guarantees the convergence of the IFT algorithms and gives a useful condition to set the step size. Second, a thorough discussion of an extensive set of real-time experimental results is done.

The second-order servo systems as controlled processes are characterized by the state-space model [45]

$$\dot{\underline{x}} = \begin{bmatrix} 0 & 1 \\ 0 & -\frac{1}{T_S} \end{bmatrix} \underline{x} + \begin{bmatrix} 0 \\ \frac{K_S}{T_S} \end{bmatrix} u \,, \qquad \begin{bmatrix} y_1 \\ y_2 \end{bmatrix} = \underline{I}_2 \, \underline{x} \,, \tag{2.11.1}$$

where $\underline{x} = [x_1 = \alpha \quad x_2 = \omega]^T$ is the state vector, α is the (angular) position, ω is the (angular) speed, u is the control signal, y_1 and y_2 are the controlled outputs, $\underline{I}_2$ is the second-order identity matrix, and the superscript T indicates the matrix transposition. The two parameters in (1) are the process gain $K_S, K_S > 0$, and the small time constant or the sum of parasitic time constants $T_S, T_S > 0$.

The two transfer functions considering the input u and output ω, and the input u and output α are $P_{\omega,u}(s)$ and $P_{\alpha,u}(s)$, respectively, with the following expressions:

$$P_{\omega,u}(s) = \frac{K_S}{(1+sT_S)}, P_{\alpha,u}(s) = \frac{K_S}{s(1+sT_S)} \,. \tag{2.11.2}$$

The integral component can be observed in $P_{\alpha,u}(s)$ when the controlled output is $y_1 = x_1 = \alpha$. Such situations correspond to positioning systems.

The state feedback control system structure is presented in Fig. 2.11.1. The dotted connection is used only when the experiments specific to IFT are conducted. That connection is not applied during the normal control system operation, therefore the control system structure is not a model reference adaptive one.

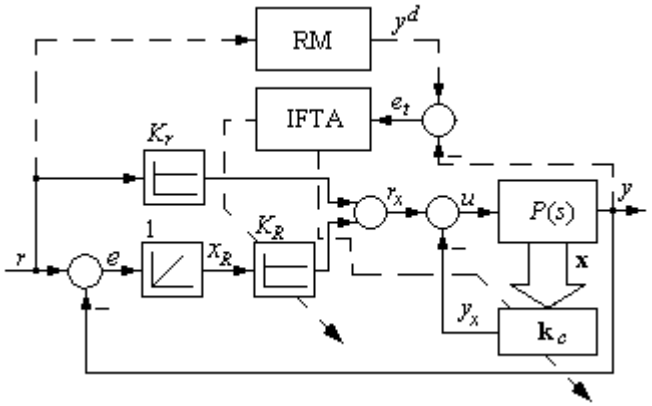

Fig. 2.11.1. IFT-based state feedback control system structure with integrator in the state feedback controller.

The main variables and blocks in Fig. 2.11.1 are: IFTA – the IFT algorithm, RM – the reference model, r – the reference input, $e = r - y$ – the control error, $\underline{k}_C = [K_1 \quad K_2]$ – the state feedback gain matrix to be tuned by means of the IFT algorithm, $P(s) = P_{\alpha,u}(s)$ – the transfer function of the controlled process with the controlled output $y = x_1 = \alpha$, y^d – the reference model (desired) output, $e_t = y^d - y$ – the tracking error.

The state-space model (2.11.1) can be reconsidered by including one additional state variable $x_3 = x_R$ which corresponds to the integrator inserted to the state feedback controller. Thus its gain K_R will be subject to IFT as it is illustrated in Fig. 2.11.1. The extended state-space model of the process becomes then

$$\dot{\underline{x}}_E = \begin{bmatrix} 0 & 1 & 0 \\ -K_s K_1 & -\frac{1}{T_s} - K_s K_2 & K_s K_R \\ -1 & 0 & 0 \end{bmatrix} \underline{x}_E + \begin{bmatrix} 0 \\ \frac{K_s}{T_s} K_r \\ 1 \end{bmatrix} r \,, \qquad (2.11.3)$$

$$y = I_3 \, \underline{x}_E \,,$$

where $\underline{x}_E = [\alpha \quad \omega \quad x_R]^T = [x \quad x_R]^T$ is the extended state vector, $\underline{I}_3$ is the second-order identity matrix, $\underline{y} = [y_1 \quad y_2 \quad y_3]^T$ is the controlled output vector, and the parameter K_r is not included in the tuning scheme. K_r is set prior to the application of IFT. One way to choose K_r is to keep a connection between the steady-state value of r and the steady-state value of r_x for which the desired r can be tracked by the steady-state value of $\underline{y}$. That value of r_x can be subject to the experimental identification of the state feedback control system.

For the purpose of the next study, all the continuous time transfer functions and signals are substituted by their discrete-time equivalents.

The objective function J defined over the finite time horizon N is

$$J(\underline{\rho}) = \frac{1}{2N} \sum_{k=1}^{N} (e_t(k, \underline{\rho}))^2 \,, \qquad (2.11.4)$$

where $\underline{\rho} \in R^m$ is the parameter vector, which for $m = 2$ is $\underline{\rho} = [\rho_1 = K_1 \quad \rho_2 = K_2]^T = \underline{k_c}^T$.

The IFT algorithms [14], [16], [18]-[20], [38], [39], [45], [58], are applied to find the solution $\underline{\rho}^*$ to the optimization problem

$$\underline{\rho}^* = \underset{\underline{\rho} \in SD}{\boldsymbol{arg\,min}} \, J(\underline{\rho}) \,, \qquad (2.11.5)$$

where several constraints can be imposed in relation with the controlled process and the state feedback control system. One of these constraints concerns the stability of the system and *SD* stands for the stability domain with this regard [75], [76].

Solving the optimization problem (2.11.5) requires finding the parameter vectors that make the gradient $\frac{\partial J}{\partial \underline{\rho}}$ equal to zero:

$$\frac{\partial J}{\partial \underline{\rho}} = [\frac{\partial J}{\partial \rho_1} \quad \ldots \quad \frac{\partial J}{\partial \rho_m}]^T = \underline{0} \,. \qquad (2.11.6)$$

Since the controlled output depends on $\underline{\rho}$ as $\underline{y}(\underline{\rho})$ and $\underline{y}^d$ not, use is made of (2.11.4) and equation (2.11.6) becomes

$$\frac{1}{N} \sum_{k=1}^{N} \frac{\partial y}{\partial \underline{\rho}}^T [y(\underline{\rho}) - y^d] = \underline{0} \,. \qquad (2.11.7)$$

The partial derivatives $\frac{\partial y}{\partial \rho_i}$ should be calculated to obtain the components of the gradient, $\frac{\partial J}{\partial \rho_i}$, $i = 1...m$. The experiments specific to IFT are conducted to obtain those components. Use is made of the notation [45]

$$\alpha' = \frac{\partial \alpha}{\partial \rho_i} \tag{2.11.8}$$

to highlight the partial derivative of the variable α with respect to the parameter ρ_i, $i = \overline{1,m}$.

To derive the IFT algorithms the following relations can be extracted from the state feedback control system structure presented in Fig. 2.11.1:

$$\begin{aligned} \underline{y} &= P(q^{-1})\, u\,, \\ r_x &= K_r r + \underline{K}_R \underline{x}_R\,, \\ u &= K_r r + \underline{K}_c \underline{x}_E\,, \end{aligned} \tag{2.11.9}$$

where the extended state feedback gain matrix $\underline{K}_c$ is

$$\underline{K}_c = [-K_1 \quad -K_2 \quad K_R] = [-k_c \quad K_R]\,. \tag{2.11.10}$$

The matrix $\underline{K}_c$ in (2.11.10) highlights the parameter vector $\underline{\rho}$ which for $m = 3$ is

$$\underline{\rho} = [K_1 \quad K_2 \quad K_R]^T\,. \tag{2.11.11}$$

Since $\underline{y}$ and u are functions of $\underline{\rho}$ the first and third equations in (2.11.9) yield

$$\begin{aligned} \underline{y}' &= P(q^{-1})\, u'\,, \\ u' &= \underline{K}_c{}' \underline{x}_E + \underline{K}_c \underline{x}_E{}'\,. \end{aligned} \tag{2.11.12}$$

Next the second equation in (2.11.3) enables the following transformation of the second equation in (2.11.12):

$$u' = \underline{K}_c{}' \underline{y} + \underline{K}_c \underline{y}'\,. \tag{2.11.13}$$

The first term in the right-hand side of (2.11.13), $\underline{K}_c{}' \underline{y}$, needs to be added to the control signal to obtain the experimental scheme. That term contains the unmodified output vector (in the MIMO framework) obtained from the first experiment [16]. The second term in the right-hand side of (2.11.13), $\underline{K}_c \underline{y}'$, is measured from the state feedback control system structure. Therefore the experimental scheme to calculate the gradients is presented in Fig. 2.11.2 where the blocks RM and IFTA (in Fig. 2.11.1) are omitted for simplicity.

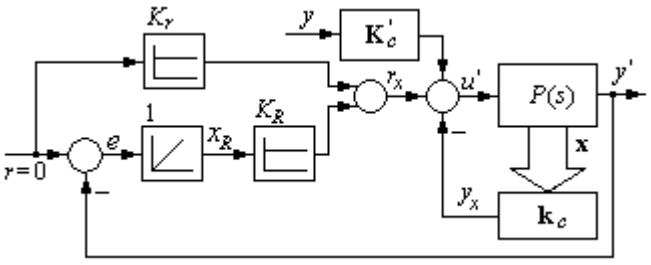

Fig. 2.11.2. Experimental scheme to calculate the gradients in the IFT-based state feedback control system structure.

The first experiment specific to IFT, referred to also as the normal one, is conducted with the control system structure presented in Fig. 2.11.1 to measure the controlled output $\underline{y}$. The next $m = 3$ experiments, i.e. the gradient experiments, are conducted with the experimental scheme presented in Fig. 2.11.2. These experiments are done separately for each parameter in $\underline{K}_C$ considering the zero values of the other $m - 1 = 2$ parameters because their derivatives with respect to the currently considered parameter are zero.

The parameter vector must be updated after the experiments are finished. Newton's algorithm is generally used as a convenient technique which iteratively approaches a zero of a function without knowing its expression. The update law to calculate the next parameter vector $\underline{\rho}^{i+1}$ is

$$\underline{\rho}^{i+1} = \underline{\rho}^{i} - \gamma_i \, (\underline{R}^{i})^{-1} \, est[\frac{\partial J}{\partial \underline{\rho}}(\underline{\rho}^{i})] \,, \tag{2.11.14}$$

where i is the index of the current iteration / experiment, $\gamma_i > 0$ is the step size, $est[\frac{\partial J}{\partial \underline{\rho}}(\underline{\rho}^{i})]$ is the estimate of the gradient, and the regular matrix $\underline{R}^{i}$ can be the estimate of the (positive definite) Hessian matrix or the identity matrix.

Popov's hyperstability analysis results will be applied as follows to the parameter update law (2.11.14) in order to derive a condition to guarantee the convergence of the IFTAs. First the domain of attraction of the update law as part of an IFTA is defined in terms of the following definition which is equivalent to that presented in [47].

Definition 2.11.1: Let $\underline{\rho}^{*}$ be the global minimum of the function $J : R^m \to R^+$ defined in (2.11.4). The set $\underline{\Pi} \subset R^m$ is called a domain of attraction of the update law (2.11.14) for the function J if

$$lim_{i \to \infty} \, \underline{\rho}^{i} = \underline{\rho}^{*} \,, \;\; \forall \underline{\rho}^{0} \in \underline{\Pi} \,, \tag{2.11.15}$$

where $\underline{\rho}^{0}$ is the initial parameter vector.

The convergence result is next expressed in terms of Theorem 2.11.1.

Theorem 2.11.1: Let $i_1 \geq 0$ be an arbitrary index of experiments / iterations and $\varepsilon_0 = const$, $\varepsilon_0 \neq 0$. If the condition

$$\underline{\Pi} = \left\{ \underline{\rho} \middle| I(i_1) = \sum_{j=0}^{i_1} \gamma_j (est[\frac{\partial J}{\partial \underline{\rho}}(\underline{\rho}^{j})])^T ((\underline{R}^{j})^{-1})^T \underline{\rho}^{j} \geq -\varepsilon_0^2 \,, \;\; \forall i_1 \geq 0 \right\} \tag{2.11.16}$$

is satisfied for the isolated global minimum $\underline{\rho}^{*}$ then $\underline{\Pi}$ is a domain of attraction of $\underline{\rho}^{*}$.

Proof: The relationship (2.11.14) is expressed as follows as a dynamical feedback MIMO system in the parameter space and iteration domain in terms of the structure presented in Fig. 2.11.3, where the feedforward discrete-time linear time-invariant (LTI) block is

$$\underline{\rho}^{i+1} = \underline{A}\,\underline{\rho}^{i} + \underline{B}\,\underline{\mu}^{i} ,$$
$$\underline{v}^{i} = \underline{C}\,\underline{\rho}^{i} + \underline{D}\,\underline{\mu}^{i} , \qquad (2.11.17)$$
$$\underline{A} = \underline{B} = \underline{C} = \underline{I} , \ \underline{D} = \underline{0} ,$$

and the nonlinear (NL) feedback block is

$$\underline{w}^{i} = \gamma_i \, (\underline{R}^{i})^{-1} est[\frac{\partial J}{\partial \underline{v}}(\underline{v}^{i})] . \qquad (2.11.18)$$

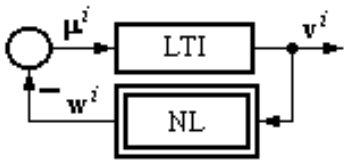

Fig. 2.11.3. Dynamical feedback MIMO system structure of (2.11.14) used in the convergence analysis.

LTI is completely controllable and completely observable. The discrete transfer function matrix of the LTI, $H(z)$, obtains the expression

$$H(z) = \underline{C}(z\underline{I} - \underline{A})^{-1}\underline{B} + \underline{D} = (z\underline{I} - \underline{I})^{-1}$$
$$= diag(1/(z-1),\ 1/(z-1),\ \ldots,\ 1/(z-1)) , \qquad (2.11.19)$$

and it is a positive real discrete transfer function matrix. Since NL satisfies the Popov type inequality

$$I(i_1) = \sum_{j=0}^{i_1} (\underline{w}^{j})^{T} \underline{v}^{j} \geq -\varepsilon_0^2 , \ \forall i_1 \geq 0 , \qquad (2.11.20)$$

which is equivalent to (2.11.16), the conditions for the hyperstability of the system (2.11.17), (2.11.18) are fulfilled [73], [74]. Thus the convergence of the IFTAs with the update law (2.11.14) is guaranteed.

The new family of IFTAs dedicated to the considered class of stat feedback control system consists of the following steps.

Step 1. Conduct the normal experiment making use of the control system structure presented in Fig. 2.11.1, measure $\underline{y}(\underline{\rho}^{i}) = \underline{x}$ and calculate the reference model output vector $\underline{y}^{d}$. Next conduct the three gradient experiments in terms of the experimental scheme presented in Fig. 2.11.2 and measure the outputs that give the gradient of the controlled output $\frac{\partial y}{\partial \underline{\rho}}(\underline{\rho}^{i})$.

Step 2. Calculate the estimate of the gradient of the objective function

$$est[\frac{\partial J}{\partial \underline{\rho}}(\underline{\rho}^{i})] = \frac{1}{N}\sum_{t=1}^{N} est\{[\frac{\partial \underline{y}}{\partial \underline{\rho}}(\underline{\rho}^{i})]^{T}\}[\underline{y}(\underline{\rho}^{i}) - \underline{y}^{d}] . \qquad (2.11.21)$$

Step 3. Calculate the Popov sums $I(i_1)$ in (2.11.16) and set the step size γ_i such that to fulfill the convergence condition (2.11.16) for any $i_1,\ 0 \leq i_1 \leq i$ and any $\varepsilon_0 = const,\ \varepsilon_0 \neq 0$.

Step 4. Calculate the next set of parameters $\underline{\rho}^{i+1}$ according to the parameter update law (2.11.14).

Some implementation issues are emphasized as follows. Setting the reference model (Fig. 2.11.1) is important. This aspect should be related to the imposed control system performance indices and the accepted model of the controlled process although it is achievable. Over ambitious reference models can results in the impossible fulfillment of the performance specifications.

The first task of the state feedback controller is to ensure an initially stable control system. The pole placement design can be used with this regard in order to set the initial parameter vector $\underline{\rho}^{0}$.

The identity matrix is recommended to play the role of the positive definite matrix $\underline{R}^{i}$ in (2.11.14) for low-cost implementations. Another alternative is to calculate the estimate of the Hessian matrix to play the role of $\underline{R}^{i}$. That calculation should be included in the step 3 of the IFTAs and an additional experiment can be employed with this regard.

In many cases the actuator is characterized by a nonlinear input-output map caused by the actuator saturation. That is a problem because it introduces usually nonlinear behaviors in the process's dynamics, thus it must be avoided. When making use of the integrator in the controller the importance of the actuator saturation is increased because actuators which enter deep saturation regions require usually longer time periods to re-enter the active regions of normal operation.

The structure illustrated in Fig. 2.11.2 highlights that when the state vector is fed over the control signal it may cause the saturation effects. Therefore the experiments will provide estimates of the gradients which are different with respect to the correct ones.

For the sake of simplicity an actuator with the active input range within -1 to $+1$ is considered as follows. One solution to solve the actuator saturation problem is to design the experiments such that the actuator does not enter saturation. Therefore the injected variable (in Fig. 2.11.2) must be in the active region of the actuator's input-output static map. The injected variable can be scaled to its maximum value $M,\ M>0$, of its measured dynamics. Generally speaking for an injected variable $z_t,\ t=1...N$, its scaled value added to the control signal is

$$(z_s)_t = z_t / M,\ M = \max_{k=1...N} |z_t| . \qquad (2.11.22)$$

Therefore it is guaranteed that the new variable to be injected, $(z_s)_t$, is within the accepted domain of the actuator input. Some details concerning the way that the gradient experiments are influenced are offered in [45].

The validation of the new state feedback control solution and IFT algorithms is done in terms of a case study dedicated to the position control of a DC servo system with backlash. The experimental setup illustrated in Fig. 2.11.4 is built around the INTECO DC motor laboratory equipment. It makes use of an optical encoder for the angle measurement and a tacho-generator for the measurement of the angular speed. The tacho-generator measurements are very noisy. The speed can also be observed from the angle measurements. The control system performance indices such as settling time and overshoot can be assessed easily.

It is accepted that $y = x_1 = \alpha$ in relation with (2.11.1), (2.11.3) and Fig. 2.11.1. The process is characterized by the parameters $K_S = 139.88$ and $T_S = 0.9198\ s$, obtained in terms of experimental identification. Part of the real-time experiments is presented here and it makes of the initial parameter vector set to set to $\underline{\rho}^0 = [0.0132 \quad 0.0126 \quad 0.005]^T$ in order to stabilize the control system.

An $r = 150\ rad$ step type modification of the reference input was applied. Therefore the parameter K_r was tuned at the value $K_r = 0.0133$ and dropped out of the objective function (2.11.4). That value of K_r was obtained by steady-state calculations to ensure a desired gain between r and *y*. The sampling period was set to 0.01 s. The continuous-time RM is characterized by the transfer function

$$G_{RM}(s) = 1/(s^2 + 1.5s + 1) \tag{2.11.23}$$

which is next discretized.

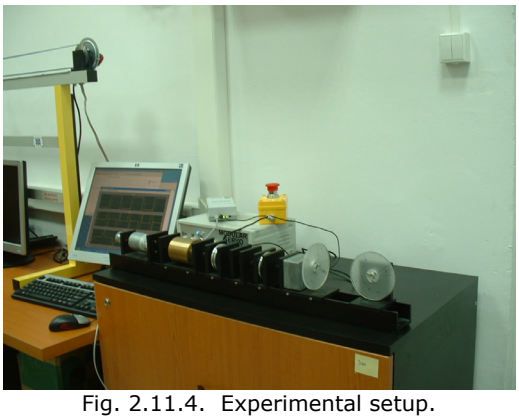

Fig. 2.11.4. Experimental setup.

The real-time experimental results that illustrate the behavior of the control system in terms of the evolution of the controlled output before the application of the IFT algorithm are presented in Fig. 2.11.5.

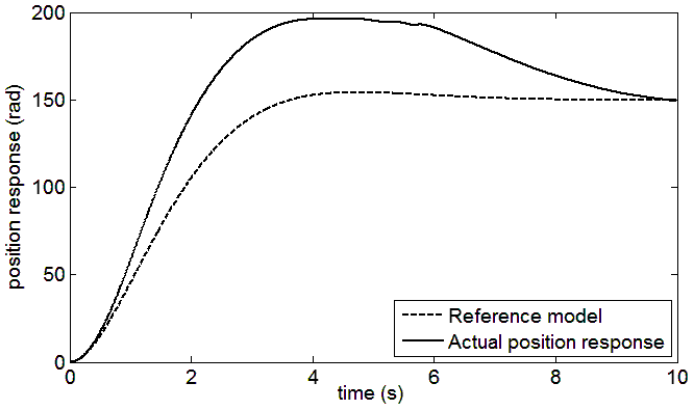

Fig. 2.11.5. y^d (dotted line) and *y* (continuous line) versus time considered before IFT.

The IFTA presented in Section 3 was applied. The parameters in the IFTA were set to $\gamma_i = 0.0001$ and $\underline{R}^i = \underline{I}_3$. After 12 iterations the parameter set reaches $\underline{\rho} = [0.0157 \quad 0.0142 \quad 0.0020]^T$. The evolution of the controlled output after 12 iterations is presented in Fig. 2.11.6.

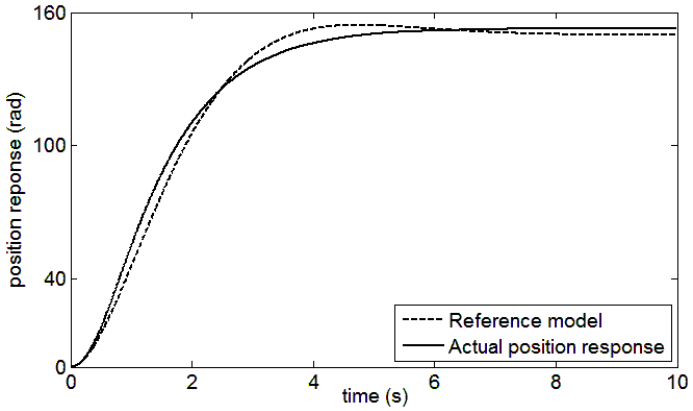

Fig. 2.11.6. y^d (dotted line) and y (continuous line) versus time considered after IFT.

The control system performance enhancement due to IFT is highlighted. It is reflected by smaller overshoot and settling time. The control system performance enhancement is also pointed out in the evolutions of the control signal and speed $x_2 = \omega$ illustrated in Fig. 2.11.7 and Fig. 2.11.8, respectively. The oscillations in the control signal and speed are caused by the backlash.

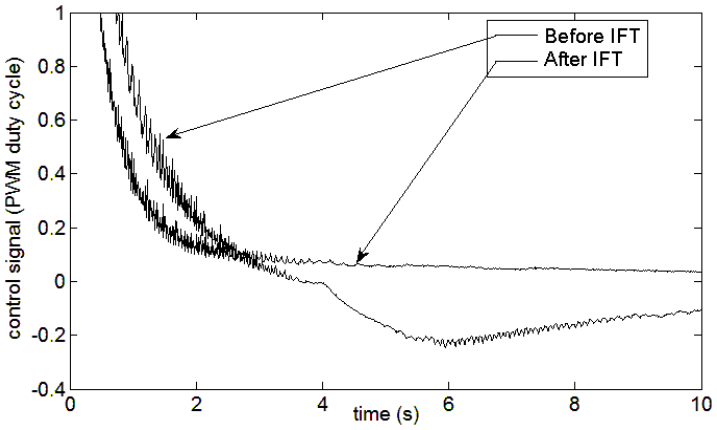

Fig. 2.11.7. u versus time considered before and after IFT.

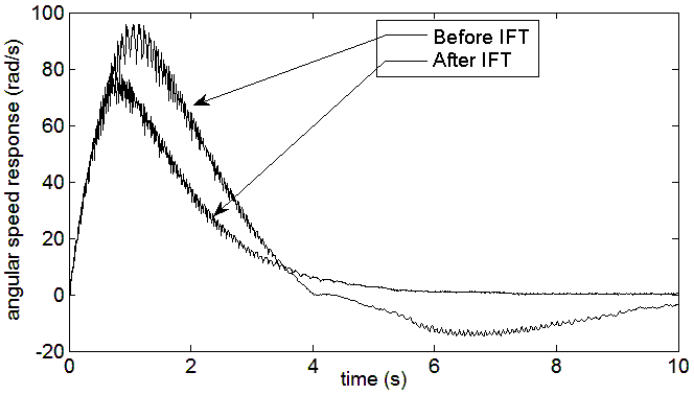

Fig. 2.11.8. x_2 versus time considered before and after IFT.

The states time responses before and after tuning with IFT are shown in Fis. 2.11.9 and 2.11.10. The evolution of the parameters throughout the iterations and the objective function decrease are presented in Figs. 2.11.11 and 2.11.12 respectively.

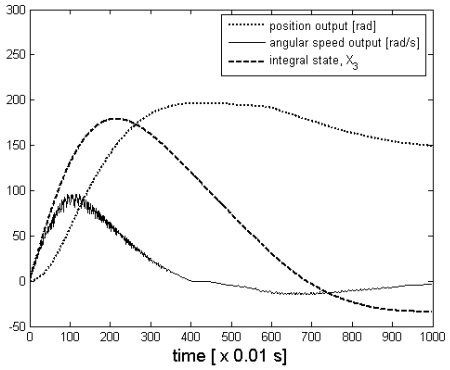

Fig. 2.11.9. The states evolution after IFT.

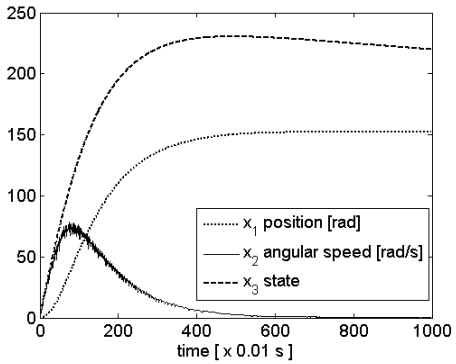

Fig. 2.11.10. The response of the system before the IFT tuning being applied on the parameters.

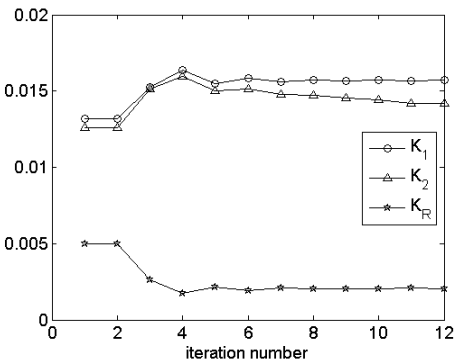

Fig. 2.11.11. Evolution of parameters.

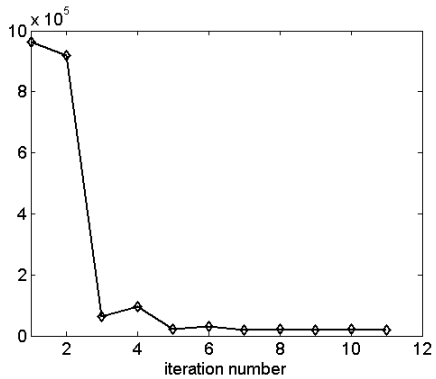

Fig. 2.11.12. The objective function after 12 iterations.

A new approach to the convergent IFT-based design of a class of state feedback control systems meant for a class of second-order systems with integral component has been presented. The convergent IFT algorithm proposed here is sufficiently general to be applied without additional difficulties to the state feedback control of systems of arbitrary order.

The real-time experimental results in the case study validate the optimal state feedback control solution. It shows the power of IFT because the IFT-based design of the control system offers better performance indices compared to the situation prior to the application of the IFT algorithm. The performance indices are very good for the nonlinear controlled process although the theoretical approach is based on the linear or linearized mathematical model of the controlled process.

2.12. Data-based improvement for Linear-Quadratic Regulator (LQR) solution using IFT

The state feedback control systems (CSs) are widely used due to the advantages offered by the state-space mathematical modeling [62], [63], [77]. They are highlighted in positioning systems and in servo systems that belong to a wide range of applications.

The improvement and optimization of the CS performance is normally obtained by minimizing objective functions (OFs) expressed as integral quadratic performance indices [78]-[81]. This also provides a convenient way to deal with the degrees of freedom associated to the pole placement design of Multi Input-Multi Output (MIMO) systems.

The Linear-Quadratic Regulator (LQR) approach which is frequently used for the tuning of the optimal state feedback CSs can actually be used only when linearized or linear models of the process and the knowledge on all state variables available for feedback are assumed [82], [83], [84].

Alternatively, the Iterative Feedback Tuning (IFT) offers a direct data-based offline-adaptive controller tuning approach. IFT performs a gradient-based minimization of the OF, and it provides an efficient way to deal with some of the specific problems of nonlinear or ill-defined processes. The OF minimization algorithm uses data obtained from the real-time experiments conducted with the real-world CS.

Good overviews of the standard IFT are given in [14], [27]. The first comprehensive treatment of IFT in a journal paper is conducted in [16]. The extension of IFT according to [38] provides additional steps to improve the convergence properties of IFT while rejecting the disturbances. Several extensions of IFT to MIMO systems are discussed in [18]-[20]. Linear applications related to digitally simulated benchmarks are presented in [18], [19]. The need for faster gradient approximations and local convergence in IFT for multivariable processes are thoroughly discussed in [20]. The input-output signals of the process are employed in [85] to identify a linear time-varying model of the process which is further used in IFT. IFT applications to industrial control problems are reported in the literature, for example, for the control of chemical processes [58] and for servo drive control [39], [75]. Discussions of the IFT approach to the nonlinear process control are given in [15], [59], [60].

As shown in [14], [16], [27], we need to conduct several experiments per

iteration in order to collect the input-output data from the closed-loop system, which are needed to calculate the gradients of the OFs in order to update the IFT-based controller parameters. In the case of one-degree-of-freedom IFT-based controllers only two experiments per iteration are needed. An additional experiment is needed to tune the two-degree-of-freedom IFT-based controllers. Even more experiments are needed for more complex CS structures including the state feedback and MIMO ones. The need to reduce the number of experiments per iteration is emphasized in [18], [20], [38], [43].

This section presents an original combination of the IFT and of optimal state feedback control techniques. Our state feedback controller estimates the OF gradients directly on the basis of measurements during the CS operation. Therefore our controller is different from other IFT-based controllers [14], [16], [18]-[20], [27], [38], that use the transfer function representation of the system. A new approach is proposed here to obtain the partial derivatives needed in the calculation of the gradient of the OF. An original experimental technique is then suggested as an alternative MIMO approach to IFT with focus on single input processes.

In our recent paper [43] we discussed the signal processing aspects of the IFT-based state feedback control for second-order positioning systems which have an integral component. A state-space formulation of IFT is analyzed in [61], and the solution converges to the analytical solutions to the state feedback gain matrix and to the Kalman gain. The typical experiments specific to one- and two-degree-of-freedom controllers are conducted in [61], [86], and they are accompanied by digital simulation results.

A recent and very good follow-up of [58] and [61] is offered in [87] using a Linear Quadratic Gaussian (LQG) formulation supported by the transfer function formulation. The results are validated by digital simulation on a first order process, and the IFT-based observer tuning is studied.

This section presents the following new contributions with respect to the analyzed literature:

- An original IFT-based approach based on a data-based algorithm to improve the performance of state feedback control systems for single input processes is offered.
- A comparison between the model-based design for state feedback optimal control systems (the LQR problem) and the experimental-based design using IFT is carried out.
- A new IFT algorithm based on an experimental setup to calculate the gradients of the OF is proposed.

The new contributions are important with respect to the state-of-the-art analyzed above because the LQR approach is used to ensure the initial tuning of the parameters of the state feedback controller, and our approach ensures the further improvement of the CS performance. The CS performance improvement is achieved by the alleviation of the OF using information from the experiments conducted with the real-world CS.

Our approach is really different from the original IFT algorithm. We develop a tuning potential for state feedback optimal control systems which are an alternative to the popular pole placement design for state feedback control systems. The optimal state feedback control systems are known for their robustness properties and stabilizing capabilities. The certainty equivalence principle upon which the optimal design is set is merely an idealization since all models are imperfect. The improvements are possible under experiment-based tuning using IFT and the conditions under which this is possible are discussed. Our tuning via IFT is

done initially in the simulation case for the pure deterministic framework while in the experimental case the stochastic framework is accounted for, and the differences between the results are explained.

This section deals with the following problems:

- the discussion of the general framework to tune the state feedback CSs by means of IFT,
- the proposal of a new IFT algorithm (IFTA),
- the treatment of the representative case study of an IFT-based angular position controller for a DC servo system with actuator dead zone and control signal saturation; the experimental laboratory setup and real-time experimental results are also presented,
- a discussion on the advantages and limitations of the new approach,
- the connection between the LQR objective function which drives the analytical solutions of the optimization problem and the IFT objective function that is subject to practical evaluations in the new data-based algorithm.

A new IFT algorithm for state feedback control systems is proposed as follows. Let us consider a process characterized by the single input discrete-time linear time-invariant (LTI) state-space model

$$\begin{aligned} \underline{x}(k+1) &= \underline{A}\,\underline{x}(k) + \underline{B}\,u(k) + \overline{B}\,\underline{w}(k), \\ \underline{y}(k) &= \underline{C}\,\underline{x}(k) + \overline{C}\,\underline{v}(k), \end{aligned} \tag{2.12.1}$$

where $k \in N$ is the discrete time argument, u is the control signal, $\underline{x} = [x_1 \ \ldots \ x_n]^T \in R^n$ is the state vector, n is the system order, $\underline{y} \in R^{n_y}$ is the controlled output, $\underline{A} \in R^{n \times n}$, $\underline{B} \in R^{n \times 1}$, $\overline{B} \in R^{n \times n}$, $\underline{C} \in R^{n_y \times n}$, $\overline{C} \in R^{n_y \times n}$ are constant matrices, $\underline{w} \in R^n$ and $\underline{v} \in R^{n_y}$ are the uncorrelated process noise vector and measurement noise vector, respectively, which are vectors of normal independent identically distributed random variables with zero means and the variances σ_w^2 and σ_v^2, respectively. Zero initial conditions are assumed throughout this section for the process dynamics without affecting the generality. It is accepted that the process is controllable and observable.

The vector y is the controlled position and speed in the cases of positioning systems and of servo systems in several applications [88]-[90], but our approach is not limited to positioning systems or servo systems. The transfer characteristics of the actuator and of the measurement instrumentation of the state variables x_i, $i = 1...n$, are both included in the process.

The corresponding deterministic discrete-time LTI state-space model of the process is

$$\begin{aligned} \underline{x}(k+1) &= \underline{A}\,\underline{x}(k) + \underline{B}\,u(k), \\ \underline{y}(k) &= \underline{C}\,\underline{x}(k). \end{aligned} \tag{2.12.2}$$

The following infinite horizon quadratic performance index can be imposed as performance specification of the CS such that its minimization can ensure very good CS performance:

$$I(\underline{\rho}) = \sum_{k=0}^{\infty} [\underline{x}^T(\underline{\rho}, k)\,\underline{Q}\,\underline{x}(\underline{\rho}, k) + \lambda\,u^2(\underline{\rho}, k)], \tag{2.12.3}$$

where $\underline{\rho} = [\rho_1 \ \ ... \ \ \rho_n]^T$ is a parameter vector, and the weights are

$$\underline{Q} \geq 0, \ \underline{Q} = [q_{ij}]_{i,j=\overline{1,n}}, q_{ij} = q_{ji}, \ i,j = 1...n, \ \lambda > 0 . \tag{2.12.4}$$

The optimization of the state feedback control systems can be formulated as the following optimization problem of finding the optimal parameter vector $\underline{\rho}^*$ which corresponds to the optimal gain matrix $(\underline{\rho}^*)^T$:

$$\underline{\rho}^* = \underset{\underline{\rho}}{\textbf{arg min}} I(\underline{\rho}) . \tag{2.12.5}$$

The optimization problem defined in (2.12.5), using the OF defined in (2.12.3) and accounting for the pure deterministic process model (2.12.2), is essentially the well known discrete-time LQR problem that is appealing for its' general robustness properties with respect to the process parametric variations [91]. To apply the state feedback CS designed via LQR, it is necessary that all the states are measurable. If this is not the case, then state observers/estimators are used in the general framework of optimal estimation and control, commonly known as the LQG problem. But, as shown in [92], the robustness properties could be lost in this case, and that can be mitigated by using the Loop Transfer Recovery (LTR) technique. In this section it is assumed that all the states are measurable and are subject to process and measurement noise.

LQR can be extended in several ways to cover the nonlinear systems when the CS performance indices are deteriorated [72], [93], [94]. Due to its experiment-based characteristics mentioned in the previous section, IFT is particularly well suited to deal with these LQR tuning aspects.

Concluding, LQR is a state feedback control solution to a model-based deterministic optimization problem assuming that the real-world process model is available. However the many practical applications are far away from this assumption and that is the point where IFT plays a significant role. IFT offers a solution to a stochastic optimization problem like that defined in (2.12.5), but with respect to stochastic disturbances that are inherent to all real-time experiments conducted with the real-world CS. IFT works on the real-world process, and it does not use the process model in the tuning scheme.

The solution to the discrete-time infinite horizon optimization problem defined in (2.12.5) is the control law $u(k) = -\underline{\rho}^T \underline{x}(k)$ which together with (2.12.2) drives the state vector to zero under the imposed spectrum of the CS prescribed by the system matrix $\underline{A}^{cl} = \underline{A} - \underline{B}\,\underline{\rho}^T$. The reference inputs are commonly introduced for each state variable when it is needed to drive the state vector to a different point in the state. The resulting state feedback controller is defined in terms of the control law

$$\begin{aligned} &u(k) = \underline{\rho}^T \underline{e}(k), \ \underline{\rho}^T = [\rho_1 \ \ ... \ \ \rho_n], \\ &\underline{e}(k) = \underline{r}(k) - \underline{x}(k), \end{aligned} \tag{2.12.6}$$

where $\underline{r} = [r_1 \ \ ... \ \ r_n]^T$, is the reference input vector, r_i are the reference inputs that correspond to the state variables x_i, $i = 1...n$, $\underline{e} = [e_1 = r_1 - x_1 \ \ ... \ \ e_n = r_n - x_n]^T$ is the state control error vector that consists of the state variable errors e_i, $i = 1...n$, ρ^T is the state feedback gain matrix, referred

to also as the gain matrix, $\underline{\rho}$ is the parameter vector, and T indicates the matrix transposition. The vector $\underline{e}$ is applied as an input to the state feedback gain matrix $\underline{\rho}^T$ as shown in Fig. 1, where $\underline{P}$ is the process and $\underline{C}$ is the controller, and the difference from the matrix $\underline{C}$ in (2.12.1) will be pointed out in the sequel when necessary.

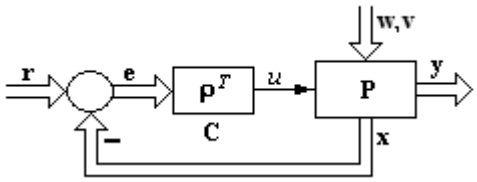

Fig. 1. State feedback control system structure.

Introducing reference inputs for the state variables, the optimization problem defined in (2.12.5) makes use of the following modified OF:

$$I(\underline{\rho}) = \sum_{k=0}^{\infty} [\underline{e}^T(\underline{\rho},k)\,\underline{Q}\,e(\underline{\rho},k) + \lambda\, e_U^2(\underline{\rho},k)]\,, \tag{2.12.7}$$

where the control signal error $e_U(\underline{\rho},k)$ is defined as the difference between the control signal and its steady-state value $u(\underline{\rho},\infty)$:

$$e_U(\underline{\rho},k) = u(\underline{\rho},k) - u(\underline{\rho},\infty)\,. \tag{2.12.8}$$

The transformation of the OF defined in (2.12.3) according to (2.12.7) is needed to ensure the convergence of the OF. Therefore, since step reference inputs are used in the sequel and the state feedback CS is asymptotically stable, the state feedback control law defined in (2.12.6) will drive the state control errors to zero and the state vector to the reference input vector during the accepted infinite time horizon.

In order to apply the IFT to solve the optimization problem defined in (2.12.5), using the OF defined in (2.12.7), we will use a modified OF, referred to as J, defined as follows over the finite time horizon N for reasons of practical evaluations of the OF:

$$J(\underline{\rho}) = \sum_{k=0}^{N} [\underline{e}^T(\underline{\rho},k)\,\underline{Q}\,\underline{e}(\underline{\rho},k) + \lambda\, e_U^2(\underline{\rho},k)]\,. \tag{2.12.9}$$

The OF defined in (2.12.9) can be represented by the approximation

$$I(\underline{\rho}) \approx J(\underline{\rho}) \tag{2.12.10}$$

if N is sufficiently large to capture all transients in the CS response.

IFT algorithms can conveniently be employed to find a solution $\underline{\rho}^*$ to the optimization problem

$$\underline{\rho}^* = \boldsymbol{arg}\ \underset{\underline{\rho}\in SD}{\boldsymbol{min}}\ J(\underline{\rho})\,, \tag{2.12.11}$$

where SD stands for the stability domain of all state feedback gain matrixes that ensure a stable CS. Several other constraints regarding the process and the closed-loop system can be considered in this context [95]-[99].

The two optimization problems defined by (2.12.7) and respectively by (2.12.11) essentially are equivalent. However, differences may appear due to:

- the infinite and respectively the finite time horizons in the OFs defined in (2.12.7) and (2.12.9),
- the discrete-time nature of the signals considered in the numerical algorithms associated with these problems [100]-[102].
- the more general stochastic framework that is necessary to be taken into consideration when the IFT problem is set.

The finite time optimal state feedback control problem is characterized by a time-varying gain matrix, while the infinite time state feedback optimal control problem is characterized by a steady-state gain matrix ρ^T. The calculation of the matrices used in both cases requires process models that are affected by modeling and identification errors.

While the LQR solution can not guarantee a global minimum of the OF because of the inherent process modeling errors, the IFT-based solution can ensure the further reduction of the OF. This reduction is ensured by the gradient experiments conducted with the real-world CS that make the IFT approach closer to the real-world process behavior.

Our approach is based on the fact that LQR finds an optimal solution for the available process model which is not optimal for the real-world process. Therefore, without using the process model the OF defined in (2.12.9) is reduced further using the real-world process. In order to provide a fair comparison between the LQR solution and the IFT-based solution, the deterministic framework is used in the simulations and the stochastic framework is next used in real-time experiments.

In order to solve the optimization problem defined in (2.12.11) a parameter vector ρ has to be found such that

$$\frac{\partial J}{\partial \underline{\rho}} = [\frac{\partial J}{\partial \rho_1} \quad ... \quad \frac{\partial J}{\partial \rho_n}]^T = [0 \quad ... \quad 0]^T , \tag{2.12.12}$$

which, for an OF J defined in (2.12.9), becomes

$$\frac{\partial J}{\partial \rho_l} = 2 \sum_{k=0}^{N} \{[\sum_{\substack{i,j=1 \\ i \geq j}}^{n} (q_{ij}\, e_i \frac{\partial e_j}{\partial \rho_l})] + \lambda\, e_u \frac{\partial e_u}{\partial \rho_l} \} = \underline{0}, \quad l = 1...n . \tag{2.12.13}$$

The cases of constrained optimization problems use Karush-Kuhn-Tucker optimality conditions instead of the null gradient given by (2.12.12).

Partial derivatives $\partial e_i / \partial \rho_l$ and $\partial e_u / \partial \rho_l$ need to be calculated first in order to obtain the derivatives $\frac{\partial J}{\partial \rho_l}$, $l = 1...n$, in the gradient of the OF. We will present in the next section an experimental technique that we developed to calculate these partial derivatives.

The IFT algorithms are presented as follows in the more general stochastic framework. Therefore the OF defined in (2.12.9) and evaluated on a finite-time horizon becomes a random variable and therefore is should be defined as

$$J(\underline{\rho}) = E\{ \sum_{k=0}^{N} [\underline{e}^T (\underline{\rho}, k)\, \underline{Q}\, \underline{e}(\underline{\rho}, k) + \lambda\, e_u^2 (\underline{\rho}, k)] \} , \tag{2.12.14}$$

where $E\{\}$ is the expectation with respect to the stochastic disturbances. However the deterministic case results in the simplification of the IFT algorithms.

The IFT algorithms can solve the optimization problem defined in (2.12.14) by using the Robbins-Monro stochastic approximation algorithm, which iteratively approaches a zero of a function without the need to know its complete expression.

There is no need for evaluations of the OF, but its first and eventually second partial derivatives are important. This result holds not only for the tuning approach based on sensitivity functions but also the stochastic convergence is ensured with useful consequences when dealing with real world processes. The parameter vector ρ values are iteratively updated according to the following equation:

$$\underline{\rho}^{i+1} = \underline{\rho}^{i} - \gamma^{i}(\underline{R}^{i})^{-1} est[\frac{\partial J}{\partial \underline{\rho}}(\underline{\rho}^{i})],\ \underline{R}^{i} > 0\,, \tag{2.12.15}$$

where $i \in N$ is the current iteration/experiment index, $\gamma^{i} > 0$ is the step size, $est[\frac{\partial J}{\partial \underline{\rho}}(\underline{\rho}^{i})]$ is the unbiased estimate of the gradient, and the regular matrix $\underline{R}^{i}$ can be the estimate of the Hessian matrix, the Gauss-Newton approximation of the Hessian, or the identity matrix in the case of less demanding and slower convergent computations.

The step size sequence $\{\gamma^{i}\}_{i \in IN}$ should evolve in time such that to satisfy some bounds. With this regard the conditions to ensure the convergence of the stochastic algorithm are [14], [19], [27], [38], [87]

$$\sum_{i=0}^{\infty} \gamma^{i} = \infty,\ \sum_{i=0}^{\infty} (\gamma^{i})^{2} < \infty\,. \tag{2.12.16}$$

A good choice of the step size sequence that ensures the divergence of the first series in (2.12.16) and the convergence of the second series in (2.12.16) is

$$\gamma^{i} = \frac{\gamma^{0}}{i},\ i \in N,\ i \geq 1\,, \tag{2.12.17}$$

where the initial step size $\gamma^{0} > 0$ is set such that to ensure a compromise to the numerical stability and to the convergence speed.

A biased estimate of the Hessian matrix can be employed in the update law (2.12.15) as the Gauss-Newton approximation

$$R^{i} = \sum_{k=1}^{N} \{est[\frac{\partial e}{\partial \rho}(\rho^{i})]^{T}\, Q\, est[\frac{\partial e}{\partial \rho}(\rho^{i})] + \lambda\ est[\frac{\partial e_{u}}{\partial \rho}(\rho^{i})]^{T} est[\frac{\partial e_{u}}{\partial \rho}(\rho^{i})]\}\,, \tag{2.12.18}$$

where the estimates of the gradients are used when the stochastic environment is accepted. An example of unbiased estimator is given in [57].

The IFT algorithm will be described as follows, and aspects concerning its implementation are pointed out as well. LQR requires always a linearized model or a collection of local models of the process (e.g., in the gain scheduling approach) in order to calculate the optimal parameter vector $\underline{\rho}^{*}$ which corresponds to the optimal gain matrix $(\underline{\rho}^{*})^{T}$. The identification problem itself is a rather complex undertaking in the case of MIMO systems, which requires a special design of the experiments.

On the other hand, the IFT-based approach does not need exact process models and special gradient experiments can be conveniently designed to avoid abnormal operation regimes. The initial tuning of the gain matrix is not a problem in the case of LQR-based approach. However, finding an initial stabilizing controller without knowing the process is not a trivial task. Finally, the IFT can be used to fine tune controllers for nonlinear processes under constraints [15].

The IFT-based approach offers a notable degree of flexibility. The OF defined in (2.12.11) is not only weighting the state variable errors and the control signal error associated to the LTI state-space model of the CS defined in (2.12.1), but it can weight the reference model tracking error trajectories as well.

As shown in [60] the IFT can be used as an alternative solution to the popular pole placement design of optimal state feedback controllers. However, the form in which it is used here is similar to the classical LQR optimization problem.

As mentioned in the previous section, the main advantage of the IFT resides in its gradient computation algorithm together with the stochastic convergence result. The MIMO IFT-based approach is particularly well suited to solve the optimization problem defined in (2.12.9). This is due to the fact that the state feedback CS can be considered as a particular case of a MIMO system with one input, which is the control signal, and with many outputs, which are the measured/observed variables as shown in the model (2.12.1).

From (2.12.1) and (2.12.6), the LTI state feedback CS is characterized by

$$\begin{cases} \underline{x}(\underline{\rho},k) = \underline{P}_{u\,\underline{x}}(q^{-1})\,u(k) + \underline{P}_{\underline{w}\,\underline{x}}(q^{-1})\,\underline{w}(k), \\ u(\underline{\rho},k) = \underline{\rho}^T \underbrace{[\underline{r}(k) - \underline{x}(\underline{\rho},k)]}_{\underline{e}(\underline{\rho},k)} \end{cases}, \tag{2.12.20}$$

where $\underline{P}_{u\,\underline{x}}(q^{-1}) \in R^{n\times 1}$ is the process pulse transfer matrix operator from the input u to the state vector $\underline{x}$, $\underline{P}_{\underline{w}\,\underline{x}}(q^{-1}) \in R^{n\times n}$ is the disturbance pulse transfer matrix operator from the process noise vector $\underline{v}$ to the state vector, and $\underline{w}$, $\underline{x}$ and u are defined in accordance with (2.12.1). The dependence of the variables involved in (2.12.20) on $\underline{\rho} = [\rho_1 \quad \dots \quad \rho_n]^T$ is underlined in (2.12.20).

As suggested in (2.12.13), we need to calculate the derivatives $\frac{\partial e_i}{\partial \rho_l}$. Taking into account the state feedback control law defined in (2.12.6) and the fact that $\underline{r}$ does not depend on $\underline{\rho}^T$, the partial derivatives obtain the expressions

$$\frac{\partial e_i(\underline{\rho},k)}{\partial \rho_l} = -\frac{\partial x_i(\underline{\rho},k)}{\partial \rho_l}, \quad \frac{\partial e_u(\underline{\rho},k)}{\partial \rho_l} = \frac{\partial u(\underline{\rho},k)}{\partial \rho_l} - \frac{\partial u(\underline{\rho},\infty)}{\partial \rho_l}, \; i,l = 1\dots n. \tag{2.12.21}$$

The derivative of the CS state vector with respect to a certain process parameter ρ_l, $l = 1\dots n$, can be written as

$$\frac{\partial \underline{x}(\underline{\rho},k)}{\partial \rho_l} = P_{u\,\underline{x}}(q^{-1})\frac{\partial u(\underline{\rho},k)}{\partial \rho_l}. \tag{2.12.22}$$

Similarly, the derivative of the control signal in the state feedback control law expressed in (2.12.6) with respect to the same parameter ρ_l, $l = 1\dots n$, is

$$\frac{\partial u(\underline{\rho},k)}{\partial \rho_l} = \frac{\partial \rho^T}{\partial \rho_l}\underline{e}(\underline{\rho},k) - \underline{\rho}^T \frac{\partial \underline{x}(\underline{\rho},k)}{\partial \rho_l}. \tag{2.12.23}$$

The derivative of the gain matrix $\underline{\rho}^T$ with respect to one parameter ρ_l is a row vector with the same dimension as $\underline{\rho}^T$, but with a single nonzero element that takes the value 1, and when multiplied by e it keeps only the l-th state variable error. The derivative of the control signal is then

$$\frac{\partial u(\underline{\rho},k)}{\partial \rho_l} = [0 \quad \ldots \quad \rho_l \quad \ldots \quad 0] \begin{bmatrix} e_1(\underline{\rho},k) \\ \vdots \\ e_l(\underline{\rho},k) \\ \vdots \\ e_n(\underline{\rho},k) \end{bmatrix} - \underline{\rho}^T \frac{\partial \underline{x}(\underline{\rho},k)}{\partial \rho_l} = e_l(\underline{\rho},k) + \underline{\rho}^T \Big(\underbrace{\underline{r}}_{=\underline{0}} - \frac{\partial \underline{x}(\underline{\rho},k)}{\partial \rho_l} \Big), \tag{2.12.24}$$

where e_l is the l-th state variable error.

Equation (2.12.24) shows how to conduct the gradient experiments with the process: by injecting an additive term in the control signal of the state feedback CS and letting the reference input vector $\underline{r}$ equal to zero, the derivatives of the state variables and of the control signal with respect to the parameter ρ_l in $\underline{\rho}^T$ are obtained. The injected term is e_l, i.e., the l-th element of the state control error vector obtained in a normal experiment. All specific experiments of IFT are described as follows.

An initial experiment, called the normal experiment, is carried out to record the evolution of the state variables and the corresponding state variable errors and control signal error respectively, in the state feedback CS shown in Fig. 2.12.1.

Other n gradient experiments are then subsequently carried out in order to calculate estimates of the derivatives $\frac{\partial x_i}{\partial \rho_l}$ and $\frac{\partial u}{\partial \rho_l}$, and use is made of equations (2.12.20) and (2.12.24). Let l denote as a superscript the l-th gradient experiment corresponding to ρ_l, $l = 1...n$:

$$\underline{x}^l(\underline{\rho},k) = \underline{P}_{u\underline{x}}(q^{-1})\, u^l(\underline{\rho},k) + \underline{P}_{\underline{w}\underline{x}}(q^{-1})\underline{w}^l(k) = \underline{P}_{u\underline{x}}(q^{-1})\,[e_l(\underline{\rho},k) - \underline{\rho}^T \underline{x}^l(\underline{\rho},k)] + \underline{P}_{\underline{w}\underline{x}}(q^{-1})\underline{w}^l(k) \tag{2.12.25}$$

that provides the basis for the experimental setup (illustrated in Fig. 2.12.2) used to calculate iteratively the partial derivatives $\frac{\partial x_i}{\partial \rho_l}$ and $\frac{\partial u}{\partial \rho_l}$ needed in the minimization of the OF. We actually obtain at each gradient experiment the estimates of the gradient of the state variables with respect to the gain matrix parameters. This is because at each experiment the process noise acts upon the CS. It is evident from (2.12.25) that $E\{\underline{x}^l\} = \frac{\partial \underline{x}}{\partial \rho_l}$. In the deterministic framework these terms are dropped out in (2.12.25).

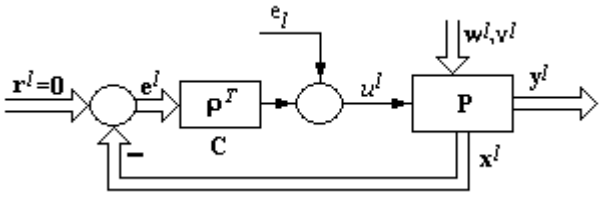

Fig. 2.12.2. Experimental setup to calculate $\frac{\partial x_i}{\partial \rho_l}$ and $\frac{\partial u}{\partial \rho_l}$.

The IFT algorithm consists of the following steps:

- *Step 0*. Set the step size, the initial controller parameters $\underline{\rho}^0$ and the weights in the OF.
- *Step 1*. Conduct the initial (normal) experiment making use of the CS structure presented in Fig. 2.12.1 and record the evolution of all state variables.
- *Step 2*. Conduct the n gradient experiments making use of the experimental setup presented in Fig. 2.12.2 to obtain all partial derivatives $\frac{\partial x_i}{\partial \rho_l}$ and $\frac{\partial u}{\partial \rho_l}$.
- *Step 3*. Conduct the normal experiment again such that the states contain realizations of noise that differ form the noise at *step 2* to ensure the unbiased estimate of the gradient.
- *Step 4*. Calculate the estimates of the gradient of the OF according to equation (2.12.13).
- *Step 5*. Calculate $\underline{\rho}^{i+1}$ in terms of the update law (2.12.15).

The *step 0* is done only once. The *steps 1* to *5* are repeated iteratively. The *step 0* of the IFT algorithm requires an initial set of parameters that stabilize the state feedback CS to be obtained here by LQR. In the case of Single Input-Single Output (SISO) systems, we can use the Ziegler-Nichols tuning [39] or other techniques like the Virtual Reference Feedback Tuning [48], [103], [104] in order to get these parameters.

There exists a difference between the deterministic case and the stochastic case in terms of the objective function and of the objectives that are targeted. Specifically, IFT is developed as an experimental-based technique in which the noise enters the CS and therefore the objective function also contains a factor that depends on the noise. This means that the minimization of the energy transfer between the noise and the state variables is also attempted, in addition to the minimization of the state control error and of the control signal energy that are objectives specific to the LQR deterministic problem. This aspect is illustrated in Appendix A.

The case study that validates the new IFT algorithm is a second-order positioning CS for a modular DC servo system with an integral component. The process is characterized by the single input discrete-time LTI state-space model defined in (2.12.4) with the matrices

$$\underline{A} = \begin{bmatrix} 1 & 0.0487 \\ 0 & 0.9471 \end{bmatrix}, \underline{B} = \begin{bmatrix} 0.1867 \\ 7.3993 \end{bmatrix}, \underline{C} = \underline{I}_2, \tag{2.12.26}$$

and with the angular position and the angular speed as state variables. The experimental setup is built around the INTECO DC servo system laboratory equipment. The main features of the experimental setup are the rated amplitude of $24\,V$, the rated current of $3.1\,A$, the rated torque of $15\,N\,cm$, the rated speed of $3000\,rpm$, the weight of inertial load of $2.03\,kg$, and the angular speed is measured by a tacho-generator. The actuator (in the power interface) is characterized by limitation since the DC motor is controlled by pulse-width modulation (PWM), and the control signal u for the accepted laboratory equipment is the PWM duty-cycle which is constrained to $-1 \le u \le 1$. The actuator exhibits a ± 0.15 width insensitivity zone applied to u and it is compensated through an inverse nonlinearity.

The simplified model presented in (2.12.26) was obtained by the parameter identification of the first-principle model of the equipment resulting in the simplified

process transfer function (considering u as the input and the angular position as the output)

$$P(s) = k_P /[s(1 + T_\Sigma s)] , \quad (2.12.27)$$

where k_P is the process gain and T_Σ is the small time constant. The values of the process parameters were obtained as $k_P = 139.88$ and $T_\Sigma = 0.92\ s$. Using the notation T_s for the sampling period, the sampling period of $T_S = 0.05\ s$ was next set.

The detailed mathematical model of the process is time variant due to the interchanging modules (inertial load, encoder and eventually backlash). The re-identification is not used in our approach.

One simulation scenario and one experimental scenario are presented as follows to illustrate the benefits of the IFT-based approach over the classical LQR-based approach.

The model used in the LQR-based approach is (2.12.26) which is obtained from (2.12.27) for the process parameters $k_P = 139.88$ and $T_\Sigma = 0.92\ s$. Setting the weights Q and λ in the infinite horizon quadratic performance index defined in (2.12.5) according to

$$\underline{Q} = \begin{bmatrix} 0.2 & 0 \\ 0 & 0.2 \end{bmatrix}, \lambda = 400 , \quad (2.12.28)$$

the gain matrix is

$$(\underline{\rho}^T)_{LQR\_1} = [\rho_1 = 0.020575 \quad \rho_2 = 0.020135] . \quad (2.12.29)$$

The results are obtained for a step angular position reference input of 40 rad and zero reference input for the angular speed, i.e., $\underline{r} = [40 \quad 0]^T$.

Accepting the time horizon of $N = 200$ samples, the OF is evaluated to $J_{LQR\_1} = 4243.42$. Next, we consider that the real-world process is generated from (2.12.27) with the process parameters $k_P = 130$ and $T_\Sigma = 1.2\ s$. This is a way to suggest that the LQR design is based on a model that is different from the real-world process as it is a very crude approximation. With the same LQR design resulting in the same gain matrix presented in (2.12.29), the OF is evaluated to $J_{LQR\_2} = 4549.30$, which is clearly non optimal since we have a different process model. However, the application of the LQR-based approach to the real-world process for the weights defined in (2.12.28), the gain matrix is

$$(\underline{\rho}^T)_{LQR\_3} = [\rho_1 = 0.020983 \quad \rho_2 = 0.022102] , \quad (2.12.30)$$

and the OF is evaluated to $J_{LQR\_3} = 4542.76$. We assume as follows that we do not know the real-world process model, but we simulate that IFT-based experiments are conducted with it starting with the gain matrix defined in (2.12.29) as initial parameter vector. A constant step size of $\gamma^i = 10^{-7}$ and $\underline{R}^i = \underline{I}_2$ are used in the IFT algorithm implemented in the deterministic framework. These results are very good because the gain matrix evolves from (2.12.29) to (2.12.30) and the OF from J_{LQR_2} to $J_{LQR\_3} < J_{LQR\_2}$. Hence we are able to find an improvement of the OF although we are not using the process model. This in fact shows that the LQR optimization problem can be improved when experimenting on the real-world process.

The evolution of the OF over 25 iterations is shown in Fig. 2.12.3. The time responses of the CS with the controller parameters defined in (2.12.29) (corresponding to J_{LQR_1}) and (2.12.30) (corresponding to J_{LQR_3}) are illustrated in Fig. 2.12.4. The system responses are very similar; therefore the state feedback CS is robust with respect to the gain matrix parameter variations and to the process parametric variations as well.

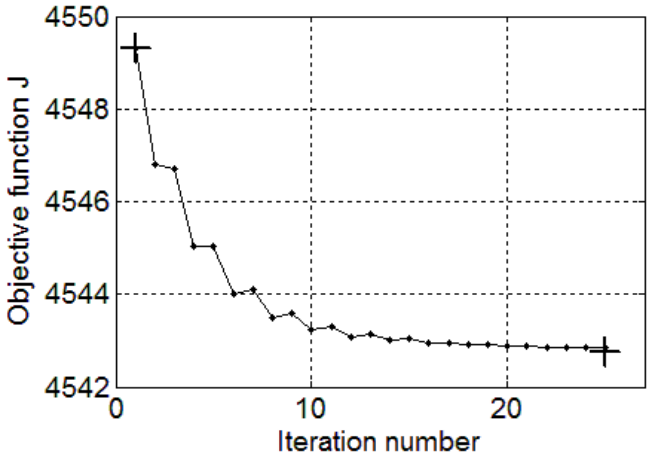

Fig. 2.12.3. Simulation results: the evolution of the objective function over 25 iterations, J_{LQR_2} and J_{LQR_3} are marked with **+**.

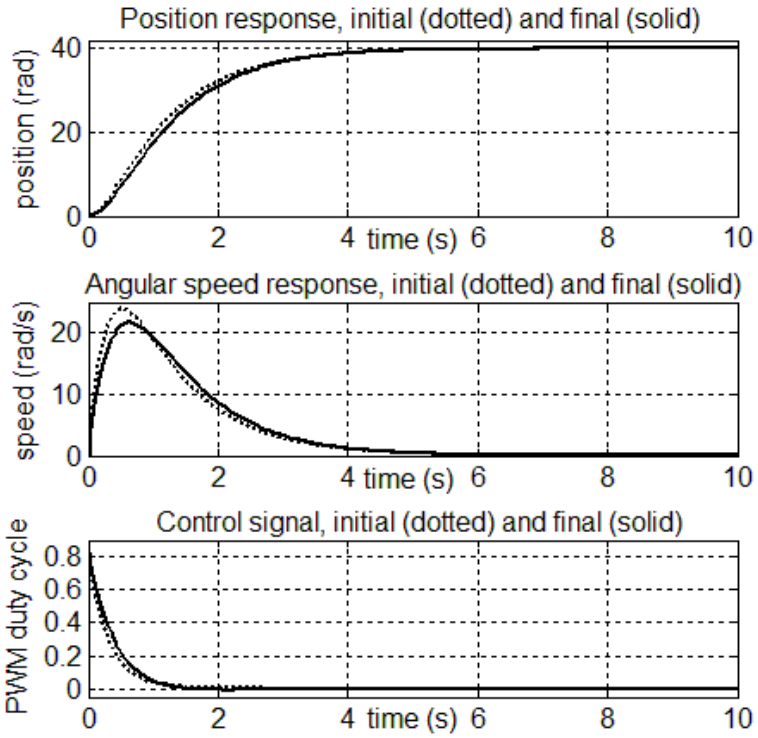

Fig. 2.12.4. Simulation results: control system responses of the CS with the initial controller parameters defined in (2.12.29) and of the CS with the final controller parameters defined in (2.12.30).

In order to illustrate how our data-based tuning evolves for a different situation, another simulation scenario is conducted. This scenario starts with an initial pole placement design, and it will be shown that the tuning actually reaches the LQR solution calculated on the basis of the real-world process. The pole placement design is based once again on the model that is different from the reality. The design is carried out in the discrete time domain. The pole placement design uses the gain matrix $(\underline{\rho}^T)_1 = (\underline{\rho}^T)_{LQR\_3}$ given in (2.12.29). The solution to the optimal design, as previously designed, is expressed as the gain matrix $(\underline{\rho}^T)_{LQR\_3}$ given in (2.12.30). For the pole placement design the closed-loop system spectrum corresponding to the continuous time case is represented by the poles $-0.93 \pm 0.44i$, and for the optimal design the poles are –0.9 and –3.88. The first design is slower than the optimal design, hence the difference in the time response is illustrated in Fig. 2.12.5.

In the IFT design, the first five iterations used the steepest descent with the estimate of the Hessian as the unity matrix and then the subsequent five iterations used the Gauss-Newton approximation since the solution was close to its minimum. The gain matrix parameters converge in ten iterations to the optimal solution designed via LQR. The evolution of the OF over these ten iterations is presented in Fig. 2.12.6.

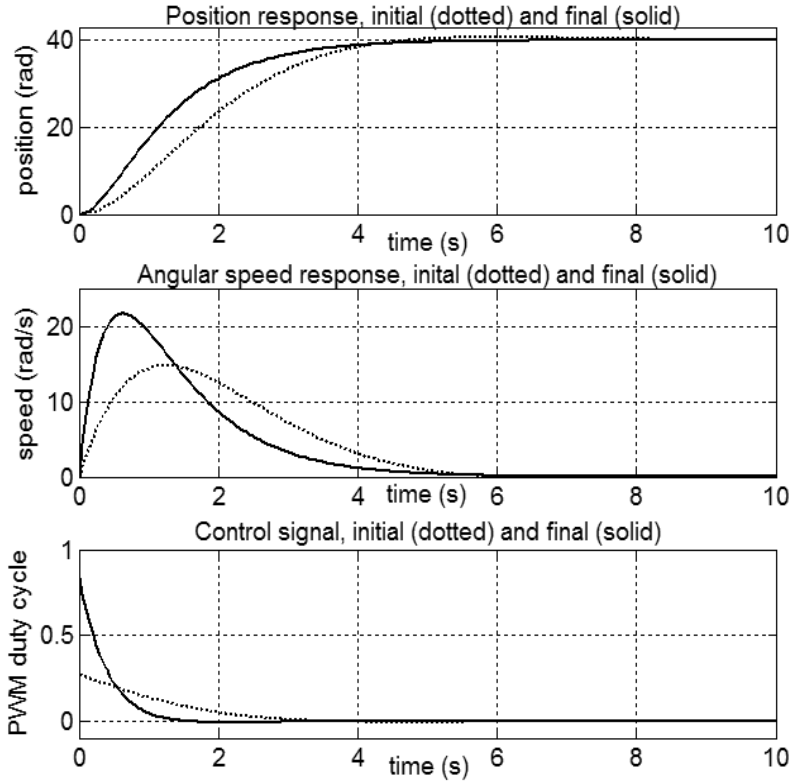

Fig. 2.12.5. Simulation results: control system responses of the CS with the initial controller parameters designed via pole placement and of the CS with the controller resulted after the optimal design towards which the tuning via IFT converges.

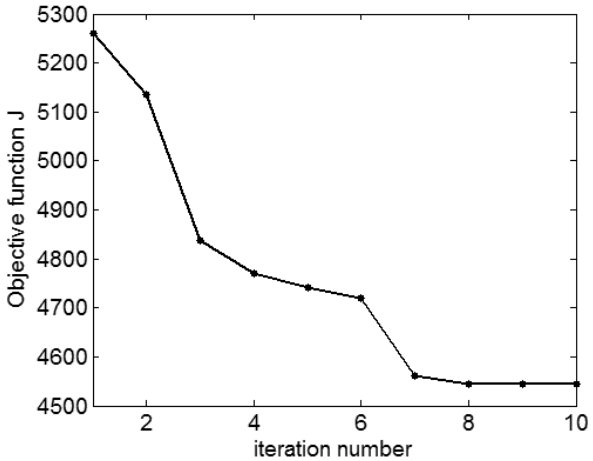

Fig. 2.12.6. The evolution of the objective function evolution for the tuning via IFT with the pole placement solution and converging to the optimal design via LQR.

The robustness properties of the pole placement design are not as good as in the case of the optimal design and this can be observed on the open-loop Bode

plots, where the phase margin and the crossover frequency get smaller. Therefore it can be motivating to use the IFT tuning to reach the optimal design when the model is imperfect and the design is based on the pole placement method.

The deterministic scenario is not acceptable in practice and if the state variables are measured the noise has to be taken into account when applying the IFT algorithm. As suggested in the Appendix A, an additional objective is targeted, viz. the minimization of the energy transfer from the process noise to the state variables. The robustness properties of the CS are normally expected to be deteriorated but this proves to be insignificant. In order to illustrate this aspect, IFT is applied in three additional scenarios, with the process noise now acting upon the CS. The noise w is considered to be zero-mean white noise with appropriate dimension with respect to (2.12.1) and with each element of equal variance. The variances corresponding to these three scenarios are $\sigma_w^2 = 1$, $\sigma_w^2 = 10$ and $\sigma_w^2 = 20$. Whereas in the deterministic case, the IFT-based solution converges to the true optimal state feedback gain matrix in (2.12.30), now IFT reaches

$$(\underline{\rho}^T) = [\rho_1 = 0.019500 \quad \rho_2 = 0.018580], \tag{2.12.31}$$

$$(\underline{\rho}^T) = [\rho_1 = 0.012323 \quad \rho_2 = 0.007201], \tag{2.12.32}$$

and

$$(\underline{\rho}^T) = [\rho_1 = 0.009623 \quad \rho_2 = 0.003569], \tag{2.12.33}$$

respectively. Due to the superposition principle the noise contribution in the objective function can be calculated for the three cases with process noise to be equal to 1.7%, 14.7% and 23.7%, respectively. The open-loop Bode plots are presented in Fig. 2.12.7.

Fig. 2.12.7 shows that with increasing noise intensity the phase margin gets smaller but still approximately 90^o. The crossover frequency also decreases which in turn lowers the closed-loop bandwidth but the decrease is not drastic. The gain margin is only reached at the Nyquist frequency and it is high, varying from 25 to 35 dB. Thus, the robustness properties still hold. This motivates the tuning to find the optimal solution that corresponds to the real-world process.

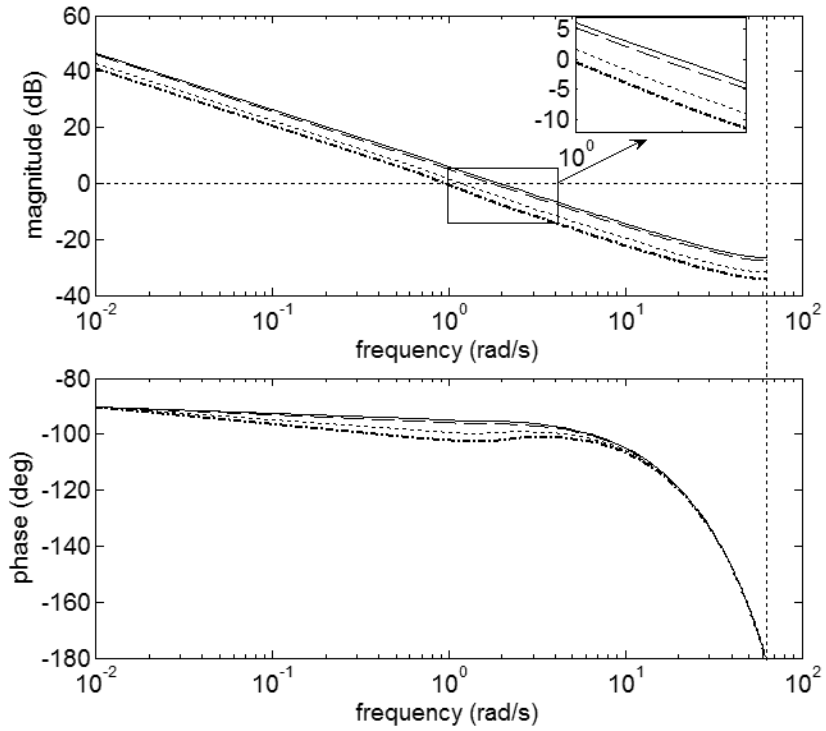

Fig. 2.12.7. The open-loop Bode plots of the state feedback CS after tuning with IFT: the true optimal solution in the deterministic scenario (solid), the scenario with the process noise of variance $\sigma_w^2 = 1$ (dashed), $\sigma_w^2 = 10$ (dotted) and $\sigma_w^2 = 20$ (dash-dotted).

In the deterministic scenario, the tuning via IFT converges to the optimal solution calculated with LQR only for constant reference inputs. This is equivalent to considering nonzero initial conditions for the process. For other reference inputs such as ramp, sine or white noise the solution does not coincide with the solution to the LQR problem. Secondly, if zero reference input is considered and the state feedback control system is excited only by the process noise and if the control signal in the objective function is not weighted anymore by setting $\lambda = 0$, the resulting system dedicated to noise rejection is not robust anymore.

A set of real-time experimental results is presented as follows. A first order low-pass digital filter with a cut-off frequency of 20 rad/s is used in the experiments to reduce the errors and the noise that occurs during the measurement of the angular speed. This filter will change the process model, but IFT is independent with this regard. This choice also supports the idea that the tuning can be carried out whenever the process model changes in time, without the need of identification and optimal redesign via LQR.

The experimental scenario is characterized by the same reference input vector, time horizon and sampling period as those used in the simulation.

The initial state feedback gain matrix is designed in terms of the LQR-based approach. The weights specific to this approach are chosen as in the simulations, and they do not cause the saturation of the actuator. Thus the undesired behavior due to the nonlinearities is avoided; this undesired behavior usually occurs in the

LQR-based approach where the nonlinear actuator is not included in the process model.

For benchmarking purposes the control system performance indices that are used are the OF, the control signal energy defined as

$$E_u = \sum_{k=0}^{N} (u(k))^2 , \tag{2.12.34}$$

the 10% to 90% rise time of the position response (t_r), and the maximum speed (ω_{max}). The IFT-based approach is next used to further reduce the OF taking advantage of the experiments conducted with the real-world process of the experimental setup.

In order to provide a relevant improvement, we start with a process model that is very different from the identified model. This is the same as assuming that the process model is time variant or that the identification is not accurate. The starting model for the LQR design uses the process parameters $k_P = 180$ and $T_\Sigma = 1.2\ s$ in the transfer function (2.12.27). For the weights set in accordance with (2.12.28) the state feedback gain matrix is

$$(\underline{\rho}^T)_{LQR\_4} = [\rho_1 = 0.020496 \quad \rho_2 = 0.021368] . \tag{2.12.35}$$

The gain matrix $(\underline{\rho}^T)_{LQR\_4}$ is further tuned using our IFT algorithm. The initial step size in the IFT algorithm employed to minimize the OF defined in (2.12.9) is set to the initial value $\gamma^0 = 2 \cdot 10^{-8}$, the values of the consequent step sizes are set in terms of (2.12.17), and $\underline{R}^i = \underline{I}_2$ is used.

The reduction of the value of the OF is emphasized to illustrate that our IFT algorithm ensures the performance improvement of the state feedback CS. The following expression of the gain matrix is obtained after 15 iterations:

$$(\underline{\rho}^T)_{LQR\_5} = [\rho_1 = 0.018900 \quad \rho_2 = 0.017355] . \tag{2.12.36}$$

The evolution of the OF with respect to the iteration number (i.e., during the tuning) is presented in Fig. 2.12.8. The evolutions of the controller parameters (i.e., the elements of the gain matrix) versus the iteration number are presented in Fig. 2.12.9. The time responses of the CS before and after the application of the IFT algorithm are presented in Fig. 2.12.10.

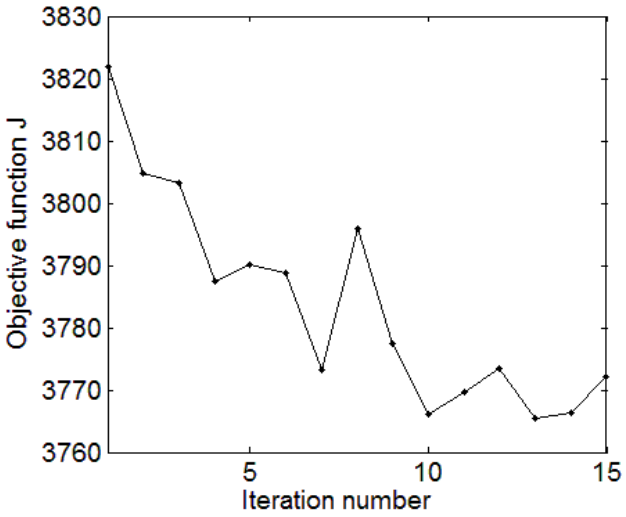

Fig. 2.12.8. Experimental results: the evolution of the objective function versus the iteration number.

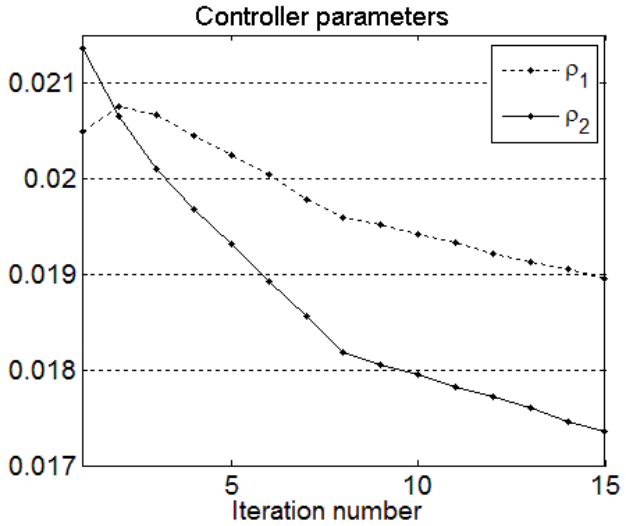

Fig. 2.12.9. Experimental results: the evolution of the controller parameters versus the iteration number.

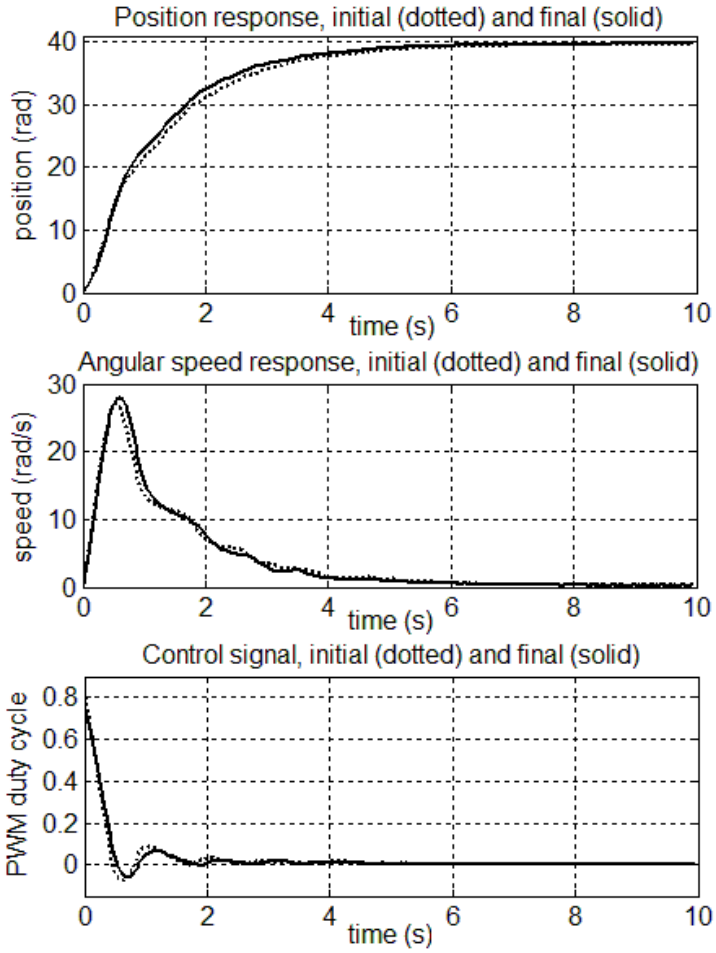

Fig. 2.12.10. Experimental results: control system responses of the CS before IFT and after IFT.

Fig. 2.12.8 illustrates that the OF is affected by random disturbances when it is evaluated on the real-world process. The values of the OF for the gain matrices defined in (2.12.35) and (2.12.36) are $J_{LQR\_4} = 3821.89$ and $J_{LQR\_5} = 3772.10$, respectively. The following performance indices were obtained:

- for the initial CS response (i.e., before IFT): $E_u = 2.5482$, $t_r = 2.94\ s$, $\omega_{max} = 27.0847\ rad/s$,
- for the final CS response (i.e., after IFT): $E_u = 2.4654$, $t_r = 2.53\ s$, $\omega_{max} = 27.9519\ rad/s$.

Since this section does not focus on using a very good model of the real-world process, the real-time experimental results were not presented in a similar style to that used for the simulation ones. As the LQR problem is developed in the deterministic case, it does not include the random elements in the design. However

the LQR was applied to the real-world process which is subject to random effects. That is the reason why the OF defined in (2.12.11) is a random variable. In other words, if no reference input is used to drive the state variables and the initial conditions are zero, the only inputs that drive the state variables are $\underline{w}$ and $\underline{v}$, therefore $J \neq 0$. In such cases the minimization of J is dedicated to reduce the energy transfer from the process noise to the state variables. Concluding, nonzero reference inputs are reflected by targeting three objectives: the minimization of the tracking error energy, the minimization of the control effort, and the noise rejection problem. The improvements via IFT shown in the previous section ensure the reduction of the OF value and of its variance, due to the lower sensitivity to noise. This idea is also backed up by the Appendix.

The time responses of the experimental results shown in Section 4 are not very different and this shows the robustness of state feedback CS with respect to the controller and process parametric variations. However, the solution is an evident improvement of the LQR design and when the noise contribution in the OF is small, it is expected that the tuning procedure gets near the optimal gain matrix which results in an optimal state feedback CS with robustness properties. When the noise contribution is important, the robustness properties of the optimal state feedback CS still hold as it is suggested by the simulation scenarios with included process noise.

The scenarios used in the previous section prove that the tuning can start with different points in the parameter space. All these different initial points lead to better results than those obtained by the LQR-based approach.

The weights in the optimization problems were set such that to ensure the linear operation of the process and of the actuator, viz., without entering saturation. The experimental results illustrate that the steady-state error of the position response is improved in spite of the process nonlinearities.

As shown in the previous section, IFT requires $1+n$ real-time experiments per iteration, n of them being successive gradient computation experiments. This number cannot be reduced using ideas similar to those presented in [18]-[20] because the number of gain matrix parameters is equal to the product between the numbers of process inputs and outputs.

Concluding, this section has presented an original IFT approach to improve the performance of state feedback CSs where the performance specifications are expressed to aim the minimization of OFs expressed as quadratic performance indices. A new IFT algorithm is suggested in this context, and comments concerning the implementation of the algorithm in several applications of single input processes are given. Our approach is general as it can be applied not only to positioning systems and to servo systems but also to other various applications [105]-[109].

The IFT approach, which is based on experiments conducted with the real-time CSs, provides an efficient way to deal with some of the specific problems of ill-defined processes when the strongly model-dependent LQR design gives solutions that are far away from the optimal solution. In such cases, when the LQR approach cannot anymore allow finding the minimum of the OF, the IFT approach can be applied to further reduce the OF. The experimental results presented in Section 4 show that the IFT approach, which allows an estimation the OF gradients on the basis of sensitivity functions' manipulation and of real-time measurements during the CS operation, can successfully be used.

A limitation of our IFT approach is that it actually ensures the strong improvement of the CS performance and the strong reduction of the OF only with

respect to the considered particular reference input. Modifications of the reference input will yield different results with different dynamic characteristics.

Our IFT approach does not use state estimators, being developed for a specific situation where all the states are measured. However, the introduction of state estimators in future research is not problematic because the estimator gain can also be included in the IFT algorithm.

Future research will deal with the extension of the proposed IFT approach to MIMO control systems and to the tuning of state feedback fuzzy control systems. Further study of the convergence of the IFT algorithms is needed for all applications including the nonlinear processes.

2.13. Stable Iterative Feedback Tuning technique for servo systems

Iterative Feedback Tuning (IFT) is a model-free direct data-based offline-adaptive controller tuning approach which has gained a lot of interest recently. It offers a solution to a stochastic optimization problem which is the translation of different control problems into Linear Quadratic Gaussian (LQG) performance criteria.

Many specific issues regarding IFT are currently solved including the IFT algorithm convergence [38], [47], [48] and the stability throughout the iterations [29], [110], [111]. Not only was the IFT algorithm merged with different control systems (CSs) paradigms but also plenty of applications have been reported that would make the subject of a long list. In order to increase the confidence in the algorithm, the stability along the iterations of the algorithm had to be tackled as already mentioned.

The idea of studying the closed-loop stability for data-based control is suggested in [110], where the objective function (OF) is expressed in frequency domain (hence the name Frequency Domain Tuning, FDT) and the gradient of the OF with respect to the controller parameters is calculated in terms of a frequency domain approach. The stability is ensured by calculating the generalized stability margin and the Vinnicombe distance between the old and the new controller. A frequency domain-based sufficient condition is proposed in [110] to guarantee the closed-loop stability, and a Spectral Analysis Algorithm (SPA) estimates the quantities involved in the computation. The need to compute the generalized stability margin was first emphasized in [29]. A relaxed sufficient condition compared to [110] is given in [111]. This test is devoted in fact to estimating, via spectral analysis, the frequency domain magnitudes of the transfer functions (t.f.s) of the output sensitivity function (S) and of the product of the process t.f. and S.

A similar approach for testing the stability under data-driven tuning of the controller for a Virtual Reference Feedback Tuning (VRFT) technique is proposed in [112]. However the testing requires the closed-loop to be opened and a filtered version of the open-loop gain is evaluated. In this approach the loop is maintained closed and thus stable, with no concerns about the regimes allowed for testing unstable processes. No assumptions are made about the stability of the process.

The above approaches are conservative in the sense that they provide only sufficient conditions for the stability of the closed-loop. Another paper which deals with stability of the loop under iterative controller design is [113] where a coprime

factor representation is proposed and the phase information derived on closed-loop is used to assert the stability through necessary and sufficient conditions. This is rather different to the wider-spread approach of using bounds on magnitude of t.f.s which give only sufficient conditions.

The new contribution of this section is a technique to guarantee the CS stability throughout the iterations of the IFT algorithm. The proposed technique makes use of a coprime factor uncertainty representation for the controller subject to tuning, and the small gain theorem for LTI discrete-time systems is applied with this regard. Bounds on the gain of the systems involved in the stability analysis are found from nonparametric models in frequency domain, which are typically easier to obtain than the parametric models. The new stable IFT technique presented in this section involves some computations concerning the same two t.f.s as those proposed in [110], and it is advantageous with respect to the state-of-the-art because of the transparency and simplicity of its three design steps.

This section gives the following results:

- The problem setup and the theoretical framework are first presented.
- Several techniques to estimate the L_2-induced gain (i.e., the H_∞ norm, referred to as the ∞-norm) of SISO Linear Time-Invariant (LTI) systems are next discussed from a comparative perspective. The discussion formulates recommendations on deciding upon using a particular estimation algorithm.
- A digitally simulated case study involving the application of the stable IFT technique to tune the controller parameters of a servo system is given.

The process is accepted to be a SISO LTI system described by

$$y(k,\underline{\rho}) = P(z^{-1})u(k,\underline{\rho}) + v(k), \tag{2.13.1}$$

where u is the input, y is the measured output, and v is the measurement noise. The process is controlled in a standard closed-loop setting with a discrete-time controller $C(q^{-1})$ such that

$$u(k,\underline{\rho}) = C(z^{-1},\underline{\rho})(r(k) - y(k,\underline{\rho})), \tag{2.13.2}$$

where r is the reference input. The main objective of IFT is to tune de controller to achieve perfect reference model (RM) tracking. The goal is achieved as an optimization problem in which the controller is parameterized and the parameter set is changed from one iteration to another in the main IFT algorithm. The IFT algorithm gathers data from the real process and it is offline. Several real-time experiments have to be performed during one iteration in order to calculate the next set of controller parameters according to the following update law:

$$\underline{\rho}^{k+1} = \underline{\rho}^{k} + \underline{\Delta}_k, \ \underline{\Delta}_k = -\gamma_k \, d\hat{J}(\underline{\rho}^{k}), \tag{2.13.3}$$

where: $\underline{\rho}^{k}$ and $\underline{\rho}^{k+1}$ – the parameter vector at the current and at the next iteration respectively, $\hat{dJ}$ – the estimate of the gradient of the OF $J(\underline{\rho})$ with respect to $\underline{\rho}$, γ_k – the step scaling coefficient, and $\underline{\Delta}_k$ is a correction term that includes both the estimate of the gradient of the OF and the step scaling coefficient. A steepest-descent algorithm in a stochastic approximation framework approach is used. The algorithm converges to the true minimum of the OF under certain assumptions on the step sequence $\{\gamma_k\}$ [16].

T he OF is usually defined as an LQG-type criterion of the general form

$$J(\underline{\rho}) = 1/(2N)E\{\sum_{k=1}^{N}[(y(k,\underline{\rho}) - y_d(k))^2 + \lambda u^2(k,\underline{\rho})]\}, \qquad (2.13.4)$$

where $y_d(k)$ is the desired RM trajectory, λ weights the control effort in the OF and the expectation operator $E\{.\}$ is taken with respect to the stochastic disturbance (which enters in the setup as in (2.13.1)). It can be seen (e.g. in [48]) that the OF can be split up in three components which correspond to three objectives of the optimization problem: RM tracking, control effort penalty and disturbance rejection.

The algorithm can only converge to a local minimum of the objective function and therefore it can not achieve global optimization. Moreover, it is not concerned with the stability of the closed-loop during the tuning procedure throughout iterations. Depending on the step size of the algorithm, problems can occur such that the closed loop becomes unstable.

In the following, a stable IFT technique is presented in a robust stability theoretical framework where the tuning of the parameters of the controller is seen as a coprime factor uncertainty as in [114]. The reason for this choice translates to a simple technique to calculated the scaling coefficient in (2.13.3).

We assume that an initial stabilizing controller exists in the beginning of the IFT algorithm that can be represented as the rational filter form

$$C(z^{-1}) = \frac{B(z^{-1})}{A(z^{-1})} = \frac{\sum_{i=1}^{m} b_i z^{-i}}{\sum_{i=0}^{n} a_i z^{-i}}. \qquad 2.13.5)$$

The controller is parameterized by the vector

$$\underline{\rho} = [b_1 \ldots b_m a_0 \ldots a_n]^T, \qquad (2.13.6)$$

which is included in an IFT-based tuning scheme subject to (2.13.3), and T indicates the matrix transposition. The correction term $\underline{\Delta}_k$ defined in (2.13.3) can be divided in two components representing the corresponding corrections for the nominator and the denominator of the controller. We can express this as

$$\underline{\Delta}_k = [\delta_B \; \delta_A]^T. \qquad (2.13.7)$$

These corrections acting on the nominator and on the denominator, respectively, will be treated in the following as uncertainties. We should make a difference between the current controller and the next controller by using the index k and k+1, respectively. The relation between them, expressed as a consequence of the IFT algorithm, is represented by

$$C_{k+1}(z^{-1}) = \frac{\sum_{i=1}^{m} b_i z^{-i} + \sum_{i=1}^{m} \delta_{Bi} z^{-i}}{\sum_{i=0}^{n} a_i z^{-i} + \sum_{i=0}^{n} \delta_{Ai} z^{-i}} = \frac{B(z) + B_\Delta(z)}{A(z) + A_\Delta(z)}$$

$$= \frac{C_k(z) + \Delta_B(z)}{1 + \Delta_A(z)}, \; C_k(z) = B(z)/A(z), \qquad (2.13.8)$$

$$\Delta_B(z) = B_\Delta(z)/A(z), \; \Delta_A(z) = A_\Delta(z)/A(z).$$

All discrete t.f.s are stable in the last form in (2.13.8) because of the division with the stable denominator polynomial $A(z)$. The insertion of the next controller in the closed-loop together with the corresponding nominator-denominator perturbations can be manipulated as in Fig. 2.13.1 (a) through the manipulation of the t.f. blocks. By aggregating the uncertainty polynomials into the line vector t.f. (matrix)

$$\underline{\Delta}_{AB}(z) = [-\Delta_A(z) \quad \Delta_B(z)] \tag{2.13.9}$$

as in Fig. 2.13.1 (b), we are able to manipulate the scheme into the standard upper linear fractional transformation (LFT) as suggested in Fig. 2.13.1 (b) in the upper right corner. This form is especially useful when analyzing the stability of the closed loop system.

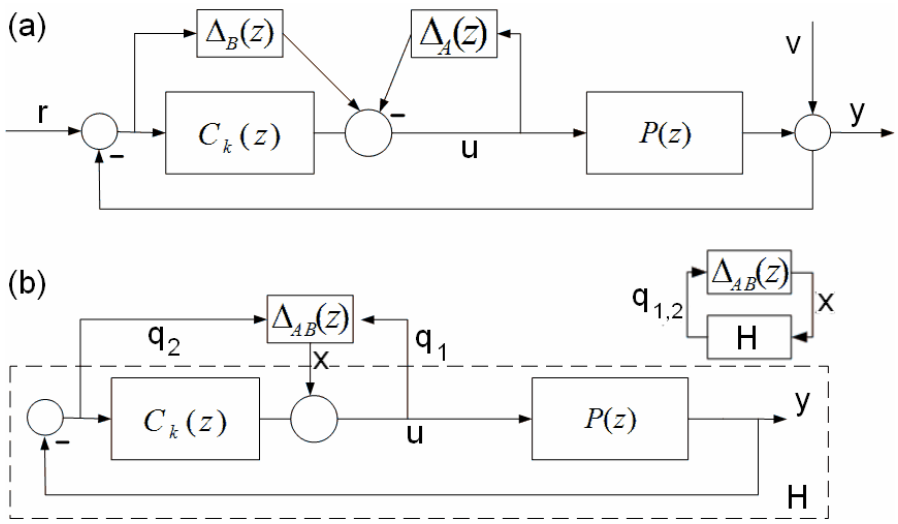

Fig. 2.13.1. Next controller built as uncertainty for the current controller (a), and reconfiguration to the standard upper LFT (b).

From the block algebra, it can be shown that the equivalent column transfer matrix $\underline{H}$ represents the transfer matrix from the scalar input x to the scalar outputs q_1 and q_2, expressed as

$$\underline{H}(z) = \begin{bmatrix} S(z) \\ -P(z)S(z) \end{bmatrix}. \tag{2.13.10}$$

The output sensitivity function denoted by $S(z)$ is

$$S(z) = 1/(1 + C_k(z)P(z)) . \tag{2.13.11}$$

A sufficient condition for the closed-loop stability for the LFT in Fig. 2.13.1 (b) is provided by a version of the small-gain theorem (e.g. [115]) applied for input/output stable (L_2 finite gain stable) discrete-time LTI systems which states that if

$$\left\|\underline{H}(z)\right\|_\infty \left\|\underline{\Delta}_{AB}(z)\right\|_\infty < 1, \tag{2.13.12}$$

then the closed-loop system is stable. The ∞-norm is the L_2-induced norm over the elements of the Hardy space H_∞.

We are sure that $\underline{H}$ is stable since we assumed previously that the current controller stabilizes the closed-loop. The term $\underline{\Delta}_{AB}(z)$ was set to be stable by construction.

In order to calculate the ∞-norm for the two transfer matrices involved in (2.13.12) it is first observed that both operators are vectors (column and line respectively) and that for a column vector $\underline{v} = [v_1 \quad v_2]^T$ or for a line vector $\underline{v} = [v_1 \quad v_2]$, we have a single singular value equal to $\sigma = \sqrt{|v_1|^2 + |v_2|^2}$. In this case, the ∞-norms for the two operators are

$$\begin{aligned} \left\|\underline{H}(z)\right\|_\infty^2 &= \sup_\omega\left(\left|S(e^{j\omega})\right|^2 + \left|P(e^{j\omega})S(e^{j\omega})\right|^2\right), \\ \left\|\underline{\Delta}_{AB}(z)\right\|_\infty^2 &= \sup_\omega\left(\left|\Delta_A(e^{j\omega})\right|^2 + \left|\Delta_B(e^{j\omega})\right|^2\right). \end{aligned} \tag{2.13.13}$$

Whereas the term corresponding to the uncertainties in (2.13.8) is known, and it can be calculated analytically, the first term depends on the process model which is unknown. However, by using an extra experiment at the current iteration of the algorithm, an estimate of the ∞-norm can be obtained experimentally. This is obtained by estimating the magnitude frequency response for the complementary sensitivity function denoted by T=1–S, which is in fact

$$T(z) = C_k(z)P(z)/(1 + C_k(z)P(z)). \tag{2.13.14}$$

The magnitude of S can next be calculated. Moreover, since we know $C_k(z)$ we can calculate the magnitude of

$$T(z)/C_k(z) = P(z)S(z), \tag{2.13.15}$$

which is exactly what we need in order to obtain the ∞-norm of $\underline{H}$, let it be α. Then, (2.13.12) results in the following sufficient condition for the closed-loop stability:

$$\left\|\underline{\Delta}_{AB}(z)\right\|_\infty < 1/\alpha. \tag{2.13.16}$$

This can be ensured since $\underline{\Delta}_{AB}(z)$ contains the step scaling coefficient from the update law in the IFT algorithm, namely $\gamma_k > 0$ which can be chosen such that to satisfy the condition (2.13.16). Thus, the norm of $\underline{\Delta}_{AB}(z)$ can be made arbitrarily small and this translates to scaling each correction term in the correction vector of the parameters of the controller.

If we use an uncertainty model for the updating controller such as

$$C_{k+1}(z) = C_k(z) + \Delta C(z), \tag{2.13.17}$$

it is not possible to pull out the scaling coefficient γ_k out of the uncertainty $\Delta C(z)$ when the denominator is also subject to tuning and thus a more complicated (expensive) search algorithm would have been necessary in order to calculate γ_k that satisfies (2.13.12).

A frequently used approach to controller design and tuning makes use of linear parameterization as in VRFT [53]. In this case, only the numerator of the controller t.f. is parameterized. This simplifies the stability analysis from our framework in the sense that $\underline{\Delta}_{AB}(z)$ consists only of $\Delta_B(z)$ and $H(z) = -P(z)S(z)$. The ∞-norm becomes more easily to calculate for $H(z)$ since it can be obtained experimentally from the magnitude-frequency characteristic. In the

case where H is a transfer matrix as in (2.13.13), one has to estimate successively the magnitude responses for $T(z)$, $S(z)$ and $-P(z)S(z)$, and next to conduct a search over the grid of frequencies at which the estimates were found to find the ∞-norm. In this case, the estimation errors add up and eventually give poor estimates. The focus should be on other approaches to estimate the ∞-norm in the MIMO case.

For the stochastic optimization to work it is necessary that [16]

$$\sum_{k=0}^{\infty}\gamma_k \text{ is divergent and } \sum_{k=0}^{\infty}\gamma_k^2 \text{ is convergent.} \tag{2.13.18}$$

Proceeding this way when getting close to the minimum the steps are smaller in order to prevent making large steps that could emerge from the noise-perturbed estimates of the gradient. A common choice for the sequence $\{\gamma_k\}$ is

$$\gamma_k = \gamma_0 / k,\ k = \overline{1,N}. \tag{2.13.19}$$

If the whole γ_k is subjected to the stability condition (2.13.16) then the steps would not respect the constraints of the stochastic algorithm. Instead of that the following choice is proposed here:

$$\gamma_k = c_k / k, \tag{2.13.20}$$

where only c_k is subjected to (2.13.16) and it is supposed to be an upper bounded positive quantity. Hence the proposed sequence still respects the conditions.

The proposed stable IFT technique can be summarized as follows.

1) Start with an initial stabilizing controller for the closed-loop system.

2) At each iteration, do the following:

- The normal experiment.
- The subsequent gradient experiments needed in the estimation of the gradient of the OF and eventually of the Hessian of the OF
- One additional experiment in order to estimate α (the ∞-norm of H). Find $\gamma_k > 0$ that satisfies (2.13.16) and calculate the next set of parameters using (2.13.3). Since the current controller stabilizes the loop so should the next controller given the small gain theorem.

3) Test the stopping condition which translates to only marginal improvements in the OF, or by calculating the Hessian of the OF near the minimum. If the condition is met, terminate the algorithm, otherwise go to step 2).

The burden is left to the gain-estimating algorithm from experimental data on the real process. Two widely spread approaches can be used to find the magnitude of the frequency response, i.e., to estimate the H_∞ norm from experiments. The advantages and drawbacks of these methods are discussed as follows.

Two popular approaches to estimate the ∞-norm are the Empirical Transfer Function Estimate (ETFE) [116] and the Frequency Response Function (FRF) [117]. The estimate of the nonparametric t.f. is basically the ratio of the Discrete Fourier Transform (DFT) (calculated using the Fast Fourier Transform (FFT) version) of the output and the input signals respectively. Under certain circumstances, this estimate is very accurate. Namely, the input is periodic and deterministic, the SNR is high on the measurement channels of the input/output, the noise acting upon the measurement channels is independent of the input/output. The periodic input eliminates the spectral leakage. The other requirements can be satisfied using high power at each input frequency so that the contribution of the noise at each

frequency is small compared to the deterministic signals. This however can be difficult and that is why the ETFE estimate is better used in narrowband systems, where it is easier to concentrate the power. One drawback is that this approach does not provide confidence intervals.

On the other hand, the Spectral Analysis Algorithm (SPA) [116] does provide confidence intervals for the estimate. It basically computes spectrum estimates of the input/output signals using a smoothed version of the (cross)-covariance functions for the input/output signals which is then Fourier transformed. The smoothing is done using a Hamming lag window of a certain width. The advantage of this approach is that it also estimates the spectrum of the noise and provides confidence bounds such as variance on the frequency response estimate. This can be used in checking the stability of the closed loop under controller tuning when estimating the gain of $\underline{H}$ is needed. The threshold of the inequality given in (2.13.12) can be lowered to account for estimation errors.

Two different approaches to estimation of the ∞-norm are presented in [112], [118]. In the first one, the ∞-norm of the systems is found as the solution of a convex optimization problem even in the presence of noise. A convex noise set is defined to keep the problem amenable to convex optimization. It makes use of only one input-output data set measured on the process.

The second solution uses successive experiments in a gradient-based search framework that aims at reshaping the input signal in order to maximize the input to output gain. The gradient of the gain objective function does not depend on the process model. The drawback in this context is that more experiments on the real system are needed.

There is an evident trade-off to these estimation algorithms to be accounted for when using different operating regimes in testing. Since the cost of the experiments on real processes can be prohibitive involving many calculations the choice of a certain estimation algorithm is subjective.

This section is dedicated to the presentation of a case study to apply the new IFT technique proposed in this section. The process is a servo system for which the angular position control is aimed. The continuous t.f. of the process is

$$P(s) = k_p /[s(1 + sT_p)], \tag{2.13.21}$$

with $k_p = 139.8$ and $T_p = 0.92\,s$ [17]. This model was not used anywhere in the application of the new IFT technique, but only for the sake of comparison. This servo system corresponds to a laboratory equipment with a DC motor and an inertial mass of 2 kg connected to the motor, and it is similar to other servo system applications [76], [121]-[123].

An initial discrete-time controller with the t.f. and the parameter vector

$$C(z,\rho) = (\rho_1 + \rho_2 z^{-1})/(1 + \rho_3 z^{-1}),$$
$$\underline{\rho} = [\rho_1 = 0.044 \quad \rho_2 = -0.03 \quad \rho_3 = -0.8181]^T, \tag{2.13.22}$$

was used. The controller design and tuning concerned only the improvement of the system response with respect to step reference inputs and not with respect to external disturbances. The pure deterministic case is considered. The CS performance specifications are expressed as RM tracking with no penalty on the control effort. The RM chosen for the achievable CS structure in terms of (2.13.21) and (2.13.22) was the discrete time equivalent of the continuous time model t.f. $M(s) = (1.556s + 15.56)/(s^3 + 21.11s^2 + 23.78s + 15.56)$, and the sampling period was set to $T_s = 0.01\,s$.

The tuning was performed only for the numerator parameters of the controller, i.e., ρ_1 and ρ_2, while the denominator is kept constant. The sequence $\{\gamma_k\}$ was implemented right from the first iteration according to (2.13.20). Since only the numerator is involved in tuning, the problem simplifies the estimation of the ∞-norm of $H(z)$ which consists only of $-P(z)S(z)$ as mentioned in Section II. Its norm is obtained by estimating the closed-loop magnitude Bode plot response from the load disturbance input to the output using Matlab's SPA. A pseudo-random binary signal was applied at the reference input.

The step response of the closed-loop with the initial controller is given in Fig. 2.13.2 (a) along with the response of the RM and the response of the CS after IFT. The estimated norm and the real norm of $-P(z)S(z)$ throughout the iterations are shown in Fig. 2.13.2 (b). The evolution of the OF is illustrated in Fig. 2.13.2 (c). The real and estimated magnitude Bode plots of the closed-loop t.f. with the initial controller are presented in Fig. 2.13.2 (d).

Fig. 2.13.2 (d) shows that the closed-loop has a resonant mode and the lag window in the SPA algorithm was chosen so that the peak in the response is revealed. The uncertainty at high frequencies is evident. The norm is underestimated at all iterations. This could affect the stability conditions. More importance was given to estimating the response at low frequencies. The peak of the initial closed-loop frequency response is matching the time response in Fig. 2.13.2 (a) for the initial controller.

The evolution of the parameters over the surface of the OF during the tuning is presented in Fig. 2.13.3. The steps lengths are suggested by segments delimited by circles. The algorithm runs in the valley where it bounces around with continuously decreasing step lengths.

The decreasing sequence $\{\gamma_k\}$ is very effective when abrupt slopes of the OF occur around the minimum, and it also prevents the possible bounces of the OF because of the stability test.

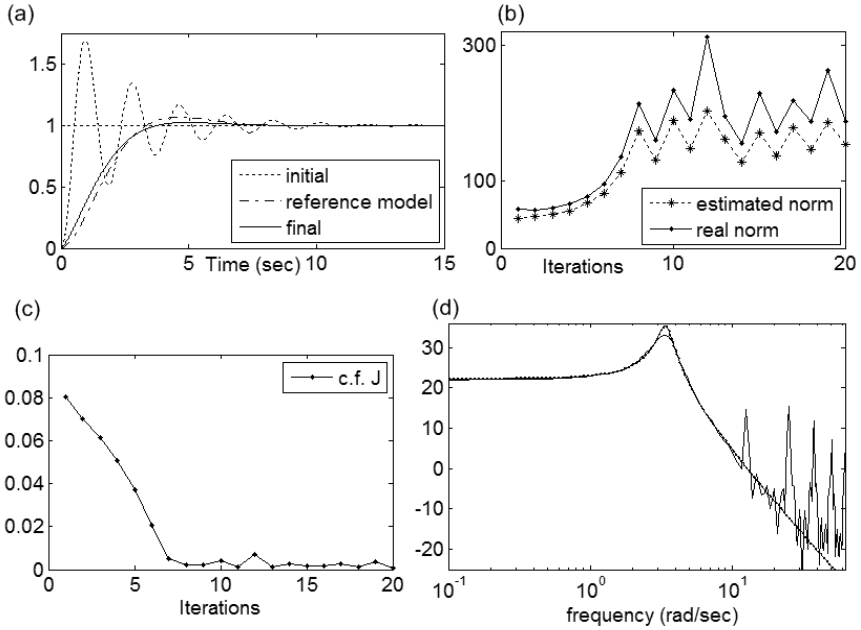

Fig. 2.13.2. Step response of control system as controlled output versus time (a), estimated and the actual norm at each iteration (b), OF evolution versus iteration number (c), and magnitude Bode plot of the closed-loop t.f. with the initial controller (d): real (solid) and estimated (dotted).

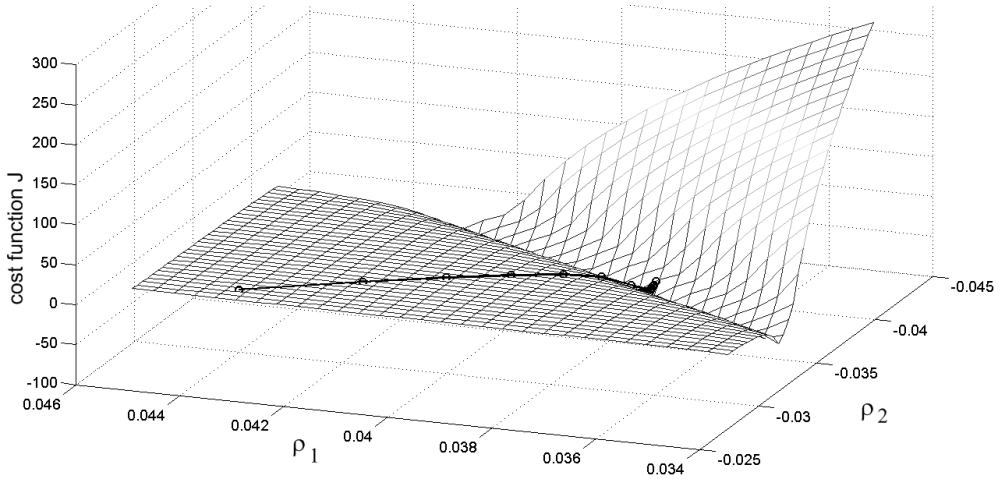

Fig. 2.13.3. Evolution of the parameters during tuning.

The proposed technique assists very well the tuning procedure of IFT. The stability condition sufficient, thus the result is conservative in the sense that better design choices are available. However the estimation of a nonparametric model in frequency domain is typically simpler than identifying parametric models, and this can be achieved using different techniques like ETFE or SPA. Just an additional experiment per iteration is needed to measure the frequency response. When the

experimenting conditions are restrictive, the testing could be done with the closed-loop in steady state by injecting a signal over the reference signal.

Concluding, the stable IFT technique proposed in this section is advantageous since it experiments on the closed-loop, so there are no concerns on experimenting unstable processes. In normal settings, the difference between the initial response and the desired response is not very large and thus we would not expect a very large number of iterations. It would be a mistake to require extreme performance from the closed-loop since it can not be guaranteed that the tuning performs in the desired direction without introducing some knowledge about the process. This implies additional information on the process leading to the existence and the uniqueness of the global minimum of the OF [48].

There is a certain need for better estimates of the ∞-norm of LTI systems in order to make them completely trustworthy. This however should be done without too much expense, and the compromise is to put an effort into a parametric model identification of the process that can be used throughout the iterations.

A limitation of our technique is the gap between the norms of the sampled-data systems which represent the true experimental conditions and the norms of their discrete-time equivalents. This can be mitigated in our case by appropriate constraints although a complicated approach is given in [119].

The future research will be focused on finalizing the laboratory implementation of the IFT algorithm developed on the basis of the stable IFT technique. The laboratory setup is characterized by the simplified mode given in (2.13.21), and it includes a motor-inertial mass setup, a backlash before the position encoder, and a dead-zone specific to the control signal. The application of our IFT algorithm is enabled by the frequency response estimation that works for smooth nonlinear processes.

2.14. Chapter conclusions

A brief summary of the results is presented in this section.

A comprehensive study of Iterative Feedback Tuning has been presented in Chapter 2. A general presentation of the tuning scheme was accomplished for one- and two-degrees of freedom controllers (1-DOF and 2-DOF). For the 2-DOF control structure, two subsequent situations are detailed for both simultaneous and separate parameter tuning. General aspects concerning the reference model selection, the search direction of the searching algorithm and issues related to the convergence of the algorithm to the solution, are presented. Subchapters 9 and 10 are dedicated to the translation of IFT to multiple-input multiple-output (MIMO) systems. Ideas on how to reduce the number of experiments at each iteration are suggested, due to the rapidly increasing number of parameters in MIMO controllers.

In subchapter 11, an original tuning scheme using IFT was presented and formulated in terms of a setup using state feedback control. The scheme shows to be effective for pole-placement-based solutions that need retuning either because of process aging or due to the large differences between the model and the real process. A solution to the search algorithm convergence is proposed in terms of Popov's hyperstability analysis theory. The results are validated on laboratory equipment represented by a modular servo system.

In subchapter 12, using the same structure with state-feedback control, the approach was translated to optimal control systems. The Linear Quadratic Regulator (LQR) and the Linear Quadratic Gaussian (LQG) control problems can be casted into optimization problems that are amenable for tuning via IFT. The optimality of the model-based paradigm in the design of optimal control systems is discussed in the light of the discrepancies between the process model and reality. In order to benefit from the guaranteed robustness properties of the LQR-based designed CSs, tuning via IFT is attempted. The case studies show some important facts: The optimal solution can be reached when we start from near a vicinity of the solution even if the process model is poor. Also, the optimal solution can be reached from an initial pole-placement solution which by its nature does not guarantee good robustness properties for the state-feedback structure. Thirdly, the inherent noise that affects the experimental-based tuning is shown to weaken the robustness of the CS but not to a substantial degree. The novel tuning scheme is also validated on laboratory equipment with a servo system.

Subchapter 13 deals with the stability issue between the iterations of the IFT. The solution makes use of a coprime factor uncertainty representation for the controller subject to tuning, and the small gain theorem for LTI discrete-time systems is applied with this regard. Bounds on the gain of the systems involved in the stability analysis are found from nonparametric models in frequency domain, which are typically easier to obtain than the parametric models. The frequency response functions can be obtained either via empirical transfer function estimate (ETFE) or by spectral correlation-based analysis (SPA). The results are supported by a simulation case study. The ideas can be considered to enlarge the overview of the iterative schemes and can render the approach into a suitable tool for maintaining the stability throughout the iterations. Several other techniques fall within the incidence of this approach, such as IRT, SPSA or CbT.

The new contributions of this chapter are:

1) The experimental validation of IFT on different laboratory equipment.
2) A novel IFT tuning scheme for state feedback controlled systems.
3) The implementation of IFT on MIMO systems with saturation on the actuator.
4) A novel approach to ensuring the search algorithm convergence by using Popov's hyperstability theory, which does not need in the formulation the knowledge of the minimum of the OF
5) A stable IFT technique that guarantees the closed-loop stability throughout IFT tuning by using a robust stability framework with the small gain theorem applied to a linear fractional transformation of the closed-loop when the modifications of controller's parameters are treated as uncertainties.
6) Solving the LQR design problem on experimental basis in terms of using the IFT technique, which is different to the model-based approach.

These new contributions were presented in the following papers:

***Rădac, M.-B.**, Precup, R.-E., Preitl, St., Tar, J. K., Fodor, J. and Petriu, E. M. (2008): Gain-Scheduling and Iterative Feedback Tuning of PI Controllers for Longitudinal Slip Control. Proceedings of 6th IEEE International Conference on Computational Cybernetics ICCC 2008, Stara Lesna, Slovakia, pp. 183-188, indexed in* **SCOPUS, INSPEC**.

*Precup, R.-E., Moşincat, I., **Rădac, M.-B.**, Preitl, St., Kilyeni, St., Petriu, E. M. and Dragoş, C.-A. (2010): Experiments in Iterative Feedback Tuning for Level Control of Three-Tank System. Proceedings of 15th IEEE Mediterranean Electromechanical*

Conference MELECON 2010, Valletta, Malta, pp. 564-569, indexed in **ISI Proceedings**.

***Rădac, M.-B.**, Precup, R.-E., Preitl, St. and Dragoş, C.-A. (2009): Iterative Feedback Tuning in MIMO Systems. Signal Processing and Application. Proceedings of 5th International Symposium on Applied Computational Intelligence and Informatics SACI 2009, Timişoara, Romania, pp. 77-82, indexed in* **ISI Proceedings**.

***Rădac, M.-B.**, Precup, R.-E., Petriu, E. M., Preitl, St. and Dragoş, C.-A. (2009): Iterative Feedback Tuning Approach to a Class of State Feedback-Controlled Servo Systems. Proceedings of 6th International Conference on Informatics in Control, Automation and Robotics ICINCO 2009, Milan, Italy, vol. 1 Intelligent Control Systems and Optimization, pp. 41-48, indexed in* **ISI Proceedings**.

***Rădac, M.-B.**, Precup, R.-E., Preitl, St., Petriu, E. M., Dragoş, C.-A., Paul, A. S. and Kilyeni, St. (2009): Signal Processing Aspects in State Feedback Control Based on Iterative Feedback Tuning. Proceedings of 2nd International Conference on Human System Interaction HSI'09, Catania, Italy, pp. 40-45, indexed in* **ISI Proceedings**.

***Rădac, M.-B.**, Precup, R.-E., Petriu, E. M., Preitl, St. and Dragoş, C.-A. (2011): Convergent Iterative Feedback Tuning of State Feedback-Controlled Servo Systems. In: Informatics in Control Automation and Robotics, Eds. Andrade Cetto, J., Filipe, J. and Ferrier, J.-L. (Springer-Verlag), pp. 99-111, indexed in* **SCOPUS**.

*Precup, R.-E., Preitl, St., **Rădac, M.-B.**, Petriu, E. M., Dragoş, C.-A. and Tar, J. K. (online first, Date of Publication: 03 August 2010): Experiment-based teaching in advanced control engineering. IEEE Transactions on Education, vol. PP, no. 99, pp. 1-11, DOI: 10.1109/TE.2010.2058575, **ISI** Science Citation Index impact factor (in 2009) = 1.157*.

***Rădac, M.-B.**, Precup, R.-E., Petriu, E. M., Preitl, St. and David, R.-C. (2011): Stable Iterative Feedback Tuning Method for Servo Systems. Proceedings of 20th IEEE International Symposium on Industrial Electronics ISIE 2011, Gdansk, Poland, pp. 1943-1948, indexată* **INSPEC**.

3. Virtual Reference Feedback Tuning (VRFT)

The idea behind the VRFT technique in model-reference control framework is related to the minimization of an objective function that penalizes the difference between the behavior of the designed closed loop and the behavior of the desired reference model [53], [54], [55]. This idea can be expressed as

$$J_{MR}(\underline{\rho}) = \left\| \left(\frac{P(z)C(z,\underline{\rho})}{1+P(z)C(z,\underline{\rho})} - M(z) \right) W(z) \right\|_2^2, \tag{3.1}$$

where $M(z)$ is the reference model expressed as a discrete-time transfer function, $P(z)$ and $C(z)$ stand for the process discrete-time transfer function and for the controller discrete-time transfer function respectively. $W(z)$ is a weighting filter and it can be understood in the frequency domain while being used as a degree of freedom in the design. The criterion makes use of the two-norm of a transfer function in discrete form. Another expression in the frequency domain can be employed due to the Parseval's theorem is

$$J_{MR}(\underline{\rho}) = \frac{1}{2\pi} \int_{-\pi}^{\pi} \left| \frac{P(e^{j\omega})C(e^{j\omega},\underline{\rho})}{1+P(e^{j\omega})C(e^{j\omega},\underline{\rho})} - M(e^{j\omega}) \right|^2 \left| W(e^{j\omega}) \right|^2 d\omega \,. \tag{3.2}$$

To solve the VRFT problem means to try and find the controller which minimizes the objective function. The solution reduces to an identification problem as explained. The following discussion assumes single input single output linear time-invariant process. The time argument is omitted for simplicity. Also, the deterministic case is considered leaving the situation when the noise affects the signals for another discussion. An excitation for the open loop process is considered as u for which the output y is recorded. The same output is considered to have been obtained by filtering a reference signal through the reference model M. Although M is causal and the inverse of it is not, the filtering can be done to obtain this virtual reference signal called r since y is available. A virtual feedback control structure is built with the controlled error $e = r - y$ feeding a controller with pre-specified structure called $C(z)$. Passing e through $C(z)$ should give us the initial signal used for excitation which is u. The parameters of the proposed structure of the controller which achieve the best fit between the filtered virtual error e and input signal u are the solution to an identification-like problem defined as an optimization problem which can be solved via least-squares if the parameterization of the controller is linear. Several manipulations lead to the fact that the solution to this problem can also be the solution to the model reference following problem. The discrete-time transfer function and the pulse transfer operator are used interchangeably for a correct notation.

Let the finite-time horizon criterion that describes the identification problem be defined as the objective function

$$J_{VR}^{N}(\underline{\rho}) = \frac{1}{N}\sum_{k=1}^{N}(u_L(k) - C(z,\underline{\rho})e_L(k))^2 \,, \tag{3.3}$$

where $u_L(k)=L(z)u(k)$ and $e_L(k)=L(z)e(k)$. The use of the filter $L(z)$ will be explained later. The objective function used in (3.3) has a solution that is denoted $\hat{\underline{\rho}}_N$ to show that it is an estimation obtained over a finite sequence of data. In the long run, as $N \to \infty$ we no longer speak about $J_{VR}^{N}(\underline{\rho})$ but we consider $J_{VR}(\underline{\rho})$ as being the asymptotic counterpart of $J_{VR}^{N}(\underline{\rho})$ which has the solution $\hat{\underline{\rho}}$. The solution $\hat{\underline{\rho}}_N$ converges to $\hat{\underline{\rho}}$ for the sequence length going to infinity. $J_{VR}(\underline{\rho})$ is defined as

$$J_{VR}(\underline{\rho}) = \lim_{N\to\infty}\frac{1}{N}\sum_{k=1}^{N}(u_L(k) - C(z,\underline{\rho})e_L(k))^2 \,. \tag{3.4}$$

Parseval's theorem can only be used for infinite length signals as is the case for the expression of the objective function in (3.4).

An important assumption is made for the analysis to follow. The existence of a controller which achieves perfect reference model following is assumed, let it be $C_0(z)$. Then it is valid to say that

$$\frac{P(z)C_0(z)}{1+P(z)C_0(z)} = M(z)\,. \tag{3.5}$$

A frequency domain expression for $J_{VR}(\underline{\rho})$ in (3.4) using Parseval's theorem leads to

$$J_{VR}(\underline{\rho}) = \frac{1}{2\pi}\int_{-\pi}^{\pi}\left|P(e^{j\omega})\right|^2\left|C(e^{j\omega},\underline{\rho}) - C_0(e^{j\omega})\right|^2\left|1-M(e^{j\omega})\right|^2\frac{\left|L(e^{j\omega})\right|^2}{\left|M(e^{j\omega})\right|^2}\varphi_u(\omega)d\omega \,. \tag{3.6}$$

We choose to omit the frequency dependent argument for simplicity. Recall that the filter $L(z)$ was intended to be used at choice. Let this choice be

$$|L|^2 = \frac{|M|^2|W|^2}{\left|1+PC(\underline{\rho})\right|^2}\frac{1}{\varphi_u}, \qquad \forall\omega\in[-\pi;\pi], \tag{3.7}$$

It can be seen that with this choice of the prefilter $L(z)$, the two objective functions in discussion become equal, $J_{VR} = J_{MR}$. Using this setting for the prefilter, while minimizing J_{VR} we also minimize J_{MR}. The only problem with this selection is that it depends on the process model $P(z)$ which is supposed to be unknown. To avoid this, another suggestion is made in choosing the prefilter as

$$|L|^2 = |1-M|^2|M|^2|W|^2\frac{1}{\varphi_u}, \qquad \forall\omega\in[-\pi;\pi], \tag{3.8}$$

which is equivalent to

$$|L|^2 = \frac{|M|^2|W|^2}{|1+PC_0|^2}\frac{1}{\varphi_u}, \qquad \forall \omega \in [-\pi;\pi]. \tag{3.9}$$

The difference between (3.7) and (3.9) is that we use C_0 instead of $C(\underline{\rho})$. So, the equality of the two criteria becomes only an approximation. In the original papers on VRFT, it is shown however that this advocated choice is in fact optimal by providing a connection between the two objective functions.

There are a few aspects that must be underlined:

- For a linear parameterization of the controller in the form $C(z,\underline{\rho}) = \underline{\beta}^T(z)\underline{\rho}$, the identification problem (3.3) rewrites:

  $$J_{VR}^N(\underline{\rho}) = \frac{1}{N}\sum_{t=1}^{N}(u_L(t) - \underline{\theta}_L^T(t)\underline{\rho})^2 ,$$

  where $\underline{\theta}_L(t) = \underline{\beta}(z)e_L(t)$. In this case, the well known least squares solution is

  $$\underline{\hat{\rho}}_N = \left[\sum_{t=1}^{N}\underline{\theta}_L(t)\underline{\theta}_L^T(t)\right]^{-1}\sum_{t=1}^{N}\underline{\hat{\theta}}_L(t)u(t) \ . \tag{3.10}$$

  This choice is at the same time restrictive but it renders the optimization problem convex in the space of the parameters, with unique solution. As will be seen, it is a good way of reaching somewhere nearby the global minimum of J_{MR}, which is by no means convex and may have more extremum points in which algorithms like CbT, IFT or IRT can get stuck.
- From the practical viewpoint, the technique requires pre specified parameterization of the controller while at the same time being model-free, as we don't need a model for the process. Chances are big that with such a parameterization, there is no possible combination of the parameters such that perfect reference model following is achieved. In the situation when we find ourselves in the class of the controllers that can achieve perfect following, the minimum of $J_{VR}^N(\underline{\rho})$ and also the one of $J_{MR}(\underline{\rho})$ are both 0 and for the same minimizing argument.
- In case we are not in the aforementioned class of controllers, because of the choice given in (3.8), the minimum of $J_{VR}^N(\underline{\rho})$ does not coincide with the minimum of $J_{MR}(\underline{\rho})$, neither do their minimizing arguments. This is an apparent obstacle but in fact creates the premises of using IFT further with the J_{MR} criterion.
- The theory was presented in a deterministic framework. When the stochastic case is also considered, noise acts on the process and therefore affects the measurements. The problem can be circumvented by the use of instrumental variable method to get the solution to the least squares identification in (3.10). One simple way is to use uncorrelated observation

vectors coming from different experiments upon which uncorrelated noise act. The effect of the noisy disturbance is that it makes the objective function $J_{VR}(\underline{\rho})$ even more different than $J_{MR}(\underline{\rho})$. This aspect is discussed in [53].

- A simple choice for the excitation signal u that affects the computation of the prefilter in (3.8) is a pseudo random binary sequence (PRBS) which approximates white noise. Apart from the fact that is has a constant spectrum – and no spectral factorization is needed to find a discrete transfer function that corresponds to this spectrum – and can be employed simple in (3.8), it also is persistently exciting helping in the identification problem.

- We must never forget that there is a difference between $J_{VR}^{N}(\underline{\rho})$ and $J_{VR}(\underline{\rho})$ (which of course have different minimizing solutions due to the difference in the time horizon) and there is also a difference between $J_{VR}(\underline{\rho})$ and $J_{MR}(\underline{\rho})$, which is because of the choice given in (3.8).

- There is no guarantee that the obtained set of parameters keeps the loop stable. In critical situations when stable operation is required, a crude model is the minimum that should be used to test stability margins, not to mention the possibility of not meeting the design specifications with the simple structure of the controller. However, the mismatch between model and reality is a constant source of problem for every control design strategy when tight specifications are required and data-based techniques become a valuable tool at hand.

3.1. Where VRFT and IFT meet

IFT differs from VRFT in the sense that it operates in closed loop and requires several "gradient" experiments per iteration. VRFT is typically a "one-shot" technique but it is limited in performance by the mismatch between the criteria. Moreover, the objective function is fixed and it is only dedicated to model reference following, with issues like disturbance rejection and robustness to parameter variations being only superficially asserted within the reference model. The sensitivity functions analysis is of course possible when process model is available. On the other hand, IFT is very flexible when it comes to formulating objective functions. One simple example is that the criterion can penalize the control effort which is important from the point of view of robust stability and robust performance. Several attempts have been made to use different objective functions [24], [25], [35]. Another very important feature of IFT is the ability of changing the objective function at any intermediate iteration, approach that has been called "windsurfing". For example, at one point the user could be interested only in model reference following and then find appropriate the penalization of the control effort. The major issues related to IFT are the need for an initial controller that stabilizes the loop and the stability analysis at each step, plus the convergence of the tuning algorithm.

The following analysis is employed in the framework of SISO time-invariant discrete-time systems, with stochastic elements. This analysis can be found in detail in [48].

Assume a process described as follows with (colored) noise acting on the output:

$$y(k) = P(q^{-1})u(k) + v(k)\,, \tag{3.1.1}$$

which in a closed loop negative feedback control structure with reference excitation on the input can be expressed as:

$$y(k) = T(q^{-1})r(k) + S(q^{-1})v(k) \tag{3.1.2}$$

The discrete transfer functions $T(q^{-1})$ and $S(q^{-1})$ are the complementary sensitivity function and the sensitivity function, respectively. The disturbance can be coloured noise obtained from white noise through linear filtering, like in $v(k) = H(q^{-1})e(k)$.

In this setting, an infinite-time horizon criterion for the purpose of applying IFT to tune the controller parameters can be expressed as

$$J_{IFT}(\underline{\rho}) = \lim_{N\to\infty} \frac{1}{N}\sum_{k=1}^{N} E\{\left(y(k,\underline{\rho}) - y_d(k)\right)^2 + \lambda u^2(k,\underline{\rho})\}\,, \tag{3.1.3}$$

although from obvious reasons, in practice we deal with finite-time horizon criterion

$$J_{IFT}^{N}(\underline{\rho}) = \frac{1}{N}\sum_{k=1}^{N} E\{\left(y(k,\underline{\rho}) - y_d(k)\right)^2 + \lambda u^2(k,\underline{\rho})\}\,.$$

The expression (3.1.3) includes both the model reference tracking and the control effort penalty. The operator $E\{.\}$ is the mathematical expectation taken with respect to the stochastic disturbance.

When the reference signal r and the disturbance v are uncorrelated, $J_{IFT}(\underline{\rho})$ can be written as

$$J_{IFT}(\underline{\rho}) = 1/N\sum_{k=1}^{N} E\left(\left(\left(T(q^{-1},\underline{\rho}) - M(q^{-1})\right)r(k)\right)^2 + \lambda u^2(k,\underline{\rho}) + \left(S(q^{-1},\underline{\rho})v(k)\right)^2\right) =$$

$$= J_y(\underline{\rho}) + J_u(\underline{\rho}) + J_e(\underline{\rho}), \tag{3.1.4}$$

where the three components in (3.1.4) are

$$J_y(\underline{\rho}) = 1/N\sum_{k=1}^{N} E\left(\left(\left(T(q^{-1},\underline{\rho}) - M(q^{-1})\right)r(k)\right)^2,\right)$$

$$J_y(\underline{\rho}) = 1/N\sum_{k=1}^{N} E\left(\lambda u^2(k,\underline{\rho})\right), \tag{3.1.5}$$

$$J_e(\underline{\rho}) = 1/N\sum_{k=1}^{N} E\left(\left(S(q^{-1},\underline{\rho})v(k)\right)^2\right).$$

In the previous expressions, $M(q^{-1})$ stands for the reference model.

In one of the simplest situations, the designer could aim for model reference closed-loop shaping. In absence of the disturbance acting on the output $J_{IFT}(\underline{\rho})$ is only comprised of $J_y(\underline{\rho})$. A frequency domain expression using Parseval's theorem is

$$J_Y(\underline{\rho}) = \frac{1}{2\pi}\int_{-\pi}^{\pi}\left|T(e^{j\omega},\underline{\rho}) - M(e^{j\omega})\right|^2 \varphi_r(\omega)\,d\omega\,. \qquad (3.1.6)$$

If the reference input spectrum $\varphi_r(\omega) = \left|W(e^{j\omega})\right|^2$ then $J_Y(\underline{\rho}) = J_{MR}(\underline{\rho})$, with J_{MR} from the VRFT setting. With this point of meeting between the two techniques, the idea is clear: since VRFT can not find the minimum of J_{MR} because of several reasons like

– the finite-time horizon in $J_{VR}^N(\underline{\rho})$,

– the contribution of the noise (in stochastic context) in $J_{VR}^N(\underline{\rho})$,

– the choice of the prefilter $L(z)$,

the search for the minimum of J_{MR} can be pursued using IFT. One thing that should not be changed at this point is the linear parameterization employed with VRFT, since the minimum of J_{MR} is yet to be found. So, in summary, VRFT helps IFT to reach somewhere close to the global minimum of J_{MR} (and saving iterations and possibly the IFT algorithm getting stuck), and then IFT carries the job further on. The advantages of using the current parameterizations are especially appealing as can be seen in the next section.

The equipment used to test and validate the VRFT technique is a INTECO DC servo system with backlash laboratory equipment. The experimental setup is illustrated in Fig. 3.1.1. An optical encoder is used for the measurement of the angle and a tacho-generator for the measurement of the angular speed. The speed can also be estimated from the angle measurements. The PWM signals proportional with the control signal u are produced by the actuator in the power interface, and use is made of the constraint $-1 \le u \le 1$.

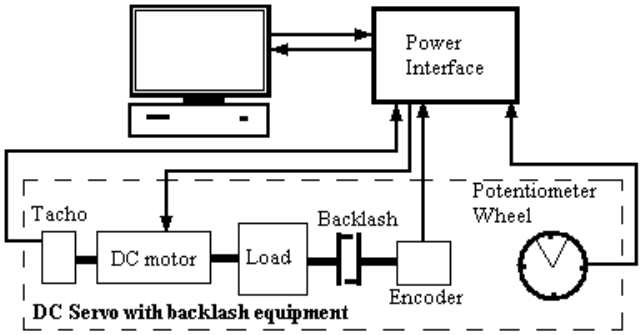

Fig. 3.1.1. Block diagram of experimental setup.

The purpose of the control is to make the position output follow a reference model trajectory for a step reference input. The reference model that is used is obtained through discretization from a second-order continuous transfer function for which the time response characteristics depend on the damping coefficient and the natural frequency as in

$$H_{Mr}(s) = \frac{\omega_0^2}{s^2 + 2\varsigma\omega_0 s + \omega_0^2}, \tag{3.1.7}$$

for which $\varsigma = 0.8$, $\omega_0 = 1$, and the sampling period is $T_s = 0.01$s.

The controller structure which contains an integrator is of the form

$$C(q^{-1}, \underline{\rho}) = (\rho_0 + \rho_1 q^{-1} + \rho_2 q^{-2} + \rho_3 q^{-3}) / (1 - q^{-1}). \tag{3.1.8}$$

For the purpose of calculating the virtual signals, an input signal that has a rich spectrum is used, namely a PRBS as shown in Fig. 3.1.2.

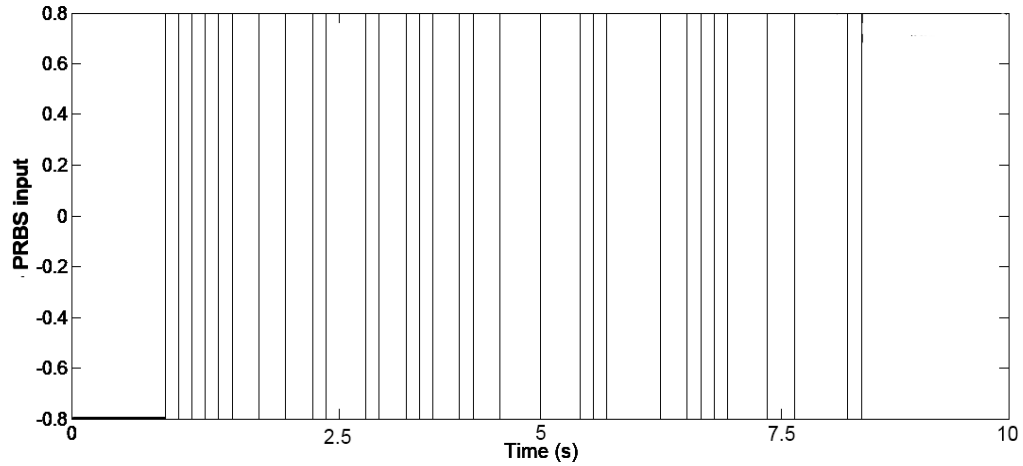

Fig. 3.1.2. PRBS input signal.

The position output that is collected in open-loop is presented in Fig. 3.1.3.

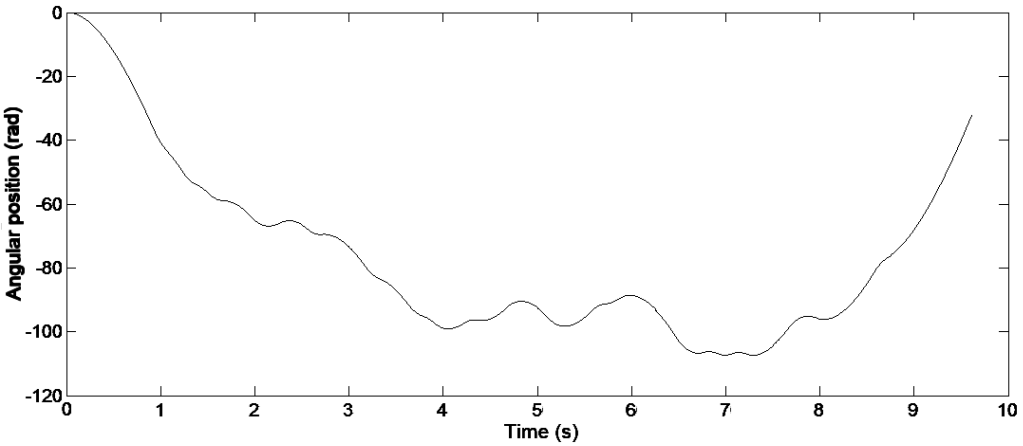

Fig. 3.1.3. Recorded position for the specific PRBS input.

To alleviate the effect of the noise on the estimate of the parameters in the least-squares solution, two observation vectors are used that come from two different experiments such that the noise coming from these experiments are uncorrelated.

The prefilter L is chosen of the form $|L|^2 = |1-M|^2|M|^2|W|^2 / \varphi_u$, with the input spectrum of the PRBS signal being constant since it is assumed to approximate white noise. For the choice of W we also choose it to be the spectral factorization of a white noise used as reference input. This choice is easier but it also implies that the J_{MR} is satisfied over the whole frequency range, and it means that any reference signal can be used since its spectrum is derived from the white noise's flat spectrum.

The obtained set of parameters with the proposed technique is $\underline{\rho} = [-0.0008 \quad 0.0177 \quad -0.0276 \quad 0.0107\ ]^T$, for which the position response compared to the response of the reference model is presented in Fig. 3.1.4.

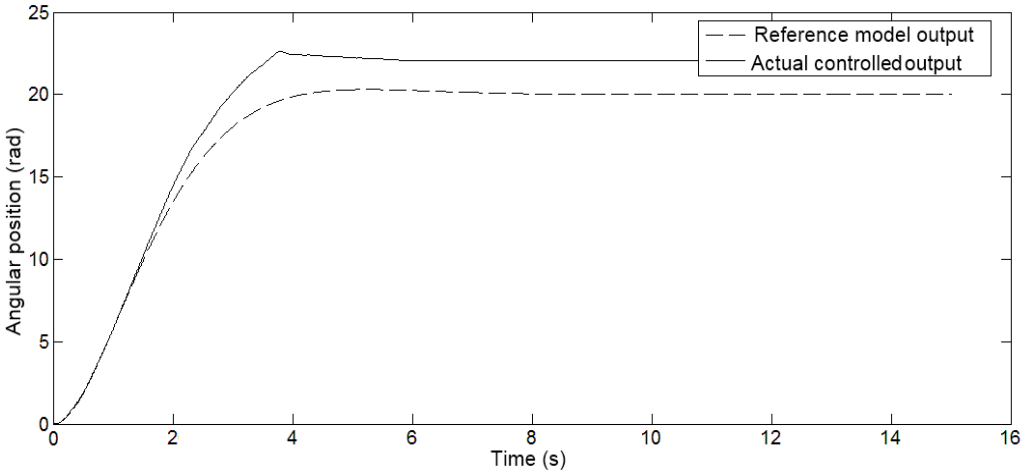

Fig. 3.1.4. Controlled position and the reference model output.

The precision is affected by the existence of a dead-zone in the actuator with a relatively large zone (spanning the interval -0.15…+0.15, about one third of the entire active zone of the actuator, that is -1…+1). This fact however was not used. The results can be further improved by the means of IFT, with inclusion of the penalty on the control input.

3.2. Computation of the estimate of the Hessian of the objective function with linear parameterized controller

Results with the computation of an unbiased estimate of the Hessian are available in the literature, but in a different context [57]. In the case of linear parameterization of the controllers and when combining IFT and VRFT, the advantages in tuning can be extremely effective.

In the following, the time argument is omitted when it necessary to simplify notation but keeping in mind it is there. Only the parameter dependency is suggested. It is assumed that

$$y(k) = T(q^{-1}, \underline{\rho})r(k) + S(q^{-1}, \underline{\rho})v(k), \tag{3.2.1}$$

where:

$$T(q^{-1},\underline{\rho}) = P(q^{-1})C(q^{-1},\underline{\rho})/(1+P(q^{-1})C(q^{-1},\underline{\rho}))\,,$$

$$S(q^{-1},\underline{\rho}) = 1/(1+P(q^{-1})C(q^{-1},\underline{\rho}))\,,$$

and ρ is the set of parameters. The partial derivative with respect to one parameter from the set of parameters is denoted as

$$\frac{\partial \bullet}{\partial \rho_i} = \bullet_i'\,. \tag{3.2.2}$$

It follows that:

$$y_i' = \frac{P(q^{-1})C_i'(q^{-1},\underline{\rho})(1+P(q^{-1})C(q^{-1},\underline{\rho})) - P(q^{-1})C_i'(q^{-1},\underline{\rho})P(q^{-1})C(q^{-1},\underline{\rho})}{(1+P(q^{-1})C(q^{-1},\underline{\rho}))^2} r -$$

$$- \frac{P(q^{-1})C_i'(q^{-1},\underline{\rho})}{(1+P(q^{-1})C(q^{-1},\underline{\rho}))^2} v =$$

$$= \frac{C_i'(q^{-1},\underline{\rho})}{C(q^{-1},\underline{\rho})} \frac{P(q^{-1})C(q^{-1},\underline{\rho})}{1+P(q^{-1})C(q^{-1},\underline{\rho})} \underbrace{\left(\frac{1}{1+P(q^{-1})C(q^{-1},\underline{\rho})} r - \frac{1}{1+P(q^{-1})C(q^{-1},\underline{\rho})} v\right)}_{e^{(1)}} =$$

$$= \frac{C_i'(q^{-1},\underline{\rho})}{C(q^{-1},\underline{\rho})} T(q^{-1}) e^{(1)}.$$

(3.2.3)

From (3.2.3), the well-known approach for computing the derivatives with respect to one parameter. These quantities are needed in the estimation of the gradient of the objective function. The way of experimenting is to inject the error from a normal experiment with usual reference input in the closed loop and then filter it through C_i'/C which can be calculated since it is known beforehand. Taking into account the fact that uncorrelated disturbances act on the closed loop at each experiment, we would obtain from the gradient experiment a perturbed version of the gradient of the objective function. Therefore, in the gradient experiment where the subscript suggests the experiment number, we have

$$y^{(2)} = \frac{P(q^{-1})C(q^{-1},\underline{\rho})}{1+P(q^{-1})C(q^{-1},\underline{\rho})} e^{(1)} + \frac{1}{1+P(q^{-1})C(q^{-1},\underline{\rho})} v^{(2)} \Bigg| \cdot \frac{C_i'}{C}\,, \tag{3.2.4}$$

and since the second term in the sum is still a noise with zero mean but with modified variance, it is valid to say that $E\{y^{(2)}\} = y_i'$. This can be used in the estimate of the gradient of the objective function.

The transformation of the recursive stochastic approximation IFT algorithm to a mixed stochastic Newton-Raphson algorithm could improve the convergence since we would have an estimate of the Hessian of the objective function. Including more information in the optimization scheme should be useful. Let the notation for partial second derivatives be $\frac{\partial^2 \bullet}{\partial \rho_i \partial \rho_j} = \bullet_{ij}''$. To compute the Hessian of the objective

function we would need terms of the form J''_{ij} which accounts for having computed y''_{ij}. The general term for the Hessian is

$$\frac{\partial^2 J}{\partial \rho_i \partial \rho_j} = \frac{2}{N}\sum_{k=1}^{N}(y'_i \cdot y'_j + \varepsilon \cdot y''_{ij}), \tag{3.2.5}$$

where $\varepsilon(k) = y(k) - y^d(k)$ is the reference model tracking error. The notation is further simplified by ommiting the dependance on ρ and q^{-1}. Continuing the calculations from (3.2.3) we will get the result

$$y''_{ij} = \frac{PC''_{ij}(1+PC)^2 - 2PC'_i(1+PC)PC'_j}{(1+PC)^4} r - \frac{PC''_{ij}(1+PC)^2 - 2PC'_i(1+PC)PC'_j}{(1+PC)^4} v =$$

$$= \ldots = -2\frac{C'_i C'_j P^2}{(1+PC)^2}\Big(\underbrace{\frac{1}{1+PC} r - \frac{1}{1+PC} v}_{e^{(1)}}\Big) = -2\frac{C'_i C'_j}{C^2}\frac{PC}{1+PC}\frac{PC}{1+PC} e^{(1)}, \tag{3.2.6}$$

where we have used the fact that because of the linear parameterization of the controller, the second derivative of the controller with respect to any parameter is zero. This simplifies the expressions in (3.2.6) showing how to do the experiments. The error from the initial normal experiments is fed as reference to the closed loop and then the output of this experiment is once more fed as reference. The resulting quantity is then filtered by a known computable filter. The useful fact is that the first gradient experiment has already been done in order to compute the first order partial derivatives and can be used in the final experiment. Now, we have to consider the noise contributions in this setting. After the first gradient experiment we obtain $y^{(2)} = \frac{PC}{1+PC} e^{(1)} + \frac{1}{1+PC} v^{(2)}$. After the third gradient experiment we obtain

$$y^{(3)} = \frac{PC}{1+PC} y^{(2)} + \frac{1}{1+PC} v^{(3)} = \frac{P^2C^2}{(1+PC)^2} e^{(1)} + \frac{PC}{(1+PC)^2} v^{(2)} + \frac{1}{1+PC} v^{(3)}. \tag{3.2.7}$$

Then, by appropriate filtering with $-2C'_i C'_j / C^2$, we obtain an estimate of the second-order derivative of the output. It can be seen that $E\{y^{(3)}\} = y''_{ij}$.

The issue that remains to be solved is concerned with the forming of unbiased second-order derivatives of the objective function in (3.2.5). We see that we have two adding terms, namely $y'_i \cdot y'_j$ and $\varepsilon \cdot y''_{ij}$. In the second term, the quantity y''_{ij} is correlated with the noises from the experiments, $v^{(1)}, v^{(2)}, v^{(3)}$. To obtain an unbiased term, the error ε should be obtained from another normal experiment, so correlated with none of $v^{(1)}, v^{(2)}, v^{(3)}$, but with a noise, say $v^{(4)}$. As for the first term of the sum, we have both y'_i and y'_j correlated with $v^{(1)}, v^{(2)}$. To avoid the problem here, the normal experiment for the error ε should be further used for a gradient experiment in order to obtain first-order partial derivatives of the output with respect to a parameter. Then, y'_j would be correlated

with the noises $v^{(4)}, v^{(5)}$, thus solving the unbiasedness property of the estimate of the hessian of the objective function. In this setting, two normal experiments and three gradient experiments are needed, with one gradient experiment of slightly different nature, in order to obtain both an unbiased estimate of the gradient of the objective function, and an unbiased estimate of the hessian of the objective function. In respect with the Robbins-Monroe stochastic approximation algorithm, what we would need for the algorithm to converge is an unbiased estimate for the gradient, a properly chosen sequence of step-scaling coefficients, and a positive definite matrix $\underline{R}^i$. It does not say anything about the matrix being an unbiased/biased estimate of the hessian of J. But this choice should be very efficient since it includes more information about the shape of the objective function.

One simple example is provided as follows to illustrate the efficiency of the combination between IFT and VRFT. Let the process be described by a discrete transfer function, $P(q^{-1})=q^{-1}/(1-0.6q^{-1})$ and a linearly parameterized controller with integrator component with a single parameter, $C=\rho/(1- q^{-1})$. The reference model is chosen as $M=0.6q^{-1} / (1 - 0.4q^{-1})$. The controller that achieves perfect reference model following is $C^*= (0.6 - 0.36q^{-1})/(1 - q^{-1})$ so we are not in the case where our controller belongs to the class of the controllers that solve perfectly the model tracking problem. With VRFT, the minimum of J_{VR}^N is $\rho=0.44$. With exhaustive search, the minimum of J_{MR} is shown to be $\rho^*=0.34$. Clearly, VRFT has a limitation but still has lead near the true minimum. Next, we employ IFT with hessian computation and without noise, with initial step-scaling coefficient being $\gamma_0 = 1$. In just one iteration, IFT hits the true minimum, $\rho^*=0.34$ showing the strength of the technique. Although the example is simple, it can be assumed the combination would work efficiently for more complex situations.

From this point, different directions can be pursued with modified criterion to include penalty on the control effort and/or modified reference model.

3.3 Chapter conclusions

In the following, a brief summary of the issues that are dealt with in this chapter are presented together with the new contributions list and the list of the disseminated results.

Chapter 3 was dedicated to the VRFT technique used as a tool in CSs tuning. VRFT and IFT can be viewed as counterparts of a complete tool aimed at CS design and fine tuning. For a proper formulation of the design objective (i.e. the objective function formulation), VRFT and IFT have an identical purpose. Benefiting from the flexibility of IFT which consists in the possibility of modifying the objective function along the iterations, different aims can be targeted such as control effort penalty or translation to control error penalty, and finally all the signals being weighted in time (or frequency domain) by using flexible filters. On the other hand, IFT can help VRFT to reach the minimum of the original objective function, an objective that is prohibited because the solution to the VRFT formulation is per se suboptimal.

The formulation of VRFT makes it suitable for the design of low complexity controllers such as the ones that predominate in industry. They have a major advantage which is also the key point of the VRFT algorithm: the linear

parameterization of the controller. Using a linear parameterization, the combination with IFT can be shown to be very effective in terms of obtaining estimates of the Hessian of the objective function, which is the major contribution of the chapter. This in turn can speed up the convergence of the algorithm since the use of the estimate of the Hessian is recommended when close to the solution. The idea is backed-up by simulations and real-time experiments on both angular velocity and angular position control for a laboratory servo system.

The new contributions of this chapter are:

1) A new tuning technique that combines the VRFT and IFT techniques to form a powerful tool to be used in controller tuning mainly for linear systems.
2) An exploitation of the linear parameterization of some very used controllers (PI, PID) used in the mixed VRFT-IFT technique, that allows for an easy computation of the Hessian estimate. This allows in turn the acceleration of the convergence of tuning and thus the reduction of the number of gradient experiments that is typical to IFT.

The results obtained in this chapter were published in:

***Rădac, M.-B.**, Grad, R.-B., Precup, R.-E., Preitl, St., Dragoş, C.-A., Petriu, E. M. and Kilyeni, A. (2011): Mixed Virtual Reference Feedback Tuning - Iterative Feedback Tuning Approach to the Position Control of a Laboratory Servo System. Proceedings of International Conference on Computer as a Tool EUROCON 2011, Lisbon, Portugal, paper index 453, 4 pp., indexed in* **INSPEC**.

***Rădac, M.-B.**, Grad. R.-B., Precup, R.-E., Petriu, E. M., Preitl, St. and Dragoş, C.-A. (2011): Mixed Virtual Reference Feedback Tuning – Iterative Feedback Tuning: Method and Laboratory Assessment. Proceedings of 20th IEEE International Symposium on Industrial Electronics ISIE 2011, Gdansk, Poland, pp. 649-654, indexed in* **INSPEC**.

4. Iterative Regression Tuning (IRT) and Simultaneous Perturbation Stochastic Approximation (SPSA)

Iterative Regression Tuning is another recent data-based algorithm for tuning controllers and is based on a computational approach [11], [12]. Similar in formulation to the IFT or VRFT approach, the idea behind this technique is to minimize a objective function which is dependent on the controller's parameters. The solution to the optimization problem however resembles with the one used in IFT. This technique uses a similar gradient descent approach to search for the set of parameters which minimize the objective function. It also assumes to be model-free in the sense that it makes no use of a process model in the tuning procedure. All fallacies of this approach are the same as in the case of IFT since the convergence of the algorithm and the stability of the loop have to be tested. Moreover, the algorithm could stop in a local minimum instead of finding the global one.

4.1. Overview of the IRT technique

The typical objective concerning IRT is to find the optimal parameter vector $\underline{\rho}^*$ to minimize the objective function (OF)

$$J(\underline{q}(\underline{\rho})) = \underline{w}^T \underline{q} = \sum_{i=1}^{M} w_i q_i \ , \tag{4.1.1}$$

where $\underline{w} = [w_1 \ \ ... \ \ w_m]^T$ is the weighting vector, $w_i \geq 0$, $i = 1...m$, are the weights, $q_i \geq 0, i = 1...m$, are the empirical CS performance indices, $\underline{q} = [q_1 \ \ ... \ \ q_m]^T$, and $\underline{\rho} = [\rho_1 \ \ ... \ \ \rho_n]^T$ is the parameter vector containing the tuning parameters of the controller. The objective can be formulated according to the definition of the optimization problem solved by IRT:

$$\underline{\rho}^* = \underset{\underline{\rho}}{\boldsymbol{arg\,min}} \, J(\underline{q}(\underline{\rho})) \, . \tag{4.1.2}$$

The IRT algorithms are employed to solve iteratively the optimization problem (4.1.2) where several constraints can be imposed, like the preservation of the closed-loop stability throughout the iterations. Measuring k samples of pairs $(\underline{q}(j), \underline{\rho}(j)), j = 1...k$, after several experiments / simulations done with the CS in the so-called k local iterations [11] the following two matrices are expressed:

$$\underline{\Theta} = \begin{bmatrix} \underline{\rho}^T(1) \\ \dots \\ \underline{\rho}^T(k) \end{bmatrix}, \ \underline{Q} = \begin{bmatrix} \underline{q}^T(1) \\ \dots \\ \underline{q}^T(k) \end{bmatrix}, \tag{4.1.3}$$

where the superscript T stands for matrix transposition.

The data preprocessing is important in the signal processing applications concerning IRT. Therefore a Gaussian assumption is made stating that the sets of data samples are centered locally and scaled to the unity variance [11], [12].

Starting with a set of data obtained by experiments / simulations, a linear model F can be estimated such that

$$\underline{q} = \underline{F}^T \ \underline{\rho}, \tag{4.1.4}$$

where $\underline{F}^T$ is the matrix of the linear map between the two linear input and output spaces:

$$\underline{F}^T : R^n \to R^m. \tag{4.1.5}$$

The application of the linear map to the set of k samples leads to the matrix form of (4.1.4):

$$\underline{Q} = \underline{\Theta}\,\underline{F}. \tag{4.1.6}$$

The linear models (4.1.4) or (4.1.6) are valid only in the vicinity of the current parameters referred to as nominal ones and considered as the elements of the vector $\underline{\rho}$. Consequently the solution to (4.1.2) can not be found in a single step, and the iterative solving by means of IRT algorithms is needed.

The use of gradient descent in IRT algorithms is convenient. The approximated gradient $\frac{dJ}{d\underline{\rho}}$ is calculated from (4.1.1) and (4.1.4):

$$\frac{dJ}{d\underline{\rho}} = \frac{d}{d\underline{\rho}}(\underline{w}^T \underline{F}^T \underline{\rho}) = \underline{F}\,\underline{w}. \tag{4.1.7}$$

The update law to calculate the next parameter vector $\underline{\rho}(K+1)$ in IRT algorithms makes use of the negative direction of the gradient:

$$\underline{\rho}(K+1) = \underline{\rho}(K) - \gamma \frac{dJ}{d\underline{\rho}} = \underline{\rho}(K) - \gamma\, \underline{F}(K)\, \underline{w}, \tag{4.1.8}$$

where K is the index of the global iteration and γ is the step size. The notation $\underline{F}(K)$ in (4.1.8) illustrates the fact that the matrix $\underline{F}$ is estimated in several local iterations at each global iteration step.

The values of γ and w can be variable during the operation of the IRT algorithm accounting for the robustness and convergence analyses. Besides (4.1.8) can be viewed as Newton's algorithm which is generally used as a convenient technique to iteratively approach a zero of a function without knowledge of its expression. The stochastic environment must be considered in all analyses.

The unimodality of the data is crucial for the approach and is used to infer the validity of the linear local model and also throws the constraint on the smoothness of the chosen performance indices as function of the parameters. The unimodality is tested by doing a lot of simulations with different combinations of the design parameters. These combinations are chosen on a stochastic basis such that each individual parameter is chosen from a normal distribution. The performance

indices are calculated after each simulation. The resulting distribution of each performance index should be Gaussian. This should occur because a linear combination of gaussian random variables is a gaussian random variable too. There is also another case when one can obtain a gaussian distribution from linear combinations of different kinds of distributions of random variables, and this is guaranteed by the central limit theorem. This however can be shown for a large number of samples.

IRT fails to solve the problem of the existing gap between the model and the real process since the data is supposed to be collected during *simulations* rather than experiments. This is an issue whenever tight specifications are required. Local linear models are developed under the unimodality assumption of data and a large numbers of simulations are necessary to test the assumptions and to derive the gradients. However, the novelty of the technique is that the objective function can be defined in a very flexible way, by aggregating performance indices of different nature, not constrained to LQG-type criteria. This is the reason for which the IRT technique could be seen as a generalization for IFT. The flexibility of the objective function is important because the performance indices can address problems like model reference tracking, sensitivity shaping for improving robustness of the CS. One other advantage could be the use of IRT on complex systems, with nonlinear behavior.

It is also important that a domain-related expert helps in defining the performance indices that form the objective function. The expertise is necessary to respect the constraints of the technique. The indices need to be continuous and relatively smooth functions of the parameters in order to approximate the derivatives. At top level, the indices that are aggregated in the objective function will usually be of contradictory nature. The solutions of the optimization could be pareto-optimal and the expertise is needed again in selecting among the best ones in order to facilitate the implementation.

It would be of great importance to use the increased flexibility of IRT when it comes to objective function definition, but use data from the real-time experiments [120]. For obvious reasons, the validation of the data unimodality of the data in the context of real experiments is prohibitive. Moreover, the real-time experiments are affected by random disturbances that we may not know of and therefore can not be modeled and included in simulations. This brings us again to the problem of the stochastic approximation theory that was employed in IFT by the Robbins-Monro procedure. Fortunately, a technique that brings the meta-heuristics to help solving optimization control problems is available: Simultaneous Perturbation Stochastic Approximation (SPSA). Otherwise, the convergence conditions of the stochastic approximation algorithms have to be proven, that is the estimate of the gradient of the objective function is unbiased and the step scaling sequence has to be chosen carefully to ensure the convergence.

The validation of the IRT algorithm is done in terms of a case study dealing with the angular position control of the INTECO DC servo system with backlash laboratory equipment [120]. An optical encoder is used for the measurement of the angle and a tacho-generator for the measurement of the angular speed. The speed can also be estimated from the angle measurements. The PWM signals proportional with the control signal u are produced by the actuator in the power interface, and use is made of the constraint $-1 \le u \le 1$. The equipment is described in Fig. 4.1.1.

The process is modeled as

$$\begin{bmatrix} \dot{\alpha} \\ \dot{\omega} \end{bmatrix} = \begin{bmatrix} 0 & 1 \\ 0 & -\frac{1}{T_S} \end{bmatrix} \begin{bmatrix} \alpha \\ \omega \end{bmatrix} + \begin{bmatrix} 0 \\ \frac{K_S}{T_S} \end{bmatrix} u, \tag{4.1.9}$$

$$y = \alpha,$$

with the t.f.

$$P(s) = K_S /[s(1 + sT_S)] . \tag{4.1.10}$$

The process modeled in (4.1.9) and (4.1.10) is characterized by the parameters $K_S = 174$ and $T_S = 0.7\ s$ obtained by experimental identification. The overshoot and the rise time are aggregated in the objective function. The applied weights are $w_1 = w_2 = 1$. Accepting the quasi-continuous digital control with the sampling period of 0.01 s, the initial parameters of the PI controller of the form $C(s) = k_C[1 + 1/(T_i s)]$ with parameter vector being $\underline{\rho} = [k_C \quad T_i]^T$, tuned by Ziegler-Nichols's method, are $k_C = 0.1$ and $T_i = 0.7\ s$.

The behavior of the CS with the initial controller parameters with respect to the step type modification of the set-point is illustrated in Figs. 4.1.2 and 4.1.3. The corresponding value of the OF is J=0.9294.

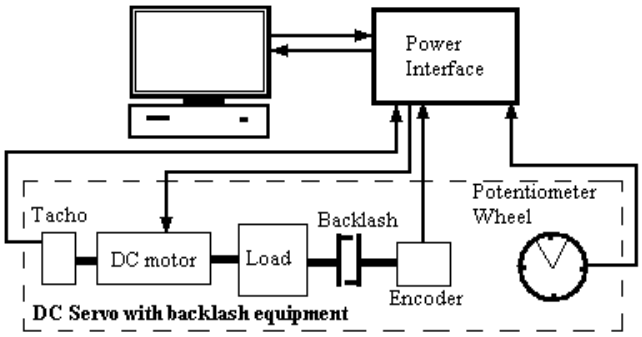

Fig. 4.1.1. Block diagram of experimental setup.

Using the step size $\gamma = 0.001$ the OF obtains the value J=0.9005 after the first global iteration. The behavior of the CS after the first iteration of the IRT algorithm is shown in Figs. 4.1.4 and 4.1.5. A rather small improvement of the CS performance indices can be observed.

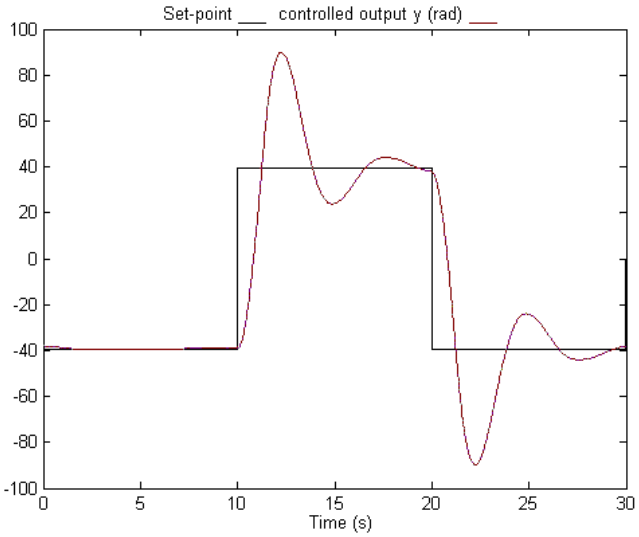

Fig. 4.1.2. Set-point and controlled output versus time for the CS with the initial parameters of PI controller parameters (before the application of the IRT algorithm).

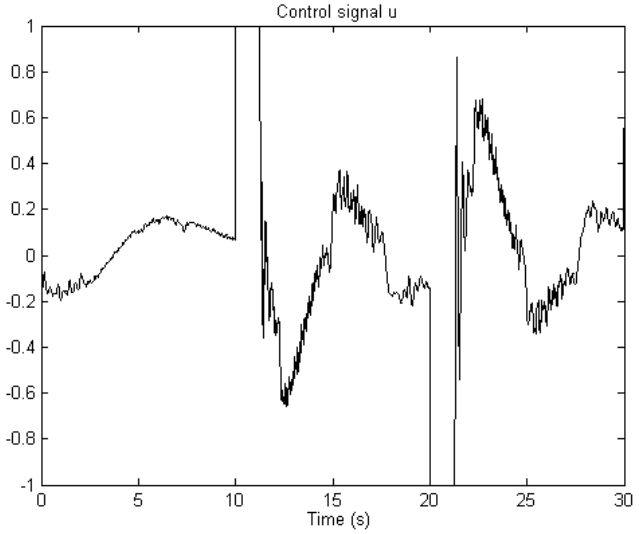

Fig. 4.1.3. Control signal versus time for the CS with the initial parameters of PI controller parameters (before the application of the IRT algorithm).

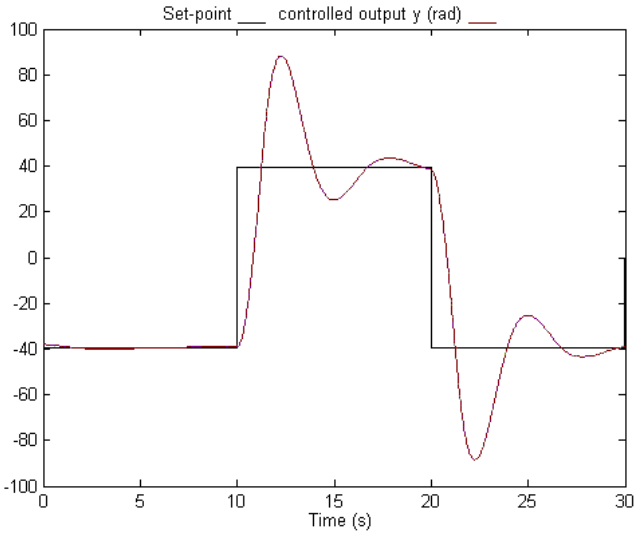

Fig. 4.1.4. Set-point and controlled output versus time for the CS with the values of PI controller parameters after the first iteration of the IRT algorithm.

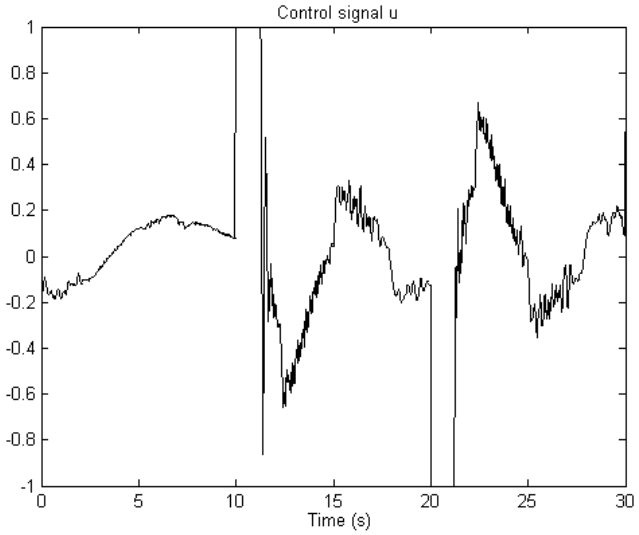

Fig. 4.1.5. Control signal versus time for the CS with the values of PI controller parameters after the first iteration of the IRT algorithm.

The controller parameters after three global iterations obtain the values $k_C = 0.004$ and $T_i = 2.8\,s$. The OF obtains the value J=0.8885. The behavior of the CS after the three iterations of the IRT algorithm is presented in Figs. 4.1.6 and 4.1.7.

The CS performance enhancement, characterized by reduced overshoot and settling time can be observed. The performance with respect to the set-point can be enhanced further if set-point filters are included. The behavior with respect to the disturbance input is not presented because the integral component in the controller ensures the disturbance rejection.

All signal processing aspects mentioned in the previous section were used in the implementation of the IRT algorithms for the considered conventional CS structure with linear PI controller. The controller is implemented as a quasi-continuous digital controller with anti-windup measure.

The conditions (4.1.12) and (4.1.13) were applied to set the value of the step size. The saturation of the actuator is shown in Figs. 4.1.3, 4.1.5 and 4.1.7, and the backlash yields oscillations in u.

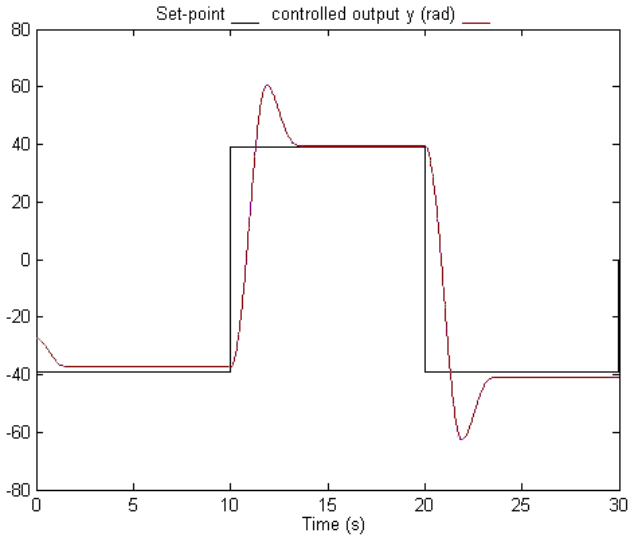

Fig. 4.1.6. Set-point and controlled output versus time for the CS with the values of PI controller parameters after the application of the IRT algorithm.

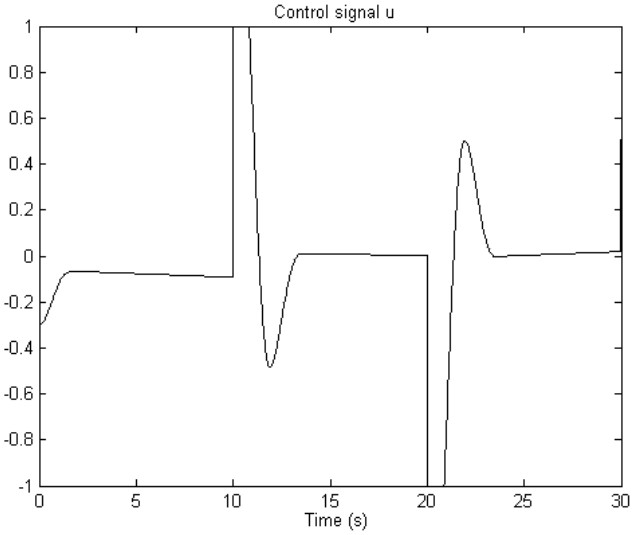

Fig. 4.1.7. Control signal versus time for the CS with the values of PI controller parameters after the application of the IRT algorithm.

4.1.1 A solution to the convergence of the IRT algorithm

To ensure the convergence of the gradient method in order so search the minimum of the OF the value of the step size γ in (4.1.8) is of crucial importance. From one application to another the step size may vary during the global iterations of the IRT algorithms. In the case of IFT algorithms the problem is mentioned in [48] and solved in [47] ensuring the convergence by guaranteeing the stability of the algorithm.

The following quadratic Lyapunov function candidate is defined to guarantee the convergence of the IRT algorithm for the nominal parameters $\underline{\rho}$:

$$V(\underline{\rho}) = (\underline{\rho} - \underline{\rho}^*)^T (\underline{\rho} - \underline{\rho}^*),\ \underline{\rho} \in \underline{D} \subset R^m . \tag{4.1.11}$$

The Lyapunov stability approach requires that the set D is a domain of attraction if

$$V(\underline{\rho}(K+1)) - V(\underline{\rho}(K)) < 0 \quad \forall\, \underline{\rho}(K) \in \underline{D},\ \underline{\rho}(K) \neq \underline{\rho}^* . \tag{4.1.12}$$

Use is made of (4.1.8), (4.1.11) and (4.1.12) to calculate

$$\begin{aligned} &V(\underline{\rho}(K+1)) - V(\underline{\rho}(K)) = -2\gamma\, [\underline{\rho}(K) - \underline{\rho}^*]^T \underline{F}(K)\, \underline{w} + \\ &+ \gamma^2 [\underline{F}(K)\, \underline{w}]^T \underline{F}(K)\, \underline{w} < 0 \quad \forall\, \underline{\rho}(K) \in \underline{D},\ \underline{\rho}(K) \neq \underline{\rho}^* , \end{aligned} \tag{4.1.13}$$

and (4.1.13) leads to the following condition guaranteeing that $\underline{D}$ is a set of attraction and the IRT algorithm is convergent:

$$\begin{aligned} &\gamma < 2[\underline{\rho}(K) - \underline{\rho}^*]^T \underline{F}(K)\, \underline{w} \,/ \\ &/\{\underline{w}^T [\underline{F}(K)]^T \underline{F}(K)\, \underline{w}\} \quad \forall\, \underline{\rho}(K) \in \underline{D},\ \underline{\rho}(K) \neq \underline{\rho}^* , \end{aligned} \tag{4.1.14}$$

which is enabled by the following sufficient condition to ensure $\gamma > 0$:

$$[\underline{\rho}(K) - \underline{\rho}^*]^T \underline{F}(K)\, \underline{w} > 0 \quad \forall\, \underline{\rho}(K) \in \underline{D},\ \underline{\rho}(K) \neq \underline{\rho}^* . \tag{4.1.15}$$

The inequalities (4.1.14) and (4.1.15) are useful in setting the value of the step size. Moreover the step size can be variable but controlled during the global iterations of the IRT algorithms such that the conditions (4.1.14) and (4.1.15) are fulfilled.

The vector $\underline{\rho}^*$ is not known in (4.1.14) and (4.1.15). The parameter vector which ensures an ideal controller can be used instead of $\underline{\rho}^*$. However the ideal controller can be obtained assuming a poor model of the controlled process is known and making use of a reference model which ensures the best possible CS performance indices for the given CS structure. This approach leads to a set of attraction which is different to D in (4.1.11).

4.2. Overview of the Simultaneous Perturbation Stochastic Approximation (SPSA)

Using the steepest descent recursive form expressed as

$$\underline{\rho}^{k+1} = \underline{\rho}^k - \gamma_k \underline{\hat{g}}_k(\underline{\rho}^k) , \tag{4.2.1}$$

we usually have the gradient of the objective function at the *k*-th iteration, at the current point in the parameter space, $\underline{\rho}^k$. Unlike with steepest descent, the stochastic approximation algorithms use estimates gradients of the objective function, $\underline{\hat{g}}_k$. In IFT, it is possible to calculate the gradients by using data from the real time experiments. However, when such schemes can not be employed, the gradients have to be estimated on the basis of the objective function noisy measurements by forming finite difference approximations (FDA) around the current point. Proven the fact that this estimates are unbiased, under specific conditions regarding the existence of a minimum of the objective function, the differentiability with respect to the parameters, and a suitable selection of the step-scaling coefficient sequence $\{\gamma_k\}$, the Robins-Monroe stochastic approximation states that the sequence of parameters $\{\underline{\rho}^k\}$ converges to the set of parameters that minimize the objective function *J*, let it be $\underline{\rho}^*$. The idea behind finite difference approximations is to evaluate the argument of the objective function around the current iterate argument and then to use the noisy measurements to form estimates of the gradient. One can use one-sided approximations, or two-sided approximations. For two-sided approximations, a general estimated gradient is

$$\underline{\hat{g}}_k(\underline{\rho}^k) = \begin{bmatrix} \dfrac{y(\underline{\rho}^k + c_k\underline{\xi}_1) - y(\underline{\rho}^k - c_k\underline{\xi}_1)}{2c_k} \\ \dots \\ \dfrac{y(\underline{\rho}^k + c_k\underline{\xi}_p) - y(\underline{\rho}^k - c_k\underline{\xi}_p)}{2c_k} \end{bmatrix}, \tag{4.2.2}$$

where ξ_i is a *p*-dimensional vector, with *p* the dimension of the parameter vector which has 1 on *i*-th place and 0 elsewhere and c_k is the difference magnitude coefficient . The quantities *y* represents noisy measurements for the objective function. The sequences $\{\gamma_k\},\{c_k\}$ are degrees of freedom in finite difference stochastic approximations (FDSA) algorithm. One problem with this approach is that the estimate is biased due to the noise and the convergence to ρ^* is ensured for gains respecting the conditions: $\gamma_k > 0$, $c_k > 0$, $\gamma_k \to 0$, $c_k \to 0$, $\sum_{k=0}^{\infty}\gamma_k = \infty$, and $\sum_{k=0}^{\infty}\gamma_k^2 / c_k^2 < \infty$ [9], [10]. Another problem is the fact that 2*p* measurements of the objective function are needed every iteration which comes in contradiction with the experiment's costs. The costs increase with the number of parameters. This is why SPSA has emerged to reduce the costs burden with the idea to use only two evaluations of the objective function per iteration. The idea is to randomly perturb the arguments and then to form the approximations to the gradient by finite difference:

$$\hat{\underline{g}}_k(\underline{\rho}^k) = \begin{bmatrix} \dfrac{y(\underline{\rho}^k + c_k\underline{\Delta}_k) - y(\underline{\rho}^k - c_k\underline{\Delta}_k)}{2c_k\Delta_{k1}} \\ \cdots \\ \dfrac{y(\underline{\rho}^k + c_k\underline{\Delta}_k) - y(\underline{\rho}^k - c_k\underline{\Delta}_k)}{2c_k\Delta_{kp}} \end{bmatrix}. \tag{4.2.3}$$

The numerator in (4.2.3) is the same for all the components in the gradient vector and only the denominator is different, proportional to the variation of the corresponding parameter in the set. The standard condition about the elements Δ_{ki} is that they are independent, identically distributed with symmetric distribution around zero, and of bounded magnitude. Moreover, there is a condition related to the inverse moments of these random variables so that a suitable distribution that respects all these requirements is a Bernoulli distribution. A normal distribution is shown to reduce the performance of the algorithm [10]. The same constraints are preserved as in the case of FDSA for the gain sequences. Also, a modified search that is similar to the deterministic Newton-Raphson algorithm can be employed, when in the same manner, attempts are made to estimate the Hessian of the objective function.

The SPSA algorithm can be employed on minimization of various objective functions, not constrained to LQG-type criteria, and maybe most important, it can be applied on nonlinear systems. These two advantages over IFT make it a very useful tool. It can only be used for tuning but not for CS design. This means that we have to start with a fixed structure used for control which stabilizes the closed-loop. The same problems that are related to the convergence speed of the algorithm and the stability of the closed-loop during iterations need to be addressed. Although it is model-free in the tuning step, asserting the robust stability and performance still needs a process model. For example, using the ν-gap distance like in [29], the stability can be checked at each step. Ideas to use SPSA with IFT are already present in the literature [51].

4.2.1. Data-based optimization of state feedback control systems for Single Input-Single Output processes

The data-based control paradigm has evolved consistently over the last years with the purpose of helping the control engineers in the design task of control system (CS) structures. The main aspect that characterizes the techniques that belong to this category is the fact that no process model is needed in the controller design and tuning. The idea could, at least theoretically, compensate for the identification efforts in trying to find a very good model or for the process complexity and some times for the modeling effort which requires multidisciplinary efforts.

An important feature of data-based control techniques is the use of additional in formation on the process by inspecting the data collected from the process's operation in terms of conducting less informative experiments that affect the normal functioning conditions. This idea narrows the general gap between the theory and the practice of control design.

The most frequently used data-based control techniques are Iterative Feedback Tuning (IFT), Virtual Reference Feedback Tuning (VRFT), Correlation-

based Tuning (CbT), Frequency Domain Tuning (FDT), Iterative Regression Tuning (IRT), and Simultaneous Perturbation Stochastic Approximation (SPSA). Two of the representative techniques, viz. IFT and SPSA, are based on Stochastic Approximation (SA) results that are used in the general context of stochastic optimization. That is really important since the stochastic effects should be considered if the data-based control techniques are applied in real-world processes.

IFT and SPSA have similar roots in gradient-based stochastic approximation algorithms. IFT uses the Robbins-Munro's SA and uses an unbiased estimate of the gradient of the objective function (OF) through experiments. SPSA starts with Kiefer-Wolfowitz's SA algorithm where an estimate of the gradient of the OF is obtained via finite differences. IFT and SPSA were developed for slightly different purposes, i.e., IFT was developed within the area of CS design and SPSA was developed for more general-purpose optimization applications.

The drawing of the complete connections of these data-based algorithms with all the related disciplines of control engineering is a tremendous effort, and it is not the intended aim of this contribution. The intended purpose of this study is to reveal the applicability of these algorithms on a large class of control design problems with focus on the data-based optimization of state feedback control systems for Single Input-Single Output (SISO) processes using Linear-Quadratic-Gaussian (LQG)-based OFs.

The state feedback CSs are widely used due to the advantages offered by the state-space mathematical modeling highlighted in various applications [124]-[126]. The improvement of the CS performance is normally obtained by optimization in terms of the minimization of OFs expressed as integral quadratic performance indices [79], [127]-[133], that also provides a convenient way to deal with the degrees of freedom associated to the pole placement design of Multi Input-Multi Output (MIMO) systems.

The Linear-Quadratic Regulator (LQR) method which is frequently used for the tuning of the optimal state feedback CSs can actually be used only when linearized or linear models of the process and the knowledge on all state variables available for feedback are assumed [134], [135]. The similar LQG problem concerns both optimal estimation and optimal control. The separation principle allows for separate design of the optimal Kalman filter and the optimal control gain.

IFT offers a direct data-based offline-adaptive controller tuning approach. IFT performs a gradient-based minimization of the OF, and it provides an efficient way to deal with some of the specific problems of nonlinear or ill-defined processes. The OF minimization algorithm uses data obtained from the real-time experiments conducted with the real-world CS.

A good overview of the standard IFT is given in [27]. The extension of IFT according to [38] provides additional steps to improve the convergence properties of IFT while rejecting the disturbances. The input-output signals of the process are employed in [85] to identify a linear time-varying model of the process which is further used in IFT. IFT applications to industrial control problems are reported in the literature, for example, for the control of chemical processes [58] and for servo drive control [39], [75]. Discussions of the IFT approach to the nonlinear process control are given in [15], [59], [60].

SPSA was introduced in [8],[136] as an efficient alternative to Finite Difference Stochastic Approximation (FDSA) algorithm in which the number of evaluations of the OF per iteration is equal to the number of the variables of the OF, viz. the number of tuning parameters in case of optimal control. SPSA uses only two

OF evaluations per iteration resulting in reduced costs with advantages when the measurements associated to the evaluations are conducted on real-world processes.

Many attractive applications of SPSA algorithms are reported in the literature in relation with parameter estimation of neural networks [137], [138], drive systems [139], model predictive control [140], intelligent control [141], neural network-based fault detection and isolation [142], filter design [143] or motion planning for mobile robots [144]. The reduction of the number of evaluations of the OF per iteration to only one is suggested in [145].

The new contributions of this section are:

- The performance comparison of IFT and SPSA is offered. These two data-based model-free gradient-based stochastic optimization techniques are analyzed in the general framework of state feedback control meant for a class of SISO processes aiming the minimization of LQG-based OFs.
- New IFT and SPSA algorithms based on a new experimental setup in the gradient experiments to calculate the gradients of the OF are proposed.
- Our theoretical approaches are validated by simulation and experimental results that correspond to the angular position of a DC servo system laboratory equipment.

This section treats the following aspects:

- The discussion of the LQG servo controller problem.
- The proposal of a new IFT algorithm and its formulation in terms of the control problem defined previously.
- The description of SPSA and of the algorithm to solve the same control problem.
- The implementation of our IFT and SPSA algorithms in a case study. Digital and experimental results concerning the optimal state space control of the angular position of a DC servo system laboratory equipment are included.
- The discussion of IFT versus SPSA.

The definition of the LQG servo controller problem uses a process characterized by the continuous-time Linear Time-Invariant (LTI) SISO state-space model

$$\begin{aligned} \underline{x}(k+1) &= \underline{A}\,\underline{x}(k) + \underline{B}\,u(k) + \overline{B}\,\underline{w}(k), \\ y(k) &= \underline{C}\,\underline{x}(k) + \underline{D}\,u(k) + \overline{D}\,\underline{w}(k) + \underline{v}(k), \end{aligned} \tag{4.1.2.1}$$

where k, $k \in N$, is the discrete time argument, u is the control signal, $\underline{x} = [x_1 \ \ldots \ x_n]^T \in R^n$ is the state vector, n is the system order, y is the controlled output, $\underline{A} \in R^{n \times n}$, $\underline{B} \in R^{n \times 1}$, $\overline{B} \in R^{n \times n}$, $\underline{C} \in R^{1 \times n}$, $\overline{D} \in R^{1 \times n}$ are constant matrices, $\underline{D} = const \in R$, $\underline{w} \in R^n$ and $v \in R$ are the uncorrelated process state noise vector and measurement noise, respectively, that include the normal independent identically distributed random variables with zero means and the variances σ_w^2 and σ_v^2, respectively. Zero initial conditions are assumed throughout this section for the process dynamics without affecting the generality. It is accepted that the process is controllable and observable.

The corresponding deterministic discrete-time LTI SISO state-space model of the process is

$$\begin{aligned} \underline{x}(k+1) &= \underline{A}\,\underline{x}(k) + \underline{B}\,u(k), \\ y(k) &= \underline{C}\,\underline{x}(k) + \underline{D}\,u(k). \end{aligned} \tag{4.1.2.2}$$

Our discussion is restricted as follows to the class of strictly causal processes with $\underline{D} = 0$ and $\overline{D} = 0$.

The LQR optimal control problem accounting for the deterministic system (4.1.2.2) is used in an iterative fashion, and it offers an alternative for the popular pole placement method. In this setting, the optimal control is concerned with minimizing infinite-horizon discrete-time quadratic performance index $I(K)$

$$I(K) = \sum_{k=0}^{\infty} [\underline{x}^T(\underline{K}(k),k)\,\underline{Q}\,\underline{x}(\underline{K}(k),k) + \lambda\, u^2(\underline{K}(k),k)]\,, \qquad (4.1.2.3)$$

subject to process dynamics (4.1.2.2), where T indicates the matrix transposition,

$$\underline{Q} \geq 0,\ \underline{Q} = [q_{ij}]_{i,j=\overline{1,n}},\ q_{ij} = q_{ji},\ i,j = 1,2,...,n,\ \lambda > 0\,, \qquad (4.1.2.4)$$

are the weights and $\underline{K}(k) \in R^{1\times n}$ is the time-varying state feedback gain matrix in the state feedback control law

$$u(k) = -\underline{K}(k)\underline{x}(k)\,. \qquad (4.1.2.5)$$

Equations (4.1.2.3) and (4.1.2.5) highlight that the evolution of the signals involved in (4.1.2.2) depend on the choice of the matrix $\underline{K}(k) \in R^{1\times n}$. The argument k will be dropped out in the sequel, but we will keep in mind that it influences the process dynamics.

The optimization of the state feedback control systems can be formulated as the problem of finding an optimal gain matrix $\underline{K}^*$ defined as

$$\underline{K}^* = \underset{\underline{K}}{\boldsymbol{arg\ min}}\, I(\underline{K})\,. \qquad (4.1.2.6)$$

The optimization problem (4.1.2.6) subject to the equality-type constraints (4.1.2.2) without noise essentially is the well known discrete-time LQR problem. The solution to this optimization problem is the solution of a Discrete time Algebraic Riccati Equation (D-ARE). For practical purposes, the steady-state solution for this equation is used very often.

The LQR is known to be very robust with respect to process parameter variations [91],[92]. It also assumes that full state feedback is employed while all state variables are measurable. However this situation is rare in practice, and the state variables should be observed or estimated using either state observers designed via pole placement or state estimators which are optimal with respect to the estimation error. This leads to the LQG estimation and control problem and the solution of it (that is also obtained as a solution to a D-ARE) finds an optimal estimator gain, further denoted L, that offers a compromise between the speed of the estimator and the noise alleviation and an optimal state feedback gain. The LQG design does not guarantee generally the robustness of the CS structure.

The OF for the LQG problem formulated in a stochastic framework is defined as

$$I(\underline{K},\underline{L}) = E\{\sum_{k=0}^{\infty} [\underline{x}^T(\underline{K},\underline{L},k)\,\underline{Q}\,\underline{x}(\underline{K},\underline{L},k) + \lambda\, u^2(\underline{K},\underline{L},k)]\}\,, \qquad (4.1.2.7)$$

where the expectation $E\{\}$ is taken with respect to the stochastic disturbances $\underline{w}$ and v. In order to design the optimal filter (i.e., the Kalman filter), the noise intensities have to be supplied, that is the covariance matrices of the noises

$$\underline{QN} = E\{\underline{w}(k)\underline{w}^T(k)\} \in R^{n\times n},\ \underline{RN} = E\{v^2(k)\} \in R\,, \qquad (4.1.2.8)$$

and the cross-covariance matrix

$$\underline{NN} = E\{\underline{w}(k)v(k)\} \in R^{n\times 1}. \tag{4.1.2.9}$$

The measurement noise stochastic properties acting on the output are easier to determine. However the properties of the state noise are more difficult to estimate, and $\underline{w}(k)$ is usually considered to be white noise in order to account for a large class of possible disturbances, model uncertainties, but also for the simplification of the optimal estimation solution.

The resulting state estimate $\underline{\hat{x}}$ minimizes the steady-state error covariance

$$\underline{P} = \lim_{k\to\infty} E\{(\underline{x}(k) - \underline{\hat{x}}(k))(\underline{x}(k) - \underline{\hat{x}}(k))^T\}. \tag{4.1.2.10}$$

The discrete time steady-state Kalman filter equations are

$$\begin{aligned}\underline{\hat{x}}(k+1\,|\,k) &= \underline{A}\,\underline{\hat{x}}(k\,|\,k-1) + \underline{B}\,u(k) + \underline{L}\,(y(k)\\ &\quad - \underline{C}\,\underline{\hat{x}}(k\,|\,k-1)),\\ \begin{bmatrix}\hat{y}(k\,|\,k)\\ \underline{\hat{x}}(k\,|\,k)\end{bmatrix} &= \begin{bmatrix}\underline{C}(\underline{I} - \underline{M}\underline{C})\\ \underline{I} - \underline{M}\underline{C}\end{bmatrix}\underline{\hat{x}}(k\,|\,k-1)\\ &\quad + \begin{bmatrix}\underline{C}\underline{M}\\ \underline{M}\end{bmatrix}y(k)\ ,\end{aligned} \tag{4.1.2.11}$$

where the first equation in (4.1.2.11) is the time update, the second set of equations are the measurement update, $\underline{L}$ is the estimation gain, and $\underline{M}$ is the innovation gain. The notations $\underline{\hat{x}}(k\,|\,k)$ and $\underline{\hat{x}}(k\,|\,k-1)$ outline the state vector at time k, given measurements up to time k and to time k–1, respectively. The state vector $\underline{\hat{x}}(k\,|\,k)$ is used for feedback in the optimal control law of type (4.1.2.5) as it is the true state vector.

In practical situations it is desired to drive the state vectors to a desired point in the state space and the introduction of input references for reference input tracking is required. In addition, the zero steady-state control error is targeted, hence an integrator is used as shown in Fig. 4.1.2.1, where an additional state variable (viz., the integrator state variable) x_I is added to the dynamics defined in equation (4.1.2.1).

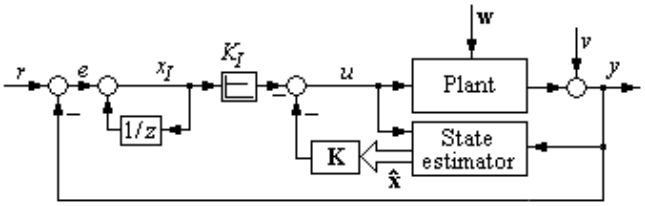

Fig. 4.1.2.1. The state-feedback control system structure with reference input and integrator to ensure zero steady-state error.

The dynamics of the integrator is expressed as follows using Fig. 4.1.2.1 and equation (4.1.2.1):

$$\begin{aligned}x_I(k+1) &= x_I(k) + e(k+1) = x_I(k)\\ &\quad + r(k+1) - y(k+1) = x_I(k) + r(k+1)\\ &\quad - \underline{C}(\underline{A}\,\underline{x}(k) + \underline{B}\,u(k) + \overline{B}\,\underline{w}(k)) - v(k+1),\end{aligned} \tag{4.1.2.12}$$

where r is the reference input and e is the control error.

The dynamics of the state feedback control system results by the combinations of equations (4.1.2.1), (4.1.2.8) and of the optimal control law obtained with LQR:

$$\underline{x}_a(k+1) = \underline{G}\,\underline{x}_a(k) + \underline{H}\,u(k) + \begin{bmatrix} 0 \\ 1 \end{bmatrix} r(k+1) + \begin{bmatrix} \overline{B} \\ -\underline{C} \end{bmatrix} \underline{w}(k) + \begin{bmatrix} 0 \\ -1 \end{bmatrix} v(k+1), \underline{x}_a(k) = [0 \quad \dots \quad 0]^T \in R^{(n+1)\times 1}, \tag{4.1.2.13}$$

$$u(k) = -\underline{K}_a \underline{x}_a(k),$$

where the matrices are

$$\underline{x}_a(k) = \begin{bmatrix} \underline{x}(k) \\ x_I(k) \end{bmatrix}, \ \underline{G} = \begin{bmatrix} \underline{A} & \underline{0} \\ -\underline{C}\underline{A} & 1 \end{bmatrix}, \ \underline{H} = \begin{bmatrix} \underline{B} \\ -\underline{C}\underline{B} \end{bmatrix}, \tag{4.1.2.14}$$

$$\underline{K}_a = [\underline{K} \quad K_I],$$

and the subscript a stands for the augmentation of the state vector and state feedback gain matrix.

The steady-state analysis of equation (4.1.2.14) for the step reference input of the magnitude $r(\infty)$ that respects

$$r(1) = \dots = r(k+1) = r(\infty) = const\ , \tag{4.1.2.15}$$

thus the result is

$$\underline{x}_a(\infty) = \underline{G}\,\underline{x}_a(\infty) + \underline{H}\,u(\infty) + \begin{bmatrix} 0 \\ 1 \end{bmatrix} r(\infty) + \begin{bmatrix} \underline{I}_n \\ -\underline{C} \end{bmatrix} \underline{w}(\infty) + \begin{bmatrix} 0 \\ -1 \end{bmatrix} v(\infty), \tag{4.1.2.16}$$

$$u(\infty) = -\underline{K}_a \underline{x}_a(\infty),$$

where the argument ∞ associated to a variable points out the steady-state value of that variable. The stochastic character with respect to w and v is preserved.

Next we define the state error with respect to the steady-state value $\underline{x}_a(\infty)$ and the control signal error with respect to the steady-state value $u(\infty)$:

$$\underline{\varepsilon}(k) = \underline{x}_a(k) - \underline{x}_a(\infty), \ u_\varepsilon(k) = u(k) - u(\infty)\,. \tag{4.1.2.17}$$

The subtraction of (4.1.2.16) out of (4.1.2.14) and the use of (4.1.2.17) lead to the following error dynamics:

$$\underline{\varepsilon}(k+1) = \underline{G}\,\underline{\varepsilon}(k) + \underline{H}\,u_\varepsilon(k) + \begin{bmatrix} \underline{I}_n \\ -\underline{C} \end{bmatrix} \underline{w}(k) + \begin{bmatrix} 0 \\ -1 \end{bmatrix} v(k+1), \underline{\varepsilon}(0) \neq [0 \quad \dots \quad 0]^T \in R^{(n+1)\times 1}, \tag{4.1.2.18}$$

$$u_\varepsilon(k) = -\underline{K}_a \underline{\varepsilon}(k).$$

The LQG problem for this dynamical system can be formulated such that to minimize the OF

$$I_\varepsilon(\underline{K}_a, \underline{L}) = E\{\sum_{k=0}^{\infty} [\underline{\varepsilon}^T(\underline{K}_a, \underline{L}, k)\,\underline{Q}\,\underline{\varepsilon}(\underline{K}_a, \underline{L}, k) + \lambda\, u_\varepsilon^2(\underline{K}_a, \underline{L}, k)]\}\,, \tag{4.1.2.19}$$

where the weights $\underline{Q}$ and λ are defined similar to the ones in (4) and with appropriate dimensions. The solution is expressed as the optimal estimator gain L and the optimal state feedback gain matrix $\underline{K}_a$, referred to as follows as the LQG servo controller problem.

In the view of applying data-based optimization to the aforementioned problems, one would have to be able to evaluate the OFs for finite time-horizon and using the estimated states when measurements are not available. A suitable OF used in this context is

$$J(\underline{K}_a, \underline{L}) = E\{\sum_{k=0}^{N} [\hat{\underline{\varepsilon}}^T(\underline{K}_a, \underline{L}, k)\, \underline{Q}\, \hat{\underline{\varepsilon}}(\underline{K}_a, \underline{L}, k) + \lambda\, u_\varepsilon^2(\underline{K}_a, \underline{L}, k)]\}, \quad (4.1.2.20)$$

where we use the state estimates to define their steady-state errors, except for the integrator state which does not need to be estimated. If the OF defined in (4.1.2.19) is minimizes by data-based optimization and the Kalman filter is already designed such that the filter gain $\underline{L}$ is fixed then the new system dynamics will be again augmented with the filter dynamics. Equations (4.1.2.13) and (4.1.2.11) are expressed as the following $2n+1$ order system:

$$\begin{aligned}
\begin{bmatrix} \underline{x}(k+1) \\ \hat{\underline{x}}(k+1\,|\,k) \\ x_I(k+1) \end{bmatrix} &= \begin{bmatrix} \underline{A} & \underline{0} & \underline{0} \\ \underline{LC} & \underline{A}-\underline{LC} & \underline{0} \\ -\underline{CA} & \underline{0} & 1 \end{bmatrix} \begin{bmatrix} \underline{x}(k) \\ \hat{\underline{x}}(k\,|\,k-1) \\ x_I(k) \end{bmatrix} \\
&+ \begin{bmatrix} \underline{B} \\ \underline{B} \\ -\underline{CB} \end{bmatrix} u(k) + \begin{bmatrix} 0 \\ 0 \\ 1 \end{bmatrix} r(k+1) + \begin{bmatrix} \underline{B} \\ 0 \\ -\underline{C}\overline{B} \end{bmatrix} \underline{w}(k) \\
&+ \begin{bmatrix} \underline{0} & \underline{0} \\ \underline{L} & \underline{0} \\ 0 & -1 \end{bmatrix} \begin{bmatrix} v(k) \\ v(k+1) \end{bmatrix}, \qquad (4.1.2.21) \\
\underline{x}(k\,|\,k) &= [\underline{MC} \quad \underline{I}-\underline{MC} \quad 0] \begin{bmatrix} \underline{x}(k) \\ \hat{\underline{x}}(k\,|\,k-1) \\ x_I(k) \end{bmatrix} + \underline{M}\, v(k), \\
u(k) &= -[\underline{0}^T \quad \underline{K} \quad K_I] \begin{bmatrix} \underline{x}(k) \\ \hat{\underline{x}}(k\,|\,k) \\ x_I(k) \end{bmatrix}.
\end{aligned}$$

In other words, if we design an optimal control law on the LQR servo controller but in (4.1.2.20) we use the state estimates to evaluate the OF, this is equivalent to using only partial state feedback for the system with the dynamics augmented with those of the Kalman filter. The following notation is introduced in order to highlight the parameterization of the optimization problem to be solved by IFT and SPSA:

$$\underline{\rho} = (\underline{K}_a)^T \in R^{(n+1)\times 1}. \quad (4.1.2.22)$$

For OFs defined in accordance with (4.1.2.20), the use of the argument vector defined in (4.1.2.22) leads to the new expression

$$J(\underline{\rho}) = E\{\sum_{k=0}^{N} [\hat{\underline{\varepsilon}}^T(\underline{\rho}, \underline{L}, k)\, \underline{Q}\, \hat{\underline{\varepsilon}}(\underline{\rho}, \underline{L}, k) + \lambda\, u_\varepsilon^2(\underline{\rho}, \underline{L}, k)]\}. \quad (4.1.2.23)$$

The IFT and the SPSA algorithms will conveniently be employed in the next sections to find a solution $\underline{\rho}^*$ to the optimization problem

$$\underline{\rho}^{*} = \boldsymbol{arg}\ \underset{\underline{\rho}\in SD}{\boldsymbol{min}}\ J(\underline{\rho}), \tag{4.1.2.24}$$

where *SD* stands for the stability domain of all state feedback gain matrices that ensure a stable CS.

In order to solve the optimization problem defined in (4.1.2.24) a parameter vector $\underline{\rho}$ has to be found such that

$$\frac{\partial J}{\partial \underline{\rho}} = [\frac{\partial J}{\partial \rho_1} \quad ... \quad \frac{\partial J}{\partial \rho_n}]^T = [0 \quad ... \quad 0]^T, \tag{4.1.2.25}$$

which, for the OF *J* defined in (4.1.2.23), becomes

$$\frac{\partial J}{\partial \rho_l} = 2\sum_{k=0}^{N}\{[\sum_{\substack{i,j=1\\ i\geq j}}^{n}(q_{ij}\hat{\varepsilon}_i\frac{\partial \hat{\varepsilon}_j}{\partial \rho_l})] + \lambda\, u_\varepsilon \frac{\partial u_\varepsilon}{\partial \rho_l}\} = 0,\ l = 1,2,...,n\,. \tag{4.1.2.26}$$

The cases of constrained optimization problems use Karush-Kuhn-Tucker optimality conditions instead of the null gradient given by equation (4.1.2.25). These constraints account for technological and/or economical conditions related to the operation of the real-world processes [72], [76], [93], [99], [102], [146].

IFT is a gradient-based stochastic approximation technique meant to find the minimum of a (objective) function that can only be known through noisy measurements. It was developed to cope with LQG like performance criteria, in a variety of problems such as combinations of reference model tracking, control effort penalty, noise rejection, optimal tracking.

The partial derivatives $\partial\hat{\varepsilon}_i / \partial\rho_l$ and $\partial u_\varepsilon / \partial\rho_l$ need to be calculated first in order to obtain the derivatives $\partial J / \partial\rho_l$, $l = 1,2,...,n$, in the gradient of the OF What can be obtained however are estimates of the gradients, $est[\partial J / \partial\rho_l]$, $l = 1,2,...,n$, by obtaining estimates of the gradients involved in the right side of (4.1.2.19). Having this gradient estimate calculated, the minimum of the OF can be aimed through iterative steps in the gradient direction in terms of the update law

$$\underline{\rho}^{i+1} = \underline{\rho}^{i} - \gamma^{i}(\underline{R}^{i})^{-1} est[\frac{\partial J}{\partial \underline{\rho}}(\underline{\rho}^{i})],\ \underline{R}^{i} > 0\,, \tag{4.1.2.27}$$

where the superscript *i*, $i \in N$, is the current iteration/experiment index, γ^{i}, $\gamma^{i} > 0$, is the step size, $est[\frac{\partial J}{\partial \underline{\rho}}(\underline{\rho}^{i})]$ is the unbiased estimate of the gradient, and the regular matrix $\underline{R}^{i}$ can be the estimate of the Hessian matrix, the Gauss-Newton approximation of the Hessian, or the identity matrix in the case of less demanding and slower convergent computations.

The step size sequence $\{\gamma^{i}\}_{i\in N}$ should evolve in time such that to satisfy some bounds. With this regard the conditions to ensure the convergence of the stochastic algorithm are [27], [38]

$$\sum_{i=0}^{\infty}\gamma^{i} = \infty,\ \sum_{i=0}^{\infty}(\gamma^{i})^{2} < \infty\,. \tag{4.1.2.28}$$

A good choice of the step size sequence that ensures the divergence of the first series in (4.1.2.28) and also the convergence of the second series in (4.1.2.28) is

$$\gamma^i = \frac{\gamma^0}{i^\alpha},\ i \in N,\ i \geq 1,\ 0.5 < \alpha \leq 1, \tag{4.1.2.29}$$

where the initial step size γ^0, $\gamma^0 > 0$, is set such that to ensure a compromise to the numerical stability and to the convergence speed.

A biased estimate of the Hessian matrix can be employed in the update law (4.1.2.27) as the Gauss-Newton approximation

$$\begin{aligned} \underline{\underline{R}}^i = \sum_{k=1}^{N} \{ & est[\frac{\partial \hat{\underline{\varepsilon}}}{\partial \underline{\rho}}(\underline{\rho}^i)]^T\ \underline{\underline{Q}}\ est[\frac{\partial \hat{\underline{\varepsilon}}}{\partial \underline{\rho}}(\underline{\rho}^i)] \\ & + \lambda\ est[\frac{\partial u_\varepsilon}{\partial \underline{\rho}}(\underline{\rho}^i)]^T est[\frac{\partial u_\varepsilon}{\partial \underline{\rho}}(\underline{\rho}^i)]\}, \end{aligned} \tag{4.1.2.30}$$

where the estimates of the gradients are used when the stochastic environment is accepted. An example of unbiased estimator is given in [57].

In order to apply IFT to the OF defined in (4.1.2.32) using the dynamics defined in (4.1.2.21) with fixed L, the derivatives of the estimated states steady-state errors have to be calculated. The definition of these errors is

$$\hat{\underline{\varepsilon}}(\underline{K}_a, k) = \begin{bmatrix} \hat{\underline{x}}(\underline{K}_a, k \mid k) - \hat{\underline{x}}(\underline{K}_a, \infty \mid \infty) \\ x_I(\underline{K}_a, k) - x_I(\underline{K}_a, \infty) \end{bmatrix}, \tag{4.1.2.31}$$

and their derivatives with respect to one parameter $K_i, i = 1,2,...,n+1$, in the matrix $\underline{K}_a = [K_1 \ \ ... \ \ K_{n+1} = K_I]$ are

$$\frac{\partial \hat{\underline{\varepsilon}}(\underline{K}_a, k)}{\partial K_i} = \begin{bmatrix} \frac{\partial \hat{\underline{x}}(\underline{K}_a, k \mid k)}{\partial K_i} - \frac{\partial \hat{\underline{x}}(\underline{K}_a, \infty \mid \infty)}{\partial K_i} \\ \frac{\partial x_I(\underline{K}_a, k)}{\partial K_i} - \frac{\partial x_I(\underline{K}_a, \infty)}{\partial K_i} \end{bmatrix}. \tag{4.1.2.32}$$

Since the partial derivatives of the state estimates are needed together with the derivative of the integrator state, and taking into account that the derivation of r, $\underline{w}$ and v with respect to the parameter K_i are zero, the derivation of the equations (4.1.2.21) with respect to K_i leads to

$$\frac{\partial}{\partial K_i}\left(\begin{bmatrix} \underline{x}(k+1) \\ \underline{\hat{x}}(k+1\,|\,k) \\ x_I(k+1) \end{bmatrix}\right) = \begin{bmatrix} \underline{A} & \underline{0} & \underline{0} \\ \underline{LC} & \underline{A}-\underline{LC} & \underline{0} \\ -\underline{CA} & \underline{0} & 1 \end{bmatrix}$$

$$\frac{\partial}{\partial K_i}\left(\begin{bmatrix} \underline{x}(k) \\ \underline{\hat{x}}(k\,|\,k-1) \\ x_I(k) \end{bmatrix}\right) + \begin{bmatrix} \underline{B} \\ \underline{B} \\ -\underline{CB} \end{bmatrix}\frac{\partial}{\partial K_i}u(k),$$

$$\frac{\partial}{\partial K_i}\underline{x}(k\,|\,k) = [\underline{MC} \quad \underline{I}-\underline{MC} \quad 0]$$

$$\frac{\partial}{\partial K_i}\left(\begin{bmatrix} \underline{x}(k) \\ \underline{\hat{x}}(k\,|\,k-1) \\ x_I(k) \end{bmatrix}\right), \tag{4.1.2.33}$$

$$\frac{\partial}{\partial K_i}u(k) = -\frac{\partial}{\partial K_i}([\underline{0}^T \quad \underline{K} \quad K_I])\begin{bmatrix} \underline{x}(k) \\ \underline{\hat{x}}(k\,|\,k) \\ x_I(k) \end{bmatrix}$$

$$-[\underline{0}^T \quad \underline{K} \quad K_I]\frac{\partial}{\partial K_i}\left(\begin{bmatrix} \underline{x}(k) \\ \underline{\hat{x}}(k\,|\,k) \\ x_I(k) \end{bmatrix}\right).$$

Equations (4.1.2.33) represent the deterministic dynamics with the state feedback gain, with zero reference input and with an additive perturbation on the control signal $u(k)$. The derivative of the gain matrix in the last equation in (4.1.2.33), calculated with respect to one of its parameters, is a gain matrix with 1 on the position of the respective parameter and 0 otherwise. Therefore, by injecting the recorded state of a normal experiment (with a reference input different from zero) into the state feedback scheme with zero reference input we obtain the derivatives of the state variables in (4.1.2.32) that are needed in order to evaluate the OF.

If i as a superscript denotes the i-th gradient experiment and as subscript the i-th state variable, then all state variables of the new dynamic system are in fact the estimates of the derivatives of the initial state variables with respect to the i-th parameter in the parameter vector $\underline{K}_a$ or $\underline{\rho}$ (via (4.1.2.22)). We talk about estimates because at each real-time experiment the dynamics are subject to the random disturbances $\underline{w}$ and v. Consequently, equations (4.1.2.21) and (4.1.2.23) result in

$$\begin{bmatrix} \underline{x}^i(k+1) \\ \underline{\hat{x}}^i(k+1|k) \\ x_I{}^i(k+1) \end{bmatrix} = \begin{bmatrix} \underline{A} & \underline{0} & \underline{0} \\ \underline{LC} & \underline{A}-\underline{LC} & \underline{0} \\ -\underline{CA} & \underline{0} & 1 \end{bmatrix} \begin{bmatrix} \underline{x}^i(k) \\ \underline{\hat{x}}^i(k|k-1) \\ x_I{}^i(k) \end{bmatrix}$$
$$+ \begin{bmatrix} \underline{B} \\ \underline{B} \\ -\underline{CB} \end{bmatrix} u^i(k) + \begin{bmatrix} \underline{B} \\ \underline{0} \\ -\underline{C}\underline{B} \end{bmatrix} \underline{w}^i(k)$$
$$+ \begin{bmatrix} \underline{0} & \underline{0} \\ \underline{L} & \underline{0} \\ 0 & -1 \end{bmatrix} \begin{bmatrix} v^i(k) \\ v^i(k+1) \end{bmatrix},$$
$$\underline{x}^i(k|k) = [\underline{MC} \quad \underline{I}-\underline{MC} \quad 0] \begin{bmatrix} \underline{x}^i(k) \\ \underline{\hat{x}}^i(k|k-1) \\ x_I{}^i(k) \end{bmatrix}$$
$$+ (\underline{I}-\underline{M})\,\underline{D}\,u^i(k) + \underline{M}\,\underline{D}\,\underline{w}^i(k) + \underline{M}\,v^i(k),$$
$$u^i(k) = -x_i - [\underline{0}^T \quad \underline{K} \quad K_I] \begin{bmatrix} \underline{x}^i(k) \\ \underline{\hat{x}}^i(k|k) \\ x_I{}^i(k) \end{bmatrix}. \tag{4.1.2.34}$$

The corresponding experimental setup is presented in Fig. 4.1.2.2. Proceeding this way we obtain the estimates of the gradients of the steady-state errors. Using the unbiased estimate of the gradient of the OF, several steps can be made in the gradient direction towards the solution.

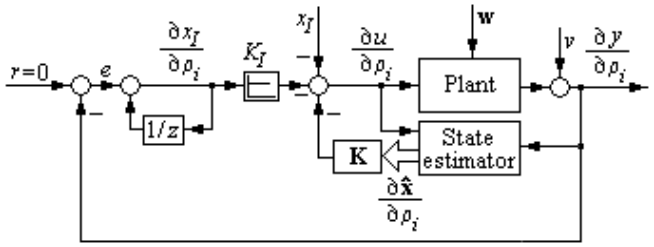

Fig. 4.1.2.2. The setup for the gradient experiment where a disturbance is added to the control signal.

The new IFT algorithm consists of the following steps:

- *Step 0*. Set the step size, the initial parameter vector $\underline{\rho}^0$ and the weights in the OF The vector $\underline{\rho}^0$ is obtained as the solution to the LQR servo controller problem applied to (4.1.2.19) in a deterministic framework.
- *Step 1*. Conduct the initial (normal) experiment making use of the CS structure presented in Fig. 4.1.2.1 and record the evolution of all state variables.

- *Step 2*. Conduct the *n* gradient experiments making use of the experimental setup presented in Fig. 4.1.2.2 to obtain all partial derivatives $\partial\hat{\varepsilon}_i / \partial\rho_l$ and $\partial u_\varepsilon / \partial\rho_l$.
- *Step 3*. Conduct the normal experiment again such that the states contain realizations of noise that differ form the noise at *step 2* to ensure the unbiased estimate of the gradient.
- *Step 4*. Calculate the estimates of the gradient of the OF according to equation (4.1.2.26).
- *Step 5*. Calculate $\underline{\rho}^{i+1}$ in terms of the update law (4.1.2.27).
- *Step 6*. If no significant decrease in the OF with the new set of parameters is obtained, stop the algorithm, otherwise go to *step 1*.

The parameter vector obtained by this IFT algorithm, referred to as the optimal parameter vector ρ^*, corresponds to the optimal state feedback gain matrix $(\underline{K}_a)^*$ expressed as (via (4.1.2.22))

$$(\underline{K}_a)^* = (\underline{\rho}^*)^T = \in R^{1\times(n+1)}. \tag{4.1.2.35}$$

To express the SPSA algorithm the use of the steepest descent recursive form [148]

$$\underline{\rho}^{i+1} = \underline{\rho}^i - a^i \frac{\partial J}{\partial \underline{\rho}}(\underline{\rho}^i), \tag{4.1.2.36}$$

usually leads to the gradient of the OF defined in (4.1.2.23) at the *i*-th iteration. $\{a^i\}_{i\in N}$ in (4.1.2.36) is the step-scaling coefficient sequence.

Unlike with steepest descent, the gradient-based stochastic approximation algorithms including IFT and SPSA use estimated gradients of the OF The parameter update law in these algorithms is

$$\underline{\rho}^{i+1} = \underline{\rho}^i - a^i est[\frac{\partial J}{\partial \underline{\rho}}(\underline{\rho}^i)]. \tag{4.1.2.37}$$

In IFT, it is possible to calculate the gradients by using data from the real time experiments. However, when such schemes cannot be employed, according to Kiefer-Wolfovitz's SA algorithm the gradients have to be estimated on the basis of the noisy measurements of the OF in terms of the calculation of finite difference approximations around the current point. Under specific conditions regarding the existence of a minimum of the OF, the differentiability with respect to the parameters, and a suitable selection of $\{a^i\}_{i\in N}$, Robbins-Monro's SA algorithm and Kiefer-Wolfowitz's SA algorithm state that the sequence of parameter vectors $\{\rho^i\}_{i\in N}$ converges to the parameter vector ρ^* that minimizes the OF *J*.

The idea behind finite difference approximations is to evaluate the argument of the OF around the current iteration argument and to use next the noisy measurements to calculate the estimates of the gradient. One-sided approximations or two-sided approximations can be used with this regard. For two-sided approximations, a general estimated gradient is

$$est[\frac{\partial J}{\partial \underline{\rho}}(\underline{\rho}^i)] = \begin{bmatrix} \frac{\tilde{J}(\underline{\rho}^i + c^i\underline{\xi}_1) - \tilde{J}(\underline{\rho}^i - c^i\underline{\xi}_1)}{2c^i} \\ \dots \\ \frac{\tilde{J}(\underline{\rho}^i + c^i\underline{\xi}_p) - \tilde{J}(\underline{\rho}^i - c^i\underline{\xi}_p)}{2c^i} \end{bmatrix}, \quad (4.1.2.38)$$

where $\underline{\xi}_i = \begin{bmatrix} 0 & \dots & \overset{i-th\ position}{\tilde{1}} & \dots & 0 \end{bmatrix}^T$ is a p-dimensional vector, with p – the dimension of the parameter vector, $p = n + 1$ in our algorithms, and c^i is the difference magnitude coefficient. The variables $\tilde{J}$ in (4.1.2.38) represent noisy measurements of the OF The sequences $\{a^i\}_{i\in N}$ and $\{c^i\}_{i\in N}$ are degrees of freedom in the FDSA algorithm. The FDSA-based estimate is biased due to the noise and the convergence to $\underline{\rho}^*$ is ensured for parameter vectors (i.e., state feedback gain matrices) that fulfill the conditions [148]

$$a^i > 0,\ c^i > 0,\ a^i \to 0,\ c^i \to 0,$$
$$\sum_{i=0}^{\infty} a^i = \infty,\ \sum_{i=0}^{\infty} (a^i / c^i)^2 < \infty. \quad (4.1.2.39)$$

Another problem of this approach is the fact that 2p measurements of the OF are needed at each iteration, and this affects the experiment's costs. The costs increase with the number of parameters. That is the reason why SPSA reduces the costs burden by means of only two evaluations of the OF per iteration. With this regard the arguments are first randomly disturbed, and next the approximations of the gradient are calculated as follows using finite differences:

$$est[\frac{\partial J}{\partial \underline{\rho}}(\underline{\rho}^i)] = \begin{bmatrix} \frac{\tilde{J}(\underline{\rho}^i + c^i\underline{\Delta}_i) - \tilde{J}(\underline{\rho}^i - c^i\underline{\Delta}_i)}{2c^i\Delta_{i1}} \\ \dots \\ \frac{\tilde{J}(\underline{\rho}^i + c^i\underline{\Delta}_i) - \tilde{J}(\underline{\rho}^i - c^i\underline{\Delta}_i)}{2c^i\Delta_{ip}} \end{bmatrix}, \quad (4.1.2.40)$$

where $\underline{\Delta}_i = [\Delta_{i1}\ \dots\ \Delta_{ip}]^T$. The numerator in (4.1.2.40) is the same for all components in the gradient vector, but the denominator is different and proportional to the variation of the corresponding parameter in the set. The standard condition imposed to the elements $\Delta_{ik}, k = 1,2,\dots,p$, is that they should be independent, identically distributed with symmetric distribution around zero, and of bounded magnitude. In addition, there is a condition related to the inverse moments of these random variables so that a suitable distribution that respects all these requirements is a Bernoulli distribution. A common choice is that the random variables $\Delta_{ik}, k = 1,2,\dots,p$, take the values ± 1 with probability 0.5. A normal or uniform distribution is shown to reduce the performance of the algorithm. The same constraints are preserved as in the case of FDSA for the gain sequences. Also, a modified search that is similar to the deterministic Newton-Raphson algorithm can

be employed, when in the same manner, attempts are made to estimate the Hessian of the OF A suitable selection of the sequences $\{a^i\}_{i\in N}$ and $\{c^i\}_{i\in N}$ is [148]

$$a^i = a^0/(i+A)^\alpha,\ c^i = c^0/i^\gamma, \tag{4.1.2.41}$$

where $a^0 > 0$, $c^0 > 0$, $A > 0$, $0 < \alpha \le 1$ and $\gamma > 0$.

Only two evaluations of the OF defined in (4.1.2.23) are needed in the application of SPSA algorithms to the LQG servo controller problem. The design is started with the LQR solution accounting for deterministic dynamics of the process augmented with the integrator, and the OF defined in (4.1.2.23) is next minimized using SPSA algorithms.

The new SPSA algorithm consists of the following steps:

- *Step 0*. Set the parameters $a^0 > 0$, $c^0 > 0$, $A > 0$, $\alpha > 0$ and $\gamma > 0$, the initial parameter vector $\underline{\rho}^0$ and the weights in the OF The vector $\underline{\rho}^0$ is obtained as the solution to the LQR servo controller problem applied to (4.1.2.19) in a deterministic framework.
- *Step 1*. Calculate $\underline{\Delta}_i$, a^i and c^i.
- *Step 2*. Evaluate $\tilde{J}(\underline{\rho}^i + c^i\underline{\Delta}_i)$ and $\tilde{J}(\underline{\rho}^i - c^i\underline{\Delta}_i)$, and find an estimate of the gradient according to (4.1.2.40).
- *Step 3*. Calculate $\underline{\rho}^{i+1}$ in terms of the update law (4.1.2.37).
- *Step 4*. Test the decrease of the OF using one of the two evaluations of the OF with the corresponding perturbed parameters. If no significant decrease is revealed then stop the algorithm, otherwise go to *step 1*. This is valid if the perturbed parameters are close to the current set of parameters.

In other words, the parameter vector is randomly disturbed only two times per iteration to evaluate the gradient in the SPSA algorithm. The parameter vector $\underline{\rho}^*$ obtained by this SPSA algorithm leads to the optimal state feedback gain matrix $(\underline{K}_a)^*$ expressed in (4.1.2.37).

The case study aims the design of a CS dedicated to the angular speed control for a modular DC servo system with an integral component. The process is characterized by the discrete time LTI SISO state-space model defined in (4.1.2.2) with the matrices

$$\underline{A} = \begin{bmatrix} 1 & 0.0487 \\ 0 & 0.9471 \end{bmatrix},\ \underline{B} = \begin{bmatrix} 0.1867 \\ 7.3993 \end{bmatrix},$$
$$\overline{B} = \underline{I}_2,\ \underline{C} = [1\ 0],\ \underline{D} = 0,\ \overline{D} = [0\ 0], \tag{4.1.2.42}$$

where $\underline{I}_2$ is the second order identity matrix, the angular position and the angular speed are the state variables x_1 and x_2 respectively.

The model defined in (4.1.2.2) with the matrices according to (4.1.2.40) is a simplified model of the process that corresponds to an experimental setup built around an INTECO DC servo system laboratory equipment. However similar processes are used in several applications [88], [90], [149]-[152].

The main features of the experimental setup are [63] the rated amplitude of $24\,V$, the rated current of $3.1\,A$, the rated torque of $15\,N\,cm$, the rated speed of

$3000\ rpm$, the weight of inertial load of $2.03\,kg$. The angular speed can be measured by a tacho-generator, but only the position is measured here and the angular speed is estimated via a Kalman filter.

This simplified model was obtained by the parameter identification of the first-principle model of the equipment resulting in the simplified process transfer function (considering the control signal u as the input and the angular position as the output, $y = x_1$)

$$P(s) = k_P /[s(1 + T_\Sigma s)], \tag{4.1.2.43}$$

where k_P is the process gain and T_Σ is the small time constant. The values of the process parameters were obtained as $k_P = 139.88$ and $T_\Sigma = 0.92\ s$. A sampling period of $T_S = 0.05\ s$ was next set.

As it is usually the case, the model-based design makes use of a model that is different from the real process. It is assumed that an initial LQR servo design is desired for the deterministic process augmented with the integrator in (4.1.2.19). Since the quadratic OF has to be convergent, the difference between the state variables and their steady-state values are weighted. Since the position measurement is available and it is affected by noise and the integrator state variable is already available, an estimation of the state variables is required in the LQR design. An optimal estimation design is carried out in order to obtain a Kalman filter. With the filter's fixed parameters, and because the estimated states are available to the user, an attempt is made to minimize the LQG-like OF defined in (4.1.2.20) over a finite time-horizon of 10 s.

A rather crude model is used to design the LQR controller and the Kalman filter, which starts from the process parameters $k_P = 150$ and $T_\Sigma = 1.2\ s$. We used the following weights in the LQR design:

$$\underline{Q} = \begin{bmatrix} 100 & 0 & 0 \\ 0 & 200 & 0 \\ 0 & 0 & 1 \end{bmatrix},\ \lambda = 300\,. \tag{4.1.2.44}$$

A white noise disturbance is acting on the state with the state noise intensity matrix $\underline{QN}$ and the measurement noise intensity matrix $\underline{RN}$:

$$\underline{QN} = \begin{bmatrix} \sigma_{w1}^2 = 2 & 0 \\ 0 & \sigma_{w1}^2 = 1 \end{bmatrix},\ \underline{RN} = \sigma_V^2 = 0.06,\ \underline{NN} = [0\ 0]^T\,. \tag{4.1.2.45}$$

Therefore the noise effect on both estimated states is alleviated. In this setup, we account for the additional estimator dynamics in the process model in the, so we are sure that the LQR-based initial solution is not optimal as far the minimization of the OF defined in (4.1.2.20) is concerned. Next, the two data-based techniques, viz. IFT and SPSA, are employed in the minimization of the OF defined in (4.1.2.15). The estimator and the innovation gains for the Kalman filter are $\underline{L} = \underline{M} = [0.0157 \quad 0.0025]^T$.

A number of 30 iterations was conducted for the IFT algorithm presented above for $N = 1000$ samples. The initial step size in the IFT algorithm was set to the initial value $\gamma^0 = 10^{-10}$, and the values of the consequent step sizes were set in terms of

$$\gamma^i = \frac{\gamma^0}{i^\alpha},\ i \in N,\ i \geq 1, \tag{4.1.2.46}$$

with $\alpha = 0.51$, such that to satisfy the conditions (4.1.2.28), and $\underline{R}^i = \underline{I}_3$ was used.

The SPSA implemented here is characterized by the same N, and the same number of iterations. The parameters in the SPSA were set to the values $a^0 = 10^{-10}$, $c^0 = 0.005$, $A = 0.1$, $\alpha = 0.4$ and $\gamma = 0.05$.

In both cases the starting point in the parameter space, as designed via LQR, was

$$\underline{K}_a = (\underline{\rho}^0)^T = [K_1 = 1.9229 \quad K_2 = 0.5163 \quad K_I = -0.0348]. \tag{4.1.2.47}$$

A step reference input of $r = 20\ rad$ was chosen for the position. The final set of parameters obtained by the IFT algorithm is

$$(\underline{K}_a)^* = (\underline{\rho}^*)^T = [K_1 = 1.9249 \quad K_2 = 0.5174 \quad K_I = -0.0778]. \tag{4.1.2.48}$$

The final set of parameters obtained by the SPS algorithm is

$$(\underline{K}_a)^* = (\underline{\rho}^*)^T = [K_1 = 1.8212 \quad K_2 = 0.4155 \quad K_I = -0.0645]. \tag{4.1.2.49}$$

The evolution of the OF versus the iteration number is presented in Fig. 4.1.2.3. The evolutions of the state feedback controller parameters are presented in Fig. 4.1.2.4. The difference in the initial value of the OF is due to the stochastic noise. For the same reason, a certain value of the OF varies because of the random factor at each evaluation. The decrease is obvious. The evolutions versus time of four variables of the state feedback CS are shown in Fig. 4.1.2.5 in three situations corresponding to the initial set of parameters, the final set of parameters after tuning with IFT and the final set of parameters after tuning with SPSA.

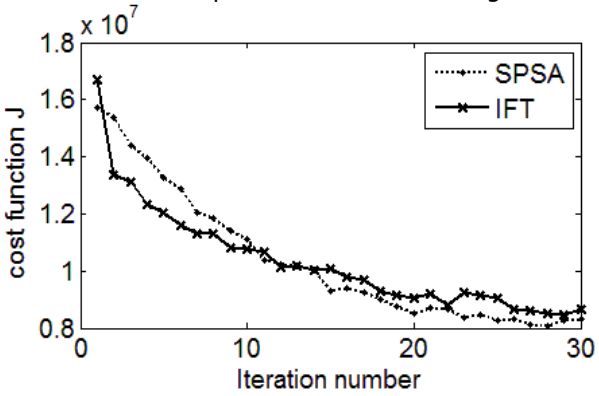

Fig. 4.1.2.3. The evolution of the OF over 30 iterations.

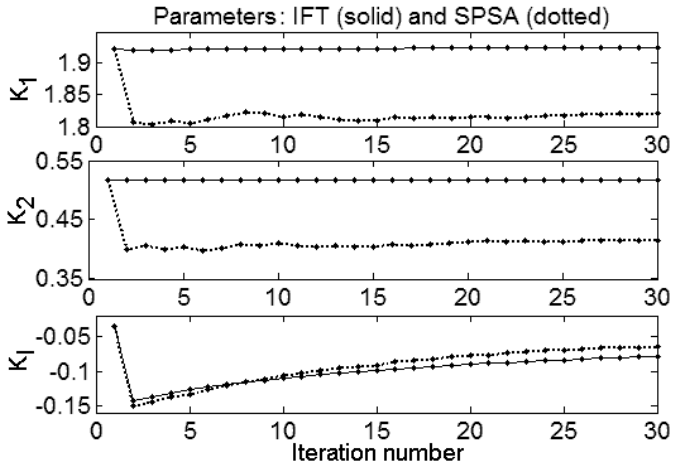

Fig. 4.1.2.4. The evolution of the state feedback controller parameters versus the iteration number.

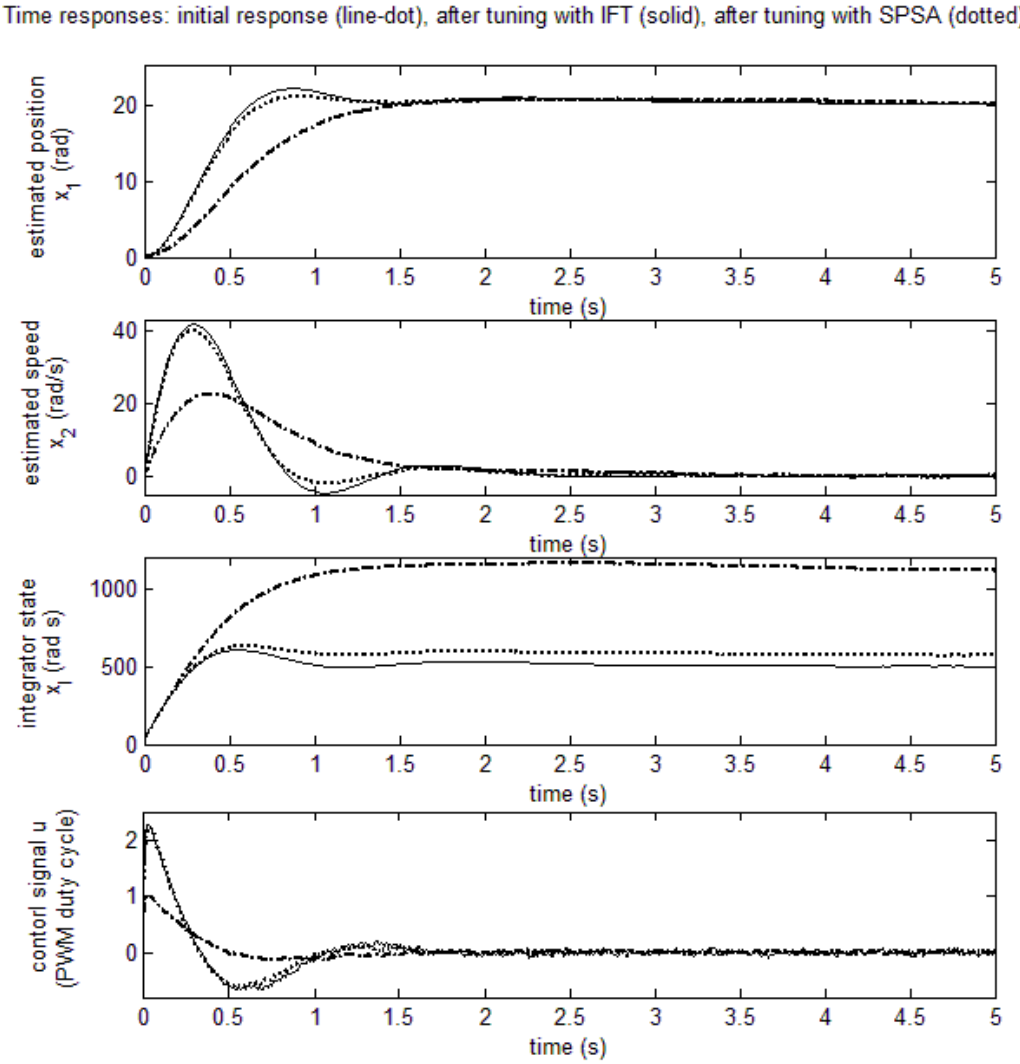

Fig. 4.1.2.5. The responses of the state feedback control system recorded from simulated results: estimated position, estimated angular speed, integrator state and control signal versus time.

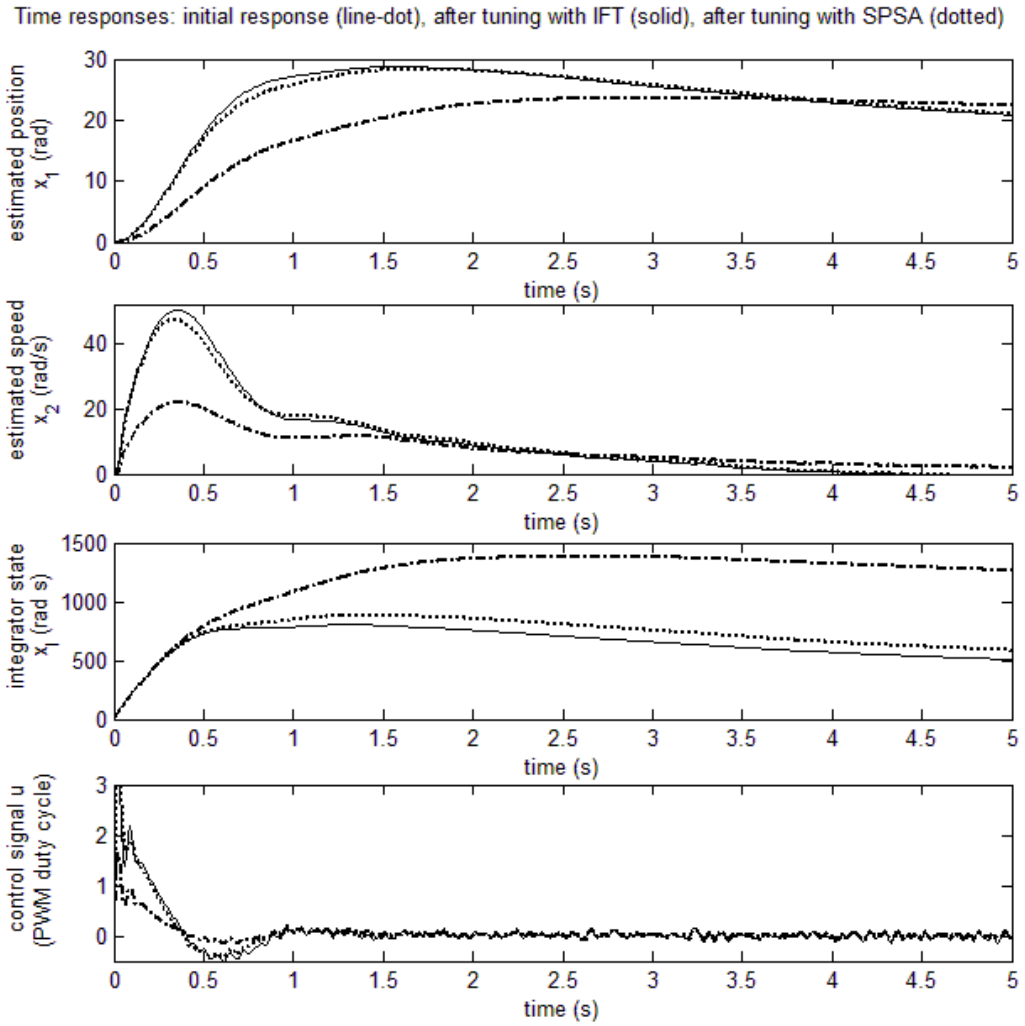

Fig. 4.1.2.6. The responses of the state feedback control system recorded from experimental results on the real process: estimated position, estimated angular speed, integrator state and control signal versus time.

The evolutions versus time of the same variables of the state feedback CS in the same three situations are presented in Fig. 4.1.2.6, but they correspond to the experiments conducted with the state feedback CS. The differences between the time responses in Fig. 4.1.2.5 and Fig. 4.1.2.6 are due to the difference between the linear process model used in the design and tuning and the real-world process model, and also to the different noise properties that act on the simulated process and the real-world process. The former difference influences the optimal controller gains and the latter influences the Kalman filter design and correspondingly the dynamics of the process plus estimator.

A discussion on the new results is conducted as follows. The LQR problem is merely an idealization as it is a model-based optimization problem that is subjected to modeling errors and linearity assumptions. Moreover it is defined in a

deterministic framework. This makes the practical evaluation of the optimality of the solution very difficult and irrelevant.

The LQG problem suffers the same drawbacks. The minimum values for the OFs can only be evaluated analytically [153]. Less problematic is the finite time horizon that can be used in practice to evaluate the OFs because for sufficiently long runs it has the enough length to capture the transients in the time response. Although the separation principle allows for independent design of the optimal estimator gain and the optimal state feedback control gain, the results can not be tested independently because the use of state estimators invalidates the possibility of evaluating the LQR OF The controller uses only the estimated state variables.

The use of the matrices $\underline{L}$ and $\underline{M}$ in the discrete time Kalman filter equations (4.1.2.11) comes in two flavors, time-varying or steady-state. The following points on the LQG are emphasized:

- Due to the certainty equivalence principle, the state feedback regulator and the estimator can be designed independently and the estimated state variables feed the gain matrix $\underline{K}$.
- The dynamics of the process is extended with the dynamics of the estimator. The robustness of the initial LQR structure is not necessarily preserved.
- The system preserves the stability as it includes the dynamics of the regulated process and the stable estimator.
- The robustness properties of closed-loop state feedback control system can be recovered via Loop Transfer Recovery (LTR).

Both IFT and SPSA are data-based stochastic optimization techniques, therefore they represent more than gradient-based search algorithm using sensitivity functions of the quantities in the control structure with respect to some design parameters. Second, they make no use of the process model in the tuning: IFT uses a successive-experiment approach to obtain the gradients of the loop variables, and then the estimate of the gradient of the OF, whereas SPSA starts with the finite difference approximation to find directly the gradient of the c. f. The derivation of the gradient experiment equations in the case of IFT can be very laborious. This is not the case with SPSA. Only two evaluations of the OF are needed with SPSA when we have a p-dimensional parameter vector but with IFT the number of experiments in this setting is p+2, one gradient experiment for each parameter and two normal experiments in order to obtain an unbiased estimate of the gradient of the OF which is critical for the performance of the algorithm.

With SPSA, the gradient estimate is biased but the convergence is preserved under the proper choice of the sequences $\{a^i\}_{i\in N}$ and $\{c^i\}_{i\in N}$. For one-degree-of-freedom controllers the number of experiments with IFT can be shown to be constant, i.e. three, but the cost is still higher in comparison with SPSA.

The IFT technique assumes linear process but SPSA is not constrained by this and it could be employed also on nonlinear processes as long as the OF is smooth as function of the parameters allowing higher order derivatives. In the same view, the OF for IFT can only be used in LQG-like form but with SPSA, performance indices of different nature could be aggregated together.

The initial starting point in the search space needs to be provided for both algorithms. In general this is not possible without using a process model, but techniques such as Ziegler-Nichols tuning or VRFT could be used for this purpose. Also, there is no automated way of finding the initial parameters of the algorithms so they are chosen by trial and error. Moreover, throughout the iterations, although the convergence of the algorithm is ensured by the choice of the corresponding

sequences, the stability of the control structure is not guaranteed. Mechanism devoted to this purpose can be used in the case where a process model is available (e.g., the ν-gap metric) as it is the case in our approaches. Otherwise, new mechanism should be developed. Since we deal with numerical algorithms, it is possible that the global minimum is never obtained, so the algorithms could get stuck in local extremum points. Different starting points in the search space may not always be available.

SPSA can be employed in the minimization of various OFs in relation with nonlinear systems, and it is not constrained just to LQG-type OFs. Therefore these two advantages over IFT make it a very useful tool. It can only be used for the further improvement and tuning of an initial designed control system. This means that we have to start with a fixed stabilizing CS structure. The same problems that are related to the convergence speed of the algorithm and the stability of the CS during iterations need to be addressed. Although it is model-free in the tuning step, asserting the robust stability and performance still needs a process model. For example, using the ν-gap distance according to [29], the stability can be checked at each step. A combination of SPSA and IFT is also suggested in [51].

4.3 Chapter conclusions

Chapter 4 has given two additional techniques that can be used in CS tuning, namely IRT and SPSA. Since their development, IRT and SPSA were seen as more "computational approach" tools rather than suitable for experiment-based tuning. The major contribution of this chapter is that it indicates different possibilities of adapting these schemes to efficient practical real-time application. The substantial advantages of the iterative schemes presented in this thesis are pinpointed again in this context since they represent more than sensitivity-based tuning schemes. They also hold a stochastic convergence results which is a crucial development that is necessary whenever we talk about real-time processes inherently affected by measurement noise. Concluding, these techniques are situated on the increasingly blurred border between the metaheuristic approach in optimization and the data-based approach.

IRT was translated to a real-process implementation for a servo system position control and was shown to be efficient. In the same setting as for the IFT and the LQG-based tuning for the process plus Kalman filter, the SPSA was also employed with results comparable in terms of efficiency with IFT. The tuning setup is novel since it is designed entirely in the state-space formulation for the ensemble formed by the process dynamics and the Kalman filter dynamics. The results allow for a thorough comparison between these two techniques.

The new contributions of this chapter are:

1) The experimental validation of the IRT and SPSA techniques on a DC servo system laboratory equipment.
2) The state-space formulation of the IFT tuning scheme and of the SPSA tuning scheme for processes with state observers (Kalman filter).
3) Solving the LQG type problems on an experimental basis using IFT and SPSA, which is different to the usual model-free approach.
4) The Successful implementation and validation of the IRT technique on a laboratory equipment.

The results were published in:

Precup, R.-E., Borchescu, C., ***Rădac, M.-B.****, Preitl, St., Dragoş, C.-A., Petriu, E. M. and Tar, J. K. (2010): Implementation and Signal Processing Aspects of Iterative Regression Tuning. Proceedings of 2010 IEEE International Symposium on Industrial Electronics ISIE 2010, Bari, Italy, pp. 1657-1662, indexed in* **SCOPUS, INSPEC**.

5. Iterative Feedback Tuning for Fuzzy Control Systems Design

5.1. Introduction

The stability analysis of fuzzy control systems (FCSs) has been investigated extensively in the context of nonlinear autonomous / nonautonomous systems in close connection with their stabilization. The current approaches reported in the literature concerning the stable design of FCSs with Takagi-Sugeno fuzzy controllers are based mainly on linear matrix inequalities (LMIs) [62], [157]-[162] making use of quadratic, piecewise quadratic, non-quadratic, parameter-dependent or polynomial Lyapunov functions [163]-[169]. Although the LMIs are computationally solvable even in relaxed versions they require numerical algorithms embedded in well acknowledged software tools.

The design of optimal control systems is of permanent interest because it ensures very good control system (CS) performance indices by the minimization of objective functions (OFs) expressed as integral quadratic performance indices [170]-[174]. The Iterative Feedback Tuning (IFT) performs the gradient-based minimization of the OFs making use of the input-output data from the closed-loop system in several experiments done per iteration [14],[16].

A good overview on IFT is given in [27] while ensuring the unbiased estimates of the gradient of the OF with respect to the controller parameters. Various extensions of IFT to Multi Input-Multi Output (MIMO) systems are investigated in [20]. The extension of IFT according to [38] provides additional ways to disturbance rejection and improves the convergence required by all iterative techniques in control design [175], [176]. Recent IFT applications to industrial control problems in servo drives and chemical processes are discussed in [39], [176].

The combination of IFT and fuzzy control aims the FCS performance enhancement. In our recent papers [75], [177], [201], [205] we discussed the parameter mapping of IFT-based PI controllers onto the parameters of Takagi-Sugeno PI-fuzzy controllers (PI-FCs) in terms of the equivalence under certain conditions between FCSs and linear / linearized CSs. A combination of IFT and fuzzy control is analyzed in [46], [177], and the FCS enables the run-time adaptation based on IFT and knowledge acquired from past experience. A fuzzy-based supervisor that modifies the parameters of an iteratively tuned PID controller is suggested in [179]. Several structures that combine the iterative and soft computing techniques are proposed in [180].

This chapter presents three new contributions in addition to the previous aspects discussed in [177]-[180]. First, original stability results for the FCS that employ a convenient formulation of Lyapunov's direct method for discrete-time systems [181]. Our stability analysis results are dedicated to processes that are modeled by discrete-time input affine SISO systems as a representative class of

nonlinear systems where thorough stability analysis approaches are offered in the literature [182]-[185]. The discrete-time input affine SISO systems considered as controlled processes enable the application of IFT-based tuning. The stability analysis is necessary for IFT-based FCSs because:

- The PI controllers are obtained initially in terms of IFT and next the parameters are mapped onto the parameters of the PI-FCs in terms of the modal equivalence principle resulting in nonlinearities specific to the FCSs.
- The stability analysis enables the systematic design of the PI-FCs to ensure the FCS performance enhancement.

Second, a transparent and attractive IFT algorithm is suggested. The convergence of the new IFT algorithm is guaranteed by the fulfillment of an inequality-type convergence condition. The convergence condition is derived from Popov's hyperstability analysis results [44], [73] applied here to the parameter update law as part of the IFT algorithm. With this regard the update law is reformulated as a nonlinear dynamical feedback system considered in the parameters space and iteration domain.

Third, a thorough discussion of a set of real-time experimental results for a different case study is conducted in this contribution.

The new contributions are important and advantageous with respect to the state-of-the-art because:

- The stability analysis is applied to the FCSs with Takagi-Sugeno PI-FCs by the transfer of the dynamics of the PI-FCs to the process dynamics. Therefore an extended nonlinear process is obtained. There is no need for the separation of the process model to consist of two parts as in the usual stability analysis of nonlinear dynamical systems, i.e., a linear part with dynamics and a static nonlinearity.
- The application of Popov's hyperstability analysis to the convergence of the IFT algorithm does not require knowledge on the global minimum as in the application of Lyapunov's results.

This chapter addresses the following topics. The new stability analysis results are presented in the next subchapter in a general formulation dedicated to a discrete-time input affine SISO systems. Subchapter 5.3 is next focused on the main aspects concerning the new IFT algorithm with guaranteed convergence. An original design approach of Takagi-Sugeno PI-FCs ensuring IFT and stable FCSs is suggested in Subchapter 5.4. Subchapter 5.5 is dedicated to the case study that applies the theoretical approaches to the angular position control of a DC servo system laboratory equipment and presents real-time experimental results. The conclusions are pointed out in Subchapter 5.6.

5.2. Stability analysis approach

The process in the FCS is modeled by the following discrete-time input affine SISO system described by state-space mathematical model [181]:

$$\begin{aligned} &\underline{x}(t+1) = \underline{f}(\underline{x}(t)) + \underline{b}(\underline{x}(t))u(t),\ t \in N, \underline{x}(0) = \underline{x}_0 \in X, \\ &y(t) = g(\underline{x}(t)), \end{aligned} \tag{5.1}$$

where y is the controlled output, $\underline{x}(t) = [x_1(t)\ \ x_2(t)\ \ \ldots\ \ x_2(t)]^T \in X \subset R^n$ is the state vector, $n \in N,\ n \geq 1$, $\underline{X}$ is the universe of discourse, T stands for matrix

transposition, the time variable t (with the initial time moment $t_0 = 0$) will be omitted as follows for simplicity, $\underline{x}_0$ is the initial state vector, the continuous functions

$$\begin{aligned} &\underline{f}, \underline{b} : R^n \times N \to R^n, \\ &\underline{f}(\underline{x}(t)) = [f_1(\underline{x}(t)) \quad f_2(\underline{x}(t)) \quad \dots \quad f_n(\underline{x}(t))]^T, \\ &\underline{b}(\underline{x}(t)) = [b_1(\underline{x}(t)) \quad b_2(\underline{x}(t)) \quad \dots \quad b_n(\underline{x}(t))]^T, \end{aligned} \tag{5.2}$$

and $g : R^n \times N \to R$ describe the dynamics of the process, and u is the control signal produced by the fuzzy controller.

The Takagi-Sugeno fuzzy controllers that control the process modeled by (5.1) and (5.2) are generally nonlinear state feedback controllers. They employ the MAX and MIN operators in the inference engine and the weighted sum method for defuzzification. The use of these operators does not restrict the generality of our approach because it does not require the differentiability of the input-output map of the fuzzy controller. Therefore other t-norms and s-norms can be used because instead of the MAX and MIN operators, respectively.

The i-th fuzzy control rule in the rule base of the fuzzy controller, referred to as R^i, $i = 1...n_{RB}$, $n_{RB} \geq 2$, is expressed as

$$R^i : IF \ x_1 \ IS \ X_1^l \ AND \ x_2 \ IS \ X_2^l \ AND \ ... \ AND \ x_n \ IS \ X_n^l \ THEN \ u = u_i(\underline{x}), \ i = 1..n_{RB}, \tag{5.3}$$

where $X_l{}^i$, $l = 1...n$ are the fuzzy sets expressed as linguistic terms (LTs) afferent to the state variables x_l, $u^i(\underline{x})$ is the control signal produced by the rule R^i with the firing strength $\alpha^i = \alpha^i(\underline{x})$, $0 \leq \alpha^i \leq 1$, $i = 1..n_{RB}$, subject to

$$\alpha^i(\underline{x}) = min(\mu_{X_1^l}(x_1), \mu_{X_2^l}(x_2), ..., \mu_{X_n^l}(x_n)), \ \forall \underline{x} \in X \ \exists i = 1..n_{RB} \ suchthat \ \alpha^i \neq 0, \tag{5.4}$$

$\mu_{X_l{}^i}$, $l = 1...n$, are the membership functions of the LTs $X_l{}^i$, $l = 1...n$, and n_{RB} is the number of rules.

An active region of the rule R^i is defined as the set

$$X_i^A = \{\underline{x} \in X \mid \alpha^i(\underline{x}) \neq 0\}, \ i = 1...n_{RB}. \tag{5.5}$$

Since the regions different to (5.5) do not affect the inference engine, the expression of the control signal produced by the fuzzy controller is

$$u(\underline{x}) = [\sum_{i=1}^{n_{RB}} \alpha^i(\underline{x}) u^i(\underline{x})] / [\sum_{i=1}^{n_{RB}} \alpha^i(\underline{x})]. \tag{5.6}$$

Let the process be characterized by the state-space model defined in (5.1) and let the radially unbounded function $V : R^n \to R$ such that $V(\underline{x}) > 0$, $\forall \underline{x} \neq 0$, $V(\underline{0}) = 0$. The first difference of the function $V(\underline{x}(t))$ along the trajectory of (5.1), denoted by $\Delta V(\underline{x}(t))$, is supposed to fulfill the condition

$$\Delta V(\underline{x}(t)) = V(\underline{x}(t+1)) - V(\underline{x}(t)) < 0. \tag{5.7}$$

Using the notation $V_k(\underline{x}(t))$ for the Lyapunov function candidate $V(\underline{x}(t))$ which is considered along the trajectory of the system (5.1) for $u(t) = u_k(\underline{x}(t))$, the first difference of $V_k(\underline{x}(t))$ is $\Delta V_k(\underline{x}(t))$:

$$\Delta V_k(\underline{x}(t)) = V_k(\underline{x}(t+1)) - V_k(\underline{x}(t)), \forall\, \underline{x} \in X_k^A, k = 1...n_{RB}. \quad (5.8)$$

The following original stability analysis theorem is derived on the basis of Lyapunov's theorem for discrete-time systems starting with the formulation given in [186].

Theorem 5.1: Let the FCS be described by the discrete-time input affine SISO system modeled in (5.1), the Takagi-Sugeno fuzzy controller characterized by (5.3)–(5.6), and $\underline{x} = \underline{0}$ an equilibrium point of (5.1). Let

$$V : X \to R,\ V(\underline{x}(t)) = \underline{x}^T(t)\,\underline{P}\,\underline{x}(t), \quad (5.9)$$

where $\underline{P}$ is an $n \times n$ positive definite matrix such that

$$\Delta V_k(\underline{x}(t)) < 0, \forall\, \underline{x} \in X_k^A, k = 1...n_{RB}. \quad (5.10)$$

Then all state vectors $\underline{x}(t)$ will converge globally asymptotically to the origin $\underline{x}(t) = \underline{0}$ as $t \to \infty$.

The proof of Theorem 5.1 is presented in Appendix B. This theorem offers the sufficient inequality-type conditions (5.10) for the globally asymptotically stability of the equilibrium point at the origin. Theorem 5.1 proves that if each subsystem is stable in the sense of Lyapunov under a common Lyapunov function, the (overall) closed-loop system is also stable in the sense of Lyapunov. Since no fuzzy model of the process is involved, the number of subsystems generated is relatively small, and the common Lyapunov function can be found easily. This approach decomposes the stability analysis to the analysis of each rule, so it is not complex. Theorem 5.1 is applied in this chapter to set the values of the parameters of the Takagi-Sugeno PI-FCs in order to offer stable FCSs.

5.3. Iterative Feedback Tuning algorithm

The structure of the linear CS with IFT algorithm is presented in Fig. 5.1, where: r – the reference input, d – the disturbance input (noise), e – the control error, u – the control signal, $\underline{\rho}$ – the parameter vector containing the controller parameters, $C(\underline{\rho})$ – the transfer function of the linear (PI) controller to be replaced by the Takagi-Sugeno PI-FC to ensure the CS performance enhancement, F – the transfer function of the reference model prescribing the desired behavior to be exhibited by the CS, P – the transfer function of the process, y – the controlled output, y_d – the desired output (of the reference model), $\delta y = y - y_d$ – the output error, and IFTA – the Iterative Feedback Tuning algorithm, and the vector **i** contains the performance specifications imposed to the CS, i.e., the desired / imposed values of performance indices including overshoot, settling time, rise time, etc.

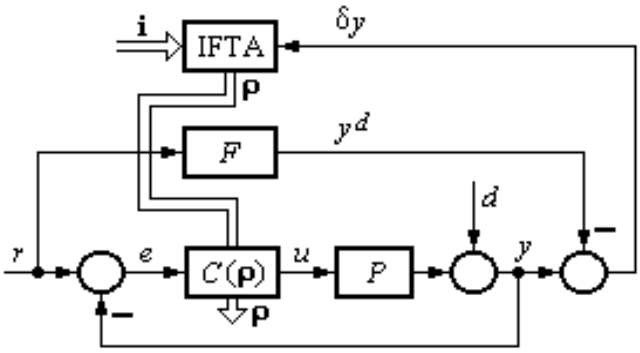

Fig. 5.1. Structure of linear control system with IFT algorithm.

One simple expression of the objective function $J(\underline{\rho})$ to be minimized by IFT is

$$J(\underline{\rho}) = (0.5/N)\sum_{t=1}^{N}[\delta y(t,\underline{\rho})]^2 , \tag{5.11}$$

where N is the number of samples setting the length of each experiment. A typical objective related to $J(\underline{\rho})$ is to find a parameter vector $\underline{\rho}^*$ to minimize $J(\underline{\rho})$ and make the error δy tend to zero as $t \to \infty$. That objective is expressed analytically in terms of the optimization problem

$$\underline{\rho}^* = \underset{\underline{\rho}\in SD}{\textbf{arg min}}\ J(\underline{\rho}), \tag{5.12}$$

where several constraints can be imposed. The most important constraint concerns the stability of the CS and *SD* stands for stability domain in (5.12). The reference model is usually chosen as a second order transfer function in normalized form where the natural frequency and the damping factor can easily be transferred to performance indices. This model also embodies the behavior of the typical CS structures which act as low-pass filters. It is of course a subject of compromise on how the performances are requested through the reference model because with a certain parameterization of the controller it may be possible that the reference model response is never matched by the CS. The a priori information on the process can be incorporated in the controller design before choosing the reference model.

The IFTAs solve the problem (5.12) by numerical stochastic approximation algorithms making use of the control signal and controlled output during the CS operation. The Robbins-Munro stochastic approximation algorithm iteratively approaches a zero of a function affected by stochastic noise without knowledge on its fully expression. The IFTA thus holds both an input-output sensitivity function-based tuning scheme, and a stochastic convergence result which is necessary in an experiment-based environment where the random factors appear every time. IFT is not only dedicated to Model Reference Adaptive Control (MRAC) schemes but also to the more generally formulated Linear-Quadratic Gaussian (LQG) criteria where flexible OFs can be formulated such that to weight the state variables, the control errors, the control signals and the controlled outputs as well. Therefore the MRAC is a particular case. Important results that back-up the application of IFT to control of nonlinear processes are presented in [15], [59]. The key requirement is its applicability to processes with smooth nonlinearities.

The update law to calculate the next parameter vector $\underline{\rho}^{i+1}$ is

$$\underline{\rho}^{i+1} = \underline{\rho}^{i} - \gamma^{i}(\underline{R}^{i})^{-1} est[\frac{\partial J}{\partial \underline{\rho}}(\underline{\rho}^{i})],\ \underline{R}^{i} > 0, \det \underline{R}^{i} \neq 0, \tag{5.13}$$

where: $i,\ i \in N$ – the index of the current iteration, $est[\frac{\partial J}{\partial \underline{\rho}}(\underline{\rho}^{i})]$ – the estimate of the gradient vector, γ^{i} – the step size, and $\underline{\rho}^{0}$ – the initial guess of the controller parameters. The usual choice for the sequence $\{\gamma^{i}\}_{i \in N}$ should ensure the convergence of the algorithm in the stochastic sense by reducing the effect of the noise around the local minimum which would otherwise lead to the lack of convergence. A common choice with this regard is [27]

$$\gamma^{i} = \frac{\gamma^{0}}{i^{\alpha}},\ i \in N,\ i \geq 1,\ 0.5 < \alpha \leq 1, \tag{5.14}$$

where the initial step size γ^{0}, $\gamma^{0} > 0$, is set to ensure a compromise to the numerical stability and to the convergence speed.

The matrix $\underline{R}^{i}$ can be an estimate of the Hessian, a Gauss-Newton approximation of the Hessian or the identity matrix to simplify the signal processing and reduce the complexity of IFTAs. Different other choices for the Hessian approximation are possible such as the Levenberg-Marquardt algorithm (LMA) as suggested in [38] and the Broyden-Fletcher-Goldfarb-Shanno algorithm according to [1]. These algorithms are expected to give very good results when the signal to noise ratio is high. However, since the LMA interpolates between the steepest descent algorithm when far from the minimum and the Gauss-Newton algorithm when close to the minimum, the Gauss-Newton approximation makes use of the first-order derivatives of the objective function which are affected by noise. In the stochastic approximation algorithm (5.13) this choice of the Hessian approximation can worsen the algorithm if the signal to noise ratio is low. As the noise that enters the closed loop has a lower intensity, it is expected that the conditions approach the deterministic case where the LMA is a better approach. On the other hand, the estimate of the Hessian is also more expensive to compute since it requires extra experiments. A good compromise is the steepest descent with the step scaling sequence chosen as to respect the convergence of the algorithm in the stochastic sense, i.e., the step sequence should tend to zero at infinity but not too fast. In the case study presented here, the noise intensity is low so the LMA can be employed.

Some hyperstability results will be applied as follows to the parameter update law (5.13) in order to ensure the convergence of the IFTA. That is the reason why (5.13) is expressed as a dynamical feedback system in the parameter space and iteration domain. In this context consider the feedforward discrete-time linear time-invariant (LTI) block

$$\begin{aligned} \underline{\rho}^{i+1} &= \underline{I}\,\underline{\rho}^{i} + \underline{I}\,\underline{\mu}^{i}, \\ \underline{v}^{i} &= \underline{I}\,\underline{\rho}^{i}, \end{aligned} \tag{5.15}$$

which is completely controllable and completely observable because of the identity matrix $\underline{I}$. Consider the nonlinear (NL) feedback block

$$\underline{w}^{i} = \gamma^{i}(\underline{R}^{i})^{-1} est[\frac{\partial J}{\partial \underline{v}}(\underline{v}^{i})]. \tag{5.16}$$

The blocks LTI and NL are connected according to the block diagram presented in Fig. 5.2. The feedback structure illustrated in Fig. 5.2 is used in the hyperstability analysis viz. convergence analysis, and it justifies that (5.15) and (5.16) are equivalent to (5.13).

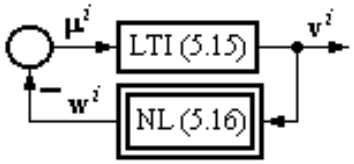

Fig. 5.2. Block diagram used in convergence analysis.

The block NL satisfies the integral inequality

$$\eta(i_0, i_1) = \sum_{i=i_0}^{i=i_1} (\underline{w}^i)^T \underline{v}^i \geq -\varepsilon_0^2, \quad \forall i_1 \geq i_0, \quad \varepsilon_0 = const, \quad \varepsilon_0 \neq 0 . \tag{5.17}$$

The necessary and sufficient condition for the nonlinear dynamical feedback system described by (5.15)–(5.17) to be hyperstable [44], [73] is that the discrete transfer function matrix

$$\underline{H}(z) = \underline{0} + (z\underline{I} - \underline{I})^{-1} = diag\big(1/(z-1), \quad 1/(z-1), \quad \ldots, \quad 1/(z-1)\big) \tag{5.18}$$

must be a positive real discrete transfer function matrix. The particular expression of the matrix $H(z)$ in (5.18) is positive real according to the definitions given in [187]. So the system (5.15)–(5.17) is hyperstable. Hence the convergence of the IFTA with the parameter update law (5.13) is guaranteed provided that the inequality (5.17) holds.

The new IFTA consists of the following steps.

- Step 0. Set the initial controller parameters in the parameter vector $\underline{\rho}^0$.
- Step 1. Conduct the two experiments for the considered CS structure and record the input-output data pairs (u_1,y_1) and (u_2,y_2). The first experiment is called the normal one, and it corresponds to the usual operation of the CS. In the second experiment, referred to as the gradient one, the reference input is the control error of the first experiment. Calculate the estimate of the gradient of output error $est[\frac{\partial \delta y}{\partial \underline{\rho}}(t, \underline{\rho}^i)]$

$$est[\frac{\partial \delta y}{\partial \underline{\rho}}(t, \underline{\rho}^i)] = \frac{1}{C(q^{-1}, \underline{\rho}^i)} \cdot \frac{\partial C}{\partial \underline{\rho}}(q^{-1}, \underline{\rho}^i) \cdot y_2(k, \underline{\rho}^i), \tag{5.19}$$

  where the subscript 2 highlights the gradient experiment.
- Step 2. Generate the output of the reference model y_d and calculate the output error δy.
- Step 3. Calculate the estimates of the gradient $\frac{\partial J}{\partial \underline{\rho}}(\underline{\rho}^i)$ and eventually of the Hessian $\underline{R}^i(\underline{\rho}^i)$ of J making use of (5.19) substituted to

$$\frac{\partial J}{\partial \underline{\rho}}(\underline{\rho}^i) = (1/N)\sum_{t=1}^{N}\{\delta y(t,\underline{\rho}^i)est[\frac{\partial \delta y}{\partial \underline{\rho}}(t,\underline{\rho}^i)]\},$$
$$\underline{R}^i(\underline{\rho}^i) = (1/N)\sum_{t=1}^{N}\{est[\frac{\partial \delta y}{\partial \underline{\rho}}(t,\underline{\rho}^i)]\}\{est[\frac{\partial \delta y}{\partial \underline{\rho}}(t,\underline{\rho}^i)\}^T. \quad (5.20)$$

- Step 4. Set the step size γ^i to fulfill the sufficient convergence condition (5.17). If no value can be found for γ^i to satisfy (5.17), the classical choice should be made according to (5.14).
- Step 5. Calculate $\underline{\rho}^{i+1}$ by the update law (5.13).

The step 0 is done only once and the other steps are repeated in all iterations till the OF has decreased sufficiently to meet the performance specifications imposed to the CS. Additional details regarding the IFT algorithms are presented in [14], [16], [38], [75], [177].

5.4. Takagi-Sugeno PI-fuzzy controllers: structure and design

The Takagi-Sugeno PI-FC is a discrete-time controller built around the two inputs-single output fuzzy controller (TISO-FC) and the structure presented in Fig. 5.3 (a) where: $\Delta e(t) = e(t) - e(t-1)$ – the increment of control error, $\Delta u(t) = u(t) - u(t-1)$ – the increment of control signal, and q^{-1} – the backward shift operator. The Takagi-Sugeno PI-FCs are characterized by the fuzzification according to Fig. 5.3 (b) (the TISO-FC includes the scaling of inputs and output), the inference engine and defuzzification in terms of Subchapter 5.2, and the inference engine is assisted by the following complete rule base ($n_{RB} = 9$):

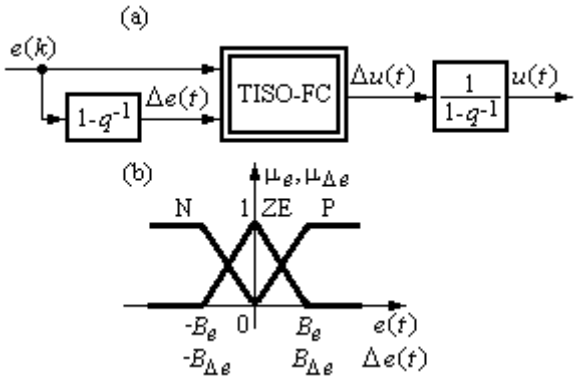

Fig. 5.3. Structure (a) and input membership functions (b) of PI-FC.

$$
\begin{aligned}
&R^1: \text{IF } e(t) \text{ IS } N \text{ AND } \Delta e(t) \text{ IS } N \text{ THEN } \Delta u(t) = \eta K_P[\Delta e(t) + \alpha e(t)],\\
&R^2: \text{IF } e(t) \text{ IS } N \text{ AND } \Delta e(t) \text{ IS } ZE \text{ THEN } \Delta u(t) = K_P[\Delta e(k) + \alpha e(t)],\\
&R^3: \text{IF } e(t) \text{ IS } N \text{ AND } \Delta e(t) \text{ IS } P \text{ THEN } \Delta u(t) = K_P[\Delta e(t) + \alpha e(t)],\\
&R^4: \text{IF } e(t) \text{ IS } ZE \text{ AND } \Delta e(t) \text{ IS } N \text{ THEN } \Delta u(t) = K_P[\Delta e(t) + \alpha e(t)],\\
&R^5: \text{IF } e(t) \text{ IS } ZE \text{ AND } \Delta e(t) \text{ IS } ZE \text{ THEN } \Delta u(t) = K_P[\Delta e(t) + \alpha e(t)],\\
&R^6: \text{IF } e(t) \text{ IS } ZE \text{ AND } \Delta e(t) \text{ IS } P \text{ THEN } \Delta u(k) = K_P[\Delta e(k) + \alpha e(t)],\\
&R^7: \text{IF } e(t) \text{ IS } P \text{ AND } \Delta e(t) \text{ IS } N \text{ THEN } \Delta u(t) = K_P[\Delta e(t) + \alpha e(t)],\\
&R^8: \text{IF } e(t) \text{ IS } P \text{ AND } \Delta e(t) \text{ IS } ZE \text{ THEN } \Delta u(t) = K_P[\Delta e(t) + \alpha e(t)],\\
&R^9: \text{IF } e(t) \text{ IS } P \text{ AND } \Delta e(t) \text{ IS } P \text{ THEN } \Delta u(t) = \eta K_P[\Delta e(t) + \alpha e(t)].
\end{aligned}
\tag{5.21}
$$

The parameters K_P and α are obtained by the continuous-time design of the linear PI controller with the transfer function (t.f.)

$$C(s) = k_C(1 + sT_i)/s = k_C[1 + 1/(sT_i)], \tag{5.22}$$

where k_C , $k_C = T_i k_c$, is the controller gain and T_i is the integral time constant. Tustin's method is next applied to obtain the incremental discrete-time linear PI controller in the consequents of all rules except R^1 and R^9, with the parameters

$$K_P = k_C[1 - T_S/(2T_i)], \alpha = 2T_S/(2T_i - T_S), \tag{5.23}$$

where T_s is the sampling period.

Three important aspects are highlighted in relation with the rule base (5.21). First, the number of rules in this complete rule base can be reduced further to support the low-cost implementation where other measures specific to digital control can be applied [188]-[193]. Second, the additional parameter η with typical values within $0 < \eta < 1$ was introduced in (5.21) to alleviate the overshoot for the same signs of $e(t)$ and $\Delta e(t)$ [76]. Third, in order to apply Theorem 5.1 the dynamics of the Takagi-Sugeno PI-FC is moved to the dynamics of the process as follows. The state variables $x_{C,1}$ and $x_{C,2}$ are defined for the Takagi-Sugeno PI-FC:

$$x_{C,1}(t) = u(t-1), \; x_{C,2}(t) = e(t-1) \tag{5.24}$$

as illustrated in Fig. 5.4.

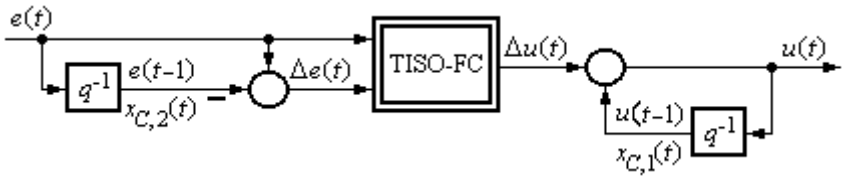

Fig. 5.4. Structure of PI-FC that includes the definitions of the state variables.

Equations (5.35) and Fig. 5.4 result in the following discrete-time state-space model of the Takagi-Sugeno PI-FC:

$$\begin{aligned} x_{C,1}(t+1) &= x_{C,1}(t) + f_{TISO-FC}(e(t), e(t) - x_{C,2}(t)), \\ x_{C,2}(t+1) &= e(t), \\ u(t) &= x_{C,1}(t) + f_{TISO-FC}(e(t), e(t) - x_{C,2}(t)), \end{aligned} \tag{5.25}$$

where the nonlinear input-output map of the TISO-FC is

$$f_{TISO-FC} : R^2 \to R, \quad \Delta u(t) = f_{TISO-FC}(e(t), \Delta e(t)) = f_{TISO-FC}(e(t), e(t) - x_{C,2}(t)) \tag{5.26}$$

Equations (5.1), (5.25) and (5.26) lead to the following expression of the state-space model (5.25):

$$\begin{aligned} x_{C,1}(t+1) &= x_{C,1}(t) + \Delta u(t), \\ x_{C,2}(t+1) &= r(t) - g(x(t)), \\ u(t) &= x_{C,1}(t) + \Delta u(t). \end{aligned} \tag{5.27}$$

The models (5.1) and (5.25) are next merged in the following discrete-time state-space model of the extended process, i.e., the process extended with the dynamics of the Takagi-Sugeno PI-FC:

$$\begin{aligned} \underline{x}(t+1) &= \underline{f}(\underline{x}(t)) + \underline{b}(\underline{x}(t))[x_{C,1}(t) + \Delta u(t)], \\ x_{C,1}(t+1) &= x_{C,1}(t) + \Delta u(t), \\ x_{C,2}(t+1) &= r(t) - g(x(t)), \\ y(t) &= g(x(t)). \end{aligned} \tag{5.28}$$

Using this model the Takagi-Sugeno PI-FC is replaced by the TISO-FC with the two input variables

$$e(t) = r(t) - g(\underline{x}(t)), \quad \Delta e(t) = r(t) - g(\underline{x}(t)) - x_{C,2}(t), \tag{5.29}$$

and the output variable $\Delta u(t)$. Therefore this transformation of the models leads to the expression of the rule base (5.21) as a particular case of (5.3).

The design approach dedicated to the accepted class of Takagi-Sugeno PI-FCs consists of the steps I to III to obtain the parameters of the PI-FCs T_s, K_P and α (specific to the linear design), and B_e, $B_{\Delta e}$ and η (specific to the fuzzy design):

- Step I. Apply a design method to tune the continuous-time linear PI controller, set T_s, apply (5.23) to calculate the initial parameter vector $\underline{\rho}^0 = [K_P \quad \alpha]^T$, set the reference model structure and its parameters according to the performance specifications imposed to the CS.
- Step II. Do the steps 0 to 5 of the IFTA presented in Subchapter 3 to obtain the optimal parameter vector $\underline{\rho}^* = [K_P \quad \alpha]^T$.
- Step III. Express the discrete-time state-space model of the extended process, set the values of the parameters B_e and η according to the performance specifications and to the stability analysis approach such that to fulfill the stability conditions (5.10) in Theorem 5.1, and apply the modal equivalence principle to map the linear controller parameters onto the Takagi-Sugeno PI-FC ones:

$$B_{\Delta e} = \alpha B_e . \tag{5.30}$$

The steps I and II correspond to the linear design, and the step III corresponds to the fuzzy design. The value of the parameter B_e depends on the reference input such that to ensure the firing of all rules, and the smaller the value of the parameter η is, $0 < \eta < 1$, the smaller the overshoot will be. This design

approach produces Takagi-Sugeno PI-FCs which exhibit as bumpless interpolators between the two discrete-time PI controllers in the consequents of the rule base (5.20).

5.5. Digital simulations results and real-time experimental results

The experimental setup is built around the INTECO DC servo system with backlash laboratory equipment. It is characterized by rated amplitude equal to 24 V, rated current equal to 3.1 A, rated torque equal to 15 N cm, rated speed equal to 3000 rpm, and inertial load mass equal to 2.030 kg. The position controllers are implemented digitally on a PC making use of an FPGA-based A/D-D/A interface connected by USB to the PC.

The nonlinear process used in the angular position control is characterized by the nonlinear continuous-time state-space model

$$m(t)=\begin{cases} 0, & \text{if } |u(t)|\le u_a, \\ k_{u,m}(u(t)-u_a\,sgn(u(t))), & \text{if } u_a<|u(t)|<u_b, \\ k_{u,m}(u_b-u_a)\,sgn(u(t)), & \text{if } |u(t)|\ge u_b, \end{cases}$$

$$\dot{\underline{x}}(t)=\begin{bmatrix} 0 & 1 \\ 0 & -1/T_\Sigma \end{bmatrix}\underline{x}(t)+\begin{bmatrix} 0 \\ k_P/T_\Sigma \end{bmatrix}m(t), \qquad (5.31)$$

$$y(t)=[1 \quad 0]\,\underline{x}(t),$$

where t is the independent continuous time argument, $t\in R, t\ge 0$, the control signal u is a pulse width modulation duty cycle, m is the output of the saturation and dead zone static nonlinearity represented by the first equation in (5.31), the state vector $\underline{x}(t)$ is

$$\underline{x}(t)=[x_1(t)=\alpha(t) \quad x_2(t)=\omega(t)]^T, \qquad (5.32)$$

$x_1(t)=\alpha(t)$ is the first state variable that represents the angular position, and $x_2(t)=\omega(t)$ is the second state variable that represents the angular speed. The disturbance inputs and the initial conditions were omitted in (5.31) for the sake of simplicity. The parameters of the linear dynamics represented by the second and third equation in (5.31) are the gain $k_P=139.88$ and the small time constant $T_\Sigma=0.9198\ s$. The parameters of the saturation and dead zone static nonlinearity in (5.41) are identified by nonlinear least squares as $k_{u,m}=1$, $u_a=0.13$ and $u_b=1.13$.

The process has an input nonlinearity related to the actuator, i.e., a saturation and dead zone static nonlinearity. However, this is not included in the following simplified model of the process expressed as the transfer function $P(s)$

$$P(s)=k_P/[s(1+sT_\Sigma)], \qquad (5.33)$$

is used in the IFTA. However the case study is dealt with from a linear perspective in the initial step when the PI controller is tuned and the CS performance indices are obtained with this simple controller.

The design approach presented in Subchapter 5.4 is applied as follows. The continuous-time linear PI controller has been obtained in the step I by the frequency domain design imposing the phase margin of 60^o resulting in the controller tuning parameters $k_C = 0.01036$ and $T_i = 3.1043\ s$. Setting $T_s = 0.01\,s$ the initial discrete-time linear PI controller parameters calculated in terms of (5.23) are

$$\underline{\rho}^0 = [K_P = 0.01034 \quad a = 0.0032]^T . \tag{5.34}$$

The continuous-time transfer function of the reference model is

$$F(s) = 1/(s^2 + 0.6s + 1) . \tag{5.35}$$

A filter was introduced on the reference input in order to alleviate the overshoot that is motivated by the presence of the integrator components in both the process (since it is a servo system for position control) and the controller. The filter's continuous-time transfer function is $F_r(s) = 1/(1.5s + 1)$. The discrete-time forms of reference model and of the reference input filter were used in the simulation and in the real-time experiments as well. All the above settings were applied in both the simulations and the experiments.

The simulation results are first presented. The IFTA was applied in the step II. The parameters obtained after 35 iterations for $\underline{R}^i = \underline{I}_2$ and $\gamma^i = 5 \cdot 10^{-9}$, $i = 0...35$ (that satisfy (5.17) for $\varepsilon_0 = 1$ at all iterations), are

$$\underline{\rho}^0 = [K_P = 0.02255 \quad a = 0.00040]^T . \tag{5.36}$$

The step III starts with the derivation of the discrete-time state-space model of the extended process. Accepting that the control signal u and the reference input r are changing at the discrete sampling intervals the discrete-time state-space model of the extended process becomes then (5.28), where

$$\underline{f}(\underline{x},t) = \begin{bmatrix} x_1(t) + T_\Sigma[1 - exp(-T_s/T_\Sigma)]x_2(t) \\ [exp(-T_s/T_\Sigma)]x_2(t) \end{bmatrix},$$

$$\underline{b}(\underline{x},t) = \begin{bmatrix} k_P[T_s + T_\Sigma\, exp(-T_s/T_\Sigma) - T_\Sigma] \\ k_P[1 - exp(-T_s/T_\Sigma)] \end{bmatrix} m(t), \tag{5.37}$$

$$g(\underline{x}(t)) = [1 \quad 0], \; m(t) = \begin{cases} 0, & if\ |u(t)| \le u_a, \\ k_{u,m}(u(t) - u_a\, sgn(u(t))), & if\ u_a < |u(t)| < u_b, \\ k_{u,m}(u_b - u_a)\, sgn(u(t)), & if\ |u(t)| \ge u_b. \end{cases}$$

For comparison reasons, an FCS is designed from the initial PI controller before tuning, and another one is designed from the resulting PI controller obtained by IFT-based tuning. A good choice of B_e for a constant reference input of $r = 40\ rad$ is $B_e = 20$ for both Takagi-Sugeno PI-FCs and the other parameter of the Takagi-Sugeno PI-FC, namely $B_{\Delta e}$, results from (5.30). The values of the parameter η and of the parameter $B_{\Delta e}$ were $\eta = 0.65$ and $B_{\Delta e} = 0.064$ for the initial fuzzy controller, and $\eta = 0.99$ and $B_{\Delta e} = 0.0080$ for the final one. The Lyapunov function candidate that fulfils the stability conditions (5.10) for this FCS is defined in (5.9), where

$$\underline{P} = diag(1,1,1,1), \; \underline{x} = [x_1 \quad x_2 \quad x_3 = x_{C,1} \quad x_4 = x_{C,2}]^T . \tag{5.38}$$

A band-limited white noise of variance 0.01 has been fed to the disturbance input d in the real-time experiments. All controllers were also tested on the

simplified linear process model (5.33) in order to outline the differences between the behavior of the CSs with the simplified model and the behavior of the CSs with the nonlinear process model. The digital simulation results are presented in Figs. 5.5 to 5.8.

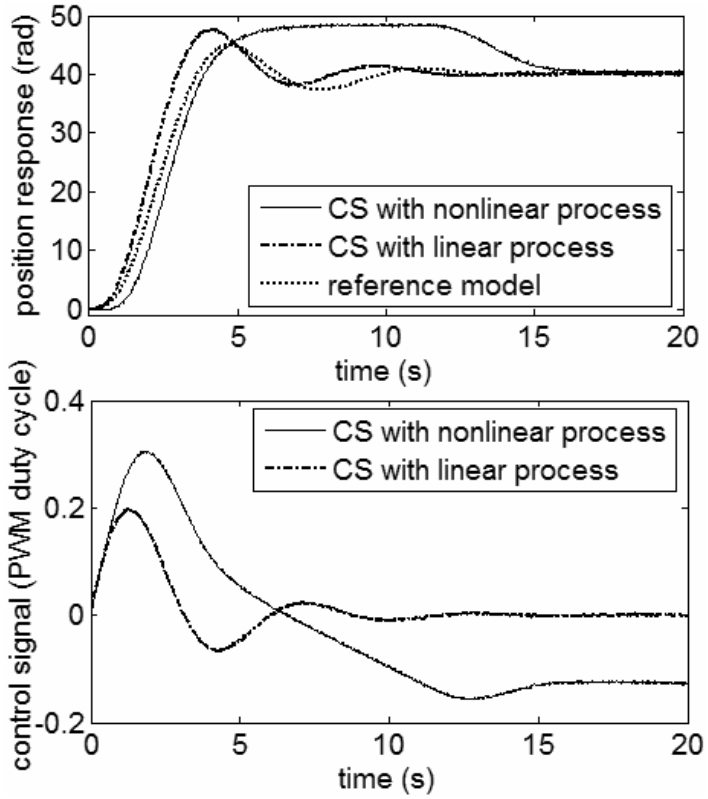

Fig. 5.5. Simulation results: controlled output (angular position) and control signal versus time for the linear CS with the PI controller before IFT.

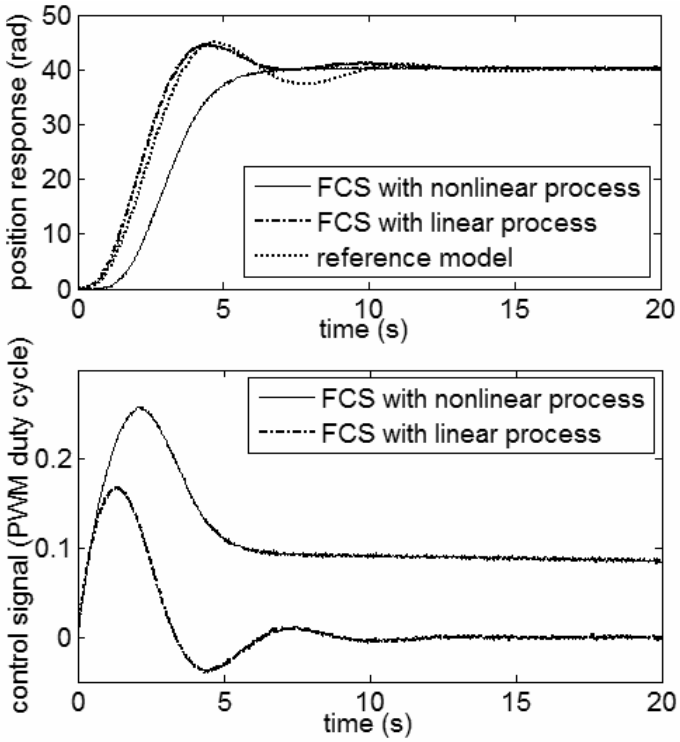

Fig. 5.6. Simulation results: controlled output (angular position) and control signal versus time for the FCS with the Takagi-Sugeno PI-FC before IFT.

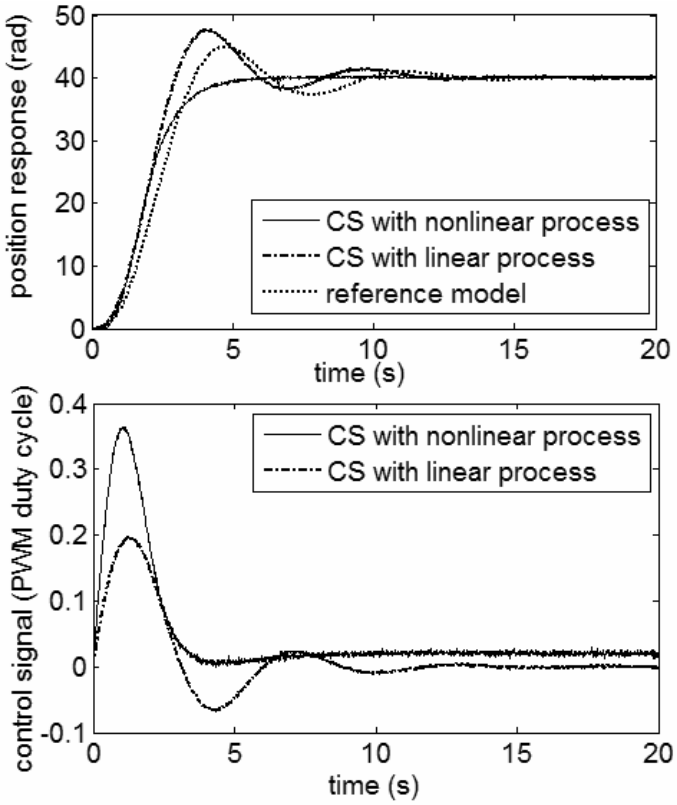

Fig. 5.7. Simulation results: controlled output (angular position) and control signal versus time for the linear CS with the PI controller after IFT.

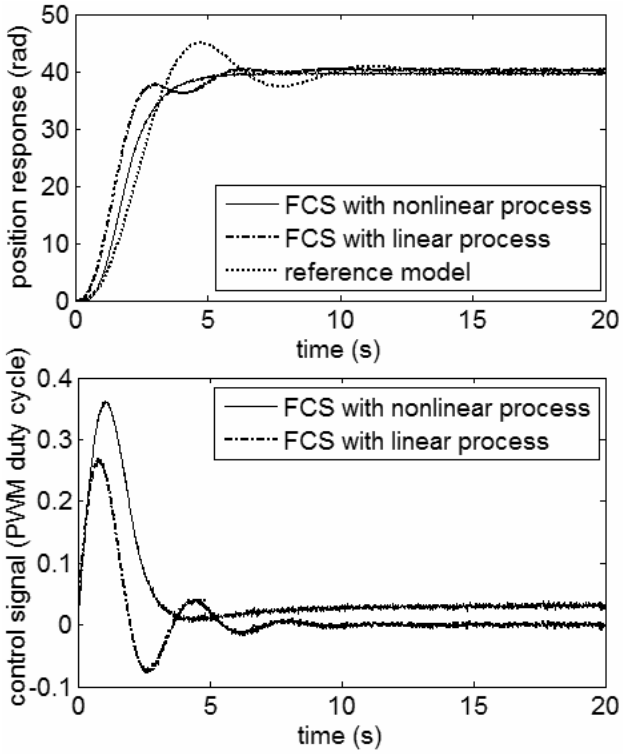

Fig. 5.8. Simulation results: controlled output (angular position) and control signal versus time for the FCS with the Takagi-Sugeno PI-FC after IFT.

The fuzzy controller developed from the initial PI controller deals better with the dead zone that causes the large overshoot in Fig. 5.5. After IFT-based tuning, the linear PI controller offers an aperiodic CS response that is closer to the reference model response in the sense given by the OF of the optimization problem. Both CSs with the IFT-based tuned PI controller and with the subsequent Takagi-Sugeno PI-FC derived from it offer a faster response than the initial FCS, and the two controllers also deal with the process nonlinearity. The values of the OF in the four cases that correspond to Figs. 5.5 to 5.8 were evaluated to 16.1623, 11.0007, 2.7803 and 2.8807, respectively. The intermediate step with IFT tuning proves to be useful since the FCS with the final IFT-based tuned fuzzy controller is better than the FCS with the initial one due to the alleviation of the OF.

The same scenario was applied in the real-time experiments with the servo system laboratory equipment. The same design approach was used starting with the same initial PI controller that was designed using the simplified linear process model (5.30). The fuzzy controllers were tuned starting with the initial PI controller and with the final PI controller after IFT. The experiments were conducted with the same reference model and reference input filter. The results are presented in Figs. 5.9 to 5.12.

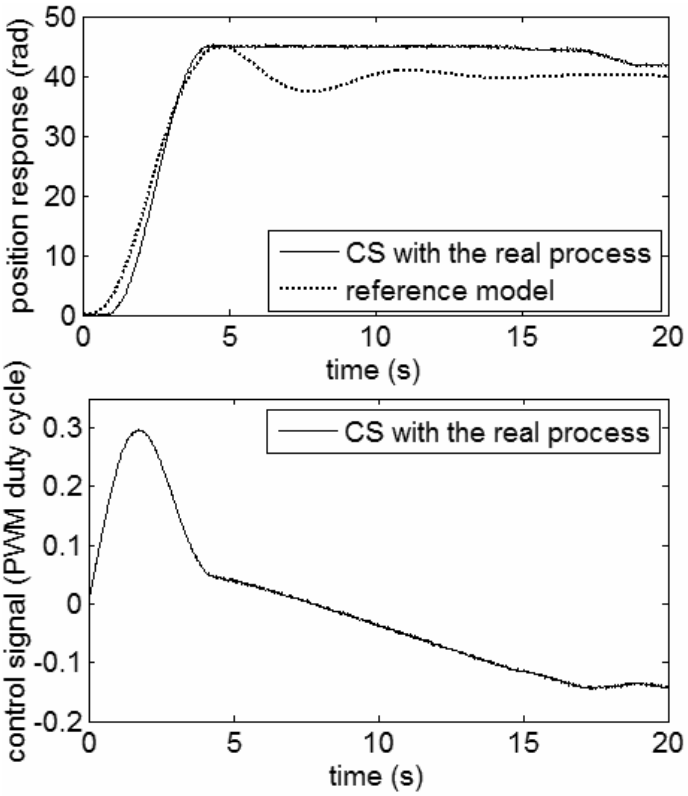

Fig. 5.9. Experimental results: controlled output (angular position) and control signal versus time for the linear CS with the PI controller before IFT.

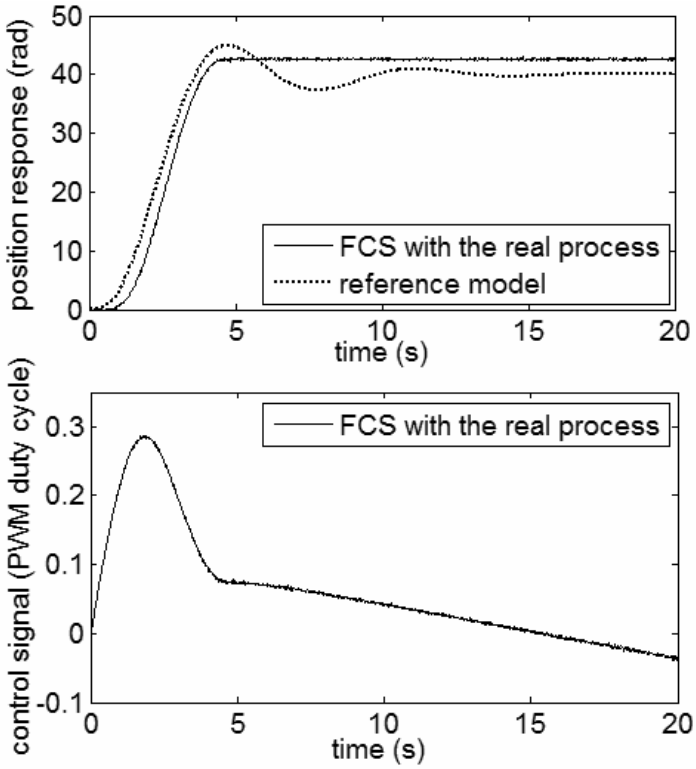

Fig. 5.10. Experimental results: controlled output (angular position) and control signal versus time for the FCS with the Takagi-Sugeno PI-FC before IFT.

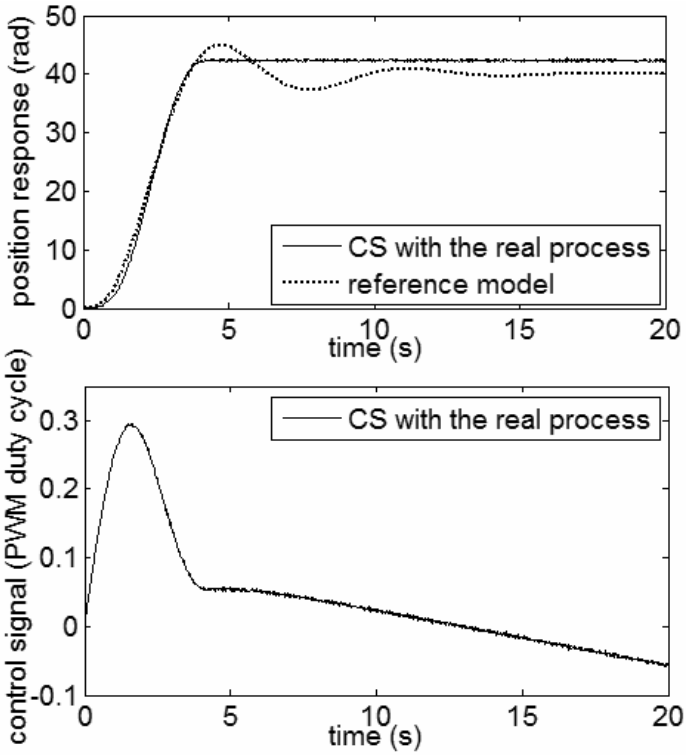

Fig. 5.11. Experimental results: controlled output (angular position) and control signal versus time for the linear CS with the PI controller after IFT.

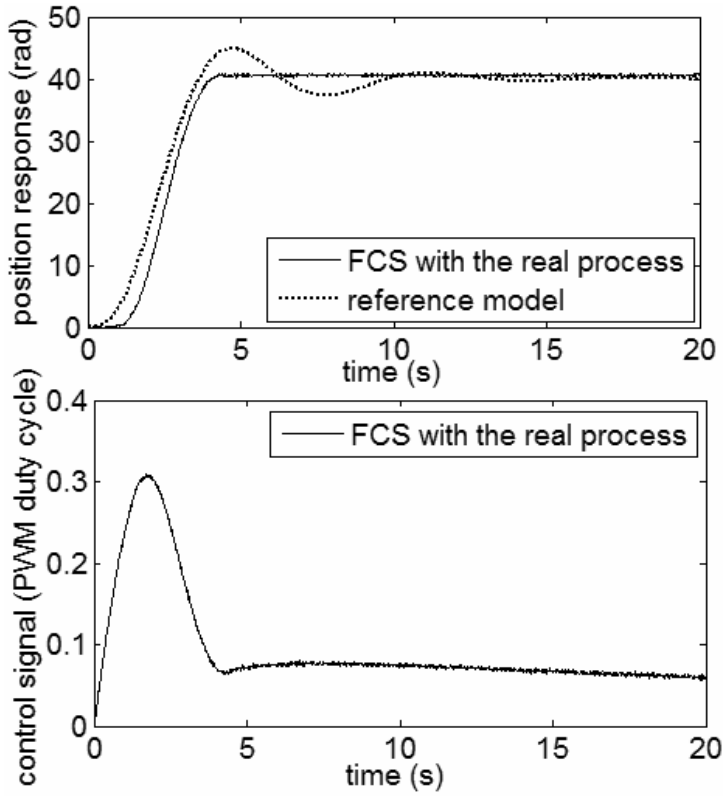

Fig. 5.12. Experimental results: controlled output (angular position) and control signal versus time for the FCS with the Takagi-Sugeno PI-FC after IFT.

For this experimental scenario the IFT-based tuning started with the same initial parameters given in (5.34). The parameters obtained after nine iterations for $\underline{R}^i = \underline{I}_2$ and $\gamma^0 = 5 \cdot 10^{-9}$, $\gamma^i = \gamma^0 / i$, $i = 1...9$ (that also satisfy (5.17) for $\varepsilon_0 = 1$ at all iterations), are

$$\underline{\rho}^9 = [K_P = 0.01199 \quad a = 0.0028]^T . \tag{5.39}$$

The values of the parameters of the Takagi-Sugeno PI-FCs were set to $B_e = 20$ for both fuzzy controllers, and the parameter $B_{\Delta e}$ of the Takagi-Sugeno PI-FCs was obtained using (5.30). The values of the parameter η and of the parameter $B_{\Delta e}$ were $\eta = 0.9$ and $B_{\Delta e} = 0.064$ for the initial fuzzy controller, and $\eta = 0.8$ and $B_{\Delta e} = 0.057$ for the final one. The Lyapunov function candidate that fulfils the stability conditions (5.10) for this FCS is defined in (5.9) and (5.38).

The FCS with the fuzzy controller that exhibits the experimental results presented in Fig. 5.10 can cope with the process nonlinearity better than the other CSs, but it still has nonzero steady-state control error. Both CSs with the IFT-based tuned PI controller and with the resulting Takagi-Sugeno PI-FC offer a slightly faster response, and the latter also ensures the zero steady-state control error. The values of the OF in the four cases that correspond to Figs. 5.9 to 5.12 were evaluated to 6.6451, 5.1081, 3.2231 and 2.4960, respectively. Therefore it is shown that the FCS

with the final IFT-based tuned fuzzy controller is better than the FCS with the initial because the OF is reduced.

The evolutions of the OF throughout the iterations of the simulation case study and of the experimental case study are illustrated in Fig. 5.13 and 5.14, respectively. The nonlinearity of the process is reflected in the OF decrease in the simulation case study where it is apparent that the OF decreasing after ten iterations, but further decreases after 20 iterations. The injected noise does not influence too much in this case the evaluation of the OF In the experimental study, the random factors that affect the evaluation of the OF are visible, they are of different nature than the injected noise, namely due to the asymmetric friction in the motor axis. However the OF decreases after several iterations. Since the evaluation of the OF on the real process has a strong variance, the more cautious steepest descent is considered in the IFTA, with small steps in order to ensure the convergence in the framework of the step 4 in the new IFTA.

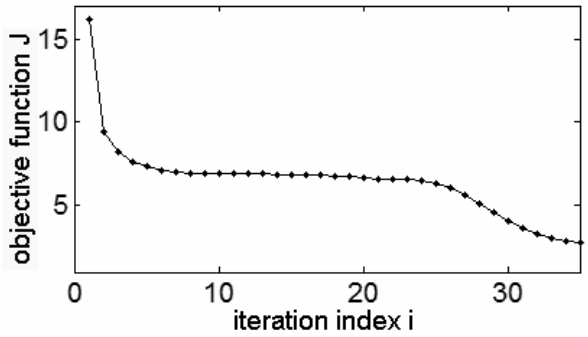

Fig. 5.13. Objective function versus iteration index in the simulations.

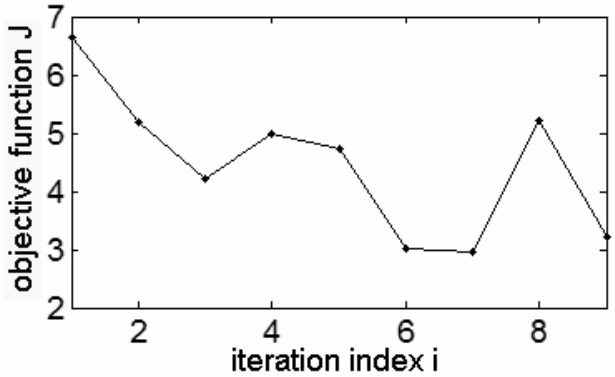

Fig. 5.14. Objective function versus iteration index in the experiments.

5.6. Chapter conclusions

Chapter 5 was devoted to studying the possible improvements that can arise from the mixing of fuzzy control with IFT. The main contribution of this chapter is a three-step stable design approach for fuzzy control systems (FCSs) with Takagi-Sugeno PI fuzzy controllers (TS-PI-FCs). The new approach is based on the

combination of IFT and fuzzy control, and it aims discrete-time input affine SISO processes. Starting with a poor process model and using a linear controller, the CS performance can be improved in two additional steps. The first step concerns the IFT, and the second step is related to the use of fuzzy control.

This chapter has suggested a three-step stable design approach for FCSs with Takagi-Sugeno PI-FCs. The new approach is based on the combination of IFT and fuzzy control, and it aims discrete-time input affine SISO processes. Starting with a poor process model and using a linear controller, the CS performance can be improved in two steps. The first step concerns the IFT, and the second step is related to the use of fuzzy control.

The stability analysis results presented here can be extended without difficulties to the design of Mamdani fuzzy controllers with singleton consequents. The application of the stability analysis is relatively simple for practitioners because it makes use of quadratic terms (5.9) in the definition of the Lyapunov function candidate.

The case study included in our contribution shows very good results in the control of a nonlinear process using the application of IFT to a simplified linear model of the process. The minimum of the OF cannot be guaranteed, but our experiment- and data-based tuning proves the improvement of the control system performance indices including the OF values. The control system performance can be improved further in terms of the fuzzy logic-based compensation of the nonlinearity of the process, but this would lead to discontinuous input-output maps of the fuzzy controllers that do not allow the systematic tuning by means of stability and convergence analysis.

The new contributions of this chapter are:

1) A mixed IFT-FCS technique to design and tune TS-PI-FCs.
2) A stability analysis approach of the resulted FCS.
3) A novel IFT algorithm with guaranteed convergence of the IFT search algorithm ensured by the use of Popov's hyperstability theory.
4) The validation of the new mixed IFT-FCS technique on a DC servo system laboratory equipment.

The results obtained in this chapter were published in:

*Precup, R.-E., **Rădac, M.-B.**, Preitl, St., Tomescu, M.-L., Petriu, E. M. and Paul, A. S. (2009): IFT-based PI-fuzzy Controllers: Signal Processing and Implementation. Proceedings of 6th International Conference on Informatics in Control, Automation and Robotics ICINCO 2009, Milan, Italy, vol. 1 Intelligent Control Systems and Optimization, pp. 207-212, indexed in* **ISI Proceedings**.

*Precup, R.-E., **Rădac, M.-B.**, Preitl, St., Petriu, E. M. and Dragoş, C.-A. (2009): Iterative Feedback Tuning in Linear and Fuzzy Control Systems. In: Towards Intelligent Engineering and Information Technology, Eds. Rudas, I. J., Fodor, J. and Kacprzyk, J. (Springer-Verlag), pp. 179-192, indexed in* **SCOPUS**.

The application of the hyperstability theory produces an elegant way to solve the problem of convergence analysis which is not a simple task. Therefore a relatively simple, general and easily algorithmic convergent IFTA is proposed. However the two indices like speed of convergence and magnitude of oscillations in the dynamics of the controller parameters are not analyzed resulting in the first limitation of the approaches given in this chapter. Measures to assess and / or impose analytically those two indices are necessary.

The second limitation is that it produces sufficient inequality-type stability and convergence conditions. Although they are more transparent than the LMIs a natural objective is to make them stronger.

Future research will be focused on extending the theoretical approaches to MIMO systems in several applications [72], [194]-[196] and controller structures [197]-[200]. The discrete-time formulation of the stability analysis will be investigated.

6. New Contributions, Future Research Directions and Dissemination of Results

6.1. New contributions

This thesis has been focused on new tuning techniques that have a **great potential** for being used in practice because of the following reasons:

- They are useful whenever retuning is needed, either because of the controlled process aging or by performance requirements changing.
- They can compensate for the lack of experience in the modeling and identification areas of the control engineer. Even if these steps would be performed, there is always a certain difference between the model and reality and therefore tight specifications can not be ensured otherwise.
- They can be used for widely spread industrial controllers of reduced complexity (such as PI, PID, PD) that predominate in the industry. The reason is their simplicity and the fact that they can be easily interpreted.
- The computations are mainly done off-line thus not affecting the computational resources that are available. This also facilitates the analysis since we are not dealing with an adaptive control context.
- To a large extend and even although the theory is developed based on the linearity assumption (for some of the techniques), they have proved to work exceptionally well in practice, for smooth nonlinear systems.

A list of **general new contributions** of this thesis is presented as follows:

- The aggregation under this thesis of different iterative and of other complementary techniques that are in recent development, and that are a current research topic in an increasing number of control engineering communities. The documentation of these techniques is very attractive since each one provides very original views on control problem formulation and solutions.
- A new IFT setup for state-feedback CSs that is used for obtaining gradients directly in the state-space formulation. This is different than other solutions found in the literature that work with transfer function representation. Different solutions for dealing with actuator saturation or for special experimentation regimes are provided.
- New iterative techniques used for optimally designed CSs such as LQR and LQG. The validity of the optimal design is questioned in the model-based design paradigm because of the discrepancies between model and reality. The tuning is attempted using experiment-based techniques. With this regard, IFT and SPSA are used and a comparison of the two techniques is also accomplished.

- An automatic selection of the step size in the search algorithm that is specific to data-based techniques. This is accomplished mainly in two settings:
    - one that is concerned with ensuring the convergence of the search algorithm to the minimum of the objective function. The development is based on the Popov's hyperstability theory. The theory is attractive because, opposed to the current developments, it makes no use of the minimum of the objective function, which prevents the use of estimated process models, thus keeping the "model-free" label intact throughout the tuning process.
    - Another setting that is concerned with the preservation of the closed-loop stability throughout the iterations. The formulation is made in a robust stability analysis framework where the controller modifications are seen as uncertainties. The stability is asserted by using a variant of the small-gain theorem for discrete-time systems. The result is that a new selection approach for the scaling coefficient of the step size is provided.
- The combination of VRFT and IFT techniques into a powerful tool in which the two techniques are complementary. The suboptimal nature of VRFT due to a sensible selection of the *L*-filter is alleviated by the use of IFT which can be used for reaching the minimum of the objective function. On the other hand, for widely spread industrial controllers such as PI or PID, for which a linear parameterization is possible, the advantage is used in a cheap estimation approach for the Hessian of the objective function which in turn translates in a faster convergence of the search algorithm. VRFT can provide at any time an initial controller as a starting point for the IFT technique.
- The combination of the iterative techniques with other conventional structures that are different from the ones in the literature has proved to be favorable in terms of the achieved improvements. In the current thesis, the combination with state-feedback controlled structures either in pole-placement or in optimal design or the combination with fuzzy CSs was successful and the premises are in favor of pursuing this direction.
- The study on how techniques such as IRT and SPSA that are of a more meta-heuristic nature are amenable to experimental-based controller tuning.

The aggregation of the specific new contributions suggested in Chapters 2, 3, 4 and 5 and presented in the chapter conclusions sections, leads to the following list of **punctual new contributions** of this thesis:

1) The experimental validation of IFT on different laboratory equipment.
2) A novel IFT tuning scheme for state feedback controlled systems.
3) The implementation of IFT on MIMO systems with saturation on the actuator.
4) A novel approach to ensuring the search algorithm convergence by using Popov's hyperstability theory, which does not need in the formulation the knowledge of the minimum of the objective function.
5) A stable IFT technique that guarantees the closed-loop stability throughout IFT tuning by using a robust stability framework with the small gain theorem

applied to a linear fractional transformation of the closed-loop when the modifications of controller's parameters are treated as uncertainties.

6) Solving the LQR design problem on experimental basis in terms of using the IFT technique, which is different to the model-based approach.
7) A new tuning technique that combines the VRFT and IFT techniques to form a powerful tool to be used in controller tuning mainly for linear systems.
8) An exploitation of the linear parameterization of some very used controllers (PI, PID) used in the mixed VRFT-IFT technique, that allows for an easy computation of the Hessian estimate. This allows in turn the acceleration of the convergence of tuning and thus the reduction of the number of gradient experiments that is typical to IFT.
9) The experimental validation of the IRT and SPSA techniques on a DC servo system laboratory equipment.
10) The state-space formulation of the IFT tuning scheme and of the SPSA tuning scheme for processes with state observers (Kalman filter).
11) Solving the LQG type problems on an experimental basis using IFT and SPSA, which is different to the usual model-free approach.
12) A mixed IFT-fuzzy control system technique to design and tune Takagi-Sugeno PI-fuzzy controllers.
13) A stability analysis approach of the resulted fuzzy control system.
14) A novel IFT algorithm with guaranteed convergence of the IFT search algorithm ensured by the use of Popov's hyperstability theory.
15) The validation of the new mixed IFT-fuzzy control system technique on a DC servo system laboratory equipment.

6.2. Future research directions

The author suggests the following **future research directions** to continue the research carried out in this thesis:

- The experimenting regimes that must not affect the normal regimes. This is of permanent concern, and it can be solved only particularly for each CS, by incorporating aprioric knowledge on the process, on the controller, on the actuators, on the excitation signals, etc. The silent run in the background of the tuning techniques would be a major step forward in their global acceptance in the industry.
- The hardware implementation using a microprocessor or a DSP-based platform that is aimed at developing prototypes for industrial application. Research in this direction is currently under work worldwide.
- The combination of the iterative techniques with other conventional CSs.
- The improvements of all aspects concerning the iterative techniques such as convergence of the search algorithm, the robust stability and robust performance assessment.

- The implementation on different industrial processes.

6.3. Dissemination of results

The new contributions of this thesis belong to the results published in 15 papers. The author of this thesis is the first author of 10 of these papers. All papers are classified as follows as function of their indexing and visibility:

- one paper published in an ISI journal with impact factor (IEEE Transactions on Education),
- six papers published in the volumes of academic conferences indexed in ISI Proceedings,
- five papers published in the volumes of academic conferences indexed in the international databases SCOPUS and/or INSPEC,
- two book chapters published in Springer-Verlag and indexed in SCOPUS as well.

All papers are visible, and this is proved by the organizing societies, IEEE (for ten papers), IFAC (for two papers) and EUCA (for one paper, published at European Control Conference ECC'09), and by Springer-Verlag (for the two book chapters). It is also highlighted that 14 out of the 15 papers are published abroad.

A list of the papers that provide new contributions of the current thesis is presented as follows:

1. ***Rădac, M.-B.****, Precup, R.-E., Preitl, St., Tar, J. K., Fodor, J. and Petriu, E. M. (2008): Gain-Scheduling and Iterative Feedback Tuning of PI Controllers for Longitudinal Slip Control. Proceedings of 6th IEEE International Conference on Computational Cybernetics ICCC 2008, Stara Lesna, Slovakia, pp. 183-188, indexed in* **SCOPUS, INSPEC**.

2. ***Rădac, M.-B.****, Precup, R.-E., Preitl, St., Petriu, E. M., Dragoş, C.-A., Paul, A. S. and Kilyeni, St. (2009): Signal Processing Aspects in State Feedback Control Based on Iterative Feedback Tuning. Proceedings of 2nd International Conference on Human System Interaction HSI'09, Catania, Italy, pp. 40-45, indexed in* **ISI Proceedings**.

3. *Precup, R.-E.,* ***Rădac, M.-B.****, Preitl, St., Tomescu, M.-L., Petriu, E. M. and Paul, A. S. (2009): IFT-based PI-fuzzy Controllers: Signal Processing and Implementation. Proceedings of 6th International Conference on Informatics in Control, Automation and Robotics ICINCO 2009, Milan, Italy, vol. 1 Intelligent Control Systems and Optimization, pp. 207-212, indexed in* **ISI Proceedings**.

4. ***Rădac, M.-B.****, Precup, R.-E., Petriu, E. M., Preitl, St. and Dragoş, C.-A. (2009): Iterative Feedback Tuning Approach to a Class of State Feedback-Controlled Servo Systems. Proceedings of 6th International Conference on Informatics in Control, Automation and Robotics ICINCO 2009, Milan, Italy, vol. 1 Intelligent Control Systems and Optimization, pp. 41-48, indexed in* **ISI Proceedings**.

5. ***Rădac, M.-B.****, Precup, R.-E., Preitl, St., Tar, J. K. and Burnham, K. J. (2009): Tire Slip Fuzzy Control of a Laboratory Anti-lock Braking System. Proceedings of the European Control Conference 2009 ECC'09, Budapest, Hungary, pp. 940-945.*

6. *Precup, R.-E., Gavriluţă, C.,* ***Rădac, M.-B.****, Preitl, St., Dragoş, C.-A., Tar, J. K. and Petriu, E. M. (2009): Iterative Learning Control Experimental Results for Inverted Pendulum Crane Mode Control. Proceedings of 7th International Symposium on Intelligent Systems and Informatics SISY 2009, Subotica, Serbia, pp. 323-328, indexed in* **ISI Proceedings**.

7. ***Rădac, M.-B.****, Precup, R.-E., Preitl, St. and Dragoş, C.-A. (2009): Iterative Feedback Tuning in MIMO Systems. Signal Processing and Application. Proceedings of 5th International Symposium on Applied Computational Intelligence and Informatics SACI 2009, Timişoara, Romania, pp. 77-82, indexed in* **ISI Proceedings**.

8. *Precup, R.-E., Moşincat, I.,* ***Rădac, M.-B.****, Preitl, St., Kilyeni, St., Petriu, E. M. and Dragoş, C.-A. (2010): Experiments in Iterative Feedback Tuning for Level Control of Three-Tank System. Proceedings of 15th IEEE Mediterranean Electromechanical Conference MELECON 2010, Valletta, Malta, pp. 564-569, indexed in* **ISI Proceedings**.

9. *Precup, R.-E., Borchescu, C.,* ***Rădac, M.-B.****, Preitl, St., Dragoş, C.-A., Petriu, E. M. and Tar, J. K. (2010): Implementation and Signal Processing Aspects of Iterative Regression Tuning. Proceedings of 2010 IEEE International Symposium on Industrial Electronics ISIE 2010, Bari, Italy, pp. 1657-1662, indexed in* **SCOPUS, INSPEC**.

10. *Precup, R.-E.,* ***Rădac, M.-B.****, Preitl, St., Petriu, E. M. and Dragoş, C.-A. (2009): Iterative Feedback Tuning in Linear and Fuzzy Control Systems. In: Towards Intelligent Engineering and Information Technology, Eds. Rudas, I. J., Fodor, J. and Kacprzyk, J. (Springer-Verlag), pp. 179-192, indexed in* **SCOPUS**.

11. *Precup, R.-E., Preitl, St.,* ***Rădac, M.-B.****, Petriu, E. M., Dragoş, C.-A. and Tar, J. K. (online first, Date of Publication: 03 August 2010): Experiment-based teaching in advanced control engineering. IEEE Transactions on Education, vol. PP, no. 99, pp. 1-11, DOI: 10.1109/TE.2010.2058575,* ***ISI*** *Science Citation Index impact factor (in 2009) = 1.157.*

12. ***Rădac, M.-B.****, Precup, R.-E., Petriu, E. M., Preitl, St. and Dragoş, C.-A. (2011): Convergent Iterative Feedback Tuning of State Feedback-Controlled Servo Systems. In: Informatics in Control Automation and Robotics, Eds. Andrade Cetto, J., Filipe, J. and Ferrier, J.-L. (Springer-Verlag), pp. 99-111, indexed in* **SCOPUS**.

13. ***Rădac, M.-B.****, Grad, R.-B., Precup, R.-E., Preitl, St., Dragoş, C.-A., Petriu, E. M. and Kilyeni, A. (2011): Mixed Virtual Reference Feedback Tuning - Iterative Feedback Tuning Approach to the Position Control of a Laboratory Servo System. Proceedings of International Conference on Computer as a Tool EUROCON 2011, Lisbon, Portugal, paper index 453, 4 pp., indexed in* **INSPEC**.

14. ***Rădac, M.-B.****, Grad. R.-B., Precup, R.-E., Petriu, E. M., Preitl, St. and Dragoş, C.-A. (2011): Mixed Virtual Reference Feedback Tuning – Iterative Feedback Tuning: Method and Laboratory Assessment. Proceedings of 20th IEEE International Symposium on Industrial Electronics ISIE 2011, Gdansk, Poland, pp. 649-654, indexed in* **INSPEC**.

15. ***Rădac, M.-B.****, Precup, R.-E., Petriu, E. M., Preitl, St. and David, R.-C. (2011): Stable Iterative Feedback Tuning Method for Servo Systems. Proceedings of 20th IEEE International Symposium on Industrial Electronics ISIE 2011, Gdansk, Poland, pp. 1943-1948, indexed in* **INSPEC**.

Appendix A

This Appendix illustrates the connection between the LQR objective function which drives the analytical solutions of the optimization problem, and the IFT objective function which is subject to practical evaluations in our data-based algorithm. We assume two cases for the objective function, defined in the deterministic case and in the stochastic case related to the state feedback CS. The dependence on the parameter vector $\underline{\rho}$ is omitted for the sake of simplicity. Our development follows a similar development to that presented in [48], and the two cases, a) and b), are presented as follows.

a) *The deterministic case*. We assume that the following operational relationships are valid:

$$\begin{aligned} &\underline{x}(\underline{\rho},k) = \underline{P}_{\underline{r}\,\underline{x}}(\underline{\rho},q^{-1})\,\underline{r}(k),\;\; u(\underline{\rho},k) = P_{\underline{r}\,u}(\underline{\rho},q^{-1})\,\underline{r}(k), \\ &\underline{e}(\underline{\rho},k) = \underline{r}(k) - \underline{x}(\underline{\rho},k) = \underline{r}(k) - \underline{P}_{r\,\underline{x}}(\underline{\rho},q^{-1})\underline{r}(k), \end{aligned} \tag{A.1}$$

where $\underline{P}_{\underline{r}\,\underline{x}}(\underline{\rho},q^{-1})$ is the *nxn* process pulse transfer matrix operator from the reference input vector $\underline{r}$ to the state vector $\underline{x}$ and $\underline{P}_{\underline{r}\,u}(\underline{\rho},q^{-1})$ is the *nx1* process pulse transfer matrix operator from $\underline{r}$ to the control signal u. The dependence on $\underline{\rho}$ is assumed but not explicitly written as follows in order to simplify notation.

The infinite horizon objective function specific to the formulation of the LQR problem corresponding to this case is

$$\begin{aligned} I(\underline{\rho}) &= \sum_{k=0}^{\infty}\{\underline{e}(k)^T\;\underline{Q}\,\underline{e}(k) + \lambda\,u^2(k)\} \\ &= \sum_{k=0}^{\infty}\{[\underline{r}(k) - \underline{P}_{\underline{r}\,\underline{x}}(q^{-1})\,\underline{r}(k)]^T\;\underline{Q}\,[\underline{r}(k) - \underline{P}_{\underline{r}\,\underline{x}}(q^{-1})\,\underline{r}(k)] + \lambda\,[\underline{P}_{\underline{r}\,u}(q^{-1})\underline{r}(k)]^2\}. \end{aligned} \tag{A.2}$$

b) *The stochastic case*. The following relations hold:

$$\begin{aligned} &\underline{x}(k) = \underline{P}_{\underline{r}\,\underline{x}}(q^{-1})\,\underline{r}(k) + \underline{P}_{\underline{w}\,\underline{x}}(q^{-1})\,\underline{w}(k),\;\; u(k) = \underline{P}_{\underline{r}\,u}(q^{-1})\,\underline{r}(k) + \underline{P}_{\underline{w}\,u}(q^{-1})\,\underline{w}(k), \\ &\underline{e}(k) = \underline{r}(k) - \underline{x}(k) = \underline{r}(k) - \underline{P}_{\underline{r}\,\underline{x}}(q^{-1})\,\underline{r}(k) - \underline{P}_{\underline{w}\,\underline{x}}(q^{-1})\,\underline{w}(k). \end{aligned} \tag{A.3}$$

The reference input vector and the process noise are assumed to be quasi-stationary and uncorrelated, i.e.,

$$E\{\underline{r}(k)\underline{w}^T(k)\} = 0\,. \tag{A.4}$$

The expression of the objective function used in IFT in this case is

$$J(\underline{\rho}) = E\{\sum_{k=0}^{\infty} \underline{e}(k)^T \underline{Q}\underline{e}(k) + \lambda u^2(k)\} =$$

$$= E\{\sum_{k=0}^{\infty} [\underline{r}(k) - \underline{P}_{\underline{r}\,\underline{x}}(q^{-1})\underline{r}(k) - \underline{P}_{\underline{w}\,\underline{x}}(q^{-1})\underline{w}(k)]^T \underline{Q}\,[\underline{r}(k) - \underline{P}_{\underline{r}\,\underline{x}}(q^{-1})\underline{r}(k) - \underline{P}_{\underline{w}\,\underline{x}}(q^{-1})\underline{w}(k)]$$

$$+ \lambda [\underline{P}_{\underline{r}\,u}(q^{-1})\underline{r}(k) + \underline{P}_{\underline{w}u}(q^{-1})\underline{w}(k)]^2\} = \sum_{k=0}^{\infty} E\{[\underline{r}(k) - \underline{P}_{\underline{r}\,\underline{x}}(q^{-1})\underline{r}(k)]^T \underline{Q}\,[\underline{r}(k) - \underline{P}_{\underline{r}\,\underline{x}}(q^{-1})\underline{r}(k)]\}$$

$$- \sum_{k=0}^{\infty} E\{[\underline{r}(k) - \underline{P}_{\underline{r}\,\underline{x}}(q^{-1})\underline{r}(k)]^T \underline{Q}\underline{P}_{\underline{w}\,\underline{x}}(q^{-1})\underline{w}(k)\} - \sum_{k=0}^{\infty} E\{[\underline{P}_{\underline{w}\,\underline{x}}(q^{-1})\underline{w}(k)]^T \underline{Q}\,[\underline{r}(k) - \underline{P}_{\underline{r}\,\underline{x}}(q^{-1})\underline{r}(k)]\}$$

$$+ \sum_{k=0}^{\infty} E\{[\underline{P}_{\underline{w}\,\underline{x}}(q^{-1})\underline{w}(k)]^T \underline{Q}\,[\underline{P}_{\underline{w}\,\underline{x}}(q^{-1})\underline{w}(k)]\} + \lambda \sum_{k=0}^{\infty} E\{[\underline{P}_{\underline{r}\,u}(q^{-1})\underline{r}(k)]^2\}$$

$$+ 2\lambda \sum_{k=0}^{\infty} E\{[\underline{P}_{\underline{r}\,u}(q^{-1})\underline{r}(k)][\underline{P}_{\underline{w}u}(q^{-1})\underline{w}(k)]\} + \lambda \sum_{k=0}^{\infty} E\{[\underline{P}_{\underline{w}u}(q^{-1})\underline{w}(k)]^2\}. \tag{A.5}$$

The second, the third and the sixth terms in (A.5) are zero due to the uncorrelation between r and w. Therefore the following expression of $J(\underline{\rho})$ is obtained:

$$J(\underline{\rho}) = I(\underline{\rho}) + \underbrace{\sum_{k=0}^{\infty} E\{[\underline{P}_{\underline{w}\,\underline{x}}(q^{-1})\underline{w}(k)]^T \underline{Q}\,[\underline{P}_{\underline{w}\,\underline{x}}(q^{-1})\underline{w}(k)]\} + \lambda \sum_{k=0}^{\infty} E\{[\underline{P}_{\underline{w}u}(q^{-1})\underline{w}(k)]^2\}}_{J_{\underline{w}}(\underline{\rho})} \tag{A.6}$$

The term $J_{\underline{w}}(\underline{\rho})$ is dedicated to the minimization of the energy transfer from the process noise to the state variables and to the control signal. Inherently, in experiment-based tuning via IFT, this objective is also targeted in addition to the objectives to minimize the state control error energy (set-point tracking) and the control signal energy. If the reference input vector **r** and the weight λ are chosen to be zero, the objective function $J(\underline{\rho})$ is dedicated to the minimization of the energy transfer from the process noise to the state variables, resulting in a non-robust structure.

Appendix B

This appendix presents the proof of Theorem 5.1 in Chapter 5 dedicated to the globally asymptotically stability of the equilibrium point at the origin of the FCSs. The theorem is supported by the following well acknowledged result based on Lyapunov's direct method for discrete-time systems [41]: let the process be characterized by the state-space model (5.1). If there exists a continuous radially unbounded Lyapunov function candidate $V : R^n \to R$ such that $V(\underline{x}) > 0$, $\forall \underline{x} \neq 0$, $V(\underline{0}) = 0$, and

$$V(\underline{x}(t+1)) < V(\underline{x}(t)), \tag{B.1}$$

then the equilibrium point at the origin $\underline{x}(t) = 0 = [0 \quad 0 \quad \ldots \quad 0]^T \in R^n$ of the system (5.1) will be globally asymptotically stable.

The hypothesis (5.10) of Theorem 5.1 leads to

$$\Delta V_k(\underline{x}(t)) = V_k(\underline{x}(t+1)) - V_k(\underline{x}(t)) < 0, \forall \underline{x} \in X_k^A, k = 1...n_{RB}. \tag{B.2}$$

The term $\underline{x}(t+1)$ is next substituted from (5.1) into (B.2):

$$\Delta V_k(\underline{x}(t)) = V_k(\underline{f}(\underline{x}(t)) + \underline{b}(\underline{x}(t))u_k(t)) - V_k(\underline{x}(t)) = [\underline{f}(\underline{x}(t)) + \underline{b}(\underline{x}(t))u_k(t)]^T \underline{P}\,[\underline{f}(\underline{x}(t)) + \underline{b}(\underline{x}(t))u_k(t)] - \underline{x}^T(t)\,\underline{P}\,\underline{x}(t) = \underline{f}^T(\underline{x}(t))\,\underline{P}\,\underline{f}(\underline{x}(t)) - \underline{x}^T(t)\,\underline{P}\,\underline{x}(t) + \underline{b}^T(\underline{x}(t))\,\underline{P}\,\underline{b}(\underline{x}(t))u_k^2(t) + [\underline{f}^T(\underline{x}(t))\,\underline{P}\,\underline{b}(\underline{x}(t)) + \underline{b}^T(\underline{x}(t))\,\underline{P}\,\underline{f}(\underline{x}(t))]u_k(t) < 0. \tag{B.3}$$

The multiplication of (B.3) by $\alpha_k(\underline{x}(t))$, and the calculation of the sum result in

$$[\underline{f}^T(\underline{x}(t))\,\underline{P}\,\underline{f}(\underline{x}(t)) - \underline{x}^T(t)\,\underline{P}\,\underline{x}(t)]\sum_{k=1}^{n_{RB}}\alpha_k(\underline{x}(t)) + \underline{b}^T(\underline{x}(t))\,\underline{P}\,\underline{b}(\underline{x}(t))\sum_{k=1}^{n_{RB}}[\alpha_k(\underline{x}(t))u_k^2(t)] + [\underline{f}^T(\underline{x}(t))\,\underline{P}\,\underline{b}(\underline{x}(t)) + \underline{b}^T(\underline{x}(t))\,\underline{P}\,\underline{f}(\underline{x}(t))]\sum_{k=1}^{n_{RB}}[\alpha_k(\underline{x}(t))u_k(t)] < 0. \tag{B.4}$$

The relation (B.4) is divided by $\sum_{k=1}^{n_{RB}}\alpha_k(\underline{x}(t)) > 0$ and the sums are manipulated as follows:

$$\underline{f}^T(\underline{x}(t))\,\underline{P}\,\underline{f}(\underline{x}(t)) - \underline{x}^T(t)\,\underline{P}\,\underline{x}(t) + \underline{b}^T(\underline{x}(t))\,\underline{P}\,\underline{b}(\underline{x}(t))\{\sum_{k=1}^{n_{RB}}[\alpha_k(\underline{x}(t))u_k^2(t)]\}/\{\sum_{k=1}^{n_{RB}}\alpha_k(\underline{x}(t))\} + [\underline{f}^T(\underline{x}(t))\,\underline{P}\,\underline{b}(\underline{x}(t)) + \underline{b}^T(\underline{x}(t))\,\underline{P}\,\underline{f}(\underline{x}(t))]\{\sum_{k=1}^{n_{RB}}[\alpha_k(\underline{x}(t))u_k(t)]\}/\{\sum_{k=1}^{n_{RB}}\alpha_k(\underline{x}(t))\} < 0. \tag{B.5}$$

The inequality (B.5) is expressed as follows accounting for (5.6):

$$\underline{f}^T(\underline{x}(t))\,\underline{P}\,\underline{f}(\underline{x}(t)) - \underline{x}^T(t)\,\underline{P}\,\underline{x}(t) + \underline{b}^T(\underline{x}(t))\,\underline{P}\,\underline{b}(\underline{x}(t))\{\sum_{k=1}^{n_{RB}}[\alpha_k(\underline{x}(t))u_k^2(t)]\}/\{\sum_{k=1}^{n_{RB}}\alpha_k(\underline{x}(t))\}$$
$$+[\underline{f}^T(\underline{x}(t))\,\underline{P}\,\underline{b}(\underline{x}(t)) + \underline{b}^T(\underline{x}(t))\,\underline{P}\,\underline{f}(\underline{x}(t))]u(t) < 0. \tag{B.6}$$

Cauchy-Buniakovski-Schwarz's inequality results next in

$$\{\sum_{k=1}^{n_{RB}}[\sqrt{\alpha_k(\underline{x}(t))}]^2\}\{\sum_{k=1}^{n_{RB}}[\sqrt{\alpha_k(\underline{x}(t))}u_k(t)]^2\} \geq \{\sum_{k=1}^{n_{RB}}[\sqrt{\alpha_k(\underline{x}(t))}\sqrt{\alpha_k(\underline{x}(t))}u_k(t)]\}^2 \tag{B.7}$$

,

which is equivalent to

$$\sum_{k=1}^{n_{RB}}[\alpha_k(\underline{x}(t))u_k^2(t)] \geq \{\sum_{k=1}^{n_{RB}}[\alpha_k(\underline{x}(t))u_k(t)]\}^2 /\{\sum_{k=1}^{n_{RB}}\alpha_k(\underline{x}(t))\}. \tag{B.8}$$

The division of (B.8) by $\sum_{k=1}^{n_{RB}}\alpha_k(\underline{x}(t)) > 0$ using (5.6) leads to

$$\{\sum_{k=1}^{n_{RB}}[\alpha_k(\underline{x}(t))u_k^2(t)]\}/\{\sum_{k=1}^{n_{RB}}\alpha_k(\underline{x}(t))\} \geq \{\{\sum_{k=1}^{n_{RB}}[\alpha_k(\underline{x}(t))u_k(t)]\}/\{\sum_{k=1}^{n_{RB}}\alpha_k(\underline{x}(t))\}\}^2 = u^2(t) \tag{B.9}$$

But the expression of $\Delta V(\underline{x}(t))$ results from (5.1) and (5.9):

$$\Delta V(\underline{x}(t)) = \underline{f}^T(\underline{x}(t))\,\underline{P}\,\underline{f}(\underline{x}(t)) - \underline{x}^T(t)\,\underline{P}\,\underline{x}(t) + \underline{b}^T(\underline{x}(t))\,\underline{P}\,\underline{b}(\underline{x}(t))u^2(t)$$
$$+[\underline{f}^T(\underline{x}(t))\,\underline{P}\,\underline{b}(\underline{x}(t) + \underline{b}^T(\underline{x}(t))\,\underline{P}\,\underline{f}(\underline{x}(t))]u(t). \tag{B.10}$$

The following inequality is next obtained from (B.9) and (B.10):

$$\Delta V(\underline{x}(t)) < \underline{f}^T(\underline{x}(t))\,\underline{P}\,\underline{f}(\underline{x}(t)) - \underline{x}^T(t)\,\underline{P}\,\underline{x}(t) + \underline{b}^T(\underline{x}(t))\,\underline{P}\,\underline{b}(\underline{x}(t))\{\sum_{k=1}^{n_{RB}}[\alpha_k(\underline{x}(t))u_k^2(t)]\}/\{\sum_{k=1}^{n_{RB}}\alpha_k(\underline{x}(t))\}$$
$$+[\underline{f}^T(\underline{x}(t))\,\underline{P}\,\underline{b}(\underline{x}(t) + \underline{b}^T(\underline{x}(t))\,\underline{P}\,\underline{f}(\underline{x}(t))]u(t). \tag{B.11}$$

Equations (B.6) and (B.11) result finally in

$$\Delta V(\underline{x}(t)) < 0. \tag{B.12}$$

Therefore the equilibrium point at the origin $\underline{x} = \underline{0}$ will be globally asymptotically stable. The proof is now complete. Concluding, Theorem 5.1 offers sufficient stability conditions concerning the class of FCSs defined in Subchapter 5.2.

References

[1] K. Hamamoto, T. Fukuda, and T. Sugie, "Iterative Feedback Tuning of controllers for a two-mass-spring system with friction," *Control Engineering Practice*, vol. 11, pp. 1061-1068, September 2003.

[2] N. Hur, K. Nam, and S. Won, "A two degree of freedom current control scheme for deadtime compensation," *IEEE Transactions on Industrial Electronics*, vol. 47, no. 3, June 2000.

[3] D. Kostić, "Data-driven robot motion control design," PhD. Thesis, Technical University of Eindhoven, Eindhoven, The Netherlands, 2004.

[4] O. Lequin, M. Gevers, M. Mossberg, E. Bosmans, and L. Triest, "Iterative Feedback Tuning of PID parameters: comparison with classical tuning rules," *Control Engineering Practice*, vol. 11, pp. 1023-1033, September 2003.

[5] M. Mihajlov, E. Wendland, O. Ivlev, and A. Gräser, "Versuchsaufbau und Reglerentwurf für modulare Leichtbaurobotergelenke mit flexiblen fluidischen Aktorelemente," in *Proceedings of 8. DFMRS Fachtagung*, Bremen, Germany, 2004, pp. 67-78.

[6] J.C. Spall and J.A. Cristion, "Model-free control of nonlinear stochastic systems with discrete-time measurements," *IEEE Transactions on Automatic Control*, vol. 43, pp. 1198-1210, September 1998.

[7] K.K Tak, Q.-G. Wang, and C.C. Hang, *Advances in PID Control*. London: Springer-Verlag, 1999.

[8] J.C. Spall, "Multivariate stochastic approximation using a simultaneous perturbation gradient approximation," *IEEE Transactions on Automatic Control*, vol. 37, pp. 332-341, March 1992.

[9] J.C. Spall, "Adaptive stochastic approximation by the simultaneous perturbation method," *IEEE Transactions on Automatic Control*, vol. 45, pp. 1839-1853, October 2000.

[10] J.C. Spall, *Introduction to Stochastic Search and Optimization: Estimation, Simulation, and Control*. Hoboken, NJ: Wiley, 2003.

[11] K. Halmevaara and H. Hyötyniemi, "Process performance optimization using iterative regression tuning," Research Report no. 139, Control Engineering Lab., Helsinki University of Technology, Helsinki, Finland, 2004.

[12] K. Halmevaara and H. Hyötyniemi, "Data-based parameter optimization of dynamic simulation models," in *Proceedings of 47th Conference on Simulation and Modelling (SIMS 2006)*, Helsinki, Finland, pp. 68–73, 2006.

[13] H. Robbins and S. Monro, "A stochastic approximation method," *Annals of Mathematical Statistics*, vol. 22, pp. 400-407, September 1951.

[14] H. Hjalmarsson, S. Gunnarsson, and M. Gevers, "A convergent iterative restricted complexity control design scheme," in *Proceedings of 33rd IEEE Conference on Decision and Control (CDC)*, Orlando, FL, USA, 1994, vol. 2, pp. 1735-1740.

[15] H. Hjalmarsson, "Control of nonlinear systems using Iterative Feedback Tuning," in *Proceedings of the American Control Conference*, Philadelphia, PA, USA, 1998, vol. 4, pp. 2083-2087.

[16] H. Hjalmarsson, M. Gevers, S. Gunnarsson, and O. Lequin, "Iterative Feedback Tuning: theory and applications," *IEEE Control Systems Magazine*, vol. 18, pp. 26-41, August 1998.

[17] B. Codrons, F. De Bruyne, M. De Wan, and M. Gevers, "Iterative Feedback Tuning of a nonlinear controller for an inverted pendulum with a flexible transmission," in *Proceedings of IEEE International Conference on Control Applications (CCA'98)*, Trieste, Italy, 1998, pp.1281-1285.

[18] H. Hjalmarsson and T. Birkeland, "Iterative Feedback Tuning of linear time-invariant MIMO systems," in *Proceedings of 37th IEEE Conference on Decision and Control (CDC)*, Tampa, FL, USA, 1998, pp. 3893-3898.

[19] H. Hjalmarsson, "Efficient tuning of linear multivariable controllers using Iterative Feedback Tuning," *International Journal of Adaptive Control and Signal Processing*, vol. 13, pp. 553-572, November 1999.

[20] H. Jansson, and H. Hjalmarsson, "Gradient approximations in Iterative Feedback Tuning for multivariable processes," *International Journal of Adaptive Control and Signal Processing*, vol. 18, pp. 665-681, October 2004.

[21] F. De Bruyne, "Iterative Feedback Tuning for internal model controllers," *Control Engineering Practice*, vol. 11, pp. 1043-1048, September 2003.

[22] R. Hildebrand, A. Lecchini, G. Solari, and M. Gevers, "Prefiltering in Iterative Feedback Tuning: optimization of the prefilter for accuracy," *IEEE Transactions on Automatic Control*, vol. 49, pp. 1801-1805, October 2004.

[23] R. Hildebrand, A. Lecchini, G. Solari, and M. Gevers, "Asymptotic accuracy of Iterative Feedback Tuning," *IEEE Transactions on Automatic Control*, vol. 50, pp. 1182-1185, August 2005.

[24] R. Hildebrand, A. Lecchini, G. Solari, and M. Gevers, "Optimal prefiltering in Iterative Feedback Tuning," *IEEE Transactions on Automatic Control*, vol. 50, pp. 1196-1200, August 2005.

[25] S. Veres and H. Hjalmarsson, "Tuning for robustness and performance using Iterative Feedback Tuning," in *Proceedings of 41st IEEE Conference on Decision and Control (CDC)*, Las Vegas, NV, USA, 2002, vol. 4, pp. 4682-4687.

[26] A. Lecchini and M. Gevers, "On Iterative Feedback Tuning for nonminimum phase processes," in *Proceedings of 41st IEEE Conference on Decision and Control (CDC)*, Las Vegas, NV, USA, 2002, vol. 4, pp. 4658-4663.

[27] H. Hjalmarsson, "Iterative Feedback Tuning – an overview," *International Journal of Adaptive Control and Signal Processing*, vol. 16, pp. 373-395, June 2002.

[28] A. Al Mamun, W.Y. Ho, W.E. Wang, and T.H. Lee, "Iterative Feedback Tuning (IFT) of hard disk drive head positioning servomechanism," in *Proceedings of 33rd Annual Conference of the IEEE Industrial Electronics Society (IECON 2007)*, Taipei, Taiwan, 2007, pp. 769-774.

[29] F. de Bruyne and L.C. Kammer, "Iterative Feedback Tuning with guaranteed stability," in *Proceedings of 1999 American Control Conference*, San Diego, CA, USA, 1999, vol. 5, pp. 3317-3321.

[30] L.C. Kammer, F. De Bruyne, and R.R. Bitmead, "Iterative Feedback Tuning via minimization of the absolute error," in *Proceedings of 38th IEEE Conference on Decision and Control*, Phoenix, AZ, USA, 1999, vol. 5, pp. 4619-4624.

[31] E.J. Sung and W.K. Sang, "Normalized Iterative Feedback Tuning with modified feedback experiment," in *Proceedings of American Control Conference (ACC 2001)*, Arlington, VA , USA, 2001, vol. 1, pp. 612-617.

[32] W.K. Ho, Y. Hong, A. Hansson, H. Hjalmarsson, and J.W. Deng, "Relay auto-tuning of PID controllers using Iterative Feedback Tuning," *Automatica*, vol. 39, pp. 149-157, January 2003.

[33] M. Mossberg, "Controller tuning via minimization of time weighted absolute error," in *Proceedings of American Control Conference*, Boston, MA, USA, 2004, vol. 3, pp. 2740-2744.

[34] I. Nilkhamhang and A. Sano, "Iterative tuning algorithm for feedforward and feedback control of two-mass motor system with physical parameter identification," in *Proceedings of IEEE Conference on Control Applications (CCA 2005)*, Toronto, Canada, 2005, pp. 1624-1629.

[35] H. Prochazka, M. Gevers, B.D.O. Anderson, and C. Ferrera, "Iterative Feedback Tuning for robust controller design and optimization," in *Proceedings of 44th IEEE Conference on Decision and Control, 2005 and 2005 European Control Conference (CDC-ECC '05)*, Seville, Spain, 2005, pp. 3602-3607.

[36] A.E. Graham, A.J. Young, and S.Q. Xie, "Rapid tuning of controllers by IFT for profile cutting machines," *Mechatronics*, vol. 17, pp. 121-128, March-April 2007.

[37] J.K. Huusom, H. Hjalmarsson, N.K. Poulsen, and S.B. Jørgensen, "Improving convergence of Iterative Feedback Tuning using optimal external perturbations," in *Proceedings of 47th IEEE Conference on Decision and Control (CDC 2008)*, Cancun, Mexico, 2008, pp. 2618-2623.

[38] J.K. Huusom, N.K. Poulsen, and S.B. Jørgensen, "Improving convergence of Iterative Feedback Tuning," *Journal of Process Control*, vol. 19, pp. 570-578, April 2009.

[39] S. Kissling, Ph. Blanc, P. Myszkorowski and I. Vaclavik, "Application of Iterative Feedback Tuning (IFT) to speed and position control of a servo drive," *Control Engineering Practice*, vol. 17, pp. 834-840, July 2009.

[40] F. De Bruyne, "Iterative Feedback Tuning for MIMO systems," in *Proceedings of 2nd International Symposium on Intelligent Control (ISIAC '98)*, Anchorage, Anchorage, AK, USA, 1998, pp. 179.1-179.8.

[41] M. Akerblad, A. Hansson, and B. Wahlberg, "Automatic tuning for classical step-response specifications using Iterative Feedback Tuning," in *Proceedings of 39th IEEE Conference on Decision and Control*, Sydney, Australia, 2000, vol. 4, pp. 3347-3348.

[42] M.-B. Rădac, R.-E. Precup, St. Preitl, J.K. Tar, J. Fodor, and E.M. Petriu, "Gain-Scheduling and Iterative Feedback Tuning of PI controllers for longitudinal slip control," in *Proceedings of 6th IEEE International Conference on Computational Cybernetics (ICCC 2008)*, Stara Lesna, Slovakia, 2008, pp. 183-188.

[43] M.-B. Rădac, R.-E. Precup, St. Preitl, E.M. Petriu, C.-A. Dragoş, A.S. Paul, and St. Kilyeni, "Signal processing aspects in state feedback control based on Iterative Feedback Tuning," in *Proceedings of 2nd International Conference on Human System Interaction (HIS'09)*, Catania, Italy, 2009, pp. 40-45.

[44] M.-B. Rădac, R.-E. Precup, St. Preitl, and C.-A. Dragos, "Iterative Feedback Tuning in MIMO systems. Signal processing and application," in *Proceedings of 5th International Symposium on Applied Computational Intelligence and Informatics (SACI 2009)*, Timisoara, Romania, 2009, pp. 77-82.

[45] M.-B. Rădac, R.-E. Precup, E. M. Petriu, St. Preitl, and C.-A. Dragoş, "Iterative Feedback Tuning approach to a class of state feedback-controlled servo systems," in *Proceedings of 6th International Conference on Informatics in Control, Automation and Robotics (ICINCO 2009)*, Milano, Italy, 2009, vol. 1, pp. 41-48.

[46] R.-E. Precup, M.-B. Rădac, St. Preitl, M.-L. Tomescu, E.M. Petriu, and A.S. Paul, "IFT-Based PI-Fuzzy Controllers: Signal Processing and Implementation," in *Proceedings of 6th International Conference on Informatics in Control, Automation and Robotics (ICINCO 2009)*, Milano, Italy, 2009, vol. 1, 207-212.

[47] D. Eckhard and A.S. Bazanella, "Optimizing the convergence of data-based controller tuning," in *Proceedings of European Control Conference 2009 (ECC 2009)*, Budapest, Hungary, 2009, pp. 9210-915.

[48] A.S. Bazanella, M. Gevers, L. Miskovic, and B.D.O. Anderson, "Iterative minimization of H_2 control performance criteria," *Automatica*, vol. 44, pp. 2549-2559, October 2008.

[49] L. Miskovic, A. Karimi, D. Bonvin, and M. Gevers, "Correlation-based Tuning of decoupling multivariable controllers," *Automatica*, vol. 43, pp. 1481-1494, September 2007.

[50] K. Ogata, *Discrete-time control systems 2/E*. Englewood Cliffs, NJ: Prentice Hall, 1994.

[51] L. Gerencser, Z. Vago, and H. Hjalmarsson, "Randomized iterative feedback tuning," in *Proceedings of 15th IFAC World Congress*, Barcelona, Spain, 2002, vol. 15, pp. 1-6.

[52] H. Hyötyniemi, "Multivariate regression - techniques and tools," Research Report no. 125, Control Engineering Laboratory, Helsinki University of Technology, Helsinki, Finland, 2001.

[53] M. C. Campi, A. Lecchini, and S.M. Savaresi, "Virtual reference feedback tuning: a direct method for the design of feedback controllers," *Automatica*, vol. 38, pp. 1337–1346, August 2002.

[54] A. Lecchini, M.C. Campi, and S.M Savaresi, "Sensitivity shaping via Virtual Reference Feedback Tuning," in *Proceedings of 40th Conference on Decision and Control*, Orlando, FL, USA, 2001, pp. 750-755.

[55] M.C. Campi, A. Lecchini, and S.M. Savaresi, "An application of the Virtual Reference Feedback Tuning (VRFT) method to a benchmark active system," *European Journal of Control*, vol. 1, pp. 66-76, 2003.

[56] M. Gevers, "Identification for control," *Annual Reviews in Control*, vol. 20, pp. 95-106, January 1996.

[57] G. Solari and M. Gevers, "Unbiased estimation of the Hessian for Iterative Feedback Tuning (IFT)," in *Proceedings of the 43rd IEEE Conference on Decision and Control (CDC)*, Atlantis, Bahamas, 2004, vol. 2, pp. 1759-1760.
[58] J.K. Huusom, N.K. Poulsen, and S.B. Jørgensen, "Data driven tuning of state space control loops with unknown state information and model uncertainty," *Computer Aided Chemical Engineering*, vol. 26, pp. 441-446, December 2009.
[59] J. Sjöberg, F. De Bruyne, M. Agarwal, B.D.O. Anderson, M. Gevers, F.J. Kraus, and N. Linard, "Iterative controller optimization for nonlinear systems," *Control Engineering Practice*, vol. 11, pp. 1079–1086, September 2003.
[60] A.J. McDaid, K.C. Aw, S.Q. Xie, and E. Haemmerle, "Gain scheduled control of IPMC actuators with 'model-free' Iterative Feedback Tuning," *Sensors and Actuators A: Physical*, vol. 164, pp. 137–147, December 2010.
[61] J.K. Huusom, N.K. Poulsen, and S.B. Jørgensen, "Data driven tuning of state space controllers with observers," in *Proceedings of European Control Conference 2009 (ECC '09)*, Budapest, Hungary, pp. 1961–1966, 2009.
[62] S. Blažič and I. Škrjanc, "Design and stability analysis of fuzzy model-based predictive control - A Case Study," *Journal of Intelligent and Robotic Systems*, vol. 49, pp. 279-292, July 2007.
[63] Z. Petres, P. Baranyi, P. Korondi, and H. Hashimoto, "Trajectory tracking by TP model transformation: case study of a benchmark problem," *IEEE Transactions on Industrial Electronics*, vol. 54, pp. 1654-1663, June 2007.
[64] J. Vaščák, "Navigation of mobile robots using potential fields and computational intelligence means," *Acta Polytechnica Hungarica*, vol. 4, pp. 63-74, March 2007.
[65] T. Orlowska-Kowalska, and K. Szabat, "Damping of torsional vibrations in two-mass system using adaptive sliding neuro-fuzzy approach," *IEEE Transactions on Industrial Informatics*, vol. 4, pp. 47-57, February 2008.
[66] M. Barut, S. Bogosyan, and M. Gokasan, "Experimental evaluation of braided EKF for sensorless control of induction motors," *IEEE Transactions on Industrial Electronics*, vol. 55, pp. 620-632, February 2008.
[67] P. Baranyi, P. Korondi, and K. Tanaka, "Parallel distributed compensation based stabilization of a 3-DOF RC helicopter: A tensor product transformation based approach," *Journal of Advanced Computional Intelligence and Intelligent Informatics*, vol. 13, pp. 25-34, January 2009.
[68] G. Klančar, D. Matko, and S. Blažič, "Wheeled mobile robots control in a linear platoon," *Journal of Intelligent and Robotic Systems*, vol. 54, pp. 709-731, May 2009.
[69] D. Hladek, J. Vaščák, and P. Sinčák, "multi-robot control system for pursuit-evasion problem," *Journal of Electrical Engineering*, vol. 60, pp. 143-148, March 2009.
[70] K.J. Åström, and T. Hägglund, "Benchmark systems for PID control," *In Proceedings of IFAC PID'00 Workshop*, Terrassa, Spain, 2000, pp. 181-182.
[71] R. Isermann, *Mechatronic Systems: Fundamentals*. Berlin, Heidelberg, New York: Springer-Verlag, 2003.
[72] L. Horváth and I.J. Rudas, *Modeling and Problem Solving Methods for Engineers*. Academic Press, Elsevier, Burlington, MA, 2004.
[73] V.M. Popov, *Hyperstability of Automatic Control Systems*. Berlin, New York: Springer-Verlag, 1973.

[74] Y.-D. Landau, *Adaptive Control: The Model Reference Approach*. New York Marcel Dekker, 1979.
[75] R.-E. Precup, St. Preitl, I.J. Rudas, M.-L. Tomescu, and J.K. Tar, "Design and experiments for a class of fuzzy controlled servo systems," *IEEE/ASME Transactions on Mechatronics*, vol. 13, pp. 22-35, February 2008.
[76] R.-E. Precup, St. Preitl, J.K. Tar, M.-L. Tomescu, M. Takács, P. Korondi, and P. Baranyi, "Fuzzy control system performance enhancement by Iterative Learning Control," *IEEE Transactions on Industrial Electronics*, vol. 55, pp. 3461-3475, September 2008.
[77] J. Ruiz-León, J.L. Orozco, and O. Begovich, "A method to obtain the semi-canonical Morse's form of a linear multivariable system," *Journal of the Franklin Institute*, vol. 347, pp. 483–501, March 2010.
[78] I. Škrjanc, S. Blažič, and O.E. Agamennoni, "Identification of dynamical systems with a robust interval fuzzy model," *Automatica*, vol. 41, pp. 327–332, February 2005.
[79] Z.C. Johanyák and S. Kovács, "Fuzzy rule interpolation by the least squares method," in *Proceedings of 7th International Symposium of Hungarian Researchers on Computational Intelligence* (HUCI 2006), Budapest, Hungary, 2006, pp. 495–506.
[80] J. Zhang, P. Shi, and J. Qiu, "Non-fragile guaranteed cost control for uncertain stochastic nonlinear time-delay systems," *Journal of the Franklin Institute*, vol 346, pp. 676-690, September 2009.
[81] M. Basin and D. Calderon-Alvarez, "Sliding mode regulator as solution to optimal control problem for non-linear polynomial systems," *Journal of the Franklin Institute*, vol. 347, 910–922, August 2010.
[82] V. Bobal, M. Kubalcik, P. Chalupa, and P. Dostal, "Self-tuning control of nonlinear servo system: Comparison of LQ and predictive approach," in *Proceedings of 17th Mediterranean Conference on Control and Automation* (MED '09), Thessaloniki, Greece, 2009, pp. 240-245.
[83] V. Azhmyakov, R. Galvan-Guerra, and A. Poznyak, "On the hybrid LQ-based control design for linear networked systems," *Journal of the Franklin Institute*, vol. 347, 1214-1226, Spemtember 2010.
[84] X. Yang, H. Gao, and P. Shi, "Robust orbital transfer for low earth orbit spacecraft with small-thrust," *Journal of the Franklin Institute*, vol. 347, pp. 1863-1887, December 2010.
[85] J. Sjöberg, P.-O. Gutman, M. Agarwal, and M. Bax, "Nonlinear controller tuning based on a sequence of identifications of linearized time-varying models," *Control Engineering Practice*, vol. 17, pp. 311-321, February 2009.
[86] F.N. Koumboulis, M.P. Tzamtzi, and C.E. Economakos, "Control of a constant turning force system via step-wise safe switching Iterative Feedback Tuning," in *Proceedings of 2008 IEEE International Conference on Emerging Technologies and Factory Automation (ETFA 2008)*, Hamburg, Germany, 2008, pp. 1416-1424.
[87] J.K. Huusom, N.K. Poulsen, and S.B. Jørgensen, "Iterative feedback tuning of uncertain state space systems," *Brazilian Journal of Chemical Engineering*, vol. 27, pp. 461-472, September 2010.
[88] J. Vaščák, "Fuzzy cognitive maps in path planning," *Acta Technica Jaurinensis, Series Intelligentia Computatorica*, vol. 1, pp. 467-479, December 2008.

[89] Y.-H. Chen and X. Zhang, "Adaptive robust approximate constraint-following control for mechanical systems," *Journal of the Franklin Institute*, vol. 347, pp. 69-86, February 2010.
[90] O. Linda and M. Manic, "Comparative analysis of type-1 and type-2 fuzzy control in context of learning behaviors for mobile robotics," in *Proceedings of 36th Annual Conference of the IEEE Industrial Electronics Society* (IEEE IECON '10), Glendale, AZ, USA, 2010, pp. 1086-1092.
[91] J. Doyle, "Guaranteed margins for LQG regulators," *IEEE Transactions on Automatic Control*, vol. 23, pp. 756-757, August 1978.
[92] J. Doyle and G. Stein, "Multivariable feedback design: Concepts for a classical/modern synthesis," *IEEE Transactions on Automatic Control*, vol. 26, pp. 4-16, February 1981.
[93] R.E. Haber, R. Haber-Haber, A. Jiménez, and R. Galán, "An optimal fuzzy control system in a network environment based on simulated annealing. An application to a drilling process," *Applied Soft Computing*, vol. 9, pp. 889-895, June 2009.
[94] Y. Wang, H. Lang, and C.W. de Silva, "A hybrid visual servo controller for robust grasping by wheeled mobile robots," *IEEE/ASME Transactions on Mechatronics*, vol. 15, pp. 757–769, October 2010.
[95] R.-E. Precup, S. Preitl, E.M. Petriu, J.K. Tar, M.L. Tomescu, and C. Pozna, "Generic two-degree-of-freedom linear and fuzzy controllers for integral processes," *Journal of the Franklin Institute*, vol. 346, pp. 980-1003, December 2009.
[96] J. Qiu and J. Cao, "Delay-dependent exponential stability for a class of neural networks with time delays and reaction–diffusion terms," *Journal of the Franklin Institute*, vol. 346, pp. 301-314, May 2009.
[97] A. Astolfi, R. Ortega, and A. Venkatraman, "A globally exponentially convergent immersion and invariance speed observer for mechanical systems with non-holonomic constraints," *Automatica*, vol. 46, pp. 182-189, January 2010.
[98] H.R. Karimi, M. Zapateiro, and N. Luo, "A linear matrix inequality approach to robust fault detection filter design of linear systems with mixed time-varying delays and nonlinear perturbations," *Journal of the Franklin Institute,* vol. 347, pp. 957-973, August 2010.
[99] A. Skoglund, B. Iliev, and R. Palm, "Programming-by-demonstration of reaching motions - A next-state-planner approach," *Robotics and Autonomous Systems*, vol. 58, pp. 607-621, May 2010.
[100] E.E. Yaz, C.S. Jeong, A. Bahakeem, and Y.I. Yaz, "Discrete-time nonlinear observer design with general criteria," *Journal of the Franklin Institute*, vol. 344, pp. 918-928, September 2007.
[101] J.S.-H. Tsai, C.-L. Wei, S.-M. Guo, L.S. Shieh, and C.R. Liu, "EP-based adaptive tracker with observer and fault estimator for nonlinear time-varying sampled-data systems against actuator failures," *Journal of the Franklin Institute*, vol 345, pp. 508-535, August 2008.
[102] G. Hulko, C. Belavy, P. Bucek, K. Ondrejkovic, and P. Zajicek, "Engineering methods and software support for control of distributed parameter systems," in *Proceedings of 7th Asian Control Conference* (ASCC 2009), Hong Kong, 2009, pp. 1432-1438.
[103] F. Previdi, T. Schauer, S.M. Savaresi, and K.J. Hunt, "Data-driven control design for neuroprotheses: A virtual reference feedback tuning

(VRFT) approach," *IEEE Transactions on Control Systems Technology*, vol 12, pp. 176-182, January 2004.

[104] M.C. Campi and S.M. Savaresi, "Direct nonlinear control design: the virtual reference feedback tuning (VRFT) approach," *IEEE Transactions on Automatic Control*, vol. 51, pp. 14-27, January 2006.

[105] M. Basin, J. Rodriguez-Gonzalez, and L. Fridman, "Optimal and robust control for linear state-delay systems," *Journal of the Franklin Institute*, vol. 344, pp. 830-845, September 2007.

[106] R.-E. Precup, and S. Preitl, "PI-fuzzy controllers for integral processes to ensure robust stability," *Information Sciences*, vol. 177, pp. 4410-4429, October 2007.

[107] J.C. Blecke, D.S. Epp, H. Sumali, and G.G. Parker, "A simple learning control to eliminate RF-MEMS switch bounce," *Journal of Microelectromechanical Systems*, vol. 18, pp. 458-465, April 2009.

[108] K. Erenturk, "Gray-fuzzy control of a nonlinear two-mass system," *Journal of the Franklin Institute*, vol. 347, pp. 1171-1185, September 2010.

[109] A.Y. Alanis, E.N. Sanchez, A.G. Loukianov, and E.A. Hernandez, "Discrete-time recurrent high order neural networks for nonlinear identification," *Journal of the Franklin Institute*, vol. 347, pp. 1253-1265, September 2010.

[110] L.C. Kammer, R.R. Bitmead, and P.L. Bartlett, "Direct iterative tuning via spectral analysis," *Automatica*, vol. 36, pp. 1301-1307, September 2000.

[111] L.C. Kammer, "Stability assessment for cautious iterative controller tuning," *Automatica*, vol. 41, pp. 1829-1834, October 2005.

[112] K. van Heusden, A. Karimi, and D. Bonvin, "Data-driven estimation of the infinity norm of a dynamical system," in *Proceedings of 46th IEEE Conference on Decision and Control*, New Orleans, LA, USA, 2007, pp. 4889-4894.

[113] A. Lanzon, A. Lecchini, A. Dehghani, and B.D.O. Anderson, "Checking if controllers are stabilizing using closed-loop data," in *Proceedings of 45th IEEE Conference on Decision and Control*, San Diego CA, USA, 2006, pp. 3660-3665.

[114] H. Kwakernaak, "Robust control and H_∞ optimization - Tutorial paper," *Automatica*, vol. 29, pp. 255-273, March 1993.

[115] H. Bourlés, "A local small gain theorem for discrete-time systems," in *Proceedings of 33rd IEEE Conference on Decision and Control*, Lake Buena Vista, FL, USA, 1994, vol. 3, pp. 2137-2138.

[116] L. Ljung, *System Identification: Theory for the User 2nd ed*. Englewood Cliffs, NJ: Prentice Hall, 1999.

[117] R. Pintelon and J. Schoukens, *System Identification: A Frequency Domain Approach*. New York: IEEE Press, 2001.

[118] B. Wahlberg, M. Barenthin Syberg, and H. Hjalmarsson, "Non-parametric methods for L_2-gain estimation using iterative experiments," *Automatica*, vol. 46, pp. 1376-1381, August 2010.

[119] T. Chen and B.A. Francis, *Optimal Sampled-Data Control Systems*. London: Springer-Verlag, 1995.

[120] R.-E. Precup, C. Borchescu, M.-B. Rădac, S. Preitl, C.-A. Dragoş, E.M. Petriu, and J.K. Tar, "Implementation and signal processing aspects of iterative regression tuning," in *Proceedings of 2010 IEEE International*

Symposium on Industrial Electronics ISIE 2010, Bari, Italy, 2010, pp. 1657-1662.

[121] M. Vašak, M. Baotić, I. Petrović, and N. Perić, "Hybrid theory-based time-optimal control of an electronic throttle," *IEEE Transactions on Industrial Electronics*, vol. 54, pp. 1483-1494, June 2007.

[122] M. Malinowski, S. Stynski, W. Kolomyjski, and M P. Kazmierkowski, "Control of three-level PWM converter applied to variable-speed-type turbines," *IEEE Transactions on Industrial Electronics*, vol. 56, pp. 69-77, January 2009.

[123] M. Cychowski, K. Szabat, and T. Orlowska-Kowalska, "Constrained model predictive control of the drive system with mechanical elasticity," *IEEE Transactions on Industrial Electronics*, vol. 56, pp. 1963-1974, June 2009.

[124] J.-H. Park, S.-H. Kim, and C.-J. Moon, "Adaptive neural control for strict-feedback nonlinear Systems without backstepping," *IEEE Transactions on Neural Networks*, vol. 20, pp. 1204-1209, July 2009.

[125] T. Chai, "Optimal operation and feedback control for complex industrial process," in *Proceedings of 2009 IEEE International Conference on Networking, Sensing and Control (ICNSC '09)*, Okayama, Japan, 2009, pp. 4-5.

[126] D. Qi, M. Liu, M. Qiu, and S. Zhang, "Exponential H_∞ synchronization of general discrete-time chaotic neural networks with or without time delays," *IEEE Transactions on Neural Networks*, vol. 21, pp. 1358-1365, August 2010.

[127] I. Škrjanc, S. Blažič, S. Oblak, and J. Richalet, "An approach to predictive control of multivariable time-delayed process: Stability and design issues," *ISA Transactions*, vol. 43, pp. 585-595, October 2004.

[128] Y. Fu and T. Chai, "Nonlinear multivariable adaptive control using multiple models and neural networks," *Automatica*, vol. 43, pp. 1101-1110, June 2007.

[129] D. Vrabie, O. Păstrăvanu, M. Abu-Khalaf, and F. L. Lewis, "Adaptive optimal control for continuous-time linear systems based on policy iteration," *Automatica*, vol. 45, pp. 477-484, February 2009.

[130] H. Zhang, Y. Luo, and D. Liu, "Neural-network-based near-optimal control for a class of discrete-time affine nonlinear systems with control constraints," *IEEE Transactions on Neural Networks*, vol. 20, pp.1490-1503, September 2009.

[131] C Yin, J.-X. Xu, and Z. Hou, "Iterative learning control design with high-order internal model for nonlinear systems," in *Proceedings of Joint 48th IEEE Conference on Decision and Control and 28th Chinese Control Conference (CDC/CCC 2009)*, Shanghai, China, 2009, pp. 434-439.

[132] Y. Hayakawa and K. Nakajima, "Design of the inverse function delayed neural network for solving combinatorial optimization problems," *IEEE Transactions on Neural Networks*, vol. 21, pp. 224-237, February 2010.

[133] Z. Liu, H. Zhang, and Q. Zhang, "Novel stability analysis for recurrent neural networks with multiple delays via line integral-type L-K functional," *IEEE Transactions on Neural Networks*, vol. 21, pp. 1710-1718, November 2010.

[134] P. Oryschuk, A. Salerno, A. M. Al-Husseini, and J. Angeles, "Experimental validation of an underactuated two-wheeled mobile robot," *IEEE/ASME Transactions on Mechatronics*, vol. 14, pp. 252-257, April 2009.

[135] V. Bobal, M. Kubalcik, P. Chalupa, and P. Dostal, "Self-tuning control of nonlinear servo system: Comparison of LQ and predictive approach," in *Proceedings of 17th Mediterranean Conference on Control and Automation (MED '09)*, Thessaloniki, Greece, 2009, pp. 240-245.

[136] J. C. Spall, "A stochastic approximation algorithm for large-dimensional systems in the Kiefer-Wolfowitz setting," in *Proceedings of 27th IEEE Conference on Decision and Control*, Austin, TX, USA, 1998, vol. 2, pp. 1544-1548.

[137] J. I. M. Martinez, K. Nakano, and K. Higuchi, "Parameter estimation in neural networks by improved version of simultaneous perturbation stochastic approximation algorithm," in *Proceedings of 2009 ICCAS-SICE Conference*, Fukuoka, Japan, 2009, pp. 4567-4572.

[138] H. Zhang, J. Zhao, T. Geng, and R. Wang, "The improved convergence of SPSA and its application in drive system," in *Proceedings of 4th IEEE Conference on Industrial Electronics and Applications (ICIEA 2009)*, Xi'an, China, 2009, pp. 662-666.

[139] H. Dong, X.-H. Tang, Y. Tong, and Y.-P. Li, "Research on model predictive control for inventory management in decentralized supply chain system," in *Proceedgins of 2009 International Conference on Information Management, Innovation Management and Industrial Engineering*, Xi'an, China, 2009, vol. 1, pp. 250-253.

[140] Y.-Y. Hong, H.-L. Chang, and C.-S. Chiu, "Hour-ahead wind power and speed forecasting using simultaneous perturbation stochastic approximation (SPSA) algorithm and neural network with fuzzy inputs," *Energy*, vol. 35, pp. 3870-3876, September 2010.

[141] O. Granichin, L. Gurevich, and A. Vakhitov, "SPSA with a fixed gain for intelligent control in tracking applications," in *Proceedings of 2009 IEEE Multi-conference on Systems and Control (MSC2009)*, Saint Petersburg, Russia, 2009, pp. 1415-1420.

[142] C. C. Hyun, J. Knowles, M. S. Fadali, and S. L. Kwon, "Fault detection and isolation of induction motors using recurrent neural networks and dynamic Bayesian modeling," *IEEE Transactions on Control Systems Technology*, vol. 18, pp. 430-437, March 2010.

[143] Y.-Y. Hong and C.-S. Chiu, "Passive filter planning using Simultaneous perturbation stochastic approximation," *IEEE Transactions on Power Delivery*, vol. 25, pp. 939-946, April 2010.

[144] M. Kumon, K. Fukushima, S. Kunimatsu, and M. Ishitobi, "Motion planning based on simultaneous perturbation stochastic approximation for mobile auditory robots," in *Proceedings of 2010 IEEE/RSJ International Conference on Intelligent Robots and Systems (IROS 2010)*, Taipei, Taiwan, 2010, pp. 431-436.

[145] A. H. Alhabsi, "Improved SPSA optimization algorithm requiring a single measurement per iteration," in *Proceedings of 10th International Conference on Information Sciences, Signal Processing and their Applications (ISSPA 2010)*, Kuala Lumpur, Malaysia, 2010, pp. 263-265.

[146] D. Vrabie and F. L. Lewis, "Neural network approach to continuous-time direct adaptive optimal control for partially unknown nonlinear systems," *Neural Networks*, vol. 22, pp. 237-246, April 2009.

[147] C. Eitzinger and H. Plach, "A new approach to perceptron training," *IEEE Transactions on Neural Networks*, vol. 14, pp. 216-221, January 2003.

[148] J. C. Spall, "Implementation of the simultaneous perturbation algorithm for stochastic optimization," *IEEE Transactions on Aerospace and Electronic Systems*, vol. 34, pp. 817-823, July 1998.

[149] R. Abdullah, A. Hussain, K. Warwick, and A. Zayed, "Autonomous intelligent cruise control using a novel multiple-controller framework incorporating fuzzy-logic-based switching and tuning," *Neurocomputing*, vol. 71, pp. 2727-2741, August 2008.

[150] W. Zuo, Y. Zhu, and L. Cai, "Fourier-neural-network-based learning control for a class of nonlinear systems with flexible components," *IEEE Transactions on Neural Networks*, vol. 20, pp. 139-151, January 2009.

[151] D. Huang, J.-X. Xu, and Z. Hou, "A discrete-time periodic adaptive control approach for parametric-strict-feedback systems," in *Proceedings of Joint 48th IEEE Conference on Decision and Control and 28th Chinese Control Conference (CDC/CCC 2009)*, Shanghai, China, 2009, pp. 6620-6625.

[152] X. Yang, J. Cao, Y. Long, and W. Rui, "Adaptive lag synchronization for competitive neural networks with mixed delays and uncertain hybrid perturbations," *IEEE Transactions on Neural Networks*, vol. 21, pp. 1656-1667, October 2010.

[153] M. Athans, "The role and use of the stochastic linear-quadratic-Gaussian problem in control system design", *IEEE Transactions on Automatic Control*, vol. 16, pp. 529-552, December 1971.

[154] K. N. Gurney, A. Hussain, J. M. Chambers, and R. Abdullah, "Controlled and automatic processing in animals and machines with application to autonomous vehicle control," *Lecture Notes in Computer Science*, vol. 5768, pp. 198-207, September 2009.

[155] W. L. Tung and C. Quek, "eFSM - A novel online neural-fuzzy semantic memory model," *IEEE Transactions on Neural Networks*, vol. 21, pp. 136-157, January 2010.

[156] A. Rodan and P. Tino, "Minimum complexity echo state network," *IEEE Transactions on Neural Networks*, vol. 22, pp. 131-144, January 2011.

[157] A. Sala, T.M. Guerra, and R. Babuška, "Perspectives of fuzzy systems and control," *Fuzzy Sets and Systems*, vol. 156, pp. 432-444, December 2005.

[158] K. Michels, F. Klawonn, R. Kruse, and A. Nürnberger, *Fuzzy Control: Fundamentals, Stability and Design of Fuzzy Controllers*. Springer-Verlag, Berlin, Heidelberg, New York, 2006.

[159] H. Gao, X. Liu, and J. Lam, "Stability analysis and stabilization for discrete-time fuzzy systems with time-varying delay," *IEEE Transactions on Systems, Man, and Cybernetics*, *Part B: Cybernetics*, vol. 39, pp. 306-317, April 2009.

[160] Z. Lendek, R. Babuška, and B. De Schutter, "Stability of cascaded fuzzy systems and observers," *IEEE Transactions on Fuzzy Systems*, vol. 17, pp. 641-653, June 2009.

[161] A. Kruszewski, R. Wang, and T.M. Guerra, "Nonquadratic stabilization conditions for a class of uncertain nonlinear discrete time TS fuzzy models: a new approach," *IEEE Transactions on Automatic Control*, vol. 53, pp. 606-611, March 2008.

[162] V.F. Montagner, R.C.L.F. Oliveira, and P.L.D. Peres, "Convergent LMI relaxations for quadratic stabilizability and H_∞ control of Takagi-Sugeno

fuzzy systems," *IEEE Transactions on Fuzzy Systems*, vol. 17, pp. 863-873, August 2009.

[163] T. Zhang, G. Feng, J. Lu, and W. Xiang, "Robust constrained fuzzy affine model predictive control with application to a fluidized bed combustion process," *IEEE Transactions on Control Systems Technology*, vol. 16, pp. 1047-1056, September 2008.

[164] H. Gao, Y. Zhao, and T. Chen, "H_∞ fuzzy control of nonlinear systems under unreliable communication links," *IEEE Transactions on Fuzzy Systems*, vol. 17, pp. 265-278, April 2009.

[165] S. Blažič, I. Škrjanc, S. Gerkšič, G. Dolanc, S. Strmčnik, M.B. Hadjiski, and A. Stathaki, "Online fuzzy identification for an intelligent controller based on a simple platform," *Engineering Applications of Artificial Intelligence*, vol. 22, pp. 628-638, June 2009.

[166] A. Poursamad, and A.H. Davaie-Markazi, "Robust adaptive fuzzy control of unknown chaotic systems," *Applied Soft Computing*, vol. 9, pp. 970–976, June 2009.

[167] H.K. Lam, and M. Narimani, "Stability analysis and performance design for fuzzy-model-based control system under imperfect premise matching," *IEEE Transactions on Fuzzy Systems*, vol. 17, pp. 949-961, August 2009.

[168] H. K. Lam, "Stability analysis of T-S fuzzy control systems using parameter-dependent Lyapunov function," *IET Control Theory & Applications*, vol. 3, pp. 750-762, June 2009.

[169] K. Tanaka, H. Yoshida, H. Ohtake, and H.O. Wang, "A sum-of-squares approach to modeling and control of nonlinear dynamical systems with polynomial fuzzy systems," *IEEE Transactions on Fuzzy Systems*, vol. 17, pp. 911-922, August 2009.

[170] V. Oduguwa, R. Roy, and D. Farrugia, "Development of a soft computing-based framework for engineering design optimisation with quantitative and qualitative search spaces," *Applied Soft Computing*, vol. 7, pp. 166–188, January 2007.

[171] I. De Falco, A. Della Cioppa, and E. Tarantino, "Facing classification problems with Particle Swarm Optimization," *Applied Soft Computing*, vol. 7, pp. 652-658, June 2007.

[172] Z. Fan, J. Wang, S. Achiche, E. Goodman, and R. Rosenberg, "Structured synthesis of MEMS using evolutionary approaches," *Applied Soft Computing*, vol. 8, pp. 579-589, January 2008.

[173] B.M. Wilamowski, N.J. Cotton, O. Kaynak, and G. Dundar, "Computing gradient vector and Jacobian matrix in arbitrarily connected neural networks," *IEEE Transactions on Industrial Electronics*, vol. 55, pp. 3784-3790, October 2008.

[174] P.M. Marusak, "Advantages of an easy to design fuzzy predictive algorithm in control systems of nonlinear chemical reactors," *Applied Soft Computing*, vol. 9, pp. 1111-1125, June 2009.

[175] N.S. Bhuvaneswari, G. Uma, and T.R. Rangaswamy, "Adaptive and optimal control of a non-linear process using intelligent controllers," *Applied Soft Computing*, vol. 9, pp. 182-190, January 2009.

[176] K.M. Zemalache, and H. Maaref, "Controlling a drone: Comparison between a based model method and a fuzzy inference system," *Applied Soft Computing*, vol. 9, pp. 553-562, March 2009.

[177] R.-E. Precup, S. Preitl, M.L. Tomescu, E.M. Petriu, J.K. Tar, and C. Bărbulescu, "Stable iterative feedback tuning-based design of Takagi-Sugeno PI-fuzzy controllers," *in Proceedings of 2008 Conference on Human System Interactions (HSI 2008)*, Krakow, Poland, 2008, pp. 542-547.

[178] A. Nafaa, Y. Hadjadj-Aoul, and A. Mehaoua, "On interaction between loss characterization and forward error correction in wireless multimedia communication," *in Proceedings of 2005 IEEE International Conference on Communications (ICC 2005)*, Seoul, Korea, 2005, vol. 2, pp. 1390-1394.

[179] M. Sanjuan, A. Kandel, and C.A. Smith, "Design and implementation of a fuzzy supervisor for on-line compensation of nonlinearities: An instability avoidance module," *Engineering Applications of Artificial Intelligence*, vol. 19, pp. 323-333, April 2006.

[180] J.-X. Xu, and Z.-S. Hou, "Notes on data-driven system approaches," *Acta Automatica Sinica*, vol. 35, pp. 668-675, June 2009.

[181] R.-E. Precup, M.L. Tomescu, S. Preitl, and E.M. Petriu, "Fuzzy logic-based stabilization of nonlinear time-varying systems," *International Journal of Artificial Intelligence*, vol. 3, pp. 24-36, 2009.

[182] F. Matia, A. Jimenez, R. Galan, and R. Sanz, "Fuzzy controllers: Lifting the linear-nonlinear frontier," *Fuzzy Sets and Systems*, vol. 52, pp. 113-128, December 1992.

[183] N. Li, and S.Y. Li, "Stability analysis and design of T-S fuzzy control system with simplified linear rule consequent," *IEEE Transactions on Systems, Man, and Cybernetics, Part B: Cybernetics*, vol. 34, pp. 788-795, February 2004.

[184] H. Ying, "Conditions for analytically determining general fuzzy controllers of Mamdani type to be nonlinear, piecewise linear or linear," *Soft Computing*, vol. 9, pp. 606-616, August 2005.

[185] D. Bellomo, D. Naso, and R. Babuška, "Adaptive fuzzy control of a non-linear servo-drive: Theory and experimental results," *Engineering Applications of Artificial Intelligence*, vol. 21, pp. 846-857, September 2008.

[186] J.J.E. Slotine and W. Li, *Applied Nonlinear Control*. Englewood Cliffs, NJ: Prentice-Hall, 1991.

[187] L. Hitz and B.D.O. Anderson, "Discrete positive real functions and their application to system stability," in *Proceedings of IEE*, vol. 116, 1969, pp. 153-155.

[188] P.C. Chang and T.W. Liao, "Combining SOM and fuzzy rule base for flow time prediction in semiconductor manufacturing factory," *Applied Soft Computing*, vol. 6, pp. 198-206, January 2006.

[189] D. Karaboga, A. Bagis, and T. Haktanir, "Controlling spillway gates of dams by using fuzzy logic controller with optimum rule number," *Applied Soft Computing*, vol. 8, pp. 232-238, January 2008.

[190] M.F. Mlynski and H.-J. Zimmermann, "An efficient method to represent and process imprecise knowledge," *Applied Soft Computing*, vol. 8, pp. 1050-1067, March 2008.

[191] B.M. Mohan and A. Sinha, "Analytical structure and stability analysis of a fuzzy PID controller," *Applied Soft Computing*, vol. 8, pp. 749-758, January 2008.

[192] Z.C. Johanyák, and A. Ádám-Majo, "Fuzzy modeling of the relation between components of thermoplastic composites and their mechanical properties," *in Proceedings of 5th International Symposium on Applied*

Computational Intelligence and Informatics (SACI 2009), Timisoara, Romania, 2009, pp. 481-486.

[193] Y. Farzaneh, and A. Akbarzadeh Tootoonchi, "A novel data reduction method for Takagi–Sugeno fuzzy system design based on statistical design of experiment," *Applied Soft Computing*, vol. 9, pp. 1367-1376, September 2009.

[194] A. Kamiya, S.J. Ovaska, R. Roy, and S. Kobayashi, "Fusion of soft computing and hard computing for large-scale processes: a general model," *Applied Soft Computing*, vol. 5, pp. 265-279, March 2005.

[195] I. B. Türkşen, "Fuzzy functions with LSE," *Applied Soft Computing*, vol. 8, pp. 1178-1188, June 2008.

[196] P. Dostál, F. Gazdoš, and V. Bobál, "Design of controllers for time delay systems. Part II: Integrating and unstable systems," *Journal of Electrical Engineering*, vol. 59, pp. 3-8, January 2008.

[197] B. Subudhi, and A.S. Morris, "Soft computing methods applied to the control of a flexible robot manipulator," *Applied Soft Computing*, vol. 9, pp. 149-158, January 2009.

[198] M. Singh, S. Srivastava, M. Hanmandlu, and J.R.P. Gupta, "Type-2 fuzzy wavelet networks (T2FWN) for system identification using fuzzy differential and Lyapunov stability algorithm," *Applied Soft Computing*, vol. 9, pp. 977-989, June 2009.

[199] S.-K. Oh, W. Pedrycz, and S.-B. Roh, "Hybrid fuzzy set-based polynomial neural networks and their development with the aid of genetic optimization and information granulation," *Applied Soft Computing*, vol. 9, pp. 1068-1089, June 2009.

[200] T.M. Jelleli, and A.M. Alimi, "On the applicability of the minimal configured hierarchical fuzzy control and its relevance to function approximation," *Applied Soft Computing*, vol. 9, pp. 1273-1284, September 2009.

[201] M.-B. Rădac, R.-E. Precup, St. Preitl, J.K. Tar, and K.J. Burnham, "Tire slip fuzzy control of a laboratory anti-lock braking system," in *Proceedings of the European Control Conference 2009 (ECC'09)*, Budapest, Hungary, 2009, pp. 940-945.

[202] R.-E. Precup, C. Gavriluţă, M.-B. Rădac, St. Preitl, C.-A. Dragoş, J.K. Tar, and E.M. Petriu, "Iterative Learning Control experimental results for inverted pendulum crane mode control," in *Proceedings of 7th International Symposium on Intelligent Systems and Informatics (SISY 2009)*, Subotica, Serbia, 2009, pp. 323-328.

[203] M. Fliess and C. Join, "Model-free control and intelligent PID controllers: towards a possible trivialization of nonlinear control?," in *Proceedings of 15th IFAC Symposium on System Identification (SYSID 2009)*, Saint-Malo, France, 2009, pp. 1531-1550.

[204] R.-E. Precup, I. Moşincat, M.-B. Rădac, St. Preitl, St. Kilyeni, E.M. Petriu, and C.-A. Dragoş, "Experiments in Iterative Feedback Tuning for level control of three-tank system," in *Proceedings of 15th IEEE Mediterranean Electromechanical Conference MELECON 2010*, Valletta, Malta, 2010, pp. 564-569.

[205] R.-E. Precup, M.-B. Rădac, St. Preitl, E.M. Petriu, and C.-A. Dragoş, "Iterative Feedback Tuning in linear and fuzzy control systems," in *Towards Intelligent Engineering and Information Technology*, I.J. Rudas, J. Fodor,

and J. Kacprzyk, Eds. Berlin, Heidelberg, New York: Springer-Verlag, 2009, pp. 179-192.

[206] R.-E. Precup, St. Preitl, M.-B. Rădac, E.M. Petriu, C.-A. Dragoş, and J.K. Tar, "Experiment-based teaching in advanced control engineering," *IEEE Transactions on Education*, vol. PP, no. 99, pp. 1-11, 2010.

[207] M.-B. Rădac, R.-E. Precup, E.M. Petriu, St. Preitl, and C.-A. Dragoş, "Convergent Iterative Feedback Tuning of state feedback-controlled servo systems," in *Informatics in Control Automation and Robotics*, J. Andrade Cetto, J. Filipe, and J.-L. Ferrier, Eds. J.-L. Berlin, Heidelberg, New York: Springer-Verlag, 2011, pp. 99-111.

[208] M.-B Rădac, R.-B. Grad, R.-E. Precup, St. Preitl, C.-A. Dragoş, E.M. Petriu, and A. Kilyeni, "Mixed Virtual Reference Feedback Tuning - Iterative Feedback Tuning approach to the position control of a laboratory servo system," in *Proceedings of International Conference on Computer as a Tool EUROCON 2011*, Lisbon, Portugal, 2011, paper index 453, 4 pp.

[209] Y.D. Landau, and G. Zito, *Digital control systems: design, identification and implementation*. London: Springer-Verlag, 2006.

[210] M.-B. Rădac, R.-B. Grad. R.-E. Precup, E.M. Petriu, St. Preitl, and C.-A. Dragoş, "Mixed Virtual Reference Feedback Tuning – Iterative Feedback Tuning: Method and laboratory assessment," in *Proceedings of 20th IEEE International Symposium on Industrial Electronics ISIE 2011*, Gdansk, Poland, 2011, pp. 649-654.

[211] M.-B. Rădac, R.-E. Precup, E.M. Petriu, St. Preitl, and R.-C. David, "Stable Iterative Feedback Tuning Method for Servo Systems," in *Proceedings of 20th IEEE International Symposium on Industrial Electronics ISIE 2011*, Gdansk, Poland, 2011, pp. 1943-194.